

# Hysteresis in the Sky

---

Sayantana Choudhury <sup>1a</sup> Shreya Banerjee <sup>b</sup>

<sup>a</sup>*Department of Theoretical Physics, Tata Institute of Fundamental Research, Colaba, Mumbai - 400005, India*

<sup>b</sup>*Department of Astronomy and Astrophysics, Tata Institute of Fundamental Research, Colaba, Mumbai - 400005, India*

*E-mail:* [sayantana@theory.tifr.res.in](mailto:sayantana@theory.tifr.res.in),  
[shreya.banerjee@tifr.res.in](mailto:shreya.banerjee@tifr.res.in)

**ABSTRACT:** Hysteresis is a phenomenon occurring naturally in several magnetic and electric materials in condensed matter physics. When applied to cosmology, aka *cosmological hysteresis*, has interesting and vivid implications in the scenario of a cyclic bouncy universe. Most importantly, this physical prescription can be treated as an alternative proposal to inflationary paradigm. *Cosmological hysteresis* is caused by the asymmetry in the equation of state parameter during expansion and contraction phase of the universe, due to the presence of a single scalar field. This process is purely thermodynamical in nature, results in a non-vanishing hysteresis loop integral ( $\oint pdV$ ) in cosmology. When applied to variants of modified gravity models -1) Dvali-Gabadadze-Porrati (DGP) brane world gravity, 2) Cosmological constant dominated Einstein gravity, 3) Loop Quantum Gravity (LQG), 4) Einstein-Gauss-Bonnet brane world gravity and 5) Randall Sundrum single brane world gravity (RSII), under certain circumstances, this phenomenon leads to the increase in amplitude of the consecutive cycles and to a universe with older and larger successive cycles, provided we have physical mechanisms to make the universe bounce and turnaround. This inculcates an arrow of time in a dissipationless cosmology. Remarkably, this phenomenon appears to be widespread in several cosmological potentials in variants of modified gravity background, which we explicitly study for- i) Hilltop, ii) Natural and iii) Coleman-Weinberg potentials, in this paper. Semi-analytical analysis of these models, for different potentials with minimum/minima, show that the conditions which creates a universe with an ever increasing expansion, depend on the signature of the hysteresis loop integral ( $\oint pdV$ ) as well as on the variants of model parameters.

**KEYWORDS:** Alternatives to inflation, Cosmological hysteresis, Cyclic cosmology, Bouncing cosmology, Cosmology beyond the standard model, Cosmology from effective theory.

---

<sup>1</sup>**Presently working as a Visiting (Post-Doctoral) fellow at DTP, TIFR, Mumbai, Alternative E-mail: [sayanphysics@gmail.com](mailto:sayanphysics@gmail.com).**

---

## Contents

<b>1</b>	<b>Introduction</b>	<b>1</b>
<b>2</b>	<b>Basics of cosmological hysteresis</b>	<b>4</b>
<b>3</b>	<b>Analogy with magnetic hysteresis</b>	<b>9</b>
<b>4</b>	<b>Hysteresis from Dvali-Gabadadze-Porrati (DGP) brane world gravity model</b>	<b>10</b>
4.1	Condition for bounce	14
4.2	Condition for acceleration	16
4.3	Condition for turnaround	19
4.4	Condition for deceleration	21
4.5	Evaluation of the work done for one cycle	23
4.6	Semi-analytical analysis for cosmological potentials	26
4.6.1	Case I: Hilltop potential	27
4.6.2	Case II: Natural potential	34
4.6.3	Case III: Coleman-Weinberg potential	38
4.7	Graphical Analysis	44
4.7.1	Case I: Hilltop potential	44
4.7.2	Case II: Natural potential	50
4.7.3	Case III: Coleman-Weinberg potential	50
<b>5</b>	<b>Hysteresis from cosmological constant dominated Einstein gravity model</b>	<b>53</b>
5.1	Condition for bounce	55
5.2	Condition for acceleration	57
5.3	Condition for turnaround	60
5.4	Condition for deceleration	60
5.5	Evaluation of work done in one cycle	64
5.6	Semi-analytical analysis for cosmological potentials	66
5.6.1	Case I: Hilltop potential	66
5.6.2	Case II: Natural potential	73
5.6.3	Case III: Coleman-Weinberg potential	79
5.7	Graphical Analysis	86
5.7.1	Case I: Hilltop potential	86
5.7.2	Case II: Natural potential	93
5.7.3	Case III: Coleman-Weinberg potential	97

<b>6</b>	<b>Hysteresis from Loop Quantum gravity (LQG) model</b>	<b>102</b>
6.1	Condition for bounce	103
6.2	Condition for acceleration	104
6.3	Condition for turnaround	106
6.4	Condition for deceleration	107
6.5	Evaluation of work done in one cycle	109
6.6	Semi-analytical analysis for cosmological potentials	111
6.6.1	Case I: Hilltop potential	111
6.6.2	Case II: Natural potential	116
6.6.3	Case III: Coleman-Weinberg potential	120
6.7	Graphical Analysis	122
6.7.1	Case I: Hilltop potential	122
6.7.2	Case II: Natural potential	126
6.7.3	Case III: Coleman-Weinberg potential	128
<b>7</b>	<b>Hysteresis from Einstein-Gauss-Bonnet brane world gravity model</b>	<b>129</b>
7.1	Condition for bounce	130
7.2	Condition for acceleration	136
7.3	Condition for turnaround	139
7.4	Condition for deceleration	142
7.5	C. Evaluation of work done for one cycle	145
7.6	RSII limit	145
7.7	Semi-analytical analysis for cosmological potentials	145
7.7.1	Case I: Hilltop potential	146
7.7.2	Case II: Natural potential	150
7.7.3	Case III: Coleman-Weinberg potential	153
7.8	Graphical Analysis	155
7.8.1	Case I: Hilltop potential	155
7.8.2	Case II: Natural potential	158
7.8.3	Case III: Coleman-Weinberg potential	159
<b>8</b>	<b>Conclusion</b>	<b>160</b>
<b>9</b>	<b>Appendix</b>	<b>163</b>
9.1	Hysteresis from RSII brane world model	163
9.1.1	Condition for bounce	163
9.1.2	Condition for acceleration	164
9.1.3	Condition for turnaround	164
9.1.4	Condition for deceleration	165
9.2	Exact expressions for $\phi$ integrals	165
9.3	Expressions of the constants in work done analysis	168

9.3.1	Dvali-Gabadadze-Porrati (DGP) brane world model	168
9.3.2	Cosmological constant dominated Einstein gravity model	169
9.3.3	Loop Quantum Gravity model	170
9.3.4	Einstein Gauss Bonnet Gravity brane world model	171

---

## 1 Introduction

Hysteresis is a phenomenon that arises in systems with a lag between its input and output. When this lag is dynamic i.e it changes with time, we get hysteresis loops. It can be evaluated by purely thermodynamical expressions where the output depends on the current and past inputs. Such phenomenon naturally occurs in many laboratory systems like ferromagnetic and ferroelectric materials and is often incorporated artificially in several electrical systems.

In analogy with hysteresis, in cosmology, we have the phenomenon of cyclic universe in which the universe re-borns repeatedly after each cycle. Just as in hysteresis, where the material undergoes through the same process over and over again, in a cyclic universe, the universe starts from big bang and ends in big crunch repeatedly. Several models of cyclic universe have been proposed in literature [1–3]. Such models also arise naturally as exact solutions of Einstein equations for a closed universe filled with perfect fluid. However in most of these models, all the cycles are identical to one another. Also all these models does not provide any prescription for avoiding singularity. Hence these models remain unsuccessful in solving some of the major problems of big bang model i.e the flatness and horizon problem, and avoidance of singularity. However Tolman [4] in his paper used a radically different approach by which one could get an oscillating universe with increasing expansion maximum after each cycle <sup>1</sup>. He postulated the presence of a viscous fluid which gave rise to asymmetric, irreversible equation of motion. This created an inequality between the pressures at the time of expansion and contraction phases which resulted in the growth of both energy and entropy. Thus he showed a novel way of linking thermodynamical principles to the model of cyclic universe. This unusual approach helped in solving the horizon and flatness problem. In later years, theory of inflation [7–9] was developed which addressed both the horizon and flatness problem. But none of these models were able to avoid big bang singularity. Also the model proposed by Tolman led to an inevitable increase in entropy with each cycle.

However, in [10, 11], the authors have proposed a method of avoiding both the presence of singularity and increasing entropy by using a cosmological analog model of hysteresis. The basic idea of generating the cyclic universe with an increasing

---

<sup>1</sup>The same phenomenon occurs naturally in other cyclic universe models as proposed in refs. [5, 6].

maximum remains the same and in the words of Tolman is “if the pressure tends to be greater during a compression than during a previous expansion, as would be expected with a lag behind equilibrium conditions, an element of fluid can return to its original volume with increased energy..”. The authors created the asymmetry in pressure using the scalar field dynamics generated during inflationary paradigm, thereby maintaining the symmetric nature of the equation of motion hence avoiding entropy production. Originally proposed in [10] and later extended in [11], the authors demonstrated that “a universe filled with a scalar field possess the intriguing property of *‘hysteresis’*.” The central idea was to show that the presence of a massive scalar field "under certain reasonable conditions at the bounce [12–25], gives rise to growing expansion cycles, the increase in expansion amplitude being related to the work done by/on the scalar field during the expansion/contraction of the universe." This leads to the production of hysteresis loop defined as  $\oint pdV$ , during each oscillatory cycle. The loop area is largest in case of inflationary potentials since they give rise to largest asymmetry between expansion and contraction pressures. But the phenomenon of hysteresis is generic i.e. independent of the nature of potential. Any potential with a proper minima which randomizes the phase of the scalar field as it oscillates around the minima during expansion, thereby making all possible values of  $\dot{\phi}$  probable at turnaround, is cable of causing the phenomenon of hysteresis. However potentials without any proper minimum will result in a unique value of  $\dot{\phi}$  which will make

$$p_{exp} = p_{cont}, \quad (1.1)$$

thereby making:

$$\oint pdV = 0. \quad (1.2)$$

Such potentials are not suitable candidates for causing hysteresis. In order to avoid big bang and big crunch, the authors have made use of the presence of existing models like brane world scenario in the early universe, and the presence of negative density or phantom like density in the late universe. These models replaces the big bang singularity by bounce and the big crunch by re-collapse or turnaround.

Our present paper is based on the analysis done by [11]. We have further investigated the phenomenon of hysteresis in different models like the variants of cosmological constant model including  $\Lambda$ CDM, higher dimensional models like Dvali-Gabadadze-Porrati (DGP) brane world gravity model, Loop Quantum Gravity model and Einstein Gauss-Bonnet brane world gravity model in brane world, and in models where the dynamics of the scalar field gets modified which can be achieved by making the cosmological constant field dependent. Our aim is to study not only the phenomenon of hysteresis in different models but also to constrain the parameters of the model using hysteresis. We have mostly studied the models which can give rise to both the phenomena of bounce in the early universe and turnaround in the late universe. We have also investigated the equivalent conditions required to achieve such

bouncing and re-collapsing scenarios. We have shown that our analysis holds true for any general form of the potential of the scalar field with a proper minimum. We have also shown that the phenomenon of hysteresis or the asymmetry in pressure can be achieved irrespective of whether the slow roll conditions of inflation are satisfied or not. A notable feature of this analysis is that an increase in expansion maximum after each cycle now depends not only on the sign of  $\oint pdV$  but also on the parameters of the models that we have considered. Thus we see that using the remarkable cosmological effect of hysteresis as proposed by [10, 11], there are numerous methods and models in which a cyclic universe with an ever increasing amplitude maximum can be achieved.

The plan of the paper is as follows:

- In section 2, we have discussed the mathematical formulation leading to the phenomenon of hysteresis in cosmological scenario.
- In section 3 we have tried to draw an analogy between the hysteresis in ferromagnetic materials and in a cyclic universe. This simple analysis leads to the conclusion that the equation of state parameter  $w$  plays the role of magnetic field  $H$  in cosmology and the scale factor mimics the behavior of magnetization  $M$ .
- In section 4, 5, 6, 7, 9.1, we have studied the behavior of each of the above mentioned models for flat, closed and open universe and have discussed various unexplored important cosmological features.
- In section 4, 6, 7, 9.1, we have explicitly studied cosmological hysteresis in the context of higher dimensional theories, where we have shown the results for both space-like and time-like extra dimensions. For the sake of simplicity we restrict ourselves up to five dimensions ( $D = 5$ ). But one can extend the computation for dimensions,  $D > 5$ .

In this paper, we have drawn various physical conclusions by explicitly solving the equations governing the dynamics of the system using the semi-analytical techniques. Though the analysis is perfectly true for any kind of cosmological potential with a proper minimum/minima, we have studied the detailed features for three different potentials - hilltop potential, natural potential and Coleman-Weinberg potential. All these potentials have well defined minimum/minima and have free parameters which can be adjusted to get the required results. Thus this analysis helps us to put stringent constraints on the characteristic parameters of these models in the bouncing scenario along with cosmological hysteresis. Though the analysis that we have performed holds good under certain physically acceptable approximations and limiting cases, but we can at least show mathematically if there are any limiting cases in which these potentials combined with the models can give rise to the phenomenon

of cosmological hysteresis i.e. make  $\oint pdV$  non-zero. In this paper we have also explicitly derived the expression for work done in one complete cycle of expansion and contraction, and have shown it to be non zero. But the sign of the integral depends on how we have chosen the sign and magnitudes of the parameters of our models. The most interesting result of our analysis is that there are several models which can give rise to a cyclic universe with an increasing amplitude of expansion.

## 2 Basics of cosmological hysteresis

Before going to the technical details of the ‘‘Cosmological hysteresis’’ let us mention clearly the underlying assumptions. It is important to note that throughout the analysis in this paper we assume that during a specified period in the time line of the universe, it is described by a single massive scalar field which is minimally interacting with the gravity sector. The presence of this scalar field is responsible to generate the required asymmetry in the pressure of the universe and this leads to an overall increase in the energy of the universe and hence an increase in its amplitude of the expansion rate.

The action governing the dynamics of this scalar field  $\phi$  with potential  $V(\phi)$  within effective field theory description, is given by

$$S = \int d^4x \sqrt{-g} \left[ \frac{M_p^2}{2} R + \frac{1}{2} g^{\mu\nu} \partial_\mu \phi \partial_\nu \phi - V(\phi) \right] = S_{EH} + S_\phi \quad (2.1)$$

where the signature of the metric throughout our analysis is  $(-, +, +, +)$ . The total action  $S$  can be written as the sum of the standard Einstein Hilbert action ( $S_{EH}$ ) and the action for the scalar field ( $S_\phi$ ). The energy-momentum tensor for the scalar field can be computed from the matter part of the action

$$S_\phi = \int d^4x \sqrt{-g} \mathcal{L}_\phi \quad (2.2)$$

as:

$$T_{\mu\nu}^\phi = -\frac{2}{\sqrt{-g}} \frac{\partial(\sqrt{-g} \mathcal{L}_\phi)}{\partial g_{\mu\nu}} = \partial_\mu \phi \partial_\nu \phi - g_{\mu\nu} \left( \frac{1}{2} \partial^\beta \phi \partial_\beta \phi + V(\phi) \right) \quad (2.3)$$

and for a homogeneous and isotropic spatially flat ( $k = 0$ ) FLRW cosmological background, the energy density and pressure for a scalar field can be computed from the energy momentum tensor as:

$$\rho = \frac{1}{2} \dot{\phi}^2 + V(\phi), \quad (2.4)$$

$$p = \frac{1}{2} \dot{\phi}^2 - V(\phi), \quad (2.5)$$

and the resulting equation of state parameter  $w$  can be written as:

$$w = \frac{p}{\rho} = \frac{\dot{\phi}^2 - 2V(\phi)}{\dot{\phi}^2 + 2V(\phi)}, \quad (2.6)$$

where we assume that the energy momentum tensor for scalar field can be approximated via perfect fluid. Also in the spatially flat FLRW cosmological background the scalar field equation of motion is given by:

$$\square\phi + \frac{dV}{d\phi} = \ddot{\phi} + 3H\dot{\phi} + \frac{dV}{d\phi} = 0, \quad (2.7)$$

where  $\square$  is the d'Alembertian operator four dimension defined as:

$$\square = \frac{1}{\sqrt{-g}}\partial_\mu(\sqrt{-g}g^{\mu\nu}\partial_\nu) = \frac{d^2}{dt^2} + 3H\frac{d}{dt}. \quad (2.8)$$

Here  $H$  is the Hubble parameter defined as:

$$H = \frac{1}{a(t)}\frac{da(t)}{dt}, \quad (2.9)$$

where  $a(t)$  is the scale factor.

**Origin of cosmic hysteresis:** If we closely look at Eq (2.7), then we can conclude that when the universe expands i.e.  $H > 0$  the second term  $3H\dot{\phi}$  mimics the role of friction and opposes the motion of the scalar field, thus serves the purpose of damping during its motion. This lowers the kinetic energy of the scalar field compared to its potential energy, giving rise to a soft equation of state ( $P = -\rho$  in case  $\dot{\phi}^2/2 \ll V(\phi)$ ) i.e. slow roll regime). By contrast, in a contracting ( $H < 0$ ) phase of the universe, the term  $3H\dot{\phi}$  behaves like anti-friction and favors the motion of the scalar field and hence accelerates it. This makes the kinetic energy of the scalar field much larger than the potential energy, giving rise to stiff equation of state ( $P = \rho$  in case  $\dot{\phi}^2/2 \gg V(\phi)$ ). As a result, from second law of thermodynamics, we can convey that a net asymmetry in the pressure (during expansion and contraction cycle) leads to a net non-zero work done by/on the scalar field. In addition, if we now postulate the presence of bouncing and recollapsing mechanisms during contraction and expansion respectively, one can expect that a non-zero work done during a given oscillatory cycle to be converted into expansion energy, resulting in the growth in the maximum amplitude and hence maximum volume of the universe of each successive expansion cycle. Thus producing older and larger cycles. In [11], using simple thermodynamic arguments, the authors have developed the equations which relate the change in maximum amplitude of the scale factor after successive cycles to the work done. The authors have shown that these equations have a universal form which is independent of the scalar field potential responsible for hysteresis. As has been discussed in [11], though the process is independent of the potential, “the presence of hysteresis



is closely linked to the ability of the field  $\phi$  to oscillate". This urges the presence of potential minimum/minima. This is because only potentials with well defined minimum can make the field oscillate. As a result Oscillations of the scalar during expansion makes its phase arbitrary, thereby making all values of  $\dot{\phi}$  equally likely at turnaround. Thus assuring that the values of  $\phi$  and  $\dot{\phi}$ , when the universe turns around and contracts, are nearly uncorrelated with its phase space value when the field  $\phi$  began oscillating. As a result, the field almost always rolls up the potential along the different phase space trajectory compared to the one along which it had descended during expansion. This gives rise to unequal pressure during expansion and contraction hence to non-zero work done.

In the present work, we have reconsidered the above phenomenon of hysteresis and applied it to models or physical mechanisms which can make the universe bounce and turnaround in the presence of potentials having well defined minimum/minima. Further solving Eq. (2.5) and Eq. (2.7) simultaneously, along with the Friedmann equations derived from various cosmological background model, and applying the proper bounce and turnaround conditions, which will be discussed in the following sections, we get the explicit expressions for the scalar field and scale factor as a function of time.

It has been first pointed out in ref.[10] that when we plot the equation of state given by  $w = p/\rho$  vs the scale factor from a specified cosmological model, we get a hysteresis loop whose area contributes to the work done by/on the scalar field during expansion and contraction of the Universe. The general expression for the work done by/on the scalar field during one cycle is given by

$$\oint pdV = \int_{cont} pdV + \int_{exp} pdV \quad (2.10)$$

where the contributions  $\int_{cont} pdV$  and  $\int_{exp} pdV$  represent the work done by/on the scalar field during the phase of contraction and expansion of the Universe respectively. The signature of the integral depends on the pressure during the phase of contraction and expansion i.e if the pressure corresponding to the contraction phase is greater than the pressure due to expansion phase i.e.

$$p_{cont} > p_{exp} \quad (2.11)$$

then the overall signature of the  $p - dV$  work done is negative i.e.

$$\oint pdV < 0. \quad (2.12)$$

On the other hand, if the pressure corresponding to the contraction phase is smaller than the pressure due to expansion phase i.e.

$$p_{cont} < p_{exp} \quad (2.13)$$

then the overall signature of the  $p - dV$  work done is positive i.e.

$$\oint pdV > 0. \tag{2.14}$$

For a universe characterized by a scale factor  $a(t)$ , the total volume at any given time is given by  $a^3(t)$  (neglecting the overall constant factor). Hence using this input, the area of the cosmological hysteresis loop or equivalently the  $p - dV$  work done is given by:

$$\oint pdV = 3 \left[ \int_{cont} pa^2 da + \int_{exp} pa^2 da \right] \tag{2.15}$$

Hence we follow the following algorithm:

- In the context of various cosmological frameworks i.e. DGP braneworld gravity, Loop Quantum gravity (LQG), Einstein-Gauss-Bonnet (EGB) gravity and in presence of pure and field dependent cosmological constant within Einstein gravity we explicitly derive an expression for this characteristic integral in terms of the scale factor and the scalar field degrees of freedom.
- Then we solve the equations of motions for the scalar field under various limiting approximations and hence elaborately study the physical conditions under which the above integral gives non zero value.
- Further we repeat this mentioned two step process for three different cosmological potentials i.e. for Hilltop potentials, Natural potential and Coleman-Weinberg potential within the framework of effective field theory prescription, which will be discussed in the next section in detail.
- We also analyze the whole process graphically to see whether we get a net increase in the amplitude of the scale factor after one cycle of expansion and contraction.

Though the phenomenon of hysteresis is commonly attached to magnetic and electric systems, its appearance for different cosmological models, almost naturally, makes us appreciate and acknowledge its importance in the field of cosmology. The various advantages which a cyclic universe along with the phenomenon of hysteresis, which is our main focus in this paper, have are:

- The phenomenon of hysteresis is important due to the simplicity with which it can be generated. Only a thermodynamic interplay between the pressure and density, creating an asymmetry during expansion and contraction phase of the universe, succeeds in causing cosmological hysteresis.

- As the phenomena of cosmological hysteresis deals with the bouncing as well as the re-collapsing phase of the universe, one can avoid the appearance of Big Bang Singularity as well as the Big Crunch at early and late times.
- Hysteresis can be generated by the presence of a single massive scalar field, which has already been studied for a wide variety of physical situations. The most exciting issue is, it do not require any other fields for its occurrence. Hence it is very easy to handle and its properties can be studied extensively in cosmological literature.
- A cyclic universe having the conditions to cause hysteresis, can solve all the Big Bang puzzles, hence acts as an alternative proposal to inflation [27–31].
- In this scenario, we can always start with a closed or open universe and after allowing the universe go through a number of cycles, we get the present observable flat universe. In this paper, we will extensively deal with several models that can give rise to such cyclic universe. Through analytical calculations, we will show that irrespective of the nature of the universe, we can get a cyclic model with increasing amplitude of the scale factor for a wide variety of models.
- It results in dissipative cosmology [10, 11, 26], which makes the whole process irreversible, which finally causes an arrow of time according to widespread belief. But recently in the ref. [35] the authors have explicitly shown that for cosmological hysteresis phenomena such an arrow of time can appear even if equations describing cosmological evolution are dissipationless, which makes the cumulative process reversible provided they possess cosmological attractors in the expanding and contracting phase of the universe. Additionally, it is important to note that for flat cosmological potential the increment in the expansion cycles are routinely observed. But for the steep potentials two fold cyclic pattern with lesser expansion cycles is observed, which being nested in the larger expansion cycles. This phenomena is exactly analogous to the ‘beat’ formation in acoustics systems. In ref. [10, 11] the authors have studied the cosmological beat formation in the context of chaotic potential  $V(\phi) = \frac{1}{2}m^2\phi^2$ .
- Cosmology in this scenario has not been explored in a very wide sense. Earlier it has been studied by the authors of refs. [10, 11, 35]. In this paper, we have further explored this phenomenon for several other models which have not been discussed earlier in refs. [10, 11, 35].
- In future we plan to connect these analyses with CMB observations, by rigorous study of the cosmological perturbation theory [32–34] in various orders of metric fluctuations and computation of two point correlations to get the expressions for scalar and tensor power spectrum in this context. Hence we extend the

study of this paper to compute the primordial non-Gaussianity in CMB from three and four point correlations [36–45]. We also plan to derive the explicit expression for various modified consistency relations between the non-Gaussian as well as other cosmological parameters in the present context.

- Also we plan to setup the formalism of magnetogenesis from the present setup which can be treated as the alternative version of the inflationary magnetogenesis [46–48].
- We also carry forward our analysis in the development of density inhomogeneities, which is the prime component to form large scale structures at late times. Also the specific role of cosmological hysteresis in the study of cosmological perturbations i.e. for interacting/decoupled dark matter and dark energy have not been explored at all earlier. We have some future plan to do some computations from this setup.
- Further using the reconstruction techniques [49, 50, 52, 53] we want to study the generic features of scalar field potentials in the framework of cosmological hysteresis.
- Last but not the least, we also plan to further study this outstanding cosmological phenomenon for different modified gravity pictures i.e. for variants of  $f(R)$  gravity [54–57], two brane-world model in presence of the Einstein-Hilbert term and the Einstein-Hilbert-Gauss-Bonnet gravity setup [58–64].

### 3 Analogy with magnetic hysteresis

The phenomenon of lagging of magnetic induction  $B$  or magnetization  $M$  behind the magnetic field  $H$  when a specimen of a magnetic material (such as iron) is subjected to a cycle of magnetization is called “magnetic hysteresis”. The closed loop that is traced by the material in the  $B - H$  or  $M - H$  plane is known as the hysteresis loop. It is related to the change in the alignment of the magnetic dipoles, as one varies the magnetic field which leads to magnetization and demagnetization of the material. It is a beautiful way of depicting the effect of varying  $H$  on the system. Fig. 1(a) is a representative schematic diagram in which we have explicitly shown one such hysteresis loop in ferromagnetic material. Since we want to draw an analogy between the phenomenon of hysteresis in magnetism and cosmology, we have also shown Fig. 1(b) to illustrate how an ideal hysteresis loop looks in the case of a cyclic universe. In a cyclic universe, the hysteresis loop is traced by the universe in the  $a - w$  plane where  $a$  is the scale factor of the universe and  $w = p/\rho$  is the equation of state parameter. Closely following the two figures we can say that just as in a magnetic material, we also vary the magnetic field and try to find the behavior of

the magnetization of the material, in this cyclic model, we vary the pressure or the equation of state in order to find the variation of the scale factor or expansion of the universe. This motivates us to consider that the parameter playing the role of  $H$  in cosmological hysteresis is  $w$  and that of  $M/B$  is  $a$ . Just as in magnetic material, where the magnetization oscillates within a specified maximum and minimum values, analogously in cyclic model, the scale factor goes through maximum and minimum values which has been clearly shown in [10, 11] for few cosmological models and will again be shown in this paper for some other cosmological models. While the primary cause of magnetic hysteresis is the asymmetry in the behavior of the alignment of the magnetic dipoles with increase and decrease of  $H$ , the cause for hysteresis in cosmology is the asymmetry in pressure during expansion and contraction phases of the universe. In magnetic hysteresis loop, the minimum and maximum corresponds to the state when all the magnetic dipoles are aligned in reverse and along the direction of  $H$  respectively. In cosmological hysteresis, the maximum is reached when the scale factor reaches its maximum value and the density of the scalar field reached at its minimum i.e when the condition for re-collapse is generated, and the corresponding minimum is reached at bounce when scale factor becomes minimum and density of the scalar field reached at its maximum value. But unlike in magnetic hysteresis where the parameters can take all kind of values i.e positive, negative and zero, in cyclic universe, one of our primary goal is to avoid singularity, i.e.  $a \neq 0$ , so that singularity is replaced by bounce. While repeated cycles of magnetic hysteresis loop results in loss of finite amount of energy, hence decrease in the area of the loop, in cosmological hysteresis, repeated cycles may be either larger or smaller in area compared to the previous one. Thus, we find that a closer look at these two phenomena draws lots of similarities in their behavior. In table. 1 we have depicted the analogy and the parallelism between the different features of these two kinds of hysteresis.

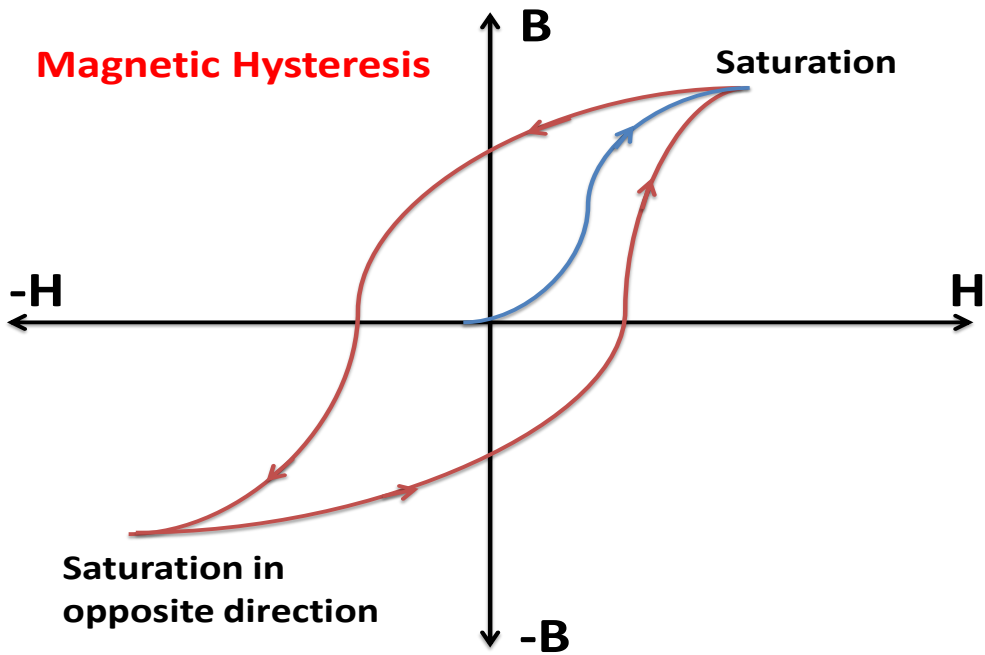
In this section we have shown the complete analysis of different models and studied the conditions under which we get an increase in the amplitude of the scale factor after each cycle. We have studied open closed and flat universe. We have also explicitly calculated the work done in one cycle for three different potentials.

## 4 Hysteresis from Dvali-Gabadadze-Porrati (DGP) brane world gravity model

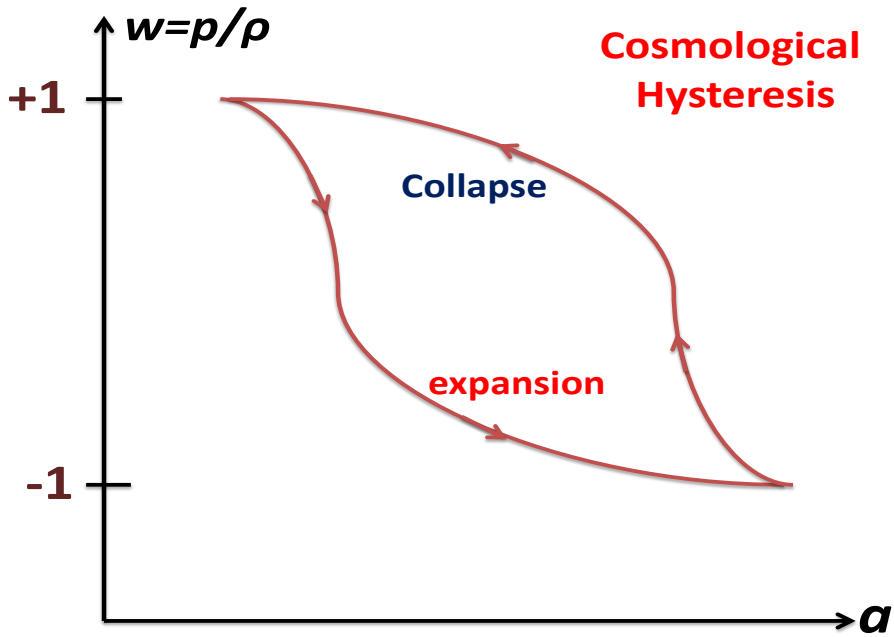
The DGP model is a model of modified gravity theory proposed by Gia Dvali, Gregory Gabadadze, and Massimo Porrati. The model consists of a 4D Minkowski brane embedded in a 5D Minkowski bulk like Randall Sundrum (RS) II model. But unlike in RSII model [65, 66]<sup>2</sup>, here the infinitely large 5th extra dimension is flat. The

---

<sup>2</sup>See also the details of Randall Sundrum (RS) I model studied in ref. [67] for completeness.



(a) An illustration of hysteresis in ferromagnetic materials. The loop has been plotted in the  $B - H$  plane.



(b) An idealised illustration of cosmological hysteresis. The loop has been plotted in the  $w - a$  plane.

**Figure 1.** Analogy between magnetic hysteresis in ferromagnetic materials and cosmological hysteresis.

Characteristics	Magnetic Hysteresis	Cosmological Hysteresis
<b>Loop parameters</b>	$B, M$ $H$	$a$ $w = p/\rho$
<b>Hysteresis loop</b>	$\oint H dB$	$\oint w da (\sim \oint p dV)$
<b>Largest value of hysteresis loop</b>	Given by hard ferromagnetic materials	Cyclic Universe with inflationary conditions
<b>Upper and lower limits of the loop</b>	No limit on maximum and minimum values of $H$	$w_{max} = +1$ $w_{min} = -1$
<b>Characteristic equation for the loop</b>	$B = \mu(H + M)$	$w = p/\rho$
<b>Nature of the loop</b>	Soft ferromagnetic materials have smaller loop area	Universe with softer equation of state have smaller loop area

**Table 1.** Table showing the analogy between magnetic hysteresis and cosmological hysteresis.

Newton's law can be recovered by adding a 4D Einstein–Hilbert action sourced by the brane curvature to the 5D action. While the DGP model recovers the standard 4D gravity for small distances, the effect from the 5D gravity manifests itself for large distances.

The DGP model is described by the following action [68]:

$$S = \frac{1}{2\kappa_{(5)}^2} \int d^5 X \sqrt{-\tilde{g}} \tilde{R} + \frac{1}{2\kappa^2} \int d^4 x \sqrt{-g} R + \int d^4 x \sqrt{-g} \mathcal{L}_M^{\text{brane}}, \quad (4.1)$$

where  $\tilde{g}_{AB}$  is the metric in the 5D bulk and

$$g_{\mu\nu} = \partial_\mu X^A \partial_\nu X^B \tilde{g}_{AB} \quad (4.2)$$

is the induced metric on the brane with  $X^A(x^c)$  being the coordinates of an event on the brane labeled by  $x^c$ . The first and second terms in Eq. (7.2) correspond to

Einstein–Hilbert actions in the 5D bulk and on the brane, respectively. Note that  $\kappa_{(5)}^2$  and  $\kappa^2$  are 5D and 4D gravitational constants, respectively, which are related with 5D and 4D Planck masses,  $M_5$  and  $M_4$ , via

$$\kappa_{(5)}^2 = \frac{1}{M_5^3}, \quad (4.3)$$

$$\kappa^2 = \frac{1}{M_4^2} = \frac{1}{M_p^2} = 8\pi G. \quad (4.4)$$

The Lagrangian  $\mathcal{L}_M^{\text{brane}}$  describes matter localized on the 3-brane.

The equations of motion read

$$G_{AB}^{(5)} = 0, \quad (4.5)$$

where  $G_{AB}^{(5)}$  is the 5D Einstein tensor. The Israel junction conditions on the brane, under which a  $Z_2$  symmetry is imposed:

$$G_{\mu\nu} - \frac{1}{r_c}(K_{\mu\nu} - g_{\mu\nu}K) = \kappa_{(4)}^2 T_{\mu\nu}, \quad (4.6)$$

where  $K_{\mu\nu}$  is the extrinsic curvature calculated on the brane,  $T_{\mu\nu}$  is the energy-momentum tensor of localized matter and  $r_c$  is the crossover length scale,

$$r_c = \frac{M_4^2}{2M_5^3}, \quad (4.7)$$

because it sets the scale above which the effect of extra dimension becomes important.

The modified Friedmann equations in this model are given by [69]:

$$H^2 + \frac{k}{a^2} = \left( \sqrt{\frac{\kappa^2 \rho}{3} + \frac{1}{4r_c^2}} + \frac{1}{2r_c} \right)^2, \quad (4.8)$$

$$\dot{H} + H^2 = -\frac{\kappa^2}{6}(\rho + p) \left[ 1 + \left( \frac{\kappa^2 \rho}{3} + \frac{1}{4r_c^2} \right)^{-1/2} \frac{1}{2r_c} \right] + \left[ \sqrt{\frac{\kappa^2 \rho}{3} + \frac{1}{4r_c^2}} + \frac{1}{2r_c} \right]^2 \quad (4.9)$$

In the present analysis, we have set the extra dimension as time-like which is necessary for getting late time acceleration in DGP model. but in generalized prescription one can consider both space and time like extra dimensions. Also it is important to note that, in Eq. (4.9) the spatial curvature  $k$  can take values 0 or  $\pm 1$ . Now following the proposal of [10, 11], we know that in order to get a cyclic universe, the condition for bounce and turn around are given by:

- **Bounce:**

$$H = \frac{\dot{a}}{a} = \frac{1}{a(t)} \frac{da(t)}{dt} = 0 \quad (4.10)$$

and

$$\ddot{a} = \frac{d^2 a(t)}{dt^2} > 0, \quad (4.11)$$



- **Turn around:**

$$H = \frac{\dot{a}}{a} = \frac{1}{a(t)} \frac{da(t)}{dt} = 0 \quad (4.12)$$

and

$$\ddot{a} = \frac{d^2 a(t)}{dt^2} < 0. \quad (4.13)$$

In the following subsections we will discuss all of these possibilities in detail for DGP brane world gravity framework.

#### 4.1 Condition for bounce

In the early universe, at high energy or equivalently in the high density regime of the brane world,  $\rho r_c^2/M_4^2 \gg 1$ , one can expand Eq. (4.9) as [74]

$$H^2 + \frac{k}{a^2} = \frac{\rho}{3M_4^2} \left[ 1 + \frac{1}{2} \left( \frac{3M_4^2}{4\rho r_c^2} \right) + \dots + \frac{1}{2r_c} \sqrt{\frac{3M_4^2}{\rho}} \right]^2 \quad (4.14)$$

At first order approximation, Eq. 4.14 reduces to the following expression:

$$H^2 + \frac{k}{a^2} = \frac{\rho}{3M_4^2} \left( 1 + \frac{1}{r_c} \sqrt{\frac{3M_4^2}{\rho}} \right) \quad (4.15)$$

This is obviously a valid assumption because at the time of bounce, the density of the matter content of the Universe (in our case scalar field) is at its maximum, hence we can neglect the contribution from the other higher order terms in Eq. (4.14). Now applying the  $\rho r_c^2/M_4^2 \gg 1$  at bounce, and setting  $H = 0$  in Eq. (2(c)), we get:

$$\rho_b = 3M_4^2 \left( \frac{\sqrt{k}}{a_b} - \frac{1}{2r_c} \right)^2 \quad (4.16)$$

where  $\rho_b$  and  $a_b$  are the density and scale factor at bounce, respectively. Similarly the mass content at bounce (neglecting the constant factor) is given by,

$$M_b = \rho_b a_b^3 = 3M_4^2 \left( \frac{\sqrt{k}}{a_b} - \frac{1}{2r_c} \right)^2 a_b^3. \quad (4.17)$$

Hence applying the energy conservation in the present context, we get:

$$\delta M + \delta W = 0, \quad (4.18)$$

where  $\delta W$  is the work done during each expansion-contraction cycle which is given by  $\oint pdV$  which includes contribution from the area of the hysteresis loop. By setting,

$$\delta M = -\delta W = -\oint pdV, \quad (4.19)$$

we get the expression for change in amplitude of the scale factor at each successive cycle as

$$\delta a_{min} = -\frac{\oint pdV}{3M_4^2 \left(\frac{\sqrt{k}}{a_b} - \frac{1}{2r_c}\right) a_b \left[3 \left(\frac{\sqrt{k}}{a_b} - \frac{1}{2r_c}\right) a_b - 2\right]} \quad (4.20)$$

Therefore we clearly observe that the change in amplitude of the scale factor after each cycle depends on the sign of the integral, the curvature parameter and the cross over length scale for DGP brane world. It is independent of the density of the matter content of the universe. During our computation we also observe that if we fix the spatial curvature parameter  $k = -1$ , this makes the energy density of the scalar field imaginary, which is not at all physically possible. Hence, for  $k = -1$  the cosmological bounce from DGP brane world model is not at all possible. But if we neglect all the higher order terms, Eq. (4.14) reduces to the standard Friedmann equation for which the condition for bounce becomes

$$\rho_b = \frac{3kM_4^2}{a_b}, \quad (4.21)$$

which is possible for both  $k = \pm 1$  but not for  $k = 0$ . Hence we see that the bouncing condition depends largely on the order of terms which we are including because our analysis is possible only under approximations. But since our present observed universe is flat ( $k = 0$ ), we will be interested to study the first case in more detail. Hence in our further analysis for DGP model, we will show the results for Eq. (2(c)) only i.e exclude the  $k = -1$  possibility. Here we have the following expression for  $\delta a_{min}$ :

$$\delta a_{min} = \begin{cases} -\frac{\oint pdV}{3M_4^2 \left(\frac{1}{a_b} - \frac{1}{2r_c}\right) a_b \left[3 \left(\frac{1}{a_b} - \frac{1}{2r_c}\right) a_b - 2\right]} & \text{for } k = +1 \\ -\frac{\oint pdV}{\frac{3M_4^2 a_b}{2r_c} \left(\frac{3}{2r_c} + 2\right)} & \text{for } k = 0. \end{cases} \quad (4.22)$$

Let us now briefly mention the characteristic feature of the results for cosmological bounce for DGP brane world model in the following:

1. For a closed universe, depending on whether the quantity appearing in the denominator for  $k = +1$  is positive or negative, an increase in the scale factor after each cycle is possible if:

- The hysteresis loop integral

$$\oint pdV < 0 \quad (4.23)$$

or equivalently

$$p_{exp} < p_{cont}, \quad (4.24)$$

- The hysteresis loop integral

$$\oint pdV > 0 \quad (4.25)$$

or equivalently

$$p_{exp} > p_{cont}. \quad (4.26)$$

2. On the other hand, for the case  $k = 0$ , the quantity in the denominator is always positive and finally we get an increase in the scale factor only if the hysteresis loop integral

$$\oint pdV < 0. \quad (4.27)$$

## 4.2 Condition for acceleration

From Eq. (4.9), at bounce or at high energy, contribution from  $1/r_c$  term is small compared to the density of the scalar field and consequently one finally gets the standard cosmology from the condition for acceleration as:

$$p < -\frac{\rho}{3} \quad (4.28)$$

which clearly implies that the cosmological bounce can be obtained by violating the strong energy condition.

Substituting the expression for  $\rho_b$  for  $k = +1, 0$ , we get the conditions for acceleration at bounce as:

$$\delta p_b < \begin{cases} -M_4^2 \left( \frac{1}{a_b} - \frac{1}{2r_c} \right)^2 & \text{for } k = +1 \\ -\frac{M_4^2}{4r_c^2} & \text{for } k = 0. \end{cases} \quad (4.29)$$

This implies that the pressure of the matter content of the Universe at the time of cosmological bounce is related to the scale factor and the cross over length scale  $r_c$ . Also we observe that the condition for acceleration depends on whether we have considered a possibility of a closed or flat universe. For flat universe, we see that the condition for acceleration is independent of the scale factor at cosmological bounce.

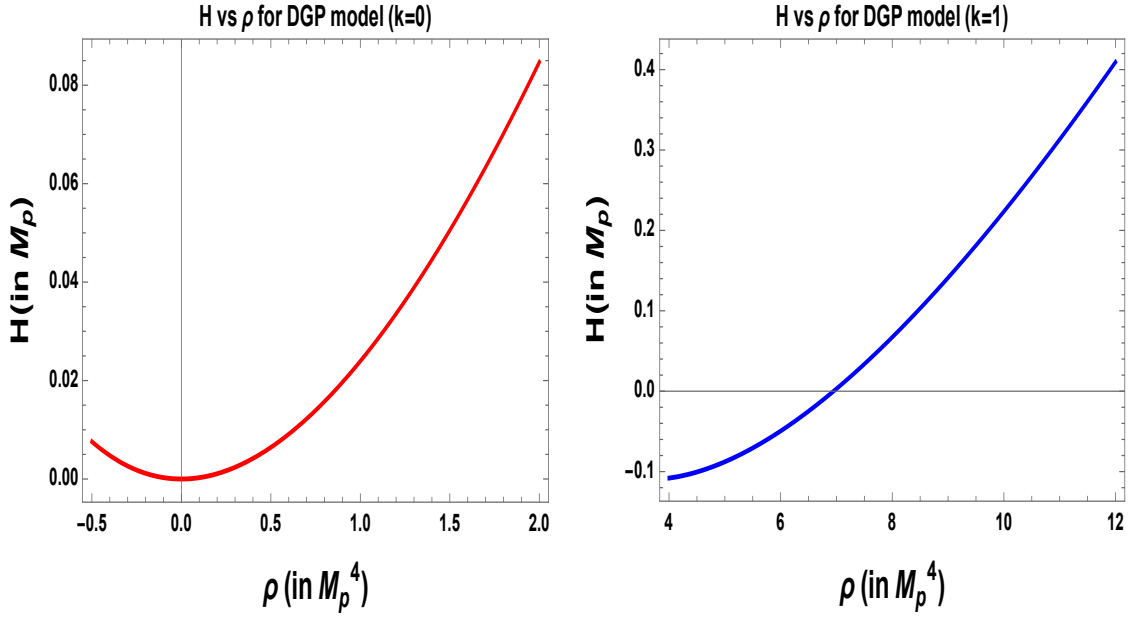
Finally substituting the expressions for the energy density  $\rho$  and pressure  $p$  from Eq. (2.5) into Eq. (9.9), we get the condition for the expansion of the Universe in terms of the scalar field degrees of freedom as:

$$\dot{\phi}^2 < V(\phi) \quad (4.30)$$

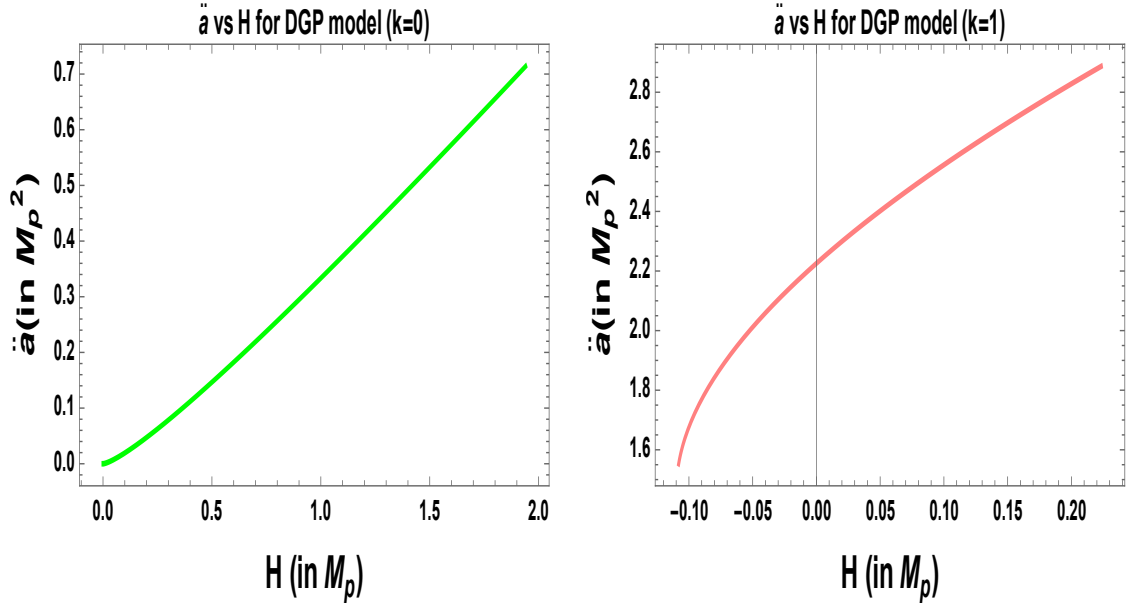
which is same as that we get for the standard cosmological inflationary scenario. Therefore, we can conclude that the conditions on the dynamics of scalar which is needed for causing acceleration in standard case remains unchanged for the DGP model at the time of cosmological bounce. This implies that the cosmological potentials in the standard cosmological scenario, capable of satisfying the above condition, will also be able to cause acceleration in a universe described by the DGP brane world model.

In Fig. 2, we have shown the phenomena of bounce and acceleration in the DGP model. We can draw the following conclusions from the above figures:

- In Fig. 2(a) and Fig. 2(b), we have plotted the r.h.s of Eq. (4.9) using the relation  $\rho = a^{-3(1+w)}$ . The graphs have been plotted only for the cases when  $k = 0, 1$ . This is because, Eq. (4.16) shows that density becomes imaginary for the case when  $k = -1$ , which is unphysical.
- We have used  $w = 0$ , since we require a soft equation of state for causing the acceleration and expansion. The case  $w = 1/3$  made  $H$  only approximately zero. The value of  $r_c$  has been chosen such that we get proper bounce and acceleration. Thus we find that we require a larger value of  $r_c$  for causing bounce in a closed universe as compared to a flat universe.
- From Fig. 2(a), we get the bounce at  $\rho = \rho_b = 0$ . Similarly from Fig. 2(b), we get  $\rho = \rho_b = 7.0M_p^4$ .
- In Fig. 2(a) and Fig. 2(b),  $H$  going to negative values may be interpreted as the universe changing its direction of motion at bounce. As had been discussed in [10], the condition of bounce/turnaround can be imposed by either the condition of making the scale factor changing sign with other quantities remaining same, or,  $\dot{a}$  going to negative values with other quantities remaining same.
- Figs. 2(c) and 4.31 show the necessary condition of acceleration ( $\ddot{a} > 0$ ) at the time of bounce. Here we have plotted the r.h.s of Eq. (4.9) and Eq. (4.9). These plots have also been obtained for the same parameter values as the earlier graphs.
- Thus Fig. 2 shows graphically that the phenomenon of bounce is possible for dgp model having  $w = 0$ .



(a) An illustration of the bouncing condition for a universe with an equation of state  $w = 0$ ,  $k = 0$ ,  $|r_c| = 1$ . (b) An illustration of the bouncing condition for a universe with an equation of state  $w = 0$ ,  $k = 1$ ,  $|r_c| = 1.44$ .



(c) An illustration of the acceleration condition at the time of bounce for a universe with an equation of state  $w = 0$ ,  $k = 0$ ,  $|r_c| = 1$ . (d) An illustration of the acceleration condition at the time of bounce for a universe with an equation of state  $w = 0$ ,  $k = 1$ ,  $|r_c| = 1.44$ .

**Figure 2.** Graphical representation of the phenomena of bounce and acceleration for DGP model.

### 4.3 Condition for turnaround

To establish the condition for turnaround we can again rewrite Eq. (4.9) as [74]:

$$\begin{aligned} H^2 + \frac{k}{a^2} &= \frac{1}{4r_c^2} \left[ \sqrt{1 + \frac{4\rho r_c^2}{3M_4^2}} + 1 \right]^2 \\ &= \frac{1}{4r_c^2} \left[ \left( 1 + \frac{4\rho r_c^2}{3M_4^2} \right) + 2\sqrt{1 + \frac{4\rho r_c^2}{3M_4^2}} + 1 \right] \end{aligned} \quad (4.31)$$

In late time universe,  $\rho r_c^2/M_4^2 \ll 1$ , hence keeping terms upto the first order we get:

$$H^2 + \frac{k}{a^2} \approx \frac{1}{r_c^2} + \frac{2\rho}{3M_4^2} \quad (4.32)$$

This is also a valid assumption because at the time of re-collapse, the density of the Universe is low or reaches at its minimum but not negligible. Hence we need to keep terms upto the first order in the binomial series expansion. Now by setting  $H = 0$ , we get:

$$\rho_t = \frac{3M_4^2}{2} \left( \frac{k}{a_t^2} - \frac{1}{r_c^2} \right) \quad (4.33)$$

where  $\rho_t$  and  $a_t$  are the density and scale factor at turnaround respectively.

Similar to the Cosmological bounce case, here we also can equate the change in energy or mass content of the Universe to the work done after each expansion-contraction cycle and finally we get:

$$\delta M_t = \frac{3M_4^2}{2} \left( k - \frac{3a_t^2}{r_c^2} \right) \delta a_t = - \oint pdV \quad (4.34)$$

Therefore the change in the scale factor after each successive cycle is given by the following expression:

$$\delta a_{max} = - \frac{2}{3M_4^2 \left( k - \frac{3a_{max}^2}{r_c^2} \right)} \oint pdV \quad (4.35)$$

Therefore, just like in the case of bounce, where the change in the amplitude is dependent on the parameters of the cosmological model, in such a physical prescription the change in the amplitude of the scale factor at turnaround also depends not only on the work done, but also on the cross over length scale  $r_c$  of the DGP brane world model.

$$\delta a_{min} = \begin{cases} -\frac{2}{3M_4^2 \left(1 - \frac{3a_{max}^2}{r_c^2}\right)} \oint pdV & \text{for } k = +1 \\ \frac{2r_c^2}{9M_4^2 a_{max}^2} \oint pdV & \text{for } k = 0 \\ \frac{2}{3M_4^2 \left(1 + \frac{3a_{max}^2}{r_c^2}\right)} \oint pdV & \text{for } k = -1. \end{cases} \quad (4.36)$$

Let us now briefly mention the characteristic feature of the results for turnaround for DGP brane world model in the following:

1. For  $k = -1$  we clearly observe that for an open universe, an increase in amplitude of the scale factor after each successive cycle is possible if the hysteresis loop integral

$$\oint pdV > 0. \quad (4.37)$$

2. For  $k = 0$  we observe that the increase in magnitude of the scale factor depends not only on work done, but also on the cross over length scale. We get a positive change in the scale factor with each successive cycle if the hysteresis loop integral

$$\oint pdV > 0. \quad (4.38)$$

Hence, this is a case where increase in expansion maximum is possible only if the work done is positive.

3. For  $k = +1$  if the denominator

$$\left(1 - \frac{3a_{max}^2}{r_c^2}\right) > 0 \quad (4.39)$$

or equivalently

$$\frac{3a_{max}^2}{r_c^2} < 1, \quad (4.40)$$

we get positive  $\delta a_{max}$  if the hysteresis loop integral

$$\oint pdV < 0 \quad (4.41)$$

and vice versa. Thus depending on the relative magnitude of the scale factor and cross over length scale at turnaround, we can get an increase in expansion for both positive and negative signature of the work done.

#### 4.4 Condition for deceleration

To establish the condition for deceleration we first take the time derivative of Eq. (3(a)), and using the energy conservation or equivalently the continuity equation,

$$\dot{\rho} + 3H(\rho + p) = 0, \quad (4.42)$$

we can write:

$$\frac{\ddot{a}}{a} = -\frac{(\rho + p)}{M_4^2} + \frac{1}{r_c^2} + \frac{2\rho}{3M_4^2}. \quad (4.43)$$

From the above equation we get the condition for deceleration as:

$$(\rho_t + 3p_t) > \frac{3M_4^2}{r_c^2} \quad (4.44)$$

Therefore, turnaround can be obtained without violating the energy condition. And just like for acceleration, here we see that the condition for deceleration depends on  $r_c$ , which was expected because in the late universe, the effect of  $r_c$  will become more important.

In place of Eq. (4.29), we get the conditions for deceleration at turnaround as:

$$p_t = \begin{cases} M_4^2 \left( \frac{1}{r_c^2} - \frac{1}{2a_t^2} \right) & \text{for } k = +1 \\ \frac{M_4^2}{r_c^2} & \text{for } k = 0 \\ M_4^2 \left( \frac{1}{r_c^2} + \frac{1}{2a_t^2} \right) & \text{for } k = -1. \end{cases} \quad (4.45)$$

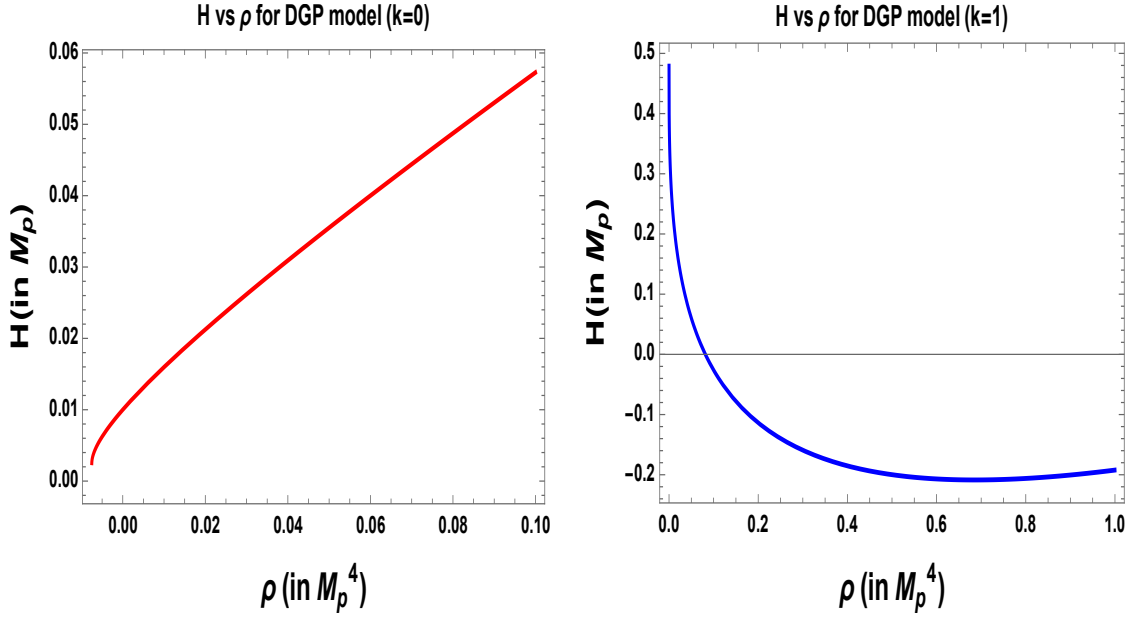
Finally substituting the expressions for the density  $\rho$  and pressure  $p$  from Eq. (2.5) into Eq. (4.44), we get the following condition for expansion of the Universe in terms of the scalar field as:

$$\dot{\phi}^2 > V(\phi) + \frac{3M_4^2}{2r_c^2} \quad (4.46)$$

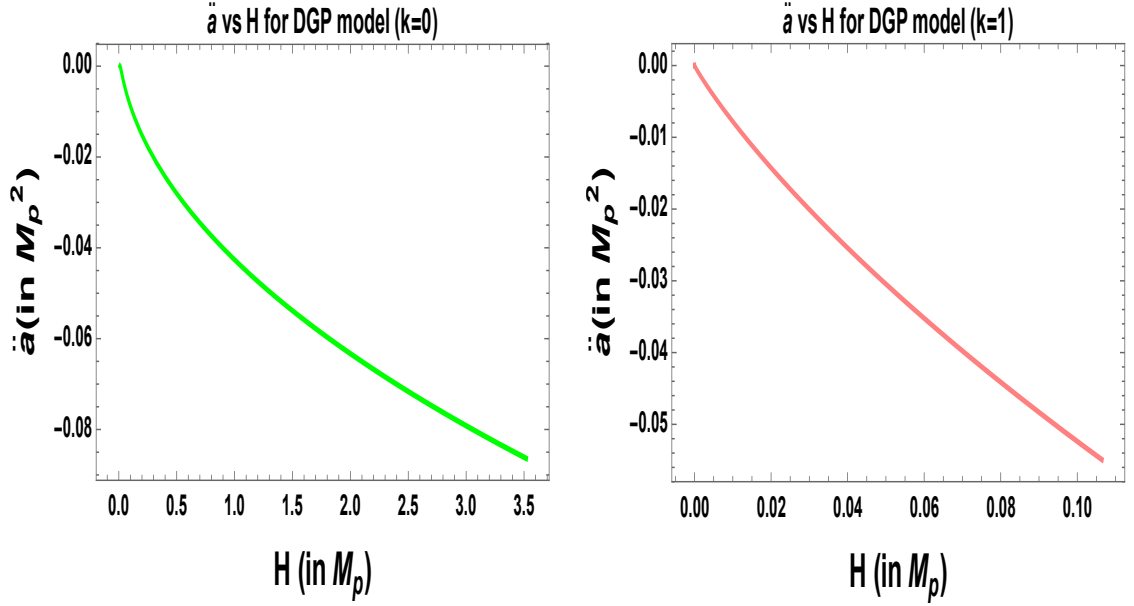
This clearly implies that the lesser the contribution from the potential energy as compared to the standard cosmological inflationary case or equivalently for the acceleration case as mentioned earlier, easier will be to achieve contraction phase of the Universe. We also clearly observe that, even if the potential satisfies the deceleration condition, just like as for standard cosmological scenario, it is not necessary that it will also cause deceleration in DGP brane world model at turnaround as of now the deceleration is also the cross over length scale  $r_c$  dependent in the present context.

In Fig. 3, we have shown the phenomena of turnaround and deceleration in dgp model. We can draw the following conclusions from the above figures:





(a) An illustration of the turnaround condition for a universe with an equation of state  $w = 1$ ,  $k = 0$ ,  $|r_c| = 10$ .  
 (b) An illustration of the turnaround condition for a universe with an equation of state  $w = 1$ ,  $k = 1$ ,  $|r_c| = 1.44$ .



(c) An illustration of the deceleration condition at turnaround for a universe with an equation of state  $w = 1$ ,  $k = 1$ ,  $|r_c| = 10$ .  
 (d) An illustration of the deceleration condition at turnaround for a universe with an equation of state  $w = 1$ ,  $k = 1$ ,  $|r_c| = 1.44$ .

**Figure 3.** Graphical representation of the phenomena of turnaround and deceleration for DGP model.

- In Figs. 3(a) and 3(b), we have plotted the r.h.s of Eqns. (4.31) and (4.9) respectively, using the relation  $\rho = a^{-3(1+w)}$ . But for this case we have used  $w = 1$ , since we require a stiff equation of state for causing contraction and deceleration.
- From Figs. 3(a) and 3(b), we get the turnaround at  $\rho = \rho_t = 0$  and at  $\rho = \rho_t = 0.08M_p^4$  respectively.
- Figs. 3(c) and 3(d) show the necessary condition of deceleration ( $\ddot{a} < 0$ ) at the time of turnaround. Here we have plotted the r.h.s of Eqns. (4.9) and (4.31), (4.9) respectively. This plot has also been obtained for the same parameter values as the earlier graph.
- Thus Fig. 3 shows graphically that the phenomenon of turnaround is possible for the DGP model having  $w = 1$ .

#### 4.5 Evaluation of the work done for one cycle

Let us now compute the explicit contribution from the work done for aone complete cycle for DGP brane world cosmological setup. To serve this purpose we start with the following closed loop integral :

$$\begin{aligned} \oint pdV &= \int_{cont} pdV + \int_{exp} pdV \\ &= \int_{a_{max}^{i-1}}^{a_{min}^{i-1}} pdV + \int_{a_{min}^i}^{a_{max}^i} pdV \end{aligned} \quad (4.47)$$

where  $i$  and  $i - 1$  refer to the two successive cycle i.e.  $i$ th and  $i - 1$ th cycle of expansion and contraction phase of the Universe. In the present context the work done corresponding to the expanding phase and the contracting phase can be expressed in terms of the work done between two successive cycle as:

$$\int_{cont} pdV = \int_{a_{max}^{i-1}}^{a_{min}^{i-1}} pdV, \quad (4.48)$$

$$\int_{exp} pdV = \int_{a_{min}^i}^{a_{max}^i} pdV \quad (4.49)$$

where  $(a_{max}^{i-1}, a_{min}^i)$  are the maximum magnitude of the scale factor for  $i - 1$ th and  $i$ th cycle of the Universe. Similarly,  $(a_{min}^{i-1})$  represents the the minimum magnitude of the scale factor for  $i - 1$ th cycle of the Universe for DGP brane world model.

Now the volume of the Universe can be written as,

$$V = a^3 \quad (4.50)$$

and an infinitesimal change in the volume can be written as,

$$dV = 3a^2 da = 3a^2(t) \frac{da(t)}{dt} dt = 3a^2 \dot{a} dt, \quad (4.51)$$

which is frequently used for further computation of the work done. And we also know from Eq. (2.5), in the presence of scalar field, the pressure for the scalar field can be written as:  $p = \dot{\phi}^2/2 - V(\phi)$ . Substituting these in Eq. (4.47), we get

$$\begin{aligned} \oint pdV &= \int_{cont} 3 \left( \frac{\dot{\phi}^2}{2} - V(\phi) \right) a^2 \dot{a} dt + \int_{exp} 3 \left( \frac{\dot{\phi}^2}{2} - V(\phi) \right) a^2 \dot{a} dt \\ &= \int_{a_{max}^{i-1}}^{a_{min}^i} 3 \left( \frac{\dot{\phi}^2}{2} - V(\phi) \right) a^2 \dot{a} dt + \int_{a_{min}^{i-1}}^{a_{max}^i} 3 \left( \frac{\dot{\phi}^2}{2} - V(\phi) \right) a^2 \dot{a} dt \end{aligned} \quad (4.52)$$

Further using the solution of scalar field  $\phi$  and the scale factor  $a$ , one can solve the above equation to get the estimation of this integral. Also it is important to mention here that the above integral can also be expressed in terms of scale factor only using Eq (4.9), Eq (4.9) and Eq (2.5). But since the Friedmann equations in case of DGP brane world model are highly complicated, we can use the late time and early time approximations of the Friedmann equations in order to get an physically relevant approximate analytical expression for the integral for the work done. Therefore, the work done can be decomposed into four parts as follows:

$$\oint pdV = \underbrace{\int_{a_{max}^{i-1}}^{a'^{i-1}} pdV + \int_{a'^{i-1}}^{a_{min}^{i-1}} pdV}_{\text{Contraction}} + \underbrace{\int_{a_{min}^{i-1}}^{a'^{i-1}} pdV + \int_{a'^{i-1}}^{a_{max}^i} pdV}_{\text{Expansion}} \quad (4.53)$$

where the first two terms corresponds to late and early times during the period of contraction respectively and the last two terms corresponds to early and late times during the period of expansion respectively. Here  $a'$  corresponds to the scale factor at the time of transition  $t'$  from early to late time or vice-versa,  $a_{max}$  and  $a_{min}$  corresponds to the values of the scale factor at the time of turnaround  $t_{max}$  and bounce  $t_{min}$  respectively.

At early time, from Eq. (4.14), keeping terms upto first order and neglecting the contribution from  $1/r_c^2$  terms in the acceleration equation [74], we get:

$$\rho = 3M_4^2 \left[ \left\{ \left( \frac{\dot{a}}{a} \right)^2 + \frac{k}{a^2} \right\}^{1/2} - \frac{1}{2r_c} \right]^2 \quad (4.54)$$

$$\frac{\ddot{a}}{a} = -\frac{(\rho + 3p)}{6M_4^2} \quad (4.55)$$

Hence using Eq. (4.54), Eq. (4.55) and Eq. (2.5) for the pressure content of the Universe  $p$ , we get:

$$\frac{\dot{\phi}^2}{2} - V(\phi) = -M_4^2 \left[ \frac{2\ddot{a}}{a} + \left[ \left\{ \left( \frac{\dot{a}}{a} \right)^2 + \frac{k}{a^2} \right\}^{1/2} - \frac{1}{2r_c} \right]^2 \right] \quad (4.56)$$

Let this equation be valid upto to a cut-off time scale  $t'$  where the value of the scale factor is  $a'$ . Therefore using Eq. (4.56) into Eq. (4.52), the second and third integral as appearing in Eq. (4.53) can be expressed as:

$$\int_{a^{i-1}}^{a_{min}^{i-1}} p dV = \int_{a_{min}^{i-1}}^{a^{i-1}} p dV \quad (4.57)$$

$$= \int -3M_4^2 \left[ \frac{2\ddot{a}}{a} + \left[ \left\{ \left( \frac{\dot{a}}{a} \right)^2 + \frac{k}{a^2} \right\}^{1/2} - \frac{1}{2r_c} \right]^2 \right] a^2 \dot{a} dt \quad (4.58)$$

At late time, using Eq. (3(a)) and Eq. (4.44), we get:

$$\rho = \frac{3M_4^2}{2} \left[ \left( \frac{\dot{a}}{a} \right)^2 + \frac{k}{a^2} - \frac{1}{r_c^2} \right] \quad (4.59)$$

$$\frac{\ddot{a}}{a} = -\frac{(\rho + p)}{M_4^2} + \frac{1}{r_c^2} + \frac{2\rho}{3M_4^2} \quad (4.60)$$

Further using Eq. (4.59), Eq. (4.60) and Eq. (2.5) for the pressure content of the Universe  $p$ , we get:

$$\frac{\dot{\phi}^2}{2} - V(\phi) = M_4^2 \left[ \frac{3}{2r_c^2} - \frac{\ddot{a}}{a} - \frac{1}{2} \left( \frac{\dot{a}}{a} \right)^2 - \frac{k}{2a^2} \right] \quad (4.61)$$

This equation is also valid upto to a cut-off time scale  $t'$  where the value of the scale factor is  $a'$ . Therefore using Eq. (4.61) into Eq. (4.52), the first and last integral as appearing in Eq. (4.53) can be expressed as:

$$\int_{a_{max}^{i-1}}^{a^{i-1}} p dV = \int_{a^{i-1}}^{a_{max}^i} p dV \quad (4.62)$$

$$= \int 3M_4^2 \left[ \frac{3}{2} a^2 \dot{a} - \ddot{a} a \dot{a} - \frac{\dot{a}^3}{2} - \frac{k \dot{a}}{2} \right] dt \quad (4.63)$$

Therefore by substituting Eq. (4.58) and Eq. (4.63) into Eq. (4.53) the complete expression for the work done in a single expansion-contraction cycle is governed by

the following expression:

$$\begin{aligned}
\oint p dV = & \underbrace{\int_{a_{min}^{i-1}}^{a_{max}^{i-1}} 3M_4^2 \left[ \frac{3}{2} a^2 \dot{a} - \ddot{a} a \dot{a} - \frac{\dot{a}^3}{2} - \frac{k \dot{a}}{2} \right] dt}_{\text{I}} \\
& - \underbrace{\int_{a^{i-1}}^{a_{min}^{i-1}} 3M_4^2 \left[ \frac{2\ddot{a}}{a} + \left[ \left( \left( \frac{\dot{a}}{a} \right)^2 + \frac{k}{a^2} \right)^{1/2} - \frac{1}{2r_c} \right]^2 \right] a^2 \dot{a} dt}_{\text{II}} \\
& - \underbrace{\int_{a_{min}^{i-1}}^{a^{i-1}} 3M_4^2 \left[ \frac{2\ddot{a}}{a} + \left[ \left( \left( \frac{\dot{a}}{a} \right)^2 + \frac{k}{a^2} \right)^{1/2} - \frac{1}{2r_c} \right]^2 \right] a^2 \dot{a} dt}_{\text{III}} \\
& + \underbrace{\int_{a^{i-1}}^{a_{max}^i} 3M_4^2 \left[ \frac{3}{2} a^2 \dot{a} - \ddot{a} a \dot{a} - \frac{\dot{a}^3}{2} - \frac{k \dot{a}}{2} \right] dt}_{\text{IV}} \tag{4.64}
\end{aligned}$$

In the present context, we clearly visualize from our analysis that, by knowing the solution of the scale factor in the early Universe and as well as in the late Universe, we can get an idea of the nature of the hysteresis loop. Additionally it is important to note that while the evaluation of work done is independent of the parameters of this model at early times, parameter dependence enters through late time evaluation of the integral for work done.

#### 4.6 Semi-analytical analysis for cosmological potentials

In this section, we try to find simple analytical expressions for the work done during one cycle of expansion and contraction from various cosmological models in order to get some idea of the behavior of the cosmological hysteresis loop. Though the analysis is independent of any particular functional form of potential, but in order to study the physical significance as well as the nature of the derived results in the previous section, we need to specify the functional form of the cosmological potential. While doing the analysis for DGP brane world model and for all the other subsequent cosmological models, we will consider three different potentials i.e. Hilltop, Natural and Coleman-Weinberg potential, which will be discussed in the next sections in detail.

Since from Eq. (4.64), we observe that the cosmological work done can be evaluated if we know the explicit form of the variation of the scale factor with time, our main motivation is to find an explicit expression for the scale factor in terms of time ‘ $t$ ’. For this we need to solve Eq. (4.9), Eq. (2.5) and Eq. (2.7) consistently. Therefore, we will basically substitute the expression for the Hubble parameter from the Friedmann equation into Eq. (2.7) and replace  $\rho$  by Eq. (2.5) with a specified form

of the cosmological potential. Then we can solve for the scalar field and substitute it back to the expression as appearing in the Friedmann equation to get an expression for scale factor in terms of  $t$ . For the sake of simplicity henceforth we will only concentrate for the case of  $k = 0$ , which is also a valid and natural assumption in the present context, since we know that our present observations predict a nearly flat universe. In order to simplify the analysis further, we will consider the case when the contribution from the kinetic term is lesser than the potential energy i.e.

$$\dot{\phi}^2 \ll V(\phi) \quad (4.65)$$

during the expansion and similarly in the physical situation where the kinetic term is larger than the potential energy i.e.

$$\dot{\phi}^2 \gg V(\phi) \quad (4.66)$$

during the contraction phase of the Universe. Hence the approximate forms of Eq. (2.5) and Eq. (2.7) during expansion and contraction phase of the Universe will be given by:

$$3H\dot{\phi} + \frac{dV}{d\phi} \approx 0, \quad \rho \approx V(\phi) \quad (\text{during expansion}) \quad (4.67)$$

$$\ddot{\phi} + 3H\dot{\phi} \approx 0, \quad \rho \approx \frac{\dot{\phi}^2}{2} \quad (\text{during contraction}) \quad (4.68)$$

Next step is to specify the specific form of the potential, in order to get further informations and the constraints from the equations. In the next subsections we have explicitly shown the analysis for three different potentials i.e. Hilltop, Natural and orientated Coleman-Weinberg potential.

#### 4.6.1 Case I: Hilltop potential

In case of hilltop models the potential can be represented by the following functional form [47]:

$$V(\phi) = V_0 \left[ 1 + \beta \left( \frac{\phi}{M_4} \right)^p \right] \quad (4.69)$$

where  $V_0 = M^4$  is the tunable energy scale and  $\beta$  is the index which characterizes the feature of the potential. In principle  $\beta$  can be both positive and negative. Additionally it is important to note that, in the present context,  $V_0$  mimics the role of vacuum energy. Since our present job is to substitute the expression for the scale factor into Eq. (4.64), we need to find separate expressions for the scale factor for both early and late times during the expansion and contraction phases of the Universe.

### A. Expansion

**i) Early time:-**

When the scale factor is lying within the window,  $a_{min} < a < a'$  or equivalently when  $\rho r_c^2/M_4^2 \gg 1$ , we can use the approximated version of the Friedmann equation as given by Eq. (4.14), with  $k = 0$ , where the energy density of the scalar field  $\rho$  is for now described by the hilltop potentials. But instead of considering only the zeroth order term (as we had done in order to find the condition for bounce), here we will consider upto the first order terms (as was done for finding an expression for cosmological work done). Then substituting the resulting expression for the Hubble parameter  $H$  into Eq. (4.67), we get the following integral equation in DGP brane world as:

$$\int d\left(\frac{\phi}{M_4}\right) \frac{\left\{ \left[ \frac{V_0}{3M_4^2} \left( 1 + \beta \left( \frac{\phi}{M_4} \right)^p \right) \right]^{1/2} + \frac{1}{2r_c} \right\}}{\beta p \left( \frac{\phi}{M_4} \right)^{p-1}} = -\frac{V_0}{3M_4^2} \int dt \quad (4.70)$$

The exact solutions of the above integral equation is given in the Appendix, which we see has a very complicated form for Randall Sundrum (RSII) limiting situation. Hence to simplify the integrals, we use the following redefinition of the field variables:

$$\frac{\phi(t)}{M_4} = e^\lambda \quad (4.71)$$

where now we will solve for  $\lambda$ . In order to further simplify the expressions, we solve for two limiting cases:

**a)  $\phi/M_4 \ll 1$ :**

For this case we can expand the exponentials upto linear order and then using the result the integral on the left hand side of Eq. (4.70) becomes:

$$\int \left[ \left( \frac{V_0}{M_4^2} \right)^{1/2} \frac{(1+\beta)^{1/2}}{\beta p} \left( 1 + \frac{\beta p \lambda}{2(1+\beta)} \right) + \frac{1}{2r_c} \right] (1+\lambda)[1-(p-1)\lambda] d\lambda = -\frac{V_0}{3M_4^2} t + c \quad (4.72)$$

which is true under the assumption that the quantity

$$\frac{\beta \lambda p}{(1+\beta)} \ll 1 \quad (4.73)$$

is small. It is important to note that in the present context  $c$  is an arbitrary integration constant.

Hence solving the above integral on the left hand side, we get the expression for  $\lambda$ , hence for  $\phi/M_4 = e^\lambda$  as:

$$\lambda = \frac{\frac{V_0}{3M_4^2}}{\left( \frac{V_0}{3M_4^2} \right)^{1/2} \frac{(1+\beta)^{1/2}}{\beta p} + \frac{1}{2r_c}} (t_i - t) + \lambda_i \quad (4.74)$$

Here  $\lambda_i$  is the value of  $\lambda$  at the initial time scale  $t = t_i$ .

Substituting the expression for  $\lambda$  back into the Friedmann equation, we get the expression for scale factor as

$$a(t) = a_i \exp \left[ \left( \left( \frac{V_0}{3M_4^2} \right)^{1/2} (1 + \beta)^{1/2} + \frac{1}{2r_c} + \beta p \frac{\left( \frac{V_0}{3M_4^2} \right)^{1/2}}{2(1 + \beta)^{1/2}} \left\{ \lambda_i + \frac{\frac{V_0}{3M_4^2}}{\left( \frac{V_0}{3M_4^2} \right)^{1/2} \frac{(1 + \beta)^{1/2}}{\beta p} + \frac{1}{2r_c}} t_i \right\} - \left( \beta p \frac{\left( \frac{V_0}{3M_4^2} \right)^{1/2}}{2(1 + \beta)^{1/2}} \right) \frac{\frac{V_0}{3M_4^2}}{2 \left( \frac{V_0}{3M_4^2} \right)^{1/2} \frac{(1 + \beta)^{1/2}}{\beta p} + \frac{1}{2r_c}} \right) t \right] \quad (4.75)$$

where  $a_i$  is the value of the scale factor at time scale  $t = t_i$  which is in our case fixed at the bouncing time scale  $t_i = t_b$ .

**b)  $\phi/M_4 \gg 1$ :**

For this physical situation Eq. (4.70) simplifies to the following expression:

$$\int \frac{1}{\beta^{1/2} p} \left[ \left( \frac{V_0}{3M_4^2} \right)^{1/2} e^{p\lambda/2} + \frac{1}{2r_c} \right] e^{(2-p)\lambda} d\lambda = -\frac{V_0}{3M_4^2} t + A_0 \quad (4.76)$$

where we use Eq. (4.71). Here we have also assumed that  $\beta e^{p\lambda} \gg 1$ , which is a valid assumption since we are working in the limit where  $\phi/M_4 \gg 1$ .

Hence solving the above integral we get the expression for  $\lambda$  as

$$\lambda = \ln \left[ \frac{\beta^{1/2} p}{\left( \frac{V_0}{3M_4^2} \right)^{1/2}} \left( A_0 - \frac{V_0}{3M_4^2} t \right) \left( 2 - \frac{p}{2} \right) \right] \quad (4.77)$$

Here  $A_0$  is an arbitrary integration constant which can be expressed as:

$$A_0 = \frac{\left( \frac{V_0}{3M_4^2} \right)^{1/2}}{\beta^{1/2} p} \left( \frac{2}{4 - p} \right) \exp \left[ \frac{(4 - p)}{2} \lambda_i \right] + \frac{V_0}{3M_4^2} t_i \quad (4.78)$$

Here we have neglected  $1/2r_c$  as the following condition holds good:

$$\frac{1}{r_c} \ll \left( \frac{V_0}{3M_4^2} \right)^{1/2} \beta^{1/2} e^{p\lambda/2}, \quad (4.79)$$

which is a valid assumption since we are studying the cosmological consequences in the context of early universe in this limiting case.



Further substituting back the expression for  $\lambda$  into the Friedmann equation and integrating, we get the following expression for the scale factor as:

$$a(t) = a_i \exp \left[ \frac{\beta p (p-4) \left( A_0 - \frac{V_0}{3M_4^2} t \right) \left( \left( 2 - \frac{p}{2} \right) \left( A_0 - \frac{V_0}{3M_4^2} t \right) \right)^{\frac{p}{4-p}}}{4 \left( \frac{V_0}{3M_4^2} \right)} \right]. \quad (4.80)$$

## ii) Late time:

When the scale factor is lying within the window,  $a' < a < a_{max}$  or equivalently when  $\rho r_c^2 / M_4^2 \ll 1$ , we can use the approximate Friedmann equation given by Eq. (3(a)) with  $k = 0$ , where  $\rho$  is now characterized by the hilltop potential. Then substituting the resulting expression for the Hubble parameter  $H$  into Eq. (4.67), we get an integral equation of the following form:

$$\int d \left( \frac{\phi}{M_4} \right) \frac{\left( \frac{2}{3} \frac{V_0}{M_4^2} + \frac{1}{r_c^2} + \frac{2}{3} \frac{\beta}{M_4^2} \left( \frac{\phi}{M_4} \right)^p \right)^{1/2}}{\beta p \left( \frac{\phi}{M_4} \right)^{p-1}} = - \frac{V_0}{3M_4^2} \int dt \quad (4.81)$$

The exact solution of the above integral is given in the Appendix for the Randall Sundrum (RSII) model. For the sake of simplicity, we follow the same procedure as we have done in the previous case i.e. first use the field redefinition  $\phi/M_4 = e^\lambda$  and then study two limiting cases.

### $\phi/M_4 \ll 1$ :

Once again expanding the exponentials upto linear order we get

$$\int d\lambda \frac{\left( \frac{2}{3} \frac{V_0 + V_0\beta}{M_4^2} + \frac{1}{r_c^2} \right)^{1/2}}{\beta p} \left( 1 + \frac{\frac{2}{3} \frac{V_0\beta}{M_4^2} p}{2 \left( \frac{2}{3} \frac{V_0 + V_0\beta}{M_4^2} + \frac{1}{r_c^2} \right)} \lambda \right) = - \frac{V_0}{3M_4^2} t + A_1 \quad (4.82)$$

where  $A_1$  is the arbitrary integration constant. The expression on the left hand side has been obtained under the underlying assumption that the following condition:

$$\frac{\frac{2}{3} \frac{V_0\beta}{M_4^2} p}{2 \left( \frac{2}{3} \frac{V_0 + V_0\beta}{M_4^2} + \frac{1}{r_c^2} \right)} \lambda \ll 1 \quad (4.83)$$

is satisfied. As we performing the analysis in late time in the present context, hence  $1/r_c^2$  is a large quantity, but to strictly satisfy this condition, we need to choose  $V_0$  in such a way that the following condition:

$$\frac{2}{3} \frac{V_0}{M_4^2} + \frac{1}{r_c^2} + \frac{2}{3} \frac{V_0\beta}{M_4^2} \gg 1 \quad (4.84)$$

is always satisfied during the late time.

Further solving the integral as stated in Eq. (4.82), we get the following simplified expression for  $\lambda$  as:

$$\lambda = \frac{\left(A_1 - \frac{V_0}{3M_4^2}t\right)}{\left(\frac{2}{3}\frac{V_0+V_0\beta}{M_4^2} + \frac{1}{r_c^2}\right)^{1/2}}\beta p \quad (4.85)$$

where  $A_1$  is given by:

$$A_1 = \frac{\lambda_f \left(\frac{2}{3}\frac{V_0+V_0\beta}{M_4^2} + \frac{1}{r_c^2}\right)^{1/2}}{\beta p} + \frac{V_0}{3M_4^2}t_f \quad (4.86)$$

where  $\lambda_f$  is the value of  $\lambda$  at turnaround corresponding to time scale  $t = t_f$ .

In order to get the expression of the scale factor, we substitute this expressions back into the Friedmann equation and integrate the equation to get the following result:

$$a(t) = A'_1 \exp \left[ \left( \left( \frac{2}{3}\frac{V_0+V_0\beta}{M_4^2} + \frac{1}{r_c^2} \right)^{1/2} + A_1 \frac{\frac{2}{3}\frac{V_0\beta}{M_4^2}p^2}{4\left(\frac{2}{3}\frac{V_0+V_0\beta}{M_4^2} + \frac{1}{r_c^2}\right)} \right) t - \frac{\frac{2}{9}\frac{V_0^2\beta}{M_4^4}p^2}{8\left(\frac{2}{3}\frac{V_0+V_0\beta}{M_4^2} + \frac{1}{r_c^2}\right)} t^2 \right] \quad (4.87)$$

where

$$A'_1 = a_f \exp \left[ - \left( \left( \frac{2}{3}\frac{V_0+V_0\beta}{M_4^2} + \frac{1}{r_c^2} \right)^{1/2} + A_1 \frac{\frac{2}{3}\frac{V_0\beta}{M_4^2}p^2}{4\left(\frac{2}{3}\frac{V_0+V_0\beta}{M_4^2} + \frac{1}{r_c^2}\right)} \right) t_f + \frac{\frac{2}{9}\frac{V_0^2\beta}{M_4^4}p^2}{8\left(\frac{2}{3}\frac{V_0+V_0\beta}{M_4^2} + \frac{1}{r_c^2}\right)} t_f^2 \right] \quad (4.88)$$

Here  $a_f$  is the value of the scale factor at the time of turnaround.

## B. Contraction

From Eq. (4.68), we observe that for the contraction phase of the Universe, under the approximation which we have assumed, the analysis becomes independent of the specific form of the cosmological potential. Hence, the results for the DGP brane world model hold for any form of the potential.

### i) Early time:

When the scale factor is lying within the window,  $a_{min} < a < a'$ , following the same analysis as we did for the case of expansion, with the new expression for density, the

integral equation is now expressed in the following form:

$$\int \frac{1}{\left(\frac{\dot{\phi}}{\sqrt{6}M_4} + \frac{1}{2r_c}\right)\dot{\phi}} d\dot{\phi} = - \int dt \quad (4.89)$$

Solving the above integral equation we get the following expression for  $\dot{\phi}$  as:

$$\dot{\phi} = \frac{\sqrt{6}M_4}{2r_c \left[ \exp\left(\frac{t-A_2}{2r_c}\right) - 1 \right]} \quad (4.90)$$

where  $A_2$  is the arbitrary integration constant given by:

$$A_2 = t_i - 2r_c \ln \left[ \frac{\sqrt{6}M_4}{2r_c\dot{\phi}_i} + 1 \right]. \quad (4.91)$$

Here  $\dot{\phi}_i$  is the value of the derivative of the scalar field at time of bounce.

Further integrating the above equation once again, we get the expression for the field  $\phi$  as:

$$\phi(t) = \frac{\sqrt{6}M_4}{r_c} \left[ \ln \left( 1 - 2e^{-\frac{A'_2}{r_c} + \frac{t}{r_c}} \right) r_c - t \right] \quad (4.92)$$

where  $A'_2$  is the arbitrary integration constant given by:

$$A'_2 = t_i - r_c \ln \left[ \frac{1}{2} \left\{ 1 - \exp \left( \left( \frac{\phi_i r_c}{\sqrt{6}M_4} + t_i \right) \frac{1}{r_c} \right) \right\} \right] \quad (4.93)$$

where  $\phi_i$  is the value of the field at the time of bounce  $t = t_i$ . Hence substituting Eq. (4.92) in the Friedmann equation, we get the following solution for the scale factor as:

$$a(t) = A''_2 \left( e^{\frac{t}{2r_c}} - e^{\frac{A_2}{2r_c}} \right) \quad (4.94)$$

where  $A''_2$  is the arbitrary integration constant given by:

$$A''_2 = \frac{a_i}{\left( e^{\frac{t}{2r_c}} - e^{\frac{A_2}{2r_c}} \right)}. \quad (4.95)$$

## ii) Late time:

When the scale factor is lying within the window,  $a' < a < a_{max}$ , using the Friedmann equation given by Eq. (3(a)) and the late time condition, we get the following solutions from DGP brane world model:

$$\dot{\phi}(t) = \frac{2}{r_c^2} \exp \left[ \frac{3}{r_c} (A_3 - t) \right] \quad (4.96)$$

$$\phi(t) = -\frac{2}{3r_c} \exp \left[ \frac{3}{r_c} (A_4 - t) \right] \quad (4.97)$$

where  $A_3$  and  $A_4$  are the arbitrary integration constants given by:

$$A_3 = \frac{r_c}{3} \ln \left[ \frac{r_c^2 \dot{\phi}_f}{2} \right] + t_f \quad (4.98)$$

$$A_4 = \frac{r_c}{3} \ln \left[ -\frac{3r_c}{2} \phi_f \right] + t_f \quad (4.99)$$

Here  $\phi_f$  and  $\dot{\phi}_f$  are the values of the scalar field and its derivative at turnaround time scale  $t = t_f$ .

Further substituting the expression for  $\dot{\phi}$  in the Friedmann equation, finally we get the expression for the scale factor as:

$$a(t) = A_5 \exp \left[ -\frac{r_c}{3} \left\{ \sqrt{\frac{1}{r_c^2} + \frac{4}{3M_4^2 r_c^4} e^{\frac{6}{r_c}(A_4-t)}} - \frac{1}{r_c} \tanh^{-1} \left( r_c \sqrt{\frac{1}{r_c^2} + \frac{4}{3M_4^2 r_c^4} e^{\frac{6}{r_c}(A_4-t)}} \right) \right\} \right] \quad (4.100)$$

where  $A_5$  is the arbitrary integration constant given by:

$$A_5 = a_f \exp \left[ \frac{r_c}{3} \left\{ \sqrt{\frac{1}{r_c^2} + \frac{4}{3M_4^2 r_c^4} e^{\frac{6}{r_c}(A_4-t_f)}} - \frac{1}{r_c} \tanh^{-1} \left( r_c \sqrt{\frac{1}{r_c^2} + \frac{4}{3M_4^2 r_c^4} e^{\frac{6}{r_c}(A_4-t_f)}} \right) \right\} \right]. \quad (4.101)$$

### C. Expression for work done

Using the solutions for the scale factor, one can further compute the expression for the integrals as appearing in Eq. (4.64), giving the work done in one cycle for the cases for which we have the final expressions for the scale factor.

For the case  $\phi/M_4 \ll 1$ , using the solutions of the scale factor as computed in the earlier section for hilltop potential, we find that the expressions for work done

for spatially flat case  $k = 0$  given by the following expression:

$$\underbrace{\int_{a_{max}^{i-1}}^{a^{i-1}} 3M_4^2 \left[ \frac{3}{2}a^2\dot{a} - \ddot{a}a\dot{a} - \frac{\dot{a}^3}{2} \right] dt}_{\text{I}} = 0, \quad (4.102)$$

$$\underbrace{\int_{a^{i-1}}^{a_{min}^{i-1}} 3M_4^2 \left[ \frac{2\ddot{a}}{a} + \left[ \frac{\dot{a}}{a} - \frac{1}{2r_c} \right]^2 \right] a^2 \dot{a} dt}_{\text{II}} = 3M_4^2 a'_2 \left[ -2e^{3a'_1 t_{min}} + 2e^{3a'_1 t'} - 18a_1(e^{a'_1 t_{min}} - e^{a'_1 t'}) \right. \\ \left. + 9a_2(e^{2a'_1 t_{min}} - e^{2a'_1 t'}) + 6a_3(t_{min} - t') \right], \quad (4.103)$$

$$\underbrace{\int_{a_{min}^{i-1}}^{a^{i-1}} 3M_4^2 \left[ \frac{2\ddot{a}}{a} + \left[ \frac{\dot{a}}{a} - \frac{1}{2r_c} \right]^2 \right] a^2 \dot{a} dt}_{\text{III}} = 3M_4^2 a_4 \left\{ \text{erf}[a_5(2a_7 t_{min} - a_6)] \right. \\ \left. - \text{erf}[a_5(2a_7 t' - a_6)] \right\}, \quad (4.104)$$

$$\underbrace{\int_{a^{i-1}}^{a_{max}^i} 3M_4^2 \left[ \frac{3}{2}a^2\dot{a} - \ddot{a}a\dot{a} - \frac{\dot{a}^3}{2} \right] dt}_{\text{IV}} = 0, \quad (4.105)$$

and consequently the total work done in a one cycle can be expressed as:

$$\oint pdV = -3M_4^2 a'_2 \left[ -2e^{3a'_1 t_{min}} + 2e^{3a'_1 t'} - 18a_1(e^{a'_1 t_{min}} - e^{a'_1 t'}) \right. \\ \left. + 9a_2(e^{2a'_1 t_{min}} - e^{2a'_1 t'}) + 6a_3(t_{min} - t') \right] \\ - 3M_4^2 a_4 (\text{Erf}[a_5(2a_7 t_{min} - a_6)] - \text{Erf}[a_5(2a_7 t' - a_6)]) \quad (4.106)$$

where  $a_1 \dots a_7$  are constants that depends on the model parameters present in the expressions for the scale factor whose explicit expressions have been given in the appendix. Here we have quoted the results corresponding to each integral of the work done as given in Eq. (4.64). Thus, we see that we get

$$\oint pdV \neq 0, \quad (4.107)$$

whose signature depends on the numerical values of the constants. Thus, one can conclude that the phenomenon of hysteresis is fruitfully achieved for small field hill-top potentials.

#### 4.6.2 Case II: Natural potential

In case of natural models the potential can be represented by the following functional form [70]:

$$V(\phi) = V_0 \left[ 1 + \cos \left( \frac{\phi}{f} \right) \right] \quad (4.108)$$

where  $V_0 = M^4$  is the tunable energy scale and  $f$  plays the mass scale of the pot. It is important to note that, the potential is periodic or equivalently shift symmetric for the shift in the field coordinate:

$$\phi \rightarrow \phi + 2\pi f, \quad (4.109)$$

where  $2\pi f$  mimics the role of angular shift in the field coordinate. Since we need to substitute the expression for the scale factor into Eq. (4.64), we need to find separate expressions for the scale factor for both early and late times during expansion and contraction phases.

## A. Expansion

### i) Early time:

When the scale factor is lying within the window,  $a_{min} < a < a'$  or equivalently when  $\rho r_c^2/M_4^2 \gg 1$ , we can use the approximate Friedmann equation given by Eq. (4.14) with spatially flat case  $k = 0$ , where  $\rho$  is now given by the potential for natural potential. But instead of considering only the zeroth order term (as we had done in order to find the condition for bounce), here we will consider upto first order terms to compute the expression for work done. Then substituting the resulting expression for Hubble parameter  $H$  into Eq. (4.67), we get an integral equation of the following form:

$$\int d\left(\frac{\phi}{f}\right) \sqrt{\frac{V_0}{3M_4^2}} \frac{\sqrt{1 + \cos\left(\frac{\phi}{f}\right)}}{\sin\left(\frac{\phi}{f}\right)} = \frac{V_0}{3f^2} \int dt \quad (4.110)$$

The exact solutions of the above integrals are given in the Appendix for Randall Sundrum single brane world model (RSII). Simplified analytical expressions could be obtained only for the small field case ( $\phi/f \ll 1$ ) which has been discussed below.

For  $\phi/f \ll 1$  case we take small argument approximations of the trigonometric functions after which we get the following solution for the scalar field  $\phi$  as:

$$\frac{\phi(t)}{f} = A_6 \exp \left[ \frac{V_0}{3\sqrt{\frac{V_0}{3M_4^2}} \sqrt{2} f^2} t \right] \quad (4.111)$$

where  $A_6$  is the arbitrary integration constant is given by:

$$A_6 = \frac{\phi_i}{f} \exp \left[ -\frac{V_0}{3\sqrt{\frac{V_0}{3M_4^2}} \sqrt{2} f^2} t_i \right] \quad (4.112)$$

Here  $\phi_i$  is the value of  $\phi$  at the initial time of bouncing time scale  $t = t_i$ .

Further substituting the expression for  $\phi$  back into the Friedmann equation, we get the following simplified expression for scale factor as:

$$a(t) = A_7 \exp \left[ \left( \sqrt{\frac{V_0}{3M_4^2}} \sqrt{2} + \frac{1}{2r_c} \right) t \right] \quad (4.113)$$

where  $A_7$  is the arbitrary integration constant is given by:

$$A_7 = a_i \exp \left[ - \left( \sqrt{\frac{V_0}{3M_4^2}} \sqrt{2} + \frac{1}{2r_c} \right) t_i \right]. \quad (4.114)$$

## ii) Late time:

When the scale factor is lying within the window,  $a' < a < a_{max}$  or equivalently when  $\rho r_c^2 / M_4^2 \ll 1$ , we can use the approximated form of the Friedmann equation given by Eq. (3(a)) with spatially flat case  $k = 0$ . Hence substituting the resulting expression for the Hubble parameter  $H$  into Eq. (4.67), we get the following integral equation as given by:

$$\int d \left( \frac{\phi}{f} \right) \frac{\sqrt{\frac{2V_0}{3M_4^2} + \frac{1}{r_c^2} + \frac{2V_0}{3M_4^2} \cos \left( \frac{\phi}{f} \right)}}{\sin \left( \frac{\phi}{f} \right)} = \frac{V_0}{3f^2} \int dt \quad (4.115)$$

The exact solution of the above integral is given in the Appendix for Randall Sundrum single brane world model (RSII). Therefore, in order to simplify the analysis, we again study small field limiting case as mentioned earlier. For  $\phi/f \ll 1$  case we take small argument approximations of the trigonometric functions and finally we get the following simplified expression for the scalar field  $\phi$  as:

$$\frac{\phi(t)}{f} = A_8 \exp \left[ \frac{1}{\sqrt{\frac{2V_0}{3M_4^2} + \frac{1}{r_c^2} + \frac{2V_0}{3M_4^2}}} \frac{V_0}{3f^2} t \right] \quad (4.116)$$

where  $A_8$  is the arbitrary integration constant is given by:

$$A_8 = \frac{\phi_F}{f} \exp \left[ - \frac{1}{\sqrt{\frac{2V_0}{3M_4^2} + \frac{1}{r_c^2} + \frac{2V_0}{3M_4^2}}} \frac{V_0}{3f^2} t_F \right]. \quad (4.117)$$

Here  $\phi_F$  is the value of the scalar field at turnaround time scale  $t = t_F$ .

In order to get the expression of the scale factor, we substitute this expression back into the Friedmann equation and integrate the equation to get following simplified expression for the scale factor as:

$$a(t) = A_9 \exp \left[ \sqrt{\left( \frac{2V_0}{3M_4^2} + \frac{1}{r_c^2} + \frac{2V_0}{3M_4^2} \right) t} \right] \quad (4.118)$$

where  $A_9$  is the arbitrary integration constant is given by:

$$A_9 = a_F \exp \left[ -\sqrt{\left( \frac{2V_0}{3M_4^2} + \frac{1}{r_c^2} + \frac{2V_0}{3M_4^2} \right) t_F} \right] \quad (4.119)$$

where  $a_F$  is the value of the scale factor at turnaround time scale  $t = t_F$ .

## B. Contraction

As has already been mentioned while performing the analysis for expansion, the conclusions for contraction phase is independent of any potential, hence the analysis remains same for natural potential also.

## C. Expression for work done

Here we also study the work done for all the cases for which we have expressions for the scale factor for all the integrals appearing in Eq. (4.64). We consider the case  $\phi/f \ll 1$  for which the expression for work done for spatially flat case  $k = 0$  is given by:

$$\underbrace{\int_{a_{max}^{i-1}}^{a^{i-1}} 3M_4^2 \left[ \frac{3}{2} a^2 \dot{a} - \ddot{a} a \dot{a} - \frac{\dot{a}^3}{2} \right] dt}_{\text{I}} = 0, \quad (4.120)$$

$$\underbrace{\int_{a^{i-1}}^{a_{min}^{i-1}} 3M_4^2 \left[ \frac{2\ddot{a}}{a} + \left[ \frac{\dot{a}}{a} - \frac{1}{2r_c} \right]^2 \right] a^2 \dot{a} dt}_{\text{II}} = 3M_4^2 a'_2 \left[ 2e^{3a'_1 t'} - 2e^{3a'_1 t_{min}} - 18a_1 (e^{a'_1 t_{min}} - e^{a'_1 t'}) \right. \\ \left. + 9a_2 (e^{2a'_1 t_{min}} - e^{2a'_1 t'}) + 6a_3 (t_{min} - t') \right], \quad (4.121)$$

$$\underbrace{\int_{a_{min}^{i-1}}^{a^{i-1}} 3M_4^2 \left[ \frac{2\ddot{a}}{a} + \left[ \frac{\dot{a}}{a} - \frac{1}{2r_c} \right]^2 \right] a^2 \dot{a} dt}_{\text{III}} = 3M_4^2 b_1 \left[ e^{3b_2 t'} - e^{3b_2 t_{min}} \right], \quad (4.122)$$

$$\underbrace{\int_{a^{i-1}}^{a_{max}^i} 3M_4^2 \left[ \frac{3}{2} a^2 \dot{a} - \ddot{a} a \dot{a} - \frac{\dot{a}^3}{2} \right] dt}_{\text{IV}} = 0, \quad (4.123)$$



and consequently the total work done in a one cycle can be expressed as:

$$\oint pdV = 0 - 3M_4^2 a_2' \left[ -2e^{3a_1' t_{min}} + 2e^{3a_1' t'} - 18a_1(e^{a_1' t_{min}} - e^{a_1' t'}) \right. \\ \left. + 9a_2(e^{2a_1' t_{min}} - e^{2a_1' t'}) + 6a_3(t_{min} - t') \right] - 3M_4^2 b_1(e^{3b_2 t'} - e^{3b_2 t_{min}}) + 0 \quad (4.124)$$

Here  $a_1..b_2$  are all constants dependent on the model parameters that appearing in the expressions for the scale factor. Their explicit forms are in the appendix. The results obtained in this section implies that, we get

$$\oint pdV \neq 0 \quad (4.125)$$

for small field limit  $\phi/f \ll 1$  and the signature of the integral is completely determined by the numerical values of the model parameters and the arbitrary integration constants. Most importantly, the analysis shows that the phenomenon of hysteresis is fruitfully achieved for natural potential.

### 4.6.3 Case III: Coleman-Weinberg potential

Let us start with a theory of five dimensional  $\mathcal{N} = 2$  bulk supergravity in which by compactifying the extra fifth dimension it is possible to derive an four dimensional effective theory described by  $\mathcal{N} = 1$  supergravity theory in brane world. Within this prescription, the four dimensional one-loop effective Coleman-Wienberg potential embedded in the brane world can be expressed as [71–73]:

$$V(\phi) = V_0 \left[ 1 + \left\{ \alpha + \beta \ln \left( \frac{\phi}{M_4} \right) \right\} \left( \frac{\phi}{M_4} \right)^4 \right] \quad (4.126)$$

where  $V_0$  sets the energy scale of supergravity theory. Additionally the model parameter  $\alpha$  signifies the tree level effect and the parameter  $\beta$  characterizes the effect of one-loop correction to the leading order result. Here  $M_4$  represents the background mass-scale of theory. For sake of simplicity one can consider  $M_4$  to be the UV cut-off i.e. the Planck scale of the gravity theory.

## A. Expansion

### i) Early time:

When the scale factor is lying within the window,  $a_{min} < a < a'$  or equivalently when  $\rho r_c^2/M_4^2 \gg 1$ , we can use the approximated form of Friedmann equation given

by Eq. (4.14) with spatially flat case  $k = 0$ , where in the present context  $\rho$  is given by the supergravity motivated potential. Instead of considering only the zeroth order term, here we will consider upto first order terms. Then substituting the resulting expression for the Hubble parameter  $H$  into Eq. (4.67), we get an integral equation of the following form:

$$\int d\left(\frac{\phi}{M_4}\right) \frac{\sqrt{\frac{V_0}{3M_4^2} \left[1 + \left\{\alpha + \beta \ln\left(\frac{\phi}{M_4}\right)\right\} \left(\frac{\phi}{M_4}\right)^4\right] + \frac{1}{2r_c}}}{\left(\frac{\phi}{M_4}\right)^3 \left[4 \left\{\alpha + \beta \ln\left(\frac{\phi}{M_4}\right)\right\} + \beta\right]} = -\frac{V_0}{3M_4^2} \int dt \quad (4.127)$$

For the sake of simplicity let us consider the following transformation or redefinition in the field:

$$\frac{\phi}{M_4} = e^\lambda, \quad (4.128)$$

as we had done for the previous cases, where now we will solve for the redefined field  $\lambda$ . In order to further simplify the expressions, we solve for two limiting cases:

**a)  $\phi/M_4 \ll 1$ :**

For this case we can expand the exponentials upto linear order after which the integral on the left hand side of Eq. (4.127) becomes

$$\int d\lambda \frac{\left[\frac{V_0}{3M_4^2} (1 + (\alpha + \beta\lambda) e^{4\lambda})\right]^{1/2} + \frac{1}{2r_c}}{e^{3\lambda} [4(\alpha + \beta\lambda) + \beta]} e^\lambda = -\frac{V_0}{3M_4^2} \int dt \quad (4.129)$$

Next we compute the above integral equation on the left hand side under the assumption that the values of model parameters,  $\alpha$  and  $\beta$  satisfy the constraint:

$$\alpha + 4\alpha\lambda + \beta\lambda \ll 1, \quad (4.130)$$

$$\frac{4\beta\lambda}{(4\alpha + \beta)} \ll 1. \quad (4.131)$$

Consequently we get the expression for  $\lambda$ , hence  $\phi/M_4 = e^\lambda$  as:

$$\lambda = \frac{\left(A_{10} - \left(\frac{V_0}{3M_4^2}\right) t\right)}{\left[\frac{\left(\frac{V_0}{3M_4^2}\right)^{1/2} \left(1 + \frac{\alpha}{2}\right) + \frac{1}{2r_c}}{(4\alpha + \beta)}\right]} \quad (4.132)$$

where  $A_{10}$  is the arbitrary integration constant given by:

$$A_{10} = \frac{\left(\frac{V_0}{3M_4^2}\right)^{1/2} \left(1 + \frac{\alpha}{2}\right) + \frac{1}{2r_c}}{(4\alpha + \beta)} \lambda_i + \left(\frac{V_0}{3M_4^2}\right) t_i \quad (4.133)$$

Here  $\lambda_i$  is the value of  $\lambda$  at the initial time  $t = t_i$  of bounce.

Substituting the expression for  $\lambda$  back into the Friedmann equation, we get the expression for scale factor as:

$$a(t) = A_{11} \exp \left[ \left( \frac{V_0}{3M_4^2} \right)^{1/2} \left( 1 + \frac{\alpha}{2} \right) t + \frac{1}{2r_c} t \right] \quad (4.134)$$

where  $A_{11}$  is the arbitrary integration constant given by:

$$A_{11} = a_i \exp \left[ - \left( \frac{V_0}{3M_4^2} \right)^{1/2} \left( 1 + \frac{\alpha}{2} \right) t_i - \frac{1}{2r_c} t_i \right] \quad (4.135)$$

Here  $a_i$  is the value of the scale factor at the time of bounce.

**b)  $\phi/M_4 \gg 1$ :**

For this case Eq. (4.127) simplifies to

$$\int \left( \frac{V_0}{3M_4^2} \right)^{1/2} \beta^{1/2} \lambda^{-1/2} d\lambda = -\frac{V_0}{3M_4^2} t + A_{12} \quad (4.136)$$

The above expression is obtained provided that the following constraints are satisfied:

$$\frac{\beta\lambda}{(1+\alpha)} \gg 1, \quad (4.137)$$

$$\frac{4\beta\lambda}{(4\alpha+\beta)} \gg 1. \quad (4.138)$$

We have also used the condition  $\rho r_c^2/M_4^2 \gg 1$ , which is true in the case of early universe. Here  $A_{12}$  is an arbitrary integration constant.

Solving the above integral equation we get the following expression for  $\lambda$  as:

$$\lambda = \left[ \left( -\frac{V_0}{3M_4^2} t + A_{12} \right) \frac{1}{2 \left( \frac{V_0}{3M_4^2} \right)^{1/2} \beta^{1/2}} \right]^2 \quad (4.139)$$

where the explicit form of  $A_{12}$  is given by:

$$A_{12} = \frac{V_0 t_i}{3M_4^2} \pm 2 \left( \frac{V_0}{3M_4^2} \right)^{1/2} \beta^{1/2} \lambda_i \quad (4.140)$$

Here  $\lambda_i$  is the value at the time of bounce  $t = t_i$ .

Further substituting back the expression for  $\lambda$  into the Friedmann equation, we get the following expression for the scale factor as:

$$a(t) = A_{13} \exp \left[ - \left( \frac{V_0}{3M_4^2} \right)^{1/2} \beta^{1/2} e^{\frac{2 \left( A_{12} - \frac{V_0}{3M_4^2} t \right)^2}{\left( 2 \left( \frac{V_0}{3M_4^2} \right)^{1/2} \beta^{1/2} \right)^2}} \frac{\left( A_{12} - \frac{V_0}{3M_4^2} t \right)}{4 \frac{V_0}{3M_4^2} \sqrt{\frac{\left( A_{12} - \frac{V_0}{3M_4^2} t \right)^2}{\left( 2 \left( \frac{V_0}{3M_4^2} \right)^{1/2} \beta^{1/2} \right)^2}}} \right] \quad (4.141)$$

where  $A_{13}$  is the arbitrary integration constant given by:

$$A_{13} = a_i \exp \left[ \left( \frac{V_0}{3M_4^2} \right)^{1/2} \beta^{1/2} e^{\frac{2 \left( A_{12} - \frac{V_0}{3M_4^2} t_i \right)^2}{\left( 2 \left( \frac{V_0}{3M_4^2} \right)^{1/2} \beta^{1/2} \right)^2}} \frac{\left( A_{12} - \frac{V_0}{3M_4^2} t_i \right)}{4 \frac{V_0}{3M_4^2} \sqrt{\frac{\left( A_{12} - \frac{V_0}{3M_4^2} t_i \right)^2}{\left( 2 \left( \frac{V_0}{3M_4^2} \right)^{1/2} \beta^{1/2} \right)^2}} \right]. \quad (4.142)$$

## ii) Late time:

When the scale factor is lying within the window,  $a' < a < a_{max}$  or equivalently when  $\rho r_c^2 / M_4^2 \ll 1$ , we can use the approximated version of the Friedmann equation given by Eq. (3(a)) with spatially flat case  $k = 0$ . Hence substituting the resulting expression for the Hubble parameter  $H$  into Eq. (4.67), we get the following integral equation given by:

$$\int d \left( \frac{\phi}{M_4} \right) \frac{\sqrt{\left[ \frac{2}{3} \frac{V_0}{M_4^2} \left( 1 + \left\{ \alpha + \beta \ln \left( \frac{\phi}{M_4} \right) \right\} \left( \frac{\phi}{M_4} \right)^4 \right) + \frac{1}{r_c^2} \right]}}{\left( \frac{\phi}{M_4} \right)^3 \left[ 4\alpha + \beta + 4\beta \ln \left( \frac{\phi}{M_4} \right) \right]} = - \frac{V_0}{3M_4^2} \int dt \quad (4.143)$$

For the sake of simplicity during the analysis, we follow the same procedure as mentioned before and use the field redefinition:

$$\frac{\phi}{M_4} = e^\lambda \quad (4.144)$$

and then study two limiting physical situations.

a)  $\phi/M_4 \ll 1$ :

For this small field limit expanding the exponentials upto linear order we get the following integral equation:

$$\int \frac{1}{r_c(4\alpha + \beta)} \left[ 1 + \frac{1}{3} \frac{V_0 r_c^2}{M_4^2} (1 + \alpha + 4\alpha\lambda + \beta\lambda) \right] (1-2\lambda) \left( 1 - \frac{4\beta}{4\alpha + \beta} \lambda \right) d\lambda = - \int \frac{V_0}{3M_4^2} dt \quad (4.145)$$

where the integral in the left hand side has been obtained under assumption that:

$$\frac{1}{3} \frac{V_0 r_c^2}{M_4^2} (1 + \alpha + 4\alpha\lambda + \beta\lambda) \ll 1, \quad (4.146)$$

which is a valid assumption since we are in the late universe and in the limit of small  $\lambda$ .

Solving the above integral, we get the expression for  $\lambda$  as

$$\lambda = \frac{\left( -\frac{V_0}{3M_4^2} t + A_{14} \right)}{\left[ \frac{1}{r_c(4\alpha + \beta)} + \frac{V_0 r_c}{3M_4^2(4\alpha + \beta)} + \frac{V_0 \alpha r_c}{3M_4^2(4\alpha + \beta)} \right]} \quad (4.147)$$

where  $A_{14}$  is the arbitrary integration constant given by:

$$A_{14} = \lambda_f \left( \frac{1}{r_c(4\alpha + \beta)} + \frac{V_0 r_c}{3M_4^2(4\alpha + \beta)} + \frac{V_0 \alpha r_c}{3M_4^2(4\alpha + \beta)} \right) + \frac{V_0}{3M_4^2} t_f \quad (4.148)$$

where  $\lambda_f$  is the value at turnaround corresponding to time  $t = t_f$ .

In order to get the expression of the scale factor, we substitute this expression back into the Friedmann equation and integrate the equation to get:

$$a(t) = A_{15} \exp \left[ \left( \frac{1}{r_c} + \frac{V_0 r_c}{3M_4^2} (1 + \alpha) + \frac{\frac{4V_0 r_c}{3M_4^2} (4\alpha + \beta) A_{14}}{\frac{1}{r_c(4\alpha + \beta)} + \frac{V_0 r_c}{3M_4^2(4\alpha + \beta)} + \frac{V_0 \alpha r_c}{3M_4^2(4\alpha + \beta)}} \right) t \right] \\ \times \exp \left[ -\frac{V_0}{3M_4^2} \frac{\frac{4V_0 r_c}{3M_4^2} (4\alpha + \beta)}{\frac{1}{r_c(4\alpha + \beta)} + \frac{V_0 r_c}{3M_4^2(4\alpha + \beta)} + \frac{V_0 \alpha r_c}{3M_4^2(4\alpha + \beta)}} \frac{t^2}{2} \right] \quad (4.149)$$

where  $A_{15}$  is the arbitrary integration constant given by:

$$A_{15} = a_f \exp \left[ - \left( \frac{1}{r_c} + \frac{V_0 r_c}{3M_4^2} (1 + \alpha) + \frac{\frac{4V_0 r_c}{3M_4^2} (4\alpha + \beta) A_{14}}{\frac{1}{r_c(4\alpha + \beta)} + \frac{V_0 r_c}{3M_4^2(4\alpha + \beta)} + \frac{V_0 \alpha r_c}{3M_4^2(4\alpha + \beta)}} \right) t_f \right] \\ \times \exp \left[ \left( \frac{V_0}{3M_4^2} \frac{\frac{4V_0 r_c}{3M_4^2} (4\alpha + \beta)}{\frac{1}{r_c(4\alpha + \beta)} + \frac{V_0 r_c}{3M_4^2(4\alpha + \beta)} + \frac{V_0 \alpha r_c}{3M_4^2(4\alpha + \beta)}} \frac{t_f^2}{2} \right) \right]. \quad (4.150)$$

**b)  $\phi \gg M_4$ :**

For this case the integral in Eq. (4.143), writing  $\phi/M_4 = e^\lambda$ , simplifies to:

$$\int \frac{\sqrt{\left(\frac{2}{3} \frac{V_0}{M_4^2} \beta \lambda e^{4\lambda} + \frac{1}{r_c^2}\right)}}{4\beta\lambda} e^{-2\lambda} d\lambda = -\frac{V_0}{3M_4^2} \int dt \quad (4.151)$$

But in order to get an solution for  $\lambda$ , we need to further simplify the integral, which is possible if we assume that the values of the parameters of the model satisfy the condition:

$$\frac{V_0\beta\lambda e^{4\lambda}}{M_4^2} \gg \frac{1}{r_c^2} \quad (4.152)$$

is satisfied. This is possible because though we are in the late time i.e.

$$\frac{\rho}{M_4^2} = \frac{V_0}{M_4^2} + \frac{V_0\alpha e^{4\lambda}}{M_4^2} + \frac{V_0\beta\lambda e^{4\lambda}}{M_4^2} \ll \frac{1}{r_c^2}, \quad (4.153)$$

we have both the above conditions being satisfied by  $1/r_c^2$  simultaneously. Under this assumption, we get the solution for  $\lambda$  as:

$$\lambda = \left(-\frac{V_0}{3M_4^2}t + A_{16}\right)^2 \frac{(4\beta)^2}{\frac{2}{3} \frac{V_0}{M_4^2} \beta} \quad (4.154)$$

where  $A_{16}$  is the arbitrary integration constant given by:

$$A_{16} = \frac{V_0}{3M_4^2}t_f \pm \frac{\left(\frac{2}{3} \frac{V_0}{M_4^2} \beta\right)^{1/2} \lambda_f^{1/2}}{4\beta} \quad (4.155)$$

Substituting the expression for  $\lambda$  back into the Friedmann equation, we get the expression for the scale factor as:

$$a(t) = A_{17} \exp \left[ -\frac{3e \left( \frac{32\beta^2 \left( A_{16} - \frac{tV_0}{3M_4^2} \right)^2}{\frac{2}{3} \frac{V_0}{M_4^2} \beta} \right) (tV_0 - 3A_{16}M_4^2)}{16 \frac{V_0}{M_4} \sqrt{\frac{\beta^2 (-3A_{16}M_4^2 + tV_0)^2}{\frac{2}{3} \frac{V_0}{M_4^2} \beta M_4^4}}} \right] \quad (4.156)$$

where  $A_{17}$  is the arbitrary integration constant given by:

$$A_{17} = a_f \exp \left[ \frac{3e \left( \frac{32\beta^2 \left( A_{16} - \frac{t_f V_0}{3M_4^2} \right)^2}{\frac{2}{3} \frac{V_0}{M_4^2} \beta} \right) (t_f V_0 - 3A_{16}M_4^2)}{16 \frac{V_0}{M_4} \sqrt{\frac{\beta^2 (-3A_{16}M_4^2 + t_f V_0)^2}{\frac{2}{3} \frac{V_0}{M_4^2} \beta M_4^4}}} \right]. \quad (4.157)$$

Here,  $a_f$  is the value of the scale factor at turnaround  $t = t_f$ .

## B. Contraction

As has already been mentioned that while performing the analysis for expansion, the conclusions for contraction phase is independent of any potential, hence rest of the analysis remains same as mentioned earlier.

## C. Expression for work done

The expression for work done in this case is same as we get for the case of natural potential with the expressions for constants now given by the parameters of this supergravity motivated model. Hence we see that in this case also, applying certain approximations and physical limits, we can get an analytical expression for work done which is non zero, thus leading to the phenomenon of cosmological hysteresis in the present context.

## 4.7 Graphical Analysis

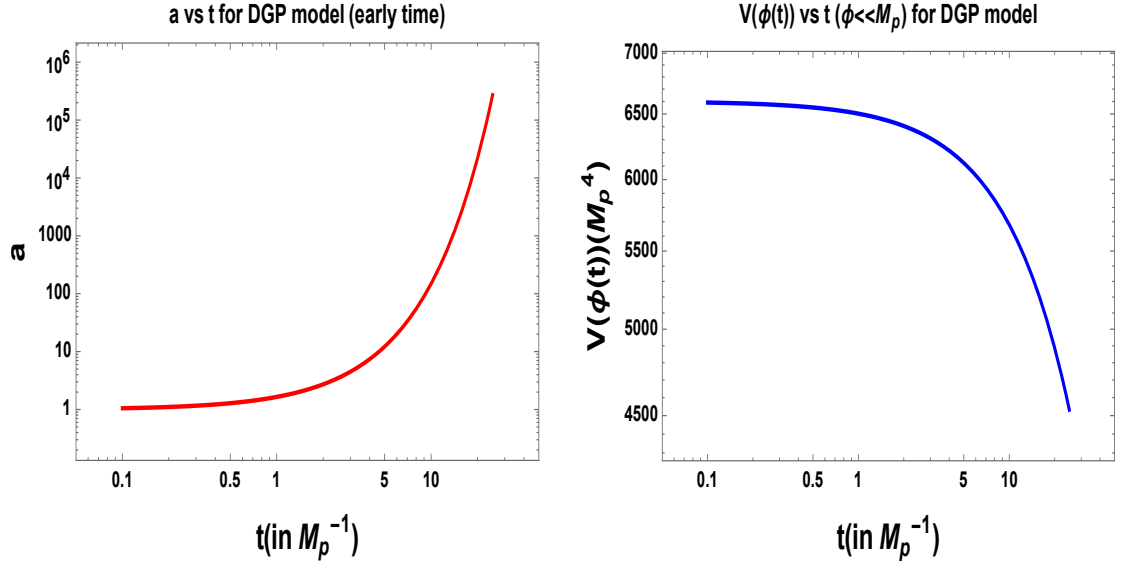
### 4.7.1 Case I: Hilltop potential

#### Graphical Analysis:

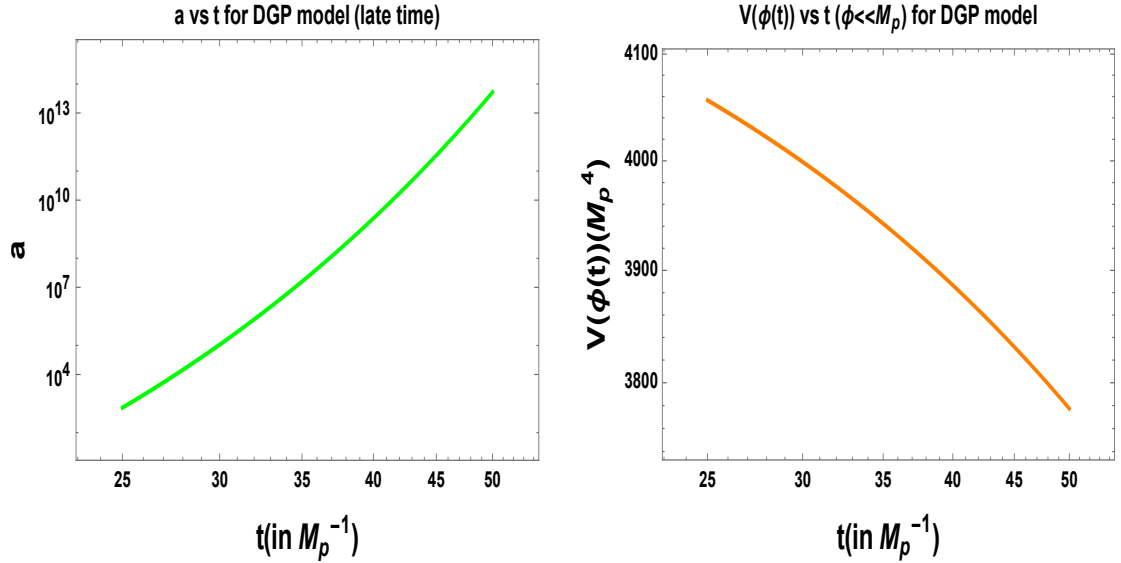
All the graphs in this section and in the following sections have been plotted in units of  $M_p = 1$ ,  $H_0 = 1$ ,  $c = 1$ , where  $M_p$  is the Planck mass,  $H_0$  is the present value of the Hubble parameter and  $c$  is the speed of light. Throughout the analysis  $r_c$  will be expressed in units of  $H_0^{-1}$ , hence only its magnitude will be written explicitly

In Fig. 4 we have shown the evolution of the scale factor and the potential for early and late time expansion phase. From the above plots, we can draw the following conclusions:

- Fig. 4(a), shows the plot of the scale factor in the small field limit for hilltop potential given by Eqn. (4.75) with the parameter values  $V_0 = 10^{-8}M_p^4$ ,  $p = 2$ ,  $\beta = 0.001$ ,  $\lambda_i = 10^{-8}$ ,  $t_i = 0.1$ ,  $a_i = 1$ ,  $r_c = 1$ .
- Higher values of the integration constants only results in an increase in the amplitude of the scale factor, not affecting the nature of the graph.
- From Eqn. (4.75), we can conclude that solution will only be possible for  $\beta \geq 0$ . Changing the value of  $\beta$  mildly modifies the amplitude of expansion,



(a) An illustration of the behavior of the scale factor with time during the early expansion phase for  $\phi \ll M_p$  with  $V_0 = 10^{-8} M_p^4$ ,  $p = 2$ ,  $\beta = 0.001$ ,  $\lambda_i = 10^{-8}$ ,  $t_i = 0.1$ ,  $r_c = 1$ . (b) An illustration of the behavior of the potential with time during early expansion phase for  $\phi \ll M_p$  with  $V_0 = 4.1 \times 10^{-3} M_p^4$ ,  $\beta = 0.72$ ,  $p = 2$ ,  $\lambda_i = 6.6$ ,  $t_i = 95 M_{pl}^{-1}$ ,  $a_i = 1$ ,  $r_c = 1$ .



(c) An illustration of the behavior of the scale factor with time during late time expansion phase for  $\phi \ll M_p$  with  $V_0 = 10^{-8} M_p^4$ ,  $p = 3$ ,  $\beta = 0.001$ ,  $A_1 = 10^{-8} M_p$ ,  $A'_1 = 10^{-8}$ ,  $r_c = 1.0$ . (d) An illustration of the behavior of the potential with time during late time expansion phase for  $\phi \ll M_p$  with  $V_0 = 3.7 \times 10^{-3} M_p^4$ ,  $p = 3$ ,  $\beta = 0.14$ ,  $A_1 = 20.8 M_p$ ,  $r_c = 1.0$ .

**Figure 4.** Graphical representation of the evolution of the scale factor and the potential during the expansion phase for DGP model.

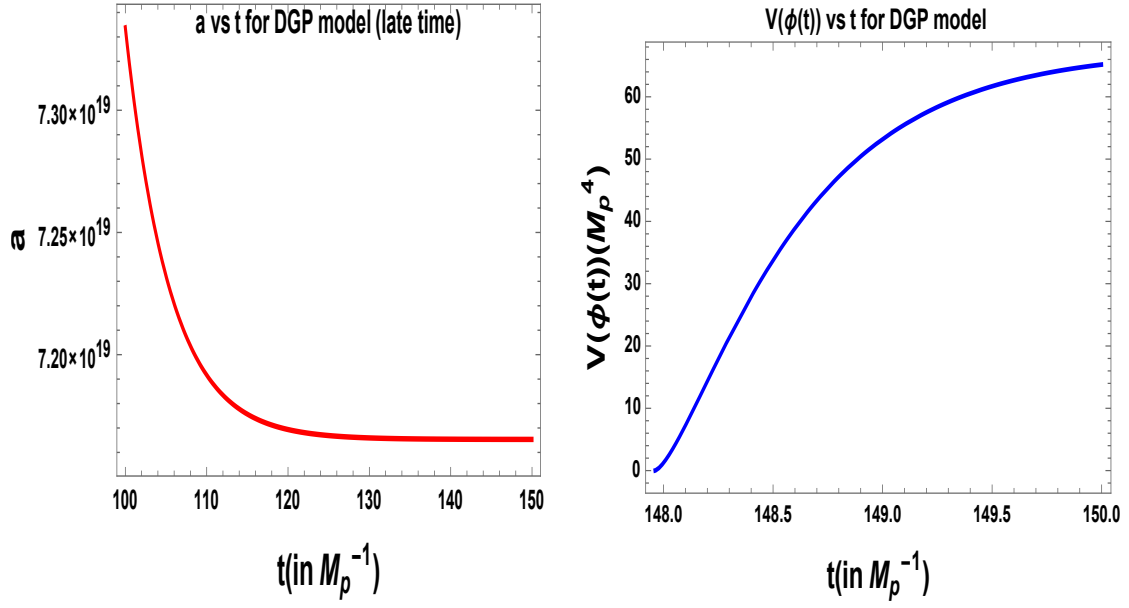
but the nature of the graph remains same. The plot is almost independent of any variation in  $p$ . Larger values of  $r_c$  increases the amplitude of the graph.



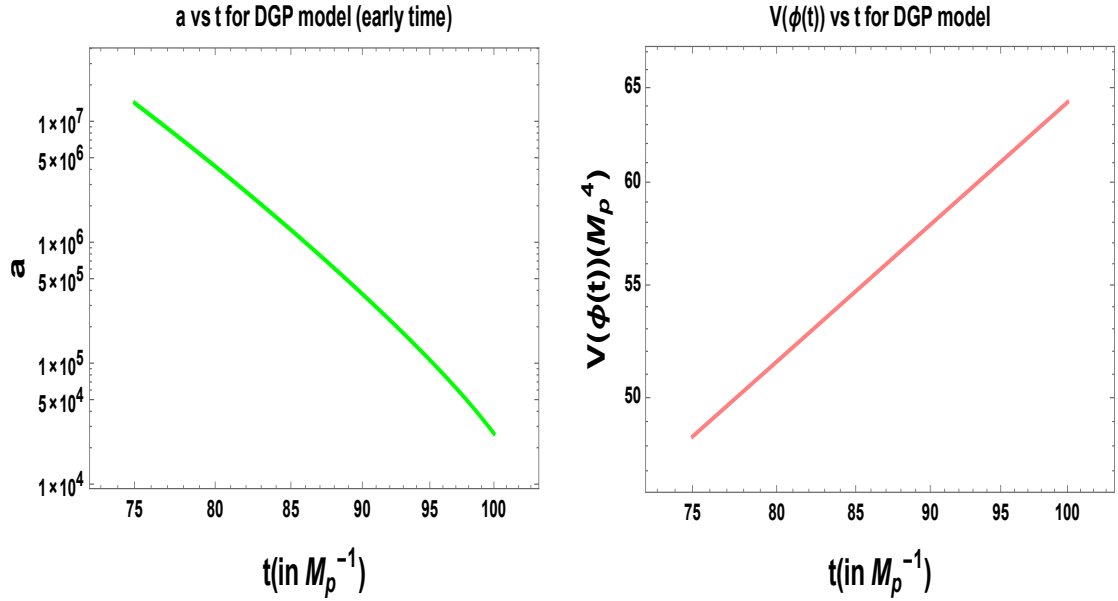
- Fig. 4(b) shows the plot of the behavior of the potential with time for small field hilltop potential. This graph has been obtained with the help of Eqn. (4.74) with parameter values  $V_0 = 4.1 \times 10^{-3} M_p^4$ ,  $\beta = 0.72$ ,  $p = 2$ ,  $\lambda_i = 6.6$ ,  $t_i = 95 M_p^{-1}$ ,  $r_c = 1$ . The evolution of the potential is not much affected by the value of  $p$ . Large values of  $r_c$  increases the height of the potential and makes the potential fall less steeply.
- Fig. 4(c) shows the plot of the scale factor in the late time expansion phase for hilltop potential given by Eqn. (4.87). This plot has been obtained for  $V_0 = 10^{-8} M_p^4$ ,  $p = 3$ ,  $\beta = 0.001$ ,  $A_1 = 10^{-8} M_p$ ,  $A'_1 = 10^{-8}$ ,  $r_c = 1.0$ . Detail graphical analysis have shown that the expansion of the universe is almost independent of the values that  $\beta$ ,  $p$ ,  $A_1$  takes i.e in this case both negative and positive values of  $\beta$  can give rise to an expanding universe. We do not get the required expansion for a value of  $r_c < 0.04$ .
- Fig. 4(d) shows the evolution of the potential in the late time expansion phase for hilltop potential. Fig. 4(d) has been obtained by with the help of Eqn. (4.85 with the parameter values  $V_0 = 3.7 \times 10^{-3} M_p^4$ ,  $p = 3$ ,  $\beta = 0.14$ ,  $A_1 = 20.8 M_p$ ,  $r_c = 1.0$ . Detail graphical analysis show that the larger the value of  $\beta$ , smaller is the the range of  $r_c$  for which we get potential giving rise to expansion. The graph is almost independent of the values that  $p$ ,  $A_1$  takes.
- If we compare Fig. 4(b) and 4(d), we find that the potential falls more steeply during the late time than in early time. This is expected because the potential is near its end of expansion phase, hence kinetic term starts dominating resulting in steeper fall of the potential.

In Fig. 5 we have shown the evolution of the scale factor and the potential for early and late time contraction phase. From the above plots, we can draw the following conclusions:

- Fig. 24(a), shows the plot of the scale factor during late time contraction phase for hilltop potential given by Eq. (4.100) with the parameter values  $A_4 = 100 M_p^{-1}$ ,  $r_c = 6$ .
- The nature of the graph (i.e the decrease in amplitude of the scale factor with time, which is expected for contraction phase) remains almost unchanged if we change the parameter values. Larger values of  $r$  decreases the amplitude of expansion (but the change is very small), but smaller values make the potential fall more steeply.
- As we can see from Fig. 24(a), the change in amplitude of the scale factor is very small. This change becomes negligibly small for very small values of  $A_4$ , and very large values of  $A_4$  are also not allowed.



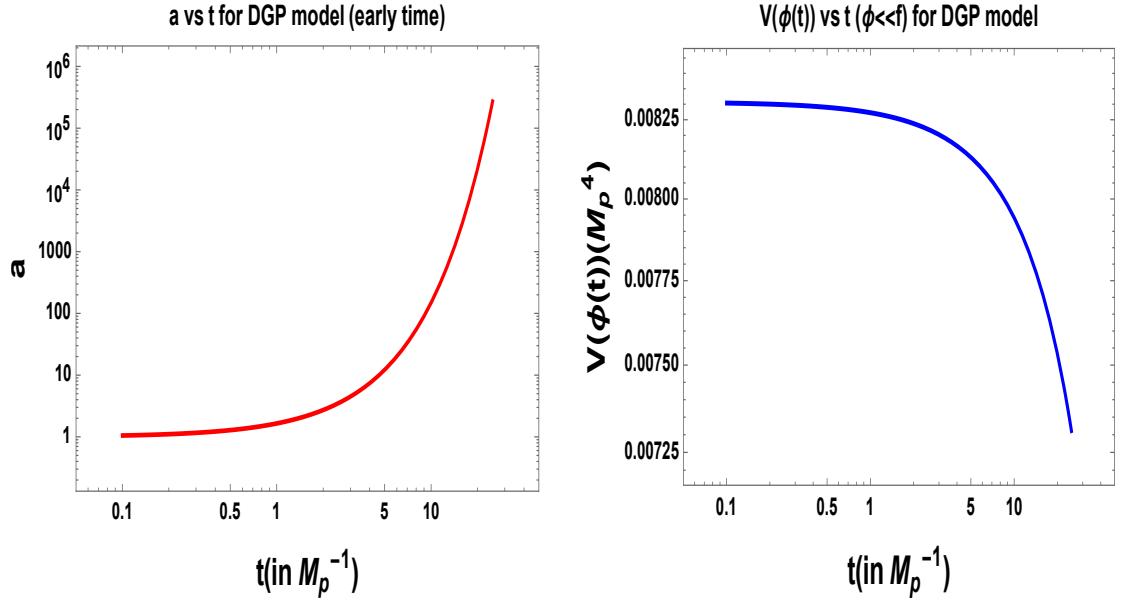
(a) An illustration of the behavior of the scale factor with time during the late contraction phase with  $A_4 = 100M_p^{-1}$ ,  $r_c = 6$ . (b) An illustration of the behavior of the potential during late contraction phase with  $V_0 = 6.1 \times 10^{-3} M_p^4$ ,  $A_3 = 152M_p^{-1}$ ,  $A_4 = 730M_p$ ,  $\beta = 0.52$ ,  $r_c = 1.62$ ,  $p = 1$ .



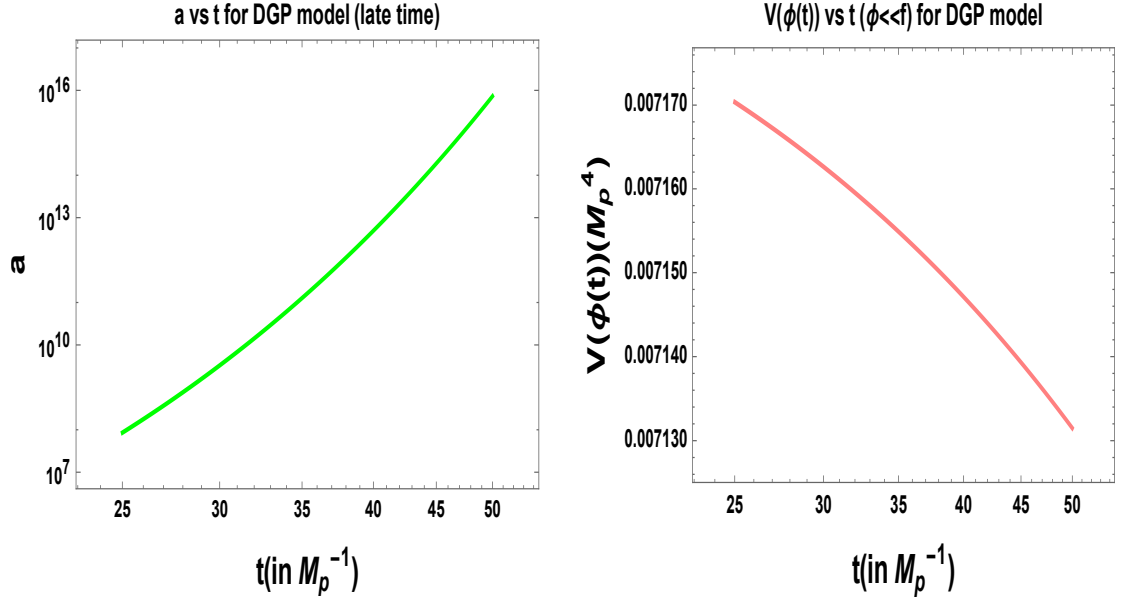
(c) An illustration of the behavior of the scale factor with time during early time contraction phase with  $A_2 = 100M_p^{-1}$ ,  $A'_2 = 1$ ,  $|r_c| = 2.0$ . (d) An illustration of the behavior of the potential during early time contraction phase with  $V_0 = 10^{-2} M_p^4$ ,  $p = 1$ ,  $\beta = 0.392$ ,  $A'_2 = 63M_p^{-1}$ ,  $|r_c| = 1.4$ .

**Figure 5.** Graphical representation of the evolution of the scale factor and the potential during the expansion phase for DGP model.

- Fig. 24(b) shows the plot of the behavior of the potential with time for late time contraction of hilltop potential. This graph has been obtained with the help of Eq. (4.97) with parameter values  $V_0 = 6.1 \times 10^{-3} M_p^4$ ,  $A_3 = 152 M_p^{-1}$ ,  $A_4 = 730 M_p$ ,  $\beta = 0.52$ ,  $r_c = 1.62$ ,  $p = 1$ .
- The potential in this case rises with time, which is expected since we are in the contraction phase and kinetic energy is dominating initially. Detail graphical analysis show that for very small value of  $r_c$ , the correct nature of the potential is obtained only if we take smaller values of the other parameters. Larger values of the parameters make the potential rise more steeply and attained the nearly flat region faster.
- Fig. 5(c) shows the plot of the scale factor in the early time contraction phase for hilltop potential given by Eq. (4.94). This plot has been obtained for  $A_2 = 100 M_p^{-1}$ ,  $A_2'' = 1$ ,  $|r_c| = 2.0$ . Detail graphical analysis have shown that as we decrease the value of  $|r_c|$ , the fall of the scale factor becomes more linear. Larger values of  $|r_c|$  increases the amplitude of the scale factor but makes contraction possible only for smaller values of  $A_2$ .
- Fig. 5(d) shows the evolution of the potential in the early time contraction phase for hilltop potential. Fig. 5(d) has been obtained by with the help of Eq. (4.92) with the parameter values  $V_0 = 10^{-2} M_p^4$ ,  $p = 1$ ,  $\beta = 0.392$ ,  $A_2' = 63 M_p^{-1}$ ,  $|r_c| = 1.4$ . Detail graphical analysis show that the nature of the graph do not depend on the parameter values. Larger values of the parameters only increases or decrease the height of the potential. But in order to get the correct nature of the potential which will result in contraction, we need  $\beta > 0$ .
- Though fig. 24(a) and Fig. 24(b) are for late time and Fig. 5(c) and Fig. 5(d) are for early time, in one complete cycle, the late time phase appears before the early time phase in contraction under the convention which we follow. But in this case, the time range has been chosen not according to the convention, but in order to get some suitable output due to the complicated nature of the equations.
- If we compare Fig. 24(a) and Fig. 5(c), we find that the decrease in the amplitude of the scale factor is much less during the late time contraction phase, as compared to early time phase.
- If we compare Fig. 5(d) with Fig. 4(a), we find that there is a net increase in the amplitude of the scale factor after one complete cycle.



(a) An illustration of the behavior of the scale factor with time during the early expansion phase for  $\phi \ll f$  with  $V_0 = 10^{-8}M_p^4$ ,  $r_c = 1$ ,  $A_7 = 1$ . (b) An illustration of the behavior of the potential during early expansion phase for  $\phi \ll f$  with  $V_0 = 4.7 \times 10^{-3}M_p^4$ ,  $r_c = 1.67$ ,  $A_6 = 32$ ,  $f = 6.7M_p$ .



(c) An illustration of the behavior of the scale factor with time during late time expansion phase for  $\phi \ll f$  with  $V_0 = 10^{-8}M_p^4$ ,  $r_c = 1.17$ ,  $A_9 = 1$ . (d) An illustration of the behavior of the potential during late time expansion phase for  $\phi \ll f$  with  $V_0 = 4.7 \times 10^{-3}M_p^4$ ,  $r_c = 1.67$ ,  $A_8 = 1$ ,  $f = 6.7M_p$ .

**Figure 6.** Graphical representation of the evolution of the scale factor and the potential during the expansion phase for the DGP model.

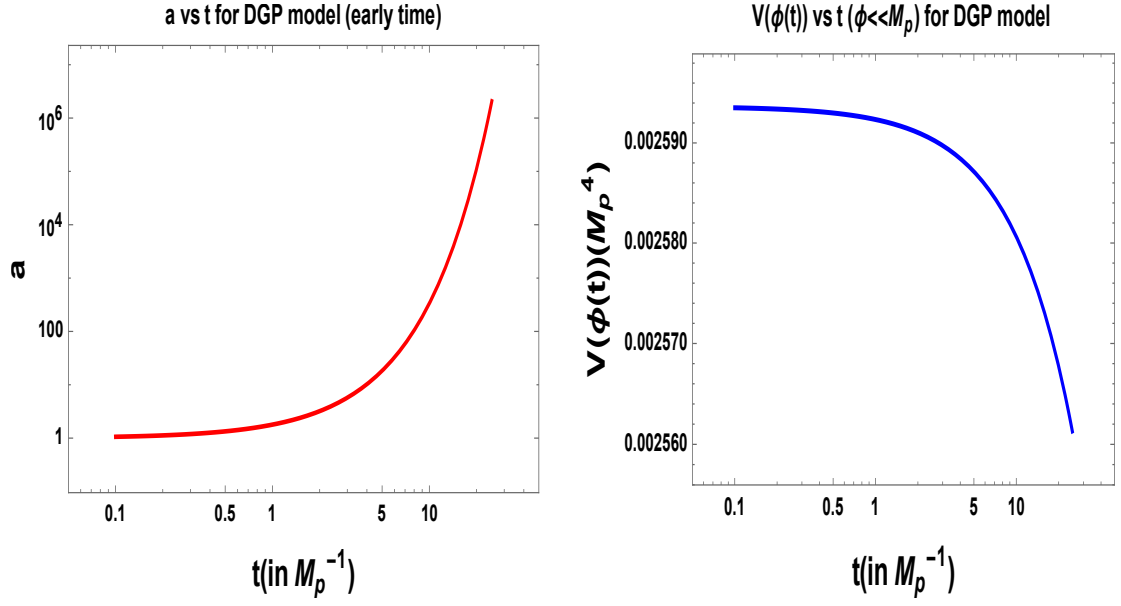
### 4.7.2 Case II: Natural potential

In Fig. 6 we have shown the evolution of the scale factor and the potential for early and late time expansion phase. From the above plots, we can draw the following conclusions:

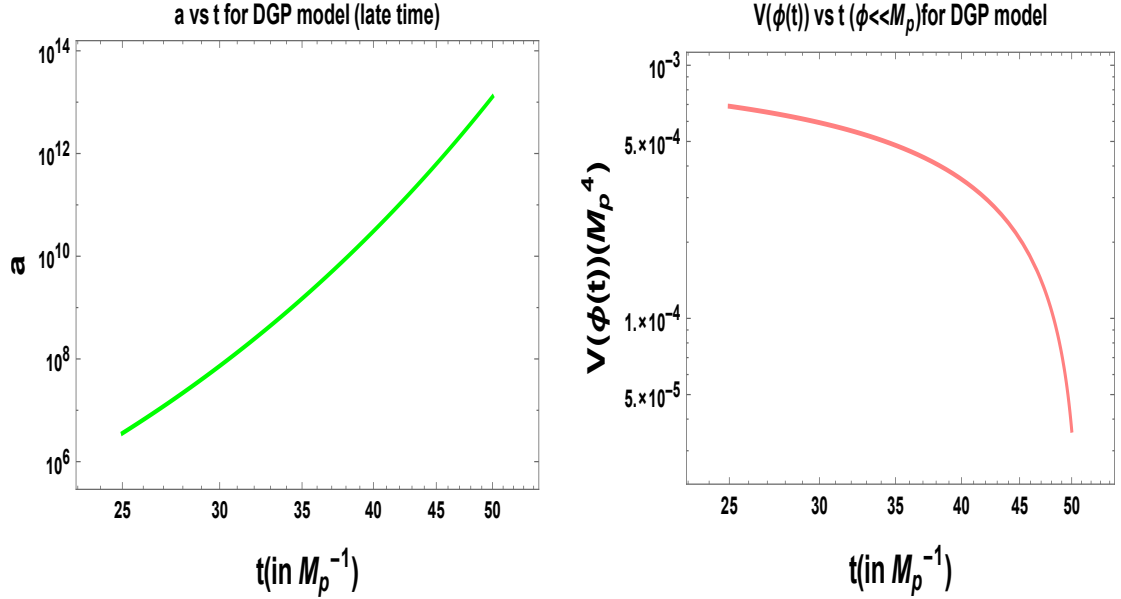
- Fig. 6(a), shows the plot of the scale factor in the small field limit for natural potential given by Eq. (4.113) with the parameter values  $V_0 = 10^{-8}M_p^4$ ,  $r_c = 1$ ,  $A_7 = 1$  during the early phase of expansion.
- Higher values of the parameters only increase the amplitude of expansion, keeping the nature of the plot unchanged.
- Fig. 6(b) shows the plot of the behavior of the potential with time for small field natural potential during the early phase of expansion. This graph has been obtained with the help of Eq. (4.111) with parameter values  $V_0 = 4.7 \times 10^{-3}M_p^4$ ,  $r_c = 1.67$ ,  $A_6 = 32$ ,  $f = 6.7M_p$ . Large values of  $r_c$  and  $f$  increases the height of the potential. Only for certain range of values of  $A_6$ , we get the required evolution of the potential (such as expansion is possible if  $A_6$  lies within (1 to 3) or (6 to 9) or (13 to 15) etc.).
- Fig. 6(c), shows the plot of the scale factor in the small field limit for natural potential given by Eq. (4.118) with the parameter values  $V_0 = 10^{-8}M_p^4$ ,  $r_c = 1.17$ ,  $A_9 = 1$  during the late phase of expansion.
- Higher values of the parameters only increase the amplitude of expansion, keeping the nature of the plot unchanged.
- Fig. 6(d) shows the plot of the behavior of the potential with time for small field natural potential. This graph has been obtained with the help of Eq. (4.116) with parameter values  $V_0 = 4.7 \times 10^{-3}M_p^4$ ,  $r_c = 1.67$ ,  $A_8 = 1$ ,  $f = 6.7M_p$ . The conclusions regarding the variation of the nature of the potential with parameters remains same as for the early time expansion.
- If we compare the amplitudes of the scale factor in Fig. 24(a) with Fig. 6(a), we find that after one cycle of expansion and contraction, we can get a net increase in amplitude of the scale factor provided the parameters are chosen properly.

### 4.7.3 Case III: Coleman-Weinberg potential

In Fig. 7 we have shown the evolution of the scale factor and the potential for early and late time small field expansion phase for supergravity potential. From the above plots, we can draw the following conclusions:



(a) An illustration of the behavior of the scale factor with time during the early expansion phase for  $\phi \ll M_p$  with  $V_0 = 10^{-8}M_p^4$ ,  $r_c = 0.86$ ,  $A_{11} = 1$ ,  $\alpha = 0.1$ . (b) An illustration of the behavior of the potential during early expansion phase for  $\phi \ll M_p$  with  $V_0 = 10^{-5}M_p^4$ ,  $r_c = 0.86$ ,  $A_{10} = 5M_p$ ,  $\alpha = 0.02$ ,  $\beta = 0.03$ .



(c) An illustration of the behavior of the scale factor with time during late time expansion phase for  $\phi \ll M_p$  with  $V_0 = 6 \times 10^{-4}M_p^4$ ,  $r_c = M_p$ ,  $A_{14} = 1.66$ ,  $A_{15} = 10^{-8}M_p$ ,  $A_{15} = 1$ ,  $\alpha = 0.145$ . (d) An illustration of the behavior of the potential during late time expansion phase for  $\phi \ll M_p$  with  $V_0 = 10^{-5}M_p^4$ ,  $r_c = 1.32$ ,  $A_{14} = 10^{-8}M_p$ ,  $\alpha = 0.032$ ,  $\beta = -1.9$ .

**Figure 7.** Graphical representation of the evolution of the scale factor and the potential during the expansion phase for the DGP model.

- Fig. 7(a), shows the plot of the scale factor in the small field limit for supergravity potential given by Eqn. (4.135) with the parameter values

$$V_0 = 10^{-8}M_p^4, r_c = 0.86, A_{11} = 1, \alpha = 0.1$$

during the early phase of expansion.

- Higher values of the parameters only increase the amplitude of expansion, keeping the nature of the plot unchanged. The variation in the nature and amplitude of the plot is almost independent of the value of  $\alpha$  parameter.
- Fig. 7(b) shows the plot of the behavior of the potential with time for small field supergravity potential during the early phase of expansion. This graph has been obtained with the help of Eqn. (4.132) with parameter values  $V_0 = 10^{-5}M_p^4$ ,  $r_c = 0.86$ ,  $A_{10} = 5M_p$ ,  $\alpha = 0.02$ ,  $\beta = 0.03$ . Large values of the parameters causes an increase in the amplitude of the expansion, keeping the nature of the plot unchanged. Largest increase in amplitude occurs for any change in value of the parameter  $\alpha$ . Detail graphical analysis have shown that we do not get the required nature of the plot for  $\beta < 0$ . Thus only positive values of  $\beta$  are allowed in this case.
- Fig. 7(c), shows the plot of the scale factor in the small field limit for supergravity potential given by Eqn. (4.149) with the parameter values  $V_0 = 6 \times 10^{-4}M_p^4$ ,  $r_c = 1.66$ ,  $A_{14} = 10^{-8}M_p$ ,  $A_{15} = 1$ ,  $\alpha = 0.145$  during the late phase of expansion.
- For  $V_0 > 6 \times 10^{-4}M_p^4$ , expansion is possible only if the values of  $\beta$ ,  $\alpha$  and  $r_c$  lie close to or lesser than unity. If we make the values of any of the parameters  $\beta, \alpha, r_c$  large, then expansion is possible only for the case when both  $A_{14}$  and  $V_0$  is  $O(10^{-4})$  or less.
- Large and positive values of  $\beta$  make the expansion more linear. Expansion is possible for  $\beta < 0$ , provided  $V_0$  takes large values and  $\alpha$  and  $A_{14}$  are smaller than unity.
- Fig. 7(d) shows the plot of the behavior of the potential with time for small field supergravity potential during late time expansion. This graph has been obtained with the help of Eqn. (4.147) with parameter values  $V_0 = 10^{-5}M_p^4$ ,  $r_c = 1.32$ ,  $A_{14} = 10^{-8}M_p$ ,  $\alpha = 0.032$ ,  $\beta = -1.9$ . Expansion is possible only if  $\beta < 2$ . Again for expansion to happen for positive value of  $\beta$ , all the other parameters must be much less than unity. Larger and positive values of  $\beta$  makes the potential fall more linearly. For expansion to occur,  $A_{14}$  must be  $\ll 1$ .

- If we compare the amplitudes of the scale factor in Fig. 24(a) with Fig. 7(a), we find that after one cycle of expansion and contraction, we can get a net increase in amplitude of the scale factor provided the parameters are chosen properly.

For large field case ( $\phi \gg M_p$ ) during expansion, the conclusions and the nature of the graphs are almost similar, hence have not been shown explicitly. Thus, a increase in the amplitude of the scale factor after one complete cycle of expansion and contraction, is possible for this case also.

## 5 Hysteresis from cosmological constant dominated Einstein gravity model

In this section we will consider three different cases by taking different functional forms of the cosmological constant like term in the effective action. One will be the case of standard model of cosmology i.e when the cosmological constant is a constant. Then we will further extend our analysis for the case when the cosmological constant is field dependent. This dependence will be included either in the form of a power series form of the scalar field or by including a dilaton field.

### Case 1: Cosmological constant of $\Lambda$ CDM model

Let us start our discussion with  $\Lambda$ CDM model, which is the standard model of Big Bang cosmology, where the Einstein's field equations are modified by the additional cosmological constant term denoted as  $\Lambda$ . The modified Friedmann equations in this model can be expressed as:

$$H^2 = \left(\frac{\dot{a}}{a}\right)^2 = \frac{\rho}{3M^2} - \frac{k}{a^2} + \frac{\Lambda}{3}, \quad (5.1)$$

$$H^2 + \dot{H} = \frac{\ddot{a}}{a} = -\frac{(\rho + 3p)}{6M^2} + \frac{\Lambda}{3}, \quad (5.2)$$

where we are denoting the Planck mass by  $M$ .

### Case 2: Scalar field dependent cosmological constant

Let us consider a situation where we make the cosmological constant term scalar field dependent i.e we replace  $\Lambda$  by  $\Lambda(\phi)$ , where

$$\Lambda(\phi) = \sum_{i=0}^4 \Lambda_i \phi^i, \quad (5.3)$$



then the representative four dimensional effective action for this case is given by:

$$\begin{aligned}
S &= \int d^4x \sqrt{-g} \left( R + \sum_{i=0}^4 \Lambda_i \phi^i + \frac{1}{2} g^{\mu\nu} \partial_\mu \phi \partial_\nu \phi - V(\phi) \right) \\
&= \underbrace{\int d^4x \sqrt{-g} (R + \Lambda_0)}_{S_{\Lambda EH}} + \underbrace{\int d^4x \sqrt{-g} \left( \sum_{i=1}^4 \Lambda_i \phi^i + \frac{1}{2} g^{\mu\nu} \partial_\mu \phi \partial_\nu \phi - V(\phi) \right)}_{S_{\Lambda\phi}}, \quad (5.4)
\end{aligned}$$

where  $\Lambda_0$  is the general cosmological constant (**denoted by  $\Lambda$  in case 1**) and  $\Lambda_1, \Lambda_2, \Lambda_3$  &  $\Lambda_4$  are the new constants.

The first action  $S_{\Lambda EH}$  is the normal action for  $\Lambda$ CDM model, hence the Friedmann equations for this part are same as Eqns. (5.1) and (5.2). The scalar field dynamics get modified due to the action  $S_{\Lambda\phi}$ . The equation of motion for the scalar field is given by:

$$\frac{\partial^\mu \delta(\sqrt{-g} \mathcal{L}_{\Lambda\phi})}{\delta \partial^\mu \phi} - \frac{\delta(\sqrt{-g} \mathcal{L}_{\Lambda\phi})}{\delta \phi} = 0 \quad (5.5)$$

where  $\mathcal{L}_{\Lambda\phi}$  is the Lagrangian density for the scalar field and for FLRW metric  $\sqrt{-g} = a^3$ . Solving the above equation we get the equation of motion for  $\phi$  as:

$$\ddot{\phi} + 3H\dot{\phi} - \sum_{i=1}^4 i\Lambda_i \phi^{i-1} + V_{,\phi} = 0 \quad (5.6)$$

where the first two terms come from the first term in Eq. (5.5) and the rest of the terms come from the last term in Eq. (5.5).

The energy momentum tensor for scalar field is given by

$$\begin{aligned}
T_{\mu\nu}^\phi &= \partial_\mu \phi \partial_\nu \phi - g_{\mu\nu} \mathcal{L}_{\Lambda\phi} \\
&= \partial_\mu \phi \partial_\nu \phi - g_{\mu\nu} \left( \frac{1}{2} \partial^\sigma \phi \partial_\sigma \phi - V(\phi) + \sum_{i=1}^4 \Lambda_i \phi^i \right)
\end{aligned} \quad (5.7)$$

For perfect fluid the expressions for the energy density  $\rho$  and pressure  $p$  can be expressed as:

$$\rho = \frac{1}{2} \dot{\phi}^2 + V(\phi) - \sum_{i=1}^4 \Lambda_i \phi^i \quad (5.8)$$

$$p = \frac{1}{2} \dot{\phi}^2 - V(\phi) + \sum_{i=1}^4 \Lambda_i \phi^i \quad (5.9)$$

Solving Eq. (5.6), Eq. (5.9) and Eq. (5.1) simultaneously, we get the solutions for the scalar field  $\phi$  and scale factor  $a$ . Thus we see that both the density, pressure as well as the equation of motion of the scalar field gets modified from the standard case,

which was expected.

### Case 3: Cosmological constant along with a dilaton field

In this case we add a dilaton field along with the general cosmological constant i.e we replace  $\Lambda$  by  $\Lambda(\phi)$ , where

$$\Lambda(\phi) = \Lambda_0 + \Lambda e^{\phi/M_p}, \quad (5.10)$$

Then the representative action for this case is then given by:

$$\begin{aligned} S &= \int d^4x \sqrt{-g} \left( R + \Lambda_0 + \Lambda e^{\phi/M_p} + \frac{1}{2} g^{\mu\nu} \partial_\mu \phi \partial_\nu \phi - V(\phi) \right) \\ &= \underbrace{\int d^4x \sqrt{-g} (R + \Lambda_0)}_{S_{\Lambda EH}} + \underbrace{\int d^4x \sqrt{-g} \left( \Lambda e^{\phi/M_p} + \frac{1}{2} g^{\mu\nu} \partial_\mu \phi \partial_\nu \phi - V(\phi) \right)}_{S_{\Lambda \phi}}, \end{aligned} \quad (5.11)$$

where  $\Lambda_0$  is the general cosmological constant and  $\Lambda$  is another constant.

Repeating the analysis as we did for the previous case 2, we get the following equation of motion for the scalar field  $\phi$  as:

$$\ddot{\phi} + 3H\dot{\phi} - \frac{\Lambda}{M_p} e^{\phi/M_p} + V_{,\phi} = 0 \quad (5.12)$$

Similarly the expressions for density and pressure for a perfect fluid in this case can be expressed as:

$$\rho = \frac{1}{2} \dot{\phi}^2 + V(\phi) - \Lambda e^{\phi/M_p} \quad (5.13)$$

$$p = \frac{1}{2} \dot{\phi}^2 - V(\phi) + \Lambda e^{\phi/M_p} \quad (5.14)$$

Solving Eq. (5.12), Eq. (5.14) and Eq. (5.1) simultaneously, we get the solutions for the scalar field  $\phi$  and scale factor  $a$ .

## 5.1 Condition for bounce

### For case 1, 2, 3

In the analysis mentioned below, we have first shown the results for open and closed universe only. The analysis for flat universe has been shown separately.

Let us start the discussion for the case 1 where at bounce, setting the Hubble parameter  $H = 0$  in Eq. (5.1) we get:

$$\rho_b = 3M^2 \left( \frac{k}{a_b^2} - \frac{\Lambda}{3} \right) \quad (5.15)$$

where  $\rho_b$  and  $a_b$  are the representative density and scale factor at bounce.

The mass content at bounce (neglecting the overall constant factor) is given by:

$$M_b = \rho_b a_b^3 = 3M^2 \left( k a_b - \frac{\Lambda a_b^3}{3} \right). \quad (5.16)$$

Therefore the infinitesimal change in the mass content can be expressed as:

$$\delta M = 3M^2 (k - \Lambda a_b^2) \delta a_b. \quad (5.17)$$

Now using energy conservation one can write:

$$\delta M + \delta W = 0, \quad (5.18)$$

where  $\delta W$  is the work done during each expansion-contraction cycle.

Further setting

$$\delta M = -\delta W = - \oint p dV, \quad (5.19)$$

we get the expression for change in amplitude of the scale factor at each successive cycle in terms of the work done as:

$$\delta a_{min} = - \frac{1}{3M^2 (k - \Lambda a_{min}^2)} \oint p dV \quad (5.20)$$

Thus we clearly observe that just like for DGP model as discussed in the earlier section, here also the increase in amplitude of the scale factor depends on the parameter of the model i.e the variants of cosmological constant as mentioned in case 1, case 2 and case 3.

$$\delta a_{min} = \begin{cases} - \frac{1}{3M^2 (1 - \Lambda a_{min}^2)} \oint p dV & \text{for } k = +1 \\ \frac{1}{3M^2 (1 + \Lambda a_{min}^2)} \oint p dV & \text{for } k = -1. \end{cases} \quad (5.21)$$

Let us now briefly mention the characteristic feature of the results for cosmological bounce for the previously mentioned variants of cosmological constant model in the following:

1. For a closed universe, with  $k = +1$ :

- The hysteresis loop integral

$$\oint p dV < 0 \quad (5.22)$$

or equivalently

$$p_{exp} < p_{cont} \quad (5.23)$$

if  $(1 - \Lambda a_{min}^2) > 0$  or  $\Lambda a_{min}^2 < 1$  and  $\delta a_{min} > 0$ ,

- The hysteresis loop integral

$$\oint pdV > 0 \quad (5.24)$$

or equivalently

$$p_{exp} > p_{cont} \quad (5.25)$$

if  $(1 - \Lambda a_{min}^2) < 0$  or  $\Lambda a_{min}^2 > 1$  and  $\delta a_{min} > 0$ .

2. On the other hand, for the open universe, with  $k = -1$ :

- The hysteresis loop integral

$$\oint pdV < 0 \quad (5.26)$$

or equivalently

$$p_{exp} < p_{cont} \quad (5.27)$$

if  $(1 + \Lambda a_{min}^2) < 0$  or  $\Lambda a_{min}^2 < -1$  and  $\delta a_{min} > 0$ ,

- The hysteresis loop integral

$$\oint pdV > 0 \quad (5.28)$$

or equivalently

$$p_{exp} > p_{cont} \quad (5.29)$$

if  $(1 + \Lambda a_{min}^2) > 0$  or  $\Lambda a_{min}^2 > -1$  and  $\delta a_{min} > 0$ .

For the other two cases i.e case 2 and case 3, since the Friedmann equations remain the same, the condition for bounce in both the cases will be given by Eq. (5.20). Hence the above analysis holds true for case 2 and case 3 also.

## 5.2 Condition for acceleration

### For case 1

From Eq. (5.2), at bounce the condition for acceleration is given by

$$\rho_b + 3p_b < 2\Lambda M^2 \quad (5.30)$$

Substituting the expression for  $\rho_b$  for different values of  $k$  we get the conditions for acceleration at bounce as:

$$p_b = \begin{cases} \Lambda M^2 - \frac{M^2}{a_b^2} \text{ for } k = +1 \\ \Lambda M^2 + \frac{M^2}{a_b^2} \text{ for } k = -1. \end{cases} \quad (5.31)$$

Thus we see that the condition for acceleration at bounce now depends not only on the scale factor but also on the cosmological constant.

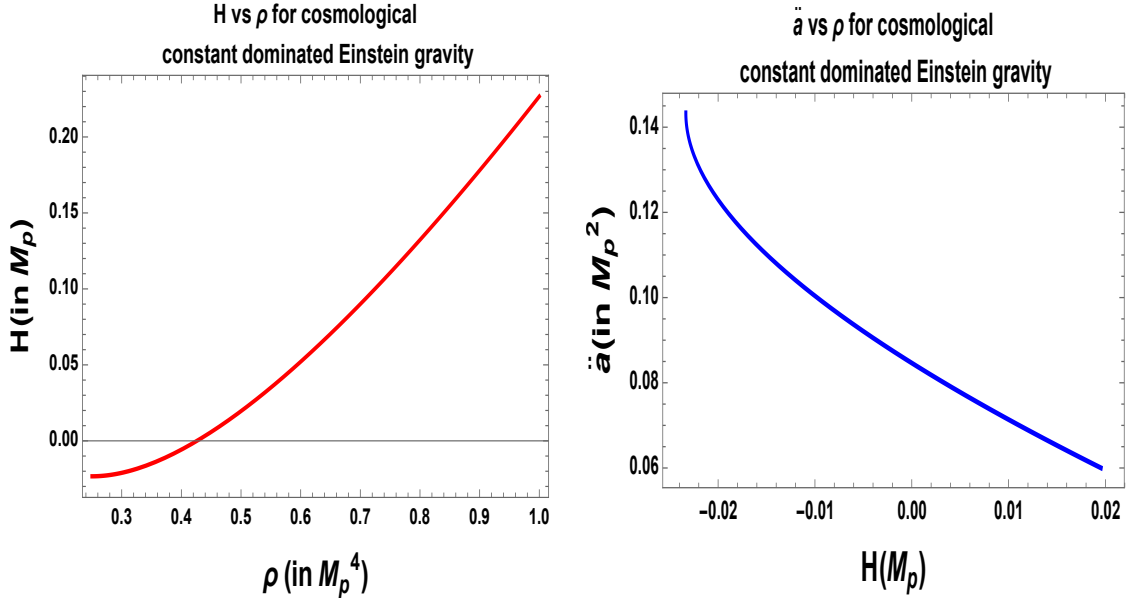
Substituting the expressions of  $\rho$  and  $p$  from Eqns. (2.5) into Eq. (5.30), we get the condition for acceleration in terms of the scalar field as

$$\dot{\phi}^2 < V(\phi) + \Lambda M^2 \quad (5.32)$$

Thus we see that even if the contribution from the potential is lesser than the standard canonical kinetic term i.e. even if  $\dot{\phi}^2 > V(\phi)$ , the above condition will still be satisfied if  $\dot{\phi}^2$  is lesser than the sum of  $V(\phi) + \Lambda M^2$ . Thus we can use potentials of smaller values than standard case and yet produce bounce. Thus the presence of cosmological constant modifies the effective potential present at bounce.

In Figs. 8(a) and 8(b), we have shown the phenomena of bounce and acceleration in this cosmological constant dominated model. We can draw the following conclusions from the above figures:

- In Fig. 8(a), we have plotted the r.h.s of Eqn. (5.1) using the relation  $\rho = a^{-3(1+w)}$ . The graph has been plotted only for the case when  $k = 1$ . This is because, Eq. (5.15) shows that density becomes negative for the cases when  $k = 0, -1$ , which is unphysical.
- We have used  $w = 1/3$ , since we require a soft equation of state for causing the acceleration and expansion. The case  $w = 0$  made  $H$  only approximately zero.
- From Fig. 8(a), using the value of  $\Lambda$  from Planck 2015 data [75], we get the bounce at  $\rho = \rho_b = 0.43M_{pl}^4$ . This value increases if we take higher values of  $\Lambda$ .
- Fig. 8(b) shows the necessary condition of acceleration ( $\ddot{a} > 0$ ) at the time of bounce. Here we have plotted the r.h.s of Eqns. (5.1) and (5.2). This plot has also been obtained for the same parameter values as the earlier graph.
- Thus Fig. 8 shows graphically that the phenomenon of bounce is possible for a closed universe dominated by cosmological constant like term and having  $w = 1/3$ .



(a) An illustration of the bouncing condition for a universe with an equation of state  $w=1/3$  and  $k=1$ . (b) An illustration of the acceleration condition at the time of bounce for a universe with an equation of state  $w=1/3$ ,  $k=1$ .

**Figure 8.** Graphical representation of the phenomena of bounce and acceleration for cosmological constant dominated Einstein gravity.

- Since the condition of bounce is true for all the three cases being studied in this section, we can say that bouncing universe is possible for all the three cases.

### For case 2

Condition for acceleration in terms of the pressure and density is again given by Eq. (5.30). Then substituting the expressions for  $\rho$  and  $p$  from Eq. (5.9), we get the condition for acceleration in terms of the scalar field as:

$$\dot{\phi}^2 < 2\Lambda_0 M^2 + V(\phi) - \sum_{i=1}^4 \Lambda_i \phi^i \quad (5.33)$$

Thus depending on the signs of constants  $(\Lambda_1, \Lambda_2, \Lambda_3, \Lambda_4)$ , we observe that less or more contribution from the potential than the canonical kinetic term as appearing in the standard case may be required. To realize the essence of this statement let us consider an example, in which all the new constants are positive or the resultant sign of the summation is positive, then this decreases the right hand side from standard case given by Eq. (5.32) and this condition for acceleration can be achieved only if the contribution from the potential is more than compared to the standard case. Again if all the constants are negative or the resultant sign of the summation terms is negative, then we need lesser contribution from the potential than the standard case

to attain the condition of acceleration. Thus we see that apart from the general cosmological constant term, the presence of different powers of scalar fields along with different constants increases or decreases the effective potential at the time of bounce.

### **For case 3**

Condition for acceleration in terms of the pressure and density is again given by Eq. (5.30). Then substituting the expressions for  $\rho$  and  $p$  from Eqns. (5.14), we get the condition for acceleration in terms of the scalar field as:

$$\dot{\phi}^2 < 2\Lambda_0 M^2 + V(\phi) - \Lambda e^{\phi/M_p} \quad (5.34)$$

Thus if  $\Lambda$  is positive, then this decreases the right hand side from standard case and this condition for acceleration can be achieved only if more potential than the standard case is present. Again if  $\Lambda$  is negative, even potential lesser than the standard case can satisfy the condition of acceleration.

Therefore from the above analysis we can conclude that, whether the standard potential will be able to cause acceleration at bounce now depends on the extra terms present in the action.

## **5.3 Condition for turnaround**

### **For case 1, 2 ,3**

The condition for turnaround is exactly same as the condition for bounce appearing in case 1 i.e. one can write:

$$\delta a_{max} = -\frac{1}{3M^2(k - \Lambda a_{max}^2)} \oint p dV \quad (5.35)$$

Rest all the conclusions remain same as what we had got for the bounce case. It is important to mention here that the conclusions for case 2 and case 3 also remains the same as appearing in the case 1.

## **5.4 Condition for deceleration**

### **For case 1**

From Eq. (5.2), at turnaround the condition for deceleration is given by

$$\rho_t + 3p_t > 2\Lambda M^2 \quad (5.36)$$

i.e turnaround can be obtained without violating the strong energy condition.

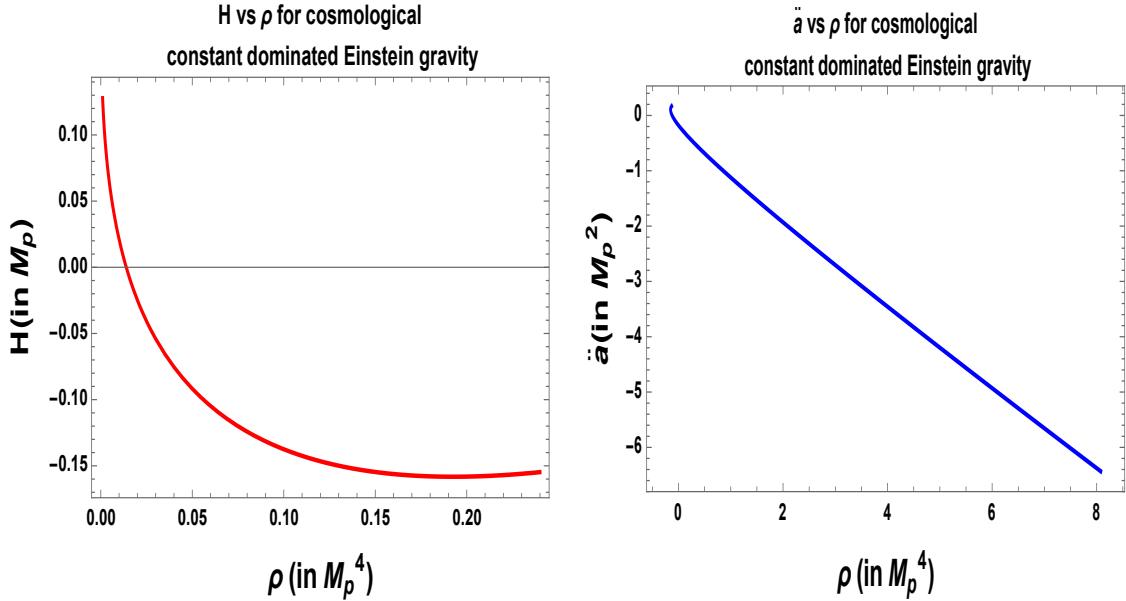
In place of Eq. (5.31), we get the conditions for deceleration at turnaround as:

$$p_t > \begin{cases} \Lambda M^2 - \frac{M^2}{a_t^2} \text{ for } k = +1 \\ \Lambda M^2 + \frac{M^2}{a_t^2} \text{ for } k = -1. \end{cases} \quad (5.37)$$

Substituting the expressions of  $\rho$  and  $p$  from Eqns. (2.5) into Eq. (5.36), we get the condition for expansion in terms of the scalar field as

$$\dot{\phi}^2 > V(\phi) + \Lambda M^2 \quad (5.38)$$

Thus we see that a potential lesser than the standard case is required to satisfy this condition because even if the condition  $\phi > V(\phi)$  is satisfied, we will get acceleration only if  $\phi > V(\phi) + \Lambda M^2$ . Thus, now the cosmological constant increases the effective potential relative to the standard case.



(a) An illustration of the turnaround condition (b) An illustration of the deceleration condition for a universe with an equation of state  $w=1$  and at turnaround for a universe with an equation of state  $w=1, k=1$ .

**Figure 9.** Graphical representation of the phenomena of turnaround and deceleration for cosmological constant dominated Einstein gravity.

In Figs. 9(a) and 9(b), we have shown the phenomena of turnaround and deceleration in this cosmological constant dominated model. We can draw the following conclusions from the above figures:



- In Fig. 9(a), we have once again plotted the r.h.s of Eq. (5.1) using the relation  $\rho = a^{-3(1+w)}$  for a closed universe. But for this case we have used  $w = 1$ , since we require a stiff equation of state for causing contraction and deceleration.
- In Fig. 9(a),  $H$  going to negative values may be interpreted as the universe changing its direction of motion at turnaround. As had been discussed in [10], the condition of bounce/turnaround can be imposed by either the condition of making the scale factor changing sign with other quantities remaining same, or,  $\dot{a}$  going to negative values with other quantities remaining same.
- From Fig. 9(a), using the value of  $\Lambda$  from Planck 2015 data [75], we get the turnaround at  $\rho = \rho_t = 0.014M_{pl}^4$ . This value increases if we take higher values of  $\Lambda$ .
- Fig. 8(b) shows the necessary condition of acceleration ( $\ddot{a} < 0$ ) at the time of turnaround. Here we have plotted the r.h.s of Eqns. (5.1) and (5.2). This plot has also been obtained for the same parameter values as the earlier graph.
- Thus Fig. 10 shows graphically that the phenomenon of turnaround is possible for a closed universe dominated by cosmological constant like term and having  $w = 1$ .
- Since the condition of turnaround is true for all the three cases being studied in this section, we can say that bouncing universe is possible for all the three cases.

### **For case 2**

Condition for deceleration in terms of the pressure and density is given by Eq. (5.36) with  $\Lambda$  replaced by  $\Lambda_0$  in this specific case. Then substituting the expressions for density  $\rho$  and pressure  $p$  from Eq. (5.9), we get the following condition for deceleration in terms of the scalar field as:

$$\dot{\phi}^2 > 2\Lambda_0 M^2 + V(\phi) - \sum_{i=1}^4 \Lambda_i \phi^i \quad (5.39)$$

Thus depending on the signs of constants ( $\Lambda_1, \Lambda_2, \Lambda_3, \Lambda_4$ ), we see that less or more contribution from the potential than the standard case may be required. To justify the validity of this statement let us consider an example, where all the new constants are independently positive or the cumulative effect appearing through their summation is positive, then this decreases the right hand side of Eq. (5.39) from standard case and the condition for deceleration can be achieved even if more contribution from the potential plays crucial role compared to the standard case. On the other

hand, if all the constants are independently negative or the cumulative effect appearing through their summation is negative, deceleration can be achieved even if the contribution from the potential is lesser than the standard case.

### **For case 3**

Condition for deceleration in terms of the pressure and density is again given by Eq. (5.36) with  $\Lambda$  replaced by  $\Lambda_0$ . Then substituting the expressions for density  $\rho$  and pressure  $p$  from Eq. (5.14), we get the condition for deceleration in terms of the scalar field as:

$$\dot{\phi}^2 > 2\Lambda_0 M^2 + V(\phi) - \Lambda e^{\phi/M_p} \quad (5.40)$$

Thus if the signature of  $\Lambda$  is positive, then this decreases the right hand side from the standard case and this condition for acceleration can be achieved even if more contribution from the potential compared to the standard case is present. On the other hand, if  $\Lambda$  is negative, we need lesser potential than the standard case to attain the condition of deceleration.

### **For $k = 0$ case**

The results below have been shown only for case 1. But they perfectly hold good for case 2 and case 3 also. In the present context the Friedmann equations for this case are given by:

$$H^2 = \left(\frac{\dot{a}}{a}\right)^2 = \frac{\rho}{3M^2} + \frac{\Lambda}{3}, \quad (5.41)$$

$$\dot{H} + H^2 = \frac{\ddot{a}}{a} = -\frac{(\rho + 3p)}{6M^2} + \frac{\Lambda}{3}. \quad (5.42)$$

From Eq. (5.42), we can infer that the same Friedmann equation cannot give rise to both bounce and turnaround condition for  $k = 0$  case. This is because  $\Lambda$  is constant in the present setup, hence it is not possible for it to be equal to both the high density at the time of bounce and low density at the time of turnaround.

For causing bounce/turnaround the following condition holds good:

$$\rho_{b/t} = -\Lambda M^2 \quad (5.43)$$

Therefore in place of Eq. (5.20), in the present context we get:

$$\delta(a_{min/max})^3 = \frac{1}{\Lambda M^2} \oint p dV \quad (5.44)$$

Thus, the amplitude of the scale factor increases:

- if  $\oint p dV > 0$  for  $\Lambda > 0$ .

- if  $\oint pdV < 0$  for  $\Lambda < 0$ .

Similarly the condition for acceleration/deceleration for  $k = 0$  case can be written as:

$$p_b < \Lambda M^2 \text{ (for acceleration at bounce)} \quad (5.45)$$

$$p_b > \Lambda M^2 \text{ (for deceleration at turnaround)} \quad (5.46)$$

Thus we observe that the pressure at bounce/turnaround required to cause acceleration/deceleration becomes independent of the scale factor at the time of bounce/turnaround. Also the results shows that it depends only on the cosmological constant.

## 5.5 Evaluation of work done in one cycle

### For case 1

Following the same procedure as we have done for DGP model, here also the general expression for the hysteresis loop is given by Eq. (4.52). In order to express the loop in terms of the scale factor only, using Eq. (5.1) and Eq. (5.2), we get:

$$\rho = \frac{\dot{\phi}^2}{2} + V(\phi) = 3M^2 \left[ \left( \frac{\dot{a}}{a} \right)^2 + \frac{k}{a^2} - \frac{\Lambda}{3} \right], \quad (5.47)$$

$$H^2 + \dot{H} = \frac{\ddot{a}}{a} = -\frac{(\rho + 3p)}{6M^2} + \frac{\Lambda}{3} \quad (5.48)$$

Further using the above equations and Eq. (2.5) for pressure  $p$  we get:

$$\frac{\dot{\phi}^2}{2} - V(\phi) = M^2 \left[ \Lambda - \frac{2\ddot{a}}{a} - \left( \frac{\dot{a}}{a} \right)^2 - \frac{k}{a^2} \right]. \quad (5.49)$$

Therefore the expression for work done is given by:

$$\oint pdV = 3M^2 \oint (\Lambda a^2 \dot{a} - 2\ddot{a}a\dot{a} - \dot{a}^3 - k\dot{a}) dt. \quad (5.50)$$

It is important to note that the total work done in one cycle now depends on the cosmological constant also.

### For case 2

For case 2 using the expression of  $p$  given by Eq. (5.9) into Eq. (4.52), we get the expression for the total work done in one expansion-contraction cycle in terms of the

$\phi$  and  $a$  as

$$\oint pdV = \int_{cont} 3 \left( \frac{1}{2} \dot{\phi}^2 - V(\phi) + \sum_{i=1}^4 \Lambda_i \phi^i \right) a^2 \dot{a} dt + \int_{exp} 3 \left( \frac{1}{2} \dot{\phi}^2 - V(\phi) + \sum_{i=1}^4 \Lambda_i \phi^i \right) a^2 \dot{a} dt \quad (5.51)$$

$$= \int_{a_{max}^{i-1}}^{a_{min}^{i-1}} 3 \left( \frac{1}{2} \dot{\phi}^2 - V(\phi) + \sum_{i=1}^4 \Lambda_i \phi^i \right) a^2 \dot{a} dt + \int_{a_{min}^i}^{a_{max}^i} 3 \left( \frac{1}{2} \dot{\phi}^2 - V(\phi) + \sum_{i=1}^4 \Lambda_i \phi^i \right) a^2 \dot{a} dt \quad (5.52)$$

Since the Friedmann equations are same as that appearing in the earlier section, the expression for the above equation in terms of the scale factor is again given by Eq. (5.50) in which  $\Lambda$  is replaced by a new constant  $\Lambda_0$ . Thus from Eq. (5.52) we find that the work done now depends on the value of all the new constants ( $\Lambda_1, \Lambda_2, \Lambda_3, \Lambda_4$ ) of the model. Thus by allowing sufficient amount of tuning in these constants we can make the signature of the representative integral positive or negative.

### **For case 3**

For case 3 using the expression for pressure  $p$  as given by Eq. (5.14), into Eq. (4.52), we get the expression for the total work done in one expansion-contraction cycle in terms of the scalar field  $\phi$  and scale factor  $a$  as:

$$\oint pdV = \int_{cont} 3 \left( \frac{1}{2} \dot{\phi}^2 - V(\phi) + \Lambda e^{\phi/M_p} \right) a^2 \dot{a} dt + \int_{exp} 3 \left( \frac{1}{2} \dot{\phi}^2 - V(\phi) + \Lambda e^{\phi/M_p} \right) a^2 \dot{a} dt \quad (5.53)$$

$$= \int_{a_{max}^{i-1}}^{a_{min}^{i-1}} 3 \left( \frac{1}{2} \dot{\phi}^2 - V(\phi) + \Lambda e^{\phi/M_p} \right) a^2 \dot{a} dt + \int_{a_{min}^i}^{a_{max}^i} 3 \left( \frac{1}{2} \dot{\phi}^2 - V(\phi) + \Lambda e^{\phi/M_p} \right) a^2 \dot{a} dt \quad (5.54)$$

In this case also, the expression for the above equation in terms of the scale factor is again given by Eq. (5.50) where  $\Lambda$  is replaced by the constant  $\Lambda_0$ . Thus adjusting

the values and signatures of the constants  $(\Lambda_0, \Lambda)$  we can change the signature of the representative integral.

## 5.6 Semi-analytical analysis for cosmological potentials

Here also we will perform the analysis for the case when  $k = 0$ . Though, the exact and complete treatment would have been for the case  $k = 1$ , simple analytical solutions were obtained only for flat universe which has been discussed below. Also, since we know that for  $k = 0$ , this model can cause either bounce or turnaround, hence to get an expression for the complete work done in one cycle, we will consider that cosmological constant is present at late times (i.e causing turnaround) whereas the early universe is governed by brane world cosmology model for which the analysis has been shown in the Appendix in the context of Randall-Sundrum single brane world (RSII). Now, if we compare Eq. (9.2) with Eq. (6.30), we see that they are both same. Hence the results for early universe which will be calculated for loop quantum model, can be used here. Below, we show the late time analysis for  $\Lambda$ CDM. In this context, we have denoted the Planck mass by  $M_p$ .

### 5.6.1 Case I: Hilltop potential

#### For Case 1:

#### A. Expansion

At late times within the window  $a' < a < a_{max}$  using Eq. (5.1) and Eq. (4.67) with the expression for density  $\rho$  now given by the hilltop potential, we get an integral equation of the following form:

$$\int d\left(\frac{\phi}{M_p}\right) \frac{\sqrt{\left[\frac{V_0\left(1+\beta\left(\frac{\phi}{M_p}\right)^p\right)}{3M_p^2} + \frac{\Lambda}{3}\right]}}{\beta p \left(\frac{\phi}{M_p}\right)^{p-1}} = -\frac{V_0}{3M_p^2} \int dt. \quad (5.55)$$

The exact solution of this integral is given in the Appendix for RSII model. To compute the left hand side of the above integral equation we again follow the same procedure as we done for DGP model i.e. we redefine the field as:

$$\frac{\phi}{M_p} = e^\lambda \quad (5.56)$$

and hence using this new definition we study two limiting cases.

#### a) $\phi/M_p \ll 1$ :

In this limit, we can expand the exponentials upto linear order and upon further simplification we get the following expression for the redefined field  $\lambda$  as:

$$\lambda = \left( -\frac{V_0}{3M_p^2}t + B_0 \right) \frac{\beta p}{\sqrt{\left( \frac{V_0}{3M_p^2}(1 + \beta) + \frac{\Lambda}{3} \right)}} \quad (5.57)$$

where  $B_0$  is the arbitrary integration constant given by:

$$B_0 = \frac{\lambda_f}{\beta p} \sqrt{\left( \frac{V_0}{3M_p^2}(1 + \beta) + \frac{\Lambda}{3} \right)} + \frac{V_0 t_f}{3M_p^2}. \quad (5.58)$$

Here  $\lambda_f$  is the value at the time of turnaround i.e at  $t = t_f$ .

The above solution has been obtained under the assumption that the quantity

$$\frac{\frac{V_0}{3M_p^2}}{\left( \frac{V_0}{3M_p^2}(1 + \beta) + \frac{\Lambda}{3} \right)} \beta p \lambda \ll 1, \quad (5.59)$$

which is possible if we choose the value of  $V_0$  and  $\Lambda$  accordingly.

Substituting this expression back into the Friedmann equation, we get the expression for the scale factor as

$$a(t) = B_1 \exp \left[ \left( \sqrt{\left( \frac{V_0}{3M_p^2}(1 + \beta) + \frac{\Lambda}{3} \right)} + \frac{\frac{V_0}{3M_p^2} \beta^2 p^2}{2 \left( \frac{V_0}{3M_p^2}(1 + \beta) + \frac{\Lambda}{3} \right)} B_0 \right) t - \frac{\left( \frac{V_0}{3M_p^2} \right)^2 \beta^2 p^2}{4 \left( \frac{V_0}{3M_p^2}(1 + \beta) + \frac{\Lambda}{3} \right)^2} t^2 \right] \quad (5.60)$$

where

$$B_1 = a_f \exp \left[ - \left( \sqrt{\left( \frac{V_0}{3M_p^2}(1 + \beta) + \frac{\Lambda}{3} \right)} + \frac{\frac{V_0}{3M_p^2} \beta^2 p^2}{2 \left( \frac{V_0}{3M_p^2}(1 + \beta) + \frac{\Lambda}{3} \right)} B_0 \right) t_f + \frac{\left( \frac{V_0}{3M_p^2} \right)^2 \beta^2 p^2}{4 \left( \frac{V_0}{3M_p^2}(1 + \beta) + \frac{\Lambda}{3} \right)^2} t_f^2 \right]. \quad (5.61)$$

Here  $a_f$  is the value of scale factor at turnaround time scale  $t = t_f$ .

**ii)  $\phi/M_p \gg 1$ :**

In this limit, the solution for the redefined field  $\lambda$  is given by:

$$\lambda = \frac{2}{p} \left[ 2 - \ln \left( \left( \frac{V_0 t}{3M_p^2} + B_2 \right) \frac{\beta^{1/2} p^2}{2 \left( \frac{V_0 t}{3M_p^2} \right)^{1/2}} \right) \right] \quad (5.62)$$

where  $B_2$  is the arbitrary integration constant given by:

$$B_2 = \frac{2 \left( \frac{V_0 t}{3M_p^2} \right)^{1/2} e^{(2-\frac{p}{2})\lambda_f}}{\beta^{1/2} p^2} - \frac{V_0 t_f}{3M_p^2}. \quad (5.63)$$

The above solution has been obtained under the assumption that the conditions:

$$\beta e^{p\lambda} \gg 1, \quad (5.64)$$

$$\frac{V_0 \beta e^{p\lambda}}{3M_p^2} \gg \frac{\Lambda}{3}, \quad (5.65)$$

are satisfied. These conditions can be satisfied since we are in the large field limit and we can choose the values of the parameters of this model  $(\beta, p, V_0)$  accordingly.

Substituting the above expression into the Friedmann equation, we get the expression for the scale factor as:

$$a(t) = B_3 \exp \left[ \left( \frac{V_0}{3M_p^2} \right)^{1/2} \beta^{1/2} e^2 \frac{\ln \left( \frac{\beta^{1/2} p^2 B_2}{2 \left( \frac{V_0}{3M_p^2} \right)^{1/2}} + \frac{\beta^{1/2} p^2 \left( \frac{V_0}{3M_p^2} \right)^{1/2} t}{2} \right)}{\left( \frac{\beta^{1/2} p^2 \left( \frac{V_0}{3M_p^2} \right)^{1/2}}{2} \right)} \right], \quad (5.66)$$

where  $B_3$  is the arbitrary integration constant given by:

$$B_3 = a_f \exp \left[ - \left( \frac{V_0}{3M_p^2} \right)^{1/2} \beta^{1/2} e^2 \frac{\ln \left( \frac{\beta^{1/2} p^2 B_2}{2 \left( \frac{V_0}{3M_p^2} \right)^{1/2}} + \frac{\beta^{1/2} p^2 \left( \frac{V_0}{3M_p^2} \right)^{1/2} t_f}{2} \right)}{\left( \frac{\beta^{1/2} p^2 \left( \frac{V_0}{3M_p^2} \right)^{1/2}}{2} \right)} \right]. \quad (5.67)$$

## B. Contraction

This phase is independent of any choice of the potential provided the condition  $\dot{\phi}^2 \gg V(\phi)$  holds good in this phase. Using Eq. (4.68) and Eq. (5.1), we get the following solutions:

$$\dot{\phi}^2 = \left[ \frac{\Lambda B_4}{3} \left( \frac{e^{\sqrt{2\Lambda}t} + 1}{e^{\sqrt{2\Lambda}t} - 1} \right)^2 - \frac{\Lambda}{3} \right], \quad (5.68)$$

where  $B_4$  is the arbitrary integration constant given by:

$$B_4 = \left( \dot{\phi}_f^2 + \frac{\Lambda}{3} \right) \frac{3}{\Lambda} \left( \frac{e^{\sqrt{2\Lambda}t_f} - 1}{e^{\sqrt{2\Lambda}t_f} + 1} \right)^2. \quad (5.69)$$

From the above expressions, we get the solution of the scale factor as:

$$a(t) = B_5 \left[ \frac{(e^{\sqrt{2\Lambda}t} - 1)^2}{e^{\sqrt{2\Lambda}t}} \right]^{\frac{1}{3M_p} \sqrt{\frac{\Lambda B_4}{2}}}, \quad (5.70)$$

where  $B_5$  is the arbitrary integration constant given by:

$$B_5 = a_f \left[ \frac{(e^{\sqrt{2\Lambda}t_f} - 1)^2}{e^{\sqrt{2\Lambda}t_f}} \right]^{-\frac{1}{3M_p} \sqrt{\frac{\Lambda B_4}{2}}}. \quad (5.71)$$

## C. Expression for work done

As will be discussed in the next section, that the expression for integral for work done in the early universe for loop quantum model contains a large no. of terms, hence will not be shown here. But the results of the integral corresponding to late universe have been discussed below.

i)  $\phi/M_p \ll 1$ :

$$\begin{aligned} \oint p dV &= b_1 (\text{erf}[-b_2 + b_3 t_{max}] - \text{erf}[-b_2 + b_3 t']) + 3M_p^2 (45 \sinh(\sqrt{\Lambda} t_{max}) \\ &\quad - 9 \sinh(2\sqrt{\Lambda} t_{max}) + \sinh(3\sqrt{\Lambda} t_{max}) - 45 \sinh(\sqrt{\Lambda} t') \\ &\quad + 9 \sinh(2\sqrt{\Lambda} t') - \sinh(3\sqrt{\Lambda} t') - 30 t_{max} + 30 t') \end{aligned} \quad (5.72)$$



ii)  $\phi/M_p \gg 1$ :

$$\begin{aligned}
\oint pdV = B_3^3 \frac{\sqrt{\frac{\pi}{2}}(-3 + \Lambda)(\text{Erfi}(\sqrt{3b_5}(b_6 + b_7t_{max})) - \text{Erfi}(\sqrt{3b_5}(b_6 + b_7t_{min})))}{2b_7} \\
+ 3M_p^2(45 \sinh(\sqrt{\Lambda}t_{max}) \\
- 9 \sinh(2\sqrt{\Lambda}t_{max}) + \sinh(3\sqrt{\Lambda}t_{max}) - 45 \sinh(\sqrt{\Lambda}t') \\
+ 9 \sinh(2\sqrt{\Lambda}t') - \sinh(3\sqrt{\Lambda}t') - 30t_{max} + 30t') \quad (5.73)
\end{aligned}$$

Here  $b_1 \dots b_7$  are constants that depend on the parameters present in the expression for the scale factor. Their explicit forms have been given in the appendix.

Including the contributions from the other integrals also we see that we get a non-zero work done for both large and small field cases for hilltop potential when we have pure cosmological constant in the background.

## For Case 2

### A. Expansion

Within the window  $a_{min} < a < a_{max}$  at late times using Eq. (5.5) and Eq. (5.9) along with energy density of scalar field,  $\rho$ , now given by the hilltop potential, we get an integral equation of the form (neglecting  $\ddot{\phi}$ ):

$$\int d\left(\frac{\phi}{M_p}\right) \frac{\sqrt{\left[\frac{V_0(1+\beta\left(\frac{\phi}{M_p}\right)^p) - \sum_{i=1}^4 \Lambda_i (M_p)^i \left(\frac{\phi}{M_p}\right)^i}{3M_p^2} + \frac{\Lambda_0}{3}\right]}}{\left[-\beta p \left(\frac{\phi}{M_p}\right)^{p-1} + \sum_{i=1}^4 \Lambda_i M_p^{i-1} \left(\frac{\phi}{M_p}\right)^{i-1}\right]} = \frac{1}{3M_p} \int dt. \quad (5.74)$$

For the sake of clarity, we again follow the same procedure as we have done for DGP model i.e. redefine the field variable, as:

$$\frac{\phi}{M_p} = e^\lambda. \quad (5.75)$$

Simplified analytical expressions can only be obtained for the small field limit given by  $\phi/M_p \ll 1$ , so that we will concentrate in this specific physical situation for this case. In this limit, we can expand the exponentials upto linear order and upon further simplification we get the following expression for  $\lambda$  as:

$$\lambda = \frac{\left(\frac{t}{3M_p} + B_{14}\right)}{\sqrt{J/K}} \quad (5.76)$$

where the arbitrary integration constants  $J$ ,  $K$  and  $B_{14}$  is given by:

$$J = \frac{V_0}{3M_p^2} + \frac{\Lambda_0}{3} + \frac{V_0\beta}{3M_p^2} - \left( \frac{\Lambda_1}{3M_p} + \frac{\Lambda_2}{3} + \frac{\Lambda_3 M_p}{3} + \frac{\Lambda_4 M_p^2}{3} \right), \quad (5.77)$$

$$K = -\frac{V_0}{M_p} p\beta + \Lambda_1 + 2\Lambda_2 M_p + 3\Lambda_3 M_p^2 + 4\Lambda_4 M_p^3, \quad (5.78)$$

$$B_{14} = \lambda_f(\sqrt{J}/K) - \frac{t_f}{3M_p}. \quad (5.79)$$

Here  $\lambda_f$  is the value at the time of turnaround i.e. at the time scale  $t = t_f$ .

The above solution has been obtained under the assumption that the conditions:

$$\frac{J\lambda}{M} \ll 1, \quad (5.80)$$

$$\frac{N\lambda}{K} \ll 1, \quad (5.81)$$

are satisfied. This is possible because we are in the small  $\lambda$  limit and we can choose the values of the other constants accordingly. Here we introduce two new constants  $M$  and  $K$  defined as:

$$M = \frac{V_0 p\beta}{3M_p^2} - \left( \frac{\Lambda_1}{3M_p} + \frac{2\Lambda_2}{3} + \frac{3\Lambda_3 M_p}{3} + \frac{4\Lambda_4 M_p^2}{3} \right) \quad (5.82)$$

$$K = -\frac{V_0}{M_p} \beta p(p-1) + 2\Lambda_2 M_p + 9\Lambda_3 M_p^2 + 12\Lambda_4 M_p^3 \quad (5.83)$$

Further substituting this expression back into the Friedmann equations, we get the following expression for the scale factor as:

$$a(t) = B_{15} \exp \left[ \sqrt{J} \left\{ t \left( 1 + \frac{B_{14} K M}{6M_p J^{3/2}} \right) + \frac{t^2}{2} \left( \frac{K M}{6M_p J^{3/2}} \right) \right\} \right], \quad (5.84)$$

where  $B_{15}$  is the arbitrary integration constant given by:

$$B_{15} = a_f \exp \left[ -\sqrt{J} \left\{ t_f \left( 1 + \frac{B_{14} K M}{6M_p J^{3/2}} \right) + \frac{t_f^2}{2} \left( \frac{K M}{6M_p J^{3/2}} \right) \right\} \right] \quad (5.85)$$

Here  $a_f$  is the value of scale factor at turnaround time scale  $t = t_f$ .

## B. Contraction

The conclusion remains same as for  $\Lambda$ CDM model, because in this case all the extra terms containing  $\phi$ , will be neglected at leading order approximation.

## C. Expression for work done

The solution of the scale factor (i.e its time dependence) is same as that for hill-top potential for constant  $\Lambda$  case. Hence the expression for work done is same except that the constant will now depend on the parameters of this model. Thus the phenomenon of hysteresis also holds true for this model.

### For Case 3

#### A. Expansion

At late times within the window  $a' < a < a_{max}$ , using Eq. (5.12) and Eq. (5.14) with scalar field density  $\rho$  now given by the hilltop potential, we get an integral equation of the following form (neglecting  $\ddot{\phi}$ ):

$$\int d\left(\frac{\phi}{M_p}\right) \frac{\sqrt{\left(\frac{V_0(1+\beta\left(\frac{\phi}{M_p}\right)^p) - \Lambda e^{\phi/M_p}}{3M_p^2} + \frac{\Lambda_0}{3}\right)}}{\left[-\frac{V_0}{M_p}\beta p\left(\frac{\phi}{M_p}\right)^{p-1} + \Lambda e^{\phi/M_p}\right]} = \frac{1}{3M_p} \int dt. \quad (5.86)$$

In order to simplify the above integral for computational purpose, we follow the same procedure as we have already done for DGP model i.e. redefine the field by using:

$$\frac{\phi}{M_p} = e^\lambda. \quad (5.87)$$

Simplified solutions were possible only for small field case i.e. for  $\phi/M_p \ll 1$ , which has been discussed below.

In this limit, we can expand the exponentials upto linear order and upon further simplification we get the expression for  $\lambda$  as

$$\lambda = \left(\frac{t}{3M_p} + B_{18}\right) \frac{\left(\frac{-V_0\beta p}{M_p} + \frac{\Lambda e}{M_p}\right)}{\sqrt{\frac{V_0}{3M_p^2} + \frac{V_0\beta}{3M_p^2} - \frac{\Lambda e}{3M_p^2} + \frac{\Lambda_0}{3}}} \quad (5.88)$$

where  $B_{18}$  is the arbitrary integration constant given by:

$$B_{18} = \frac{\lambda_f \sqrt{\frac{V_0}{3M_p^2} + \frac{V_0\beta}{3M_p^2} - \frac{\Lambda e}{3M_p^2} + \frac{\Lambda_0}{3}}}{\left(\frac{-V_0\beta p}{M_p} + \frac{\Lambda e}{M_p}\right)} - \frac{t_f}{3M_p} \quad (5.89)$$

Here  $\lambda_f$  is the value at the time of turnaround i.e at the time scale  $t = t_f$ .

The above solutions have been obtained under the assumption that the conditions:

$$\frac{(V_0\beta p - \Lambda e)\lambda}{(V_0 + V_0\beta - \Lambda e + \Lambda_0 M_p^2)} \ll 1, \quad (5.90)$$

$$\frac{((\Lambda e - V_0\beta p(p-1))/M_p)\lambda}{((-V_0\beta p + \Lambda e)/M_p)} \ll 1 \quad (5.91)$$

are satisfied, which is possible if we choose the values of the constants accordingly.

Further substituting this expression back into the Friedmann equation, we get the following expression for the scale factor as:

$$a(t) = B_{19} \exp \left[ \sqrt{O'} \left( \left( 1 + \frac{P' B_{18}}{2O'^{3/2}} \right) t + \frac{P' t^2}{12M_p O'^{3/2}} \right) \right] \quad (5.92)$$

where  $B_{19}$  is the arbitrary integration constant given by:

$$B_{19} = a_f \exp \left[ -\sqrt{O'} \left( \left( 1 + \frac{P' B_{18}}{2O'^{3/2}} \right) t_f + \frac{P' t_f^2}{12M_p O'^{3/2}} \right) \right] \quad (5.93)$$

in which we introduce two new symbols given by:

$$O' = \frac{V_0}{3M_p^2} + \frac{V_0\beta}{3M_p^2} - \frac{\Lambda e}{3M_p^2} + \frac{\Lambda_0}{3}, \quad (5.94)$$

$$P' = \left( \frac{V_0\beta p - \Lambda e}{3M_p^2} \right) \left( -\frac{V_0\beta p}{M_p} + \frac{\Lambda e}{M_p} \right). \quad (5.95)$$

Here  $a_f$  is the value of scale factor at turnaround.

## B. Contraction

Solutions remain same as obtained before. So the conclusion also remain unchanged for contraction phase of the Universe.

## C. Expression for work done

The solution of the scale factor (i.e its time dependence) is same as that obtained for hilltop potential. Hence the expression for work done is exactly same except that the constant will now depend on the parameters of this model. Thus the phenomenon of hysteresis also holds good for this model.

### 5.6.2 Case II: Natural potential

#### For Case 1:

#### A. Expansion

At late times within the window  $a' < a < a_{max}$ , using Eq. (4.67) and Eq. (5.1), we get the following integral equation of the form:

$$\int d\left(\frac{\phi}{f}\right) \frac{\sqrt{\left(\frac{V_0}{3M_p^2} + \frac{\Lambda}{3} + \frac{V_0}{3M_p^2} \cos\left(\frac{\phi}{f}\right)\right)}}{\sin\left(\frac{\phi}{f}\right)} = \frac{V_0}{3f^2} \int dt. \quad (5.96)$$

The exact solution of the left hand side of the above equation is given in the Appendix for RSII model. For the sake of simplicity, here we study solutions for two limiting physical situations.

i)  $\phi/f \ll 1$ :

Using the small argument approximations for trigonometric functions, we get the expression for scalar field  $\phi$  as:

$$\frac{\phi(t)}{f} = B_6 \exp \left[ \frac{V_0 t}{3f^2 \left(1 + \frac{V_0}{3M_p^2}\right)^{1/2} \left(\frac{V_0}{3M_p^2} + \frac{\Lambda}{3}\right)^{1/2}} \right], \quad (5.97)$$

where  $B_6$  is the arbitrary integration constant given by:

$$B_6 = \frac{\phi_F}{f} \exp \left[ - \frac{V_0 t_F}{3f^2 \left(1 + \frac{V_0}{3M_p^2}\right)^{1/2} \left(\frac{V_0}{3M_p^2} + \frac{\Lambda}{3}\right)^{1/2}} \right]. \quad (5.98)$$

Here  $\phi_F$  is the value of the scalar field at turnaround corresponding to  $t = t_F$ .

Further substituting the expression for  $\phi$  into the Friedmann equation, we get the following expression for the scale factor as:

$$a(t) = B_7 \exp \left[ \left(1 + \frac{V_0}{3M_p^2}\right)^{1/2} \left(\frac{V_0}{3M_p^2} + \frac{\Lambda}{3}\right)^{1/2} t \right] \quad (5.99)$$

where  $B_7$  is the arbitrary integration constant given by:

$$B_7 = a_F \exp \left[ - \left(1 + \frac{V_0}{3M_p^2}\right)^{1/2} \left(\frac{V_0}{3M_p^2} + \frac{\Lambda}{3}\right)^{1/2} t_F \right] \quad (5.100)$$

Here  $a_F$  is the value of the scale factor at turnaround.

**ii)  $\phi/f \gg 1$ :**

Since we know that for large argument  $\phi/f \gg 1$ , value of cosine function is very small, hence using this concept and the following constraint condition:

$$\operatorname{cosec}^2 \left( \frac{\phi}{f} \right) \gg \frac{\frac{V_0}{3M_p^2} \cos \left( \frac{\phi}{f} \right)}{2 \left( \frac{V_0}{3M_p^2} + \frac{\Lambda}{3} \right) \sin^2 \left( \frac{\phi}{f} \right)}, \quad (5.101)$$

we get the solution for the scalar field  $\phi$  as:

$$\frac{\phi(t)}{f} = 2 \tan^{-1} \left[ \left( \frac{V_0 t}{3M_p^2} + B_8 \right) \frac{1}{\sqrt{\frac{V_0}{3M_p^2} + \frac{\Lambda}{3}}} \right], \quad (5.102)$$

where  $B_8$  is the arbitrary integration constant given by:

$$B_8 = \tan \left( \frac{\phi_F}{2f} \right) \left( \sqrt{\frac{V_0}{3M_p^2} + \frac{\Lambda}{3}} - \frac{V_0 t_F}{3M_p^2} \right). \quad (5.103)$$

Here  $\phi_F$  is the value of the scalar field at turnaround.

Further using the expression for  $\phi$  in the Friedmann equation, we get the following expression for the scale factor as:

$$a(t) = B_9 \exp \left[ \left( \frac{V_0}{3M_p^2} + \frac{\Lambda}{3} \right)^{1/2} G(t) \right], \quad (5.104)$$

where  $G(t)$  is defined as:

$$G(t) = \left( \frac{\frac{\frac{V_0}{3M_p^2} \left( B_8 + \frac{V_0 t}{3M_p^2} \right) - \frac{\frac{V_0}{3M_p^2}}{\left( \frac{V_0}{3M_p^2} + \frac{\Lambda}{3} \right)^{1/2}} \tan^{-1} \left( \frac{B_8 + \frac{V_0 t}{3M_p^2}}{\left( \frac{V_0}{3M_p^2} + \frac{\Lambda}{3} \right)^{1/2}} \right)}{\left( \frac{V_0}{3M_p^2} \right)}}{t - \frac{\frac{V_0}{3M_p^2} \left( B_8 + \frac{V_0 t}{3M_p^2} \right) - \frac{\frac{V_0}{3M_p^2}}{\left( \frac{V_0}{3M_p^2} + \frac{\Lambda}{3} \right)^{1/2}} \tan^{-1} \left( \frac{B_8 + \frac{V_0 t}{3M_p^2}}{\left( \frac{V_0}{3M_p^2} + \frac{\Lambda}{3} \right)^{1/2}} \right)}{\left( \frac{V_0}{3M_p^2} \right)}} \right) \quad (5.105)$$

and  $B_9$  is the arbitrary integration constant given by:

$$B_9 = a_F \exp \left[ - \left( \frac{V_0}{3M_p^2} + \frac{\Lambda}{3} \right)^{1/2} G(t_F) \right]. \quad (5.106)$$

Here  $a_F$  is the value of the scale factor at turnaround.

## B. Contraction

This phase is independent of any choice of the potential provided the condition  $\dot{\phi}^2 \gg V(\phi)$  holds good in this phase. This implies that the final conclusion remains same as obtained for previous hilltop potential in the background of  $\Lambda$ CDM model.

## C. Expression for work done

As will be discussed in the next section, that the expression for representative integral for work done in the early universe for loop quantum model contains a large number of terms, hence will not be explicitly shown in the present context. But the results of the integral corresponding to the late universe have been discussed below.

### i) $\phi/f \ll 1$ :

In this limit, the total work done is given by:

$$\oint p dV = b_8(e^{3b_9 t'} - e^{3b_9 t_{max}}) + 3M_p^2(45 \sinh(\sqrt{\Lambda} t_{max}) - 9 \sinh(2\sqrt{\Lambda} t_{max}) + \sinh(3\sqrt{\Lambda} t_{max}) - 45 \sinh(\sqrt{\Lambda} t') + 9 \sinh(2\sqrt{\Lambda} t') - \sinh(3\sqrt{\Lambda} t') - 30t_{max} + 30t'). \quad (5.107)$$

Here  $b_4 \dots b_9$  are constants that depend on the parameters present in the expression for the scale factor whose explicit expressions have been given in the appendix.

Including the contributions from the other integrals also we see that we get a non-zero work done for small field case for hilltop potential when we have cosmological constant in the background.

### ii) $\phi/f \gg 1$ :

In this limit, the total work done is given by:

$$\oint p dV = \frac{1}{3b_{10}(-1 + b_{11}b_{12} - b_{12}b_{13})} \times \left[ -3b_{14}^3 (e^{3b_{10}(t_{max}-b_{11}+b_{13})(b_{15}+b_{12}t_{max})} - e^{3b_{10}(t_{min}-b_{11}+b_{13})(b_{15}+b_{12}t_{min})}) + b_{14}^4 (e^{3b_{10}(t_{max}-b_{11}+b_{13})(b_{15}+b_{12}t_{max})} - e^{3b_{10}(t_{min}-b_{11}+b_{13})(b_{15}+b_{12}t_{min})}) - 3b_{14} (e^{b_{10}(t_{max}-b_{11}+b_{13})(b_{15}+b_{12}t_{max})} - e^{b_{10}(t_{min}-b_{11}+b_{13})(b_{15}+b_{12}t_{min})}) + 3M_p^2(45 \sinh(\sqrt{\Lambda} t_{max}) - 9 \sinh(2\sqrt{\Lambda} t_{max}) + \sinh(3\sqrt{\Lambda} t_{max}) - 45 \sinh(\sqrt{\Lambda} t') + 9 \sinh(2\sqrt{\Lambda} t') - \sinh(3\sqrt{\Lambda} t') - 30t_{max} + 30t') \right]. \quad (5.108)$$

Here  $b_4\dots b_{14}$  are constants that depend on the parameters present in the expression for the scale factor. Thus we get a non-zero work done for large field case for hilltop potential when we have cosmological constant.

## For Case 2

### A. Expansion

Analytical solutions in this case can also be obtained for small field limit i.e. when  $\phi/f \ll 1$ . Hence taking the small angle approximations of the trigonometric functions and redefining the field using following transformation equation:

$$\frac{\phi}{f} = e^\lambda, \quad (5.109)$$

we get the following solution for the transformed field  $\lambda$  as:

$$\lambda = \left( \frac{t}{3f} + B_{16} \right) \frac{K'}{\sqrt{M'}} \quad (5.110)$$

where  $B_{16}$  is the arbitrary integration constant given by:

$$B_{16} = \lambda_F \frac{\sqrt{M'}}{K'} - \frac{t_F}{3f} \quad (5.111)$$

where we introduce two new constants  $K'$  and  $M'$  given by:

$$K' = \frac{V_0}{f} + \Lambda_1 + 2\Lambda_2 M_p + 3\Lambda_3 M_p^2 + 4\Lambda_4 M_p^3, \quad (5.112)$$

$$M' = \frac{2V_0}{3M_p^2} + \frac{\Lambda_0}{3} - \left( \frac{\Lambda_1}{3M_p} + \frac{\Lambda_2}{3} + \frac{\Lambda_3 M_p}{3} + \frac{\Lambda_4 M_p^2}{3} \right). \quad (5.113)$$

Here  $\lambda_F$  is the value at turnaround.

The above expressions have been obtained under the assumption that the following constraint conditions are satisfied:

$$\frac{L'\lambda}{M'} \ll 1, \quad (5.114)$$

$$\frac{N'\lambda}{K'} \ll 1. \quad (5.115)$$

Since we are in the small field limit, these conditions can be satisfied if we choose the numerical values of the model parameters accordingly. Here we additionally introduce two new constants  $L'$  and  $N'$  given by:

$$L' = \frac{\Lambda_1}{3M_p} + \frac{2\Lambda_2}{3} + \frac{3\Lambda_3 M_p}{3} + \frac{4\Lambda_4 M_p^2}{3}, \quad (5.116)$$



$$N' = \frac{V_0}{f} + 2\Lambda_2 M_p + 9\Lambda_3 M_p^2 + 12\Lambda_4 M_p^3. \quad (5.117)$$

The expression for the scale factor that follows from the above solution is given by:

$$a(t) = B_{17} \exp \left[ \sqrt{M'} \left( \left( 1 - \frac{L' B_{16} K'}{2M'^{3/2}} \right) t - \frac{L' K' t^2}{12M'^{3/2} f} \right) \right], \quad (5.118)$$

where  $B_{17}$  is the arbitrary integration constant given by:

$$B_{17} = a_F \exp \left[ -\sqrt{M'} \left( \left( 1 - \frac{L' B_{16} K'}{2M'^{3/2}} \right) t_F - \frac{L' K' t_F^2}{12M'^{3/2} f} \right) \right]. \quad (5.119)$$

Here  $a_F$  is the value of the scale factor at turnaround.

## B. Contraction

The conclusion remains same as for  $\Lambda$ CDM model, because in this case all the extra terms containing  $\phi$ , will be neglected at leading order approximation.

## C. Expression for work done

The solution of the scale factor (i.e its time dependence) is same as that for hill-top potential. Hence the expression for work done is same except that the constant will now depend on the parameters of this model. Thus the phenomenon of hysteresis also holds good for this model.

### For Case 3

At late times within the interval  $a' < a < a_{max}$ , using Eq. (5.12) and Eq. (5.14), we get the integral equation of the form similar to Eq. (5.86) with  $V(\phi)$  given by the natural potential. Simple analytical expressions for the scalar field and scale factor could be obtained only for the case when  $\phi/f \ll 1$  which has been discussed below. In this limiting situation using the small argument approximations for trigonometric functions, we get the following expression for the scalar field  $\phi$  as:

$$\frac{\phi(t)}{f} = \left( \frac{t}{3f} + B_{20} \right) \frac{\Lambda}{f \sqrt{\frac{2V_0}{3M_p^2} - \frac{\Lambda}{3M_p^2} + \frac{\Lambda_0}{3}}}, \quad (5.120)$$

where  $B_{20}$  is the arbitrary integration constant given by:

$$B_{20} = \frac{f \phi_F \sqrt{\frac{2V_0}{3M_p^2} - \frac{\Lambda}{3M_p^2} + \frac{\Lambda_0}{3}}}{\Lambda} - \frac{t_F}{3f}. \quad (5.121)$$

Here  $\phi_F$  is the value of the scalar field at turnaround corresponding to  $t = t_F$ .

Finally, substituting the expression for  $\phi$  into the Friedmann equation, we get the following expression for the scale factor as:

$$a(t) = B_{21} \exp \left[ \sqrt{Q'} \left( \left( 1 - \frac{B_{20}\Lambda^2}{2Q'^{3/2}fM_p^2} \right) t - \frac{\Lambda^2 t^2}{12M_p^2 f^2 Q'^{3/2}} \right) \right], \quad (5.122)$$

where  $B_{21}$  is the arbitrary integration constant given by:

$$B_{21} = a_F \exp \left[ -\sqrt{Q'} \left( \left( 1 - \frac{B_{20}\Lambda^2}{2Q'^{3/2}fM_p^2} \right) t_F - \frac{\Lambda^2 t_F^2}{12M_p^2 f^2 Q'^{3/2}} \right) \right]. \quad (5.123)$$

Here we introduce a new constant  $Q'$  defined as:

$$Q' = \frac{2V_0}{3M_p^2} - \frac{\Lambda}{3M_p^2} + \frac{\Lambda_0}{3} \quad (5.124)$$

Here  $a_F$  is the value of the scale factor at turnaround.

## B. Contraction

Solutions remain same as obtained before. So the conclusion also remain unchanged for contraction phase of the Universe.

## C. Expression for work done

The solution of the scale factor (i.e its time dependence) is same as that for hill-top potential. Hence the expression for work done is same except that the constant will now depend on the parameters of this model. Thus the phenomenon of hysteresis also holds good for this model.

### 5.6.3 Case III: Coleman-Weinberg potential

#### For Case 1:

#### A. Expansion

At late times within the interval  $a' < a < a_{max}$ , using Eq. (4.67) and Eq. (5.1), we get the following integral equation of the form:

$$\int d\left(\frac{\phi}{M_p}\right) \frac{\sqrt{\left[\frac{V_0}{3M_p^2} \left( 1 + \left( \alpha + \beta \ln \left( \frac{\phi}{M_p} \right) \right) \left( \frac{\phi}{M_p} \right)^4 \right) + \frac{\Lambda}{3} \right]}}{\left( \frac{\phi}{M_p} \right)^3 \left[ 4\alpha + \beta + 4\beta \ln \left( \frac{\phi}{M_p} \right) \right]} = -\frac{V_0}{3M_p^2} \int dt. \quad (5.125)$$

To compute the left hand side of the above integral equation, we once again use the field redefinition via the following transformation:

$$\frac{\phi}{M_p} = e^\lambda, \quad (5.126)$$

and study the two limiting physical situations as mentioned below.

i)  $\phi/M_p \ll 1$ :

In this limit, we expand the exponentials upto linear order and get the resulting solution for the transformed field  $\lambda$  as:

$$\lambda = \left( -\frac{V_0}{3M_p^2}t + B_{10} \right) \frac{(4\alpha + \beta)}{\left( \frac{V_0}{3M_p^2} + \frac{V_0\alpha}{3M_p^2} + \frac{\Lambda}{3} \right)^{1/2}}, \quad (5.127)$$

where  $B_{10}$  is the arbitrary integration constant given by:

$$B_{10} = \frac{\left( \frac{V_0}{3M_p^2} + \frac{V_0\alpha}{3M_p^2} + \frac{\Lambda}{3} \right)^{1/2} \lambda_f}{4\alpha + \beta} + \frac{V_0}{3M_p^2} t_f, \quad (5.128)$$

The above expressions have been obtained using the assumptions that the constraint conditions:

$$\frac{4\beta\lambda}{(4\alpha + \beta)} \ll 1, \quad (5.129)$$

$$\frac{\frac{V_0}{3M_p^2}(4\alpha + \beta)\lambda}{\frac{V_0}{3M_p^2} + \frac{V_0\alpha}{3M_p^2} + \frac{\Lambda}{3}} \ll 1, \quad (5.130)$$

are satisfied. Since we are already in the limit in which the value of  $\lambda$  is very small, hence by choosing the other parameters of the model properly, we can easily satisfy the above constraint conditions.

Further substituting the above expression into the Friedmann equation, we get the following expression for the scale factor as:

$$a(t) = B_{11} \exp \left[ \left( \left( \frac{V_0}{3M_p^2} + \frac{V_0\alpha}{3M_p^2} + \frac{\Lambda}{3} \right)^{1/2} + \frac{\frac{V_0}{3M_p^2}(4\alpha + \beta)}{2 \left( \frac{V_0}{3M_p^2} + \frac{V_0\alpha}{3M_p^2} + \frac{\Lambda}{3} \right)} B_{10}(4\alpha + \beta) \right) t - \frac{V_0 \frac{V_0}{3M_p^2} (4\alpha + \beta)}{12 \left( \frac{V_0}{3M_p^2} + \frac{V_0\alpha}{3M_p^2} + \frac{\Lambda}{3} \right) M_p^2} (4\alpha + \beta) t^2 \right] \quad (5.131)$$

where  $B_{11}$  is the arbitrary integration constant given by:

$$B_{11} = a_f \exp \left[ - \left( \left( \frac{V_0}{3M_p^2} + \frac{V_0\alpha}{3M_p^2} + \frac{\Lambda}{3} \right)^{1/2} + \frac{\frac{V_0}{3M_p^2}(4\alpha + \beta)}{2 \left( \frac{V_0}{3M_p^2} + \frac{V_0\alpha}{3M_p^2} + \frac{\Lambda}{3} \right)} B_{10}(4\alpha + \beta) \right) t_f + \frac{V_0 \frac{V_0}{3M_p^2}(4\alpha + \beta)}{12 \left( \frac{V_0}{3M_p^2} + \frac{V_0\alpha}{3M_p^2} + \frac{\Lambda}{3} \right) M_p^2} (4\alpha + \beta) t_f^2 \right]. \quad (5.132)$$

Here  $a_f$  is the value of the scale factor at turnaround.

ii)  $\phi/M_p \gg 1$ :

In this case we get an integral of the form

$$\int d\lambda \frac{\sqrt{\left[ \frac{V_0}{3M_p^2} + \frac{\Lambda}{3} + \frac{V_0}{3M_p^2}(\alpha + \beta\lambda)e^{4\lambda} \right]}}{(4\alpha + \beta + 4\beta\lambda)} e^{-2\lambda} = -\frac{V_0}{3M_p^2} \int dt. \quad (5.133)$$

To compute the left hand side of the above integral equation and hence to get an analytical expression for  $\lambda$ , we assume the following three constraint conditions i.e.

$$\left( \frac{V_0}{3M_p^2} + \frac{\Lambda}{3} \right) \ll \frac{V_0}{3M_p^2}(\alpha + \beta\lambda)e^{4\lambda}, \quad (5.134)$$

$$4\alpha + \beta \ll 4\beta\lambda, \quad (5.135)$$

$$\alpha \ll \beta\lambda. \quad (5.136)$$

Since we are in large  $\lambda$  limit, by choosing the values of the parameters of the model, the above conditions can be easily satisfied. Under these assumptions, we get the expression for  $\lambda$  as:

$$\lambda = \left( -\frac{V_0}{3M_p^2}t + B_{12} \right)^2 \frac{4\beta}{\frac{V_0}{3M_p^2}}, \quad (5.137)$$

where  $B_{12}$  is the arbitrary integration constant given by:

$$B_{12} = \frac{V_0}{3M_p^2}t_f \pm \left( \frac{V_0\lambda_f}{12M_p^2\beta} \right)^{1/2} \quad (5.138)$$

Here  $\lambda_f$  is the value at turnaround.

Further substituting the expression for  $\lambda$ , hence  $\phi$  into the Friedmann equation and applying the above mentioned constraint conditions, we get the following expression for the scale factor as:

$$a(t) = B_{13} \exp \left[ 2e \left( \frac{s \left( B_{12} - \frac{V_0 t}{3M_p^2} \right)^2 \beta}{\frac{V_0}{3M_p^2}} \right) t \left( \frac{\left( -\frac{V_0}{3M_p^2}t + B_{12} \right)^2 \beta^2}{\frac{V_0}{3M_p^2}} \right)^{1/2} \right], \quad (5.139)$$

where  $B_{13}$  is the arbitrary integration constant given by:

$$B_{13} = a_f \exp \left[ -2e \left( \frac{8 \left( B_{12} - \frac{V_0 t_f}{3M_p^2} \right)^2 \beta}{\frac{V_0}{3M_p^2}} \right) t_f \left( \frac{\left( -\frac{V_0}{3M_p^2} t_f + B_{12} \right)^2 \beta^2}{\frac{V_0}{3M_p^2}} \right)^{1/2} \right]. \quad (5.140)$$

Here  $a_f$  is the value of the scale factor at turnaround.

## B. Contraction

This phase is independent of any choice of the potential provided the condition  $\dot{\phi}^2 \gg V(\phi)$  holds good in this phase. This implies that the final conclusion remains same as obtained for previous hilltop and natural potential in the background of  $\Lambda$ CDM model.

## C. Expression for work done

The solution of the scale factor (i.e its time dependence) is same as that for hill-top and natural potential. Hence the expression for work done is same except that the constant will now depend on the parameters of this model. Thus the phenomenon of hysteresis also holds perfectly for this model.

### For Case 2

#### A. Expansion

At late times within the window  $a' < a < a_{max}$ , using Eq. (5.5) and Eq. (5.6), we get an integral equation similar to Eq. (5.74), with the potential  $V(\phi)$  now given by the Supregavity motivated Coleman-Weinberg potential. For the case 2 the mathematical form of the governing integral equation is exactly same as that obtained in case 2, only in the present case the constant  $\Lambda$  is replaced by the field dependent  $\Lambda(\phi)$ , which is defined earlier. To compute the left hand side of the master integral equation we will once again use the previously mentioned field redefinition:

$$\frac{\phi}{M_p} = e^\lambda. \quad (5.141)$$

One can find the analytical solutions only for the case when the small field limiting approximation is valid i.e.  $\phi/M_p \ll 1$  is satisfied.

In this limit, we expand the exponentials upto linear order and get the resulting

solution for the redefined field  $\lambda$  as:

$$\lambda = \frac{\left(\frac{t}{3M_p} + B_{16}\right) O}{\sqrt{P}} \quad (5.142)$$

where  $B_{16}$  is the arbitrary integration constant given by:

$$B_{16} = \frac{\lambda_f \sqrt{P}}{O} - \frac{t_f}{3M_p}. \quad (5.143)$$

Here we introduce two new constants  $O$  and  $P$  given by the following expressions:

$$O = -(4\alpha + \beta) + \Lambda_1 + 2\Lambda_2 M_p + 3\Lambda_3 M_p^2 + 4\Lambda_4 M_p^3, \quad (5.144)$$

$$P = \frac{V_0}{3M_p^2} + \frac{\Lambda_0}{3} - \left( \frac{\Lambda_1}{3M_p} + \frac{\Lambda_2}{3} + \frac{\Lambda_3 M_p}{3} + \frac{\Lambda_4 M_p^2}{3} \right). \quad (5.145)$$

Here  $\lambda_f$  is the value at turnaround when  $t = t_f$ .

The above expressions have been obtained using the assumptions that the conditions,

$$\frac{Q\lambda}{P} \ll 1, \quad (5.146)$$

$$\frac{L\lambda}{O} \ll 1, \quad (5.147)$$

are satisfied. Since we are already in the limit in which the value of  $\lambda$  is very small, hence by choosing the other parameters of the model properly, we can easily satisfy the above conditions. Here we introduce two new constants  $Q$  and  $L$  given by the following expressions:

$$Q = \frac{V_0\beta}{3M_p^2} + \frac{4V_0\alpha}{3M_p^2} - \left( \frac{\Lambda_1}{3M_p} + \frac{2\Lambda_2}{3} + \frac{3\Lambda_3 M_p}{3} + \frac{4\Lambda_4 M_p^2}{3} \right), \quad (5.148)$$

$$L = - \left( \frac{V_0}{M_p} \right) (7\beta + 12\alpha) + 2\Lambda_2 M_p + 6\Lambda_3 M_p^2 + 12\Lambda_4 M_p^3. \quad (5.149)$$

Further substituting the above expression into the Friedmann equation, we get the following expression for the scale factor as:

$$a(t) = B_{17} \exp \left[ \sqrt{P} \left( \left( 1 + \frac{OQB_{16}}{2P^{3/2}} \right) t + \frac{OQ}{12P^{3/2}M_p} t^2 \right) \right], \quad (5.150)$$

where  $B_{17}$  is the arbitrary integration constant given by:

$$B_{17} = a_f \exp \left[ -\sqrt{P} \left( \left( 1 + \frac{OQB_{16}}{2P^{3/2}} \right) t_f + \frac{OQ}{12P^{3/2}M_p} t_f^2 \right) \right]. \quad (5.151)$$

Here  $a_f$  is the value of the scale factor at turnaround.

## B. Contraction

The conclusion remains same as for  $\Lambda$ CDM model, because in this case all the extra terms containing  $\phi$ , will be neglected at leading order approximation.

## C. Expression for work done

The solution of the scale factor (i.e its time dependence) is same as that for hill-top and natural potential. Hence the expression for work done is same except that the constant will now depend on the parameters of this model. Thus the phenomenon of hysteresis also holds true for this model.

### For Case 3

At late times within the window  $a' < a < a_{max}$ , using Eq. (5.12) and Eq. (5.14), we get the integral equation of the form similar to Eq. (5.86) with the potential now given by the supergravity motivated Coleman-Weinberg potential. Simplified analytical solutions can be obtained if we use the following field redefinition:

$$\frac{\phi}{M_p} = e^\lambda, \quad (5.152)$$

which we have used earlier and take small field limiting approximation  $\phi/M_p \ll 1$  in the present context.

In this limit, we expand the exponentials upto linear order and get the resulting solution for the redefined field variable  $\lambda$  as:

$$\lambda = \left( \frac{t}{3M_p} + B_{22} \right) \frac{M_p^2}{\frac{1+\frac{R'}{2S'}}{\frac{U'}{V'}} + \frac{(\frac{U'}{V'} - (1+\frac{R'}{2S'}))}{\frac{U'^2}{V'^2}}}, \quad (5.153)$$

where  $B_{22}$  is the arbitrary integration constant given by:

$$B_{22} = \frac{\lambda_f}{M_p^2} \left( \frac{1 + \frac{R'}{2S'}}{\frac{U'}{V'}} + \frac{(\frac{U'}{V'} - (1 + \frac{R'}{2S'}))}{\frac{U'^2}{V'^2}} \right) - \frac{t_f}{3M_p}. \quad (5.154)$$

Here for the sake of clarity we introduce four model dependent constants  $R', S', U', V'$

given by:

$$R' = \frac{V_0}{3M_p^2}(4\alpha + \beta - \frac{\Lambda e}{V_0}), \quad (5.155)$$

$$S' = \frac{V_0}{3M_p^2} + \frac{\Lambda_0}{3} + \frac{V_0\alpha}{3M_p^2} - \frac{\Lambda e}{3M_p^2}, \quad (5.156)$$

$$U' = -\frac{4V_0\beta}{M_p} + \frac{3V_0(4\alpha + \beta)}{M_p} + \frac{\Lambda e}{M_p}, \quad (5.157)$$

$$V' = -\frac{V_0}{M_p}(4\alpha + \beta) + \frac{\Lambda e}{M_p}. \quad (5.158)$$

The above expressions have been obtained using the assumptions that the conditions,

$$\frac{R'\lambda}{S'} \ll 1, \quad (5.159)$$

$$\frac{U'\lambda}{V'} \ll 1, \quad (5.160)$$

are satisfied. Since we are already in the limit in which the value of  $\lambda$  is very small, hence by choosing the other parameters of the model properly, we can easily satisfy the above conditions.

Further substituting the above expression into the Friedmann equation, we get the following expression for the scale factor as:

$$a(t) = B_{23} \exp \left[ \sqrt{S'} \left( \left( 1 + \frac{R' M_p^2 B_{22}}{2S' \left( \frac{1+\frac{R'}{2S'}}{\frac{U'}{V'}} + \frac{(\frac{U'}{V'} - (1+\frac{R'}{2S'}))}{\frac{U'^2}{V'^2}} \right)} \right) t + \frac{R' t^2 M_p^2}{12S' \left( \frac{1+\frac{R'}{2S'}}{\frac{U'}{V'}} + \frac{(\frac{U'}{V'} - (1+\frac{R'}{2S'}))}{\frac{U'^2}{V'^2}} \right)} \right) \right], \quad (5.161)$$

where

$$B_{23} = a_f \exp \left[ -\sqrt{S'} \left( \left( 1 + \frac{R' M_p^2 B_{22}}{2S' \left( \frac{1+\frac{R'}{2S'}}{\frac{U'}{V'}} + \frac{(\frac{U'}{V'} - (1+\frac{R'}{2S'}))}{\frac{U'^2}{V'^2}} \right)} \right) t_f + \frac{R' t_f^2 M_p^2}{12S' \left( \frac{1+\frac{R'}{2S'}}{\frac{U'}{V'}} + \frac{(\frac{U'}{V'} - (1+\frac{R'}{2S'}))}{\frac{U'^2}{V'^2}} \right)} \right) \right]. \quad (5.162)$$

Here  $a_f$  is the value of the scale factor at turnaround.

## B. Contraction

Solutions remain same as obtained before. So the conclusion also remain unchanged for contraction phase of the Universe.

## C. Expression for work done



The solution of the scale factor (i.e. its time dependence) is same as that for hilltop potential. Hence the expression for work done is same except that the constant will now depend on the parameters of this model. Thus the phenomenon of hysteresis also holds true for this model.

## 5.7 Graphical Analysis

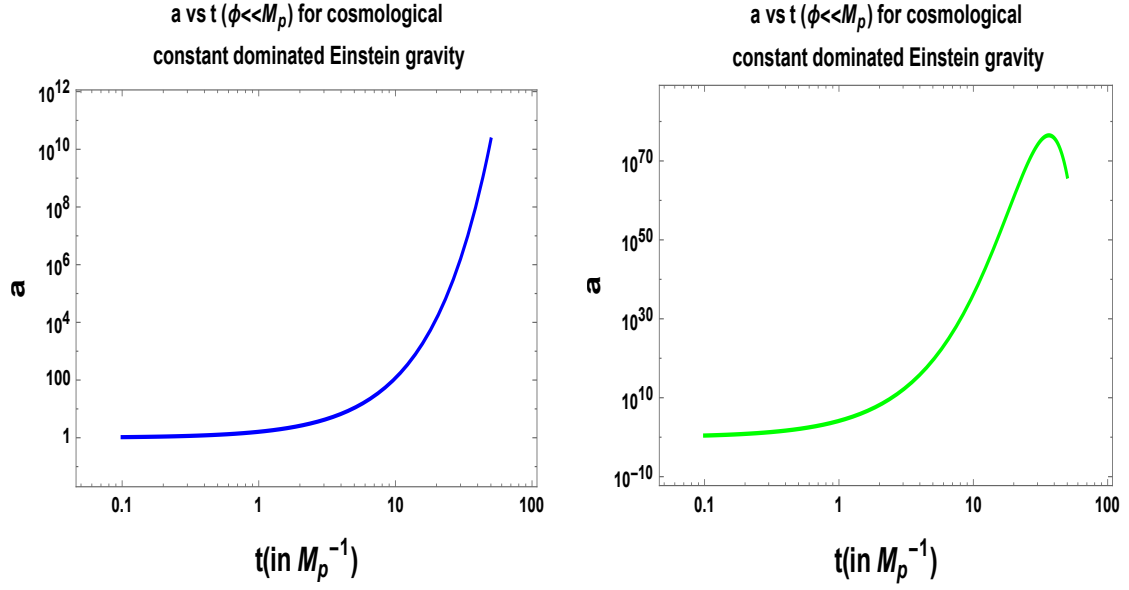
### 5.7.1 Case I: Hilltop potential

All the graphs in this section and in the following sections have been plotted in units of  $M_p = 1$ ,  $H_0 = 1$ ,  $c = 1$ , where  $M_p$  is the Planck mass,  $H_0$  is the present value of the Hubble parameter and  $c$  is the speed of light. While performing the analysis, for the value of the standard cosmological constant, we have used Planck 2015 data [75]. The analysis for all the three potentials has been done for late times since, in the early times the solutions are those that we get for Randall-Sundrum single brane world (RSII).

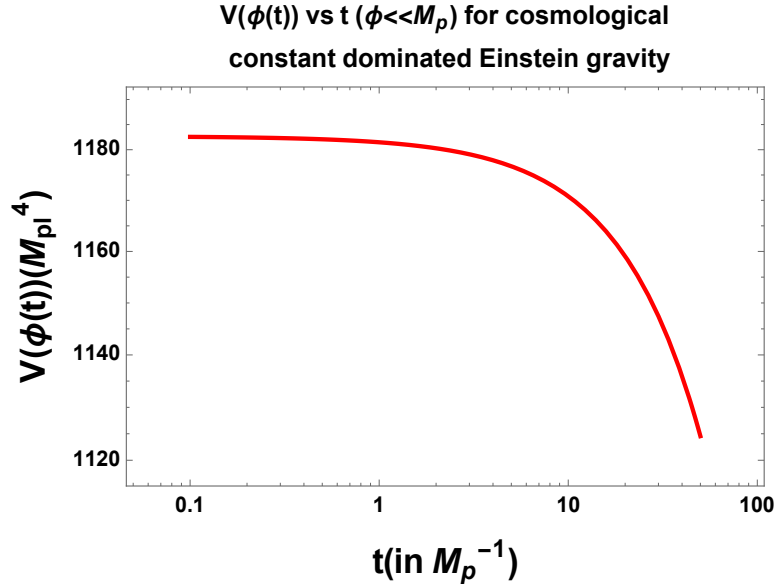
#### For Case 1:

Figs. 10 and 11 show the evolution of the scale factor and kinetic term of the potential during contraction phase. We can draw the following conclusions from the plots:

- Fig. 10(a), shows the plot of the scale factor in the small field limit for hilltop potential given by Eqn. (5.60).
- While obtaining the above plot, we kept the value of the integration constants  $B_0$  and  $B_1$  as 1. Higher values of the integration constants only results in an increase in the amplitude of the scale factor, not affecting the nature of the graph.
- In Figs. 10(a) and 10(b), the plot has been shown for two particular cases which gives interesting results. The red curve has been obtained for the case when  $V_0 = 10^{-8}M_p^4$ ,  $p = 2$ ,  $\beta = 1$ ,  $B_0 = 1$ ,  $B_1 = 1$ . While the blue curve has been obtained for the case when  $V_0 = 10^{-2}M_p^4$ ,  $p = 3$ ,  $\beta = -8$ ,  $B_0 = 1$ ,  $B_1 = 1$ .
- While analyzing the results graphically, we have found that when the value of  $V_0$  is low (for example  $\approx 10^{-8}M_p^4$ ), the universe undergoes expansion for any values of the parameters  $p$ ,  $\beta$ , etc. But if we make  $V_0 > 10^{-3}M_p^4$ , then expansion is possible for any values of the parameters provided  $B_0$  takes larger

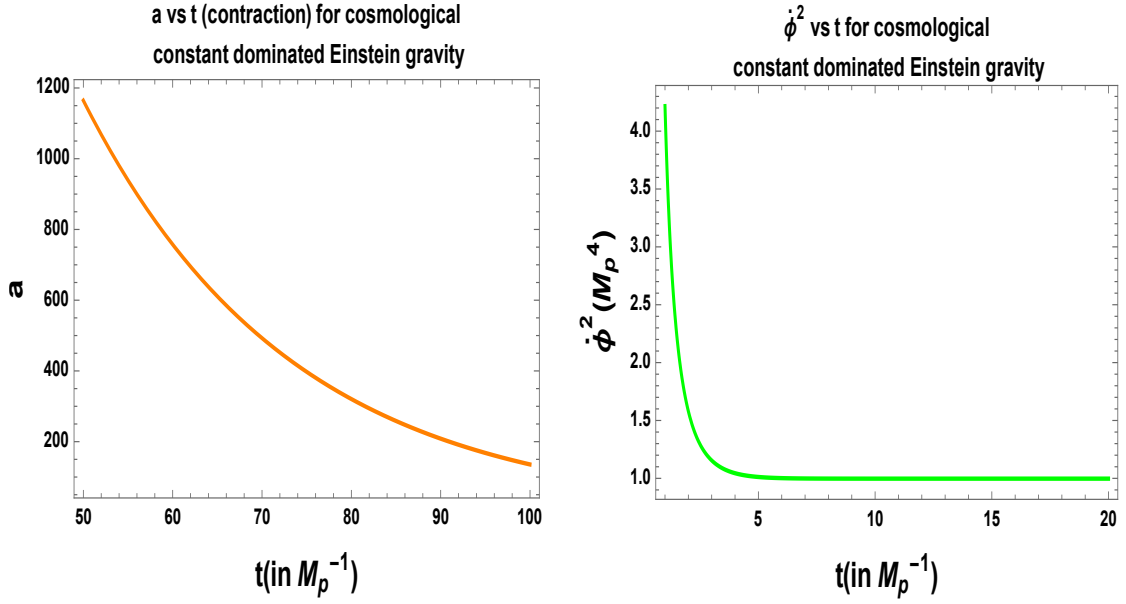


(a) An illustration of the behavior of the scale factor with time during expansion phase for  $\phi \ll M_p$  with  $V_0 = 10^{-8}M_p^4$ ,  $p = 2$ ,  $\beta = 1$ ,  $B_0 = M_p$ ,  $B_1 = 1$ .  
 (b) An illustration of the behavior of the scale factor with time during expansion phase for  $\phi \ll M_p$  with  $V_0 = 10^{-2}M_p^4$ ,  $p = 3$ ,  $\beta = -8$ ,  $B_0 = M_p$ ,  $B_1 = 1$ .



(c) An illustration of the behavior of the potential during expansion phase for  $\phi \ll M_p$  with  $V_0 = 10^{-4}M_p^4$ ,  $\beta = 2$ ,  $p = 2$ ,  $B_0 = M_p$ .

**Figure 10.** Graphical representation of the evolution of the scale factor and the potential during the expansion and contraction phase for the cosmological constant dominated Einstein gravity for case 1.

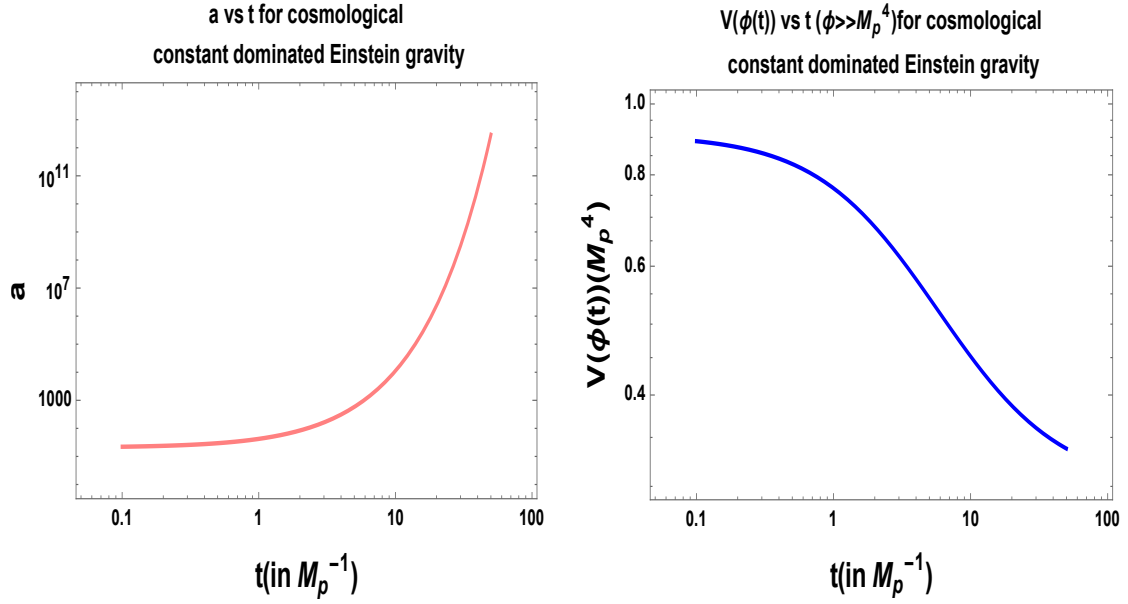


(a) An illustration of the behavior of the scale factor with time during contraction phase with  $B_4 = 10^{-3}M_p^2$ ,  $B_5 = 10^4$ . (b) An illustration of the behavior of the kinetic term of the potential with time during contraction phase with  $B_4 = 5.4M_p^2$ .

**Figure 11.** Graphical representation of the evolution of the scale factor and the kinetic term of the potential during the contraction phase for the cosmological constant dominated Einstein gravity for case 1.

value. One such example has been shown in Fig. 10(b), where the universe undergoes starts contracting instead of expanding at later times. Thus the values of parameters for which Fig. 10(b) has been obtained, are not favourable for the present scenario.

- Fig. 10(c) shows the plot of the behavior of the potential with time for small field hilltop potential. This graph has been obtained with the help of Eqn. (5.57) with parameter values  $V_0 = 10^{-4}M_p^4$ ,  $\beta = 2$ ,  $p = 2$ ,  $B_0 = 1$ . Negative values of  $\beta$  and very large values of  $B_0$  does not give the required variation of the potential for causing expansion. Thus, such values of the parameters are not favorable for our model.
- In Fig. 11(a), we have plotted Eqn. (5.70), which results in the contraction phase of the universe provided we choose the value of the constants accordingly. This plot has been obtained for  $B_4 = 10^{-3}$ ,  $B_5 = 10^4$ . Taking higher values of  $B_4$  decreases the amplitude of the scale factor, whereas higher values of  $B_5$  increases the amplitude of the scale factor. If we compare Fig. 8(a) with Fig. 11(a), we find that there occurs a net increase in the amplitude of the scale factor after one expansion-contraction cycle.



(a) An illustration of the behavior of the scale factor with time during expansion phase for  $\phi \gg M_p$  with  $V_0 = 3 \times 10^{-1} M_p^4$ ,  $p = 3$ ,  $\beta = 1$ ,  $B_2 = M_p$ ,  $B_3 = 1$ .  
(b) An illustration of the behavior of the potential with time during expansion phase for  $\phi \gg M_p$  with  $V_0 = 3 \times 10^{-1} M_p^4$ ,  $p = 3$ ,  $\beta = 1$ ,  $B_2 = M_p$ ,  $B_3 = 1$ .

**Figure 12.** Graphical representation of the evolution of the scale factor and the potential during the expansion phase for the cosmological constant dominated Einstein gravity for case 1.

- In Fig. 11(b), we have plotted the kinetic term of the potential during the contraction phase with the help of Eqn. (5.68) using  $B_4 = 5.4 M_p^2$ . Negative values of  $B_4$  do not give the correct nature of the kinetic term required for causing contraction. The graph shows a decreasing kinetic term with time because this will result in contraction phase.
- Fig. 12(a) shows the plot of the scale factor in the large field limit for hill-top potential given by Eqn. (5.66). This plot has been obtained for  $V_0 = 3 \times 10^{-1} M_p^4$ ,  $\beta = 1$ ,  $p = 3$ ,  $B_2 = M_p$ ,  $B_3 = 1$ . From Eqn. (5.66), we can conclude that negative values of  $\beta$  are not allowed in this case, since this will make the expression imaginary. Larger and positive values of  $\beta$  results in a decrease in amplitude of the scale factor. Also, if we make  $p > 3$ , then the amplitude of the scale factor decreases to a very low value. If we make  $p < 2$ , then the evolution of the scale factor becomes very uneven, i.e. it remains constant for most part of its evolution, with a sudden increase in amplitude at the end. Thus for smooth and large amplitude expansion for the values of the other parameters that we have chosen here, the allowed range of  $p$  is  $2 \leq p \leq 3$ .
- Fig. 12(b) shows the plot of the behavior of the potential with time for large

field hilltop potential. This graph has been obtained with the help of Eqn. (5.62) with parameter values  $V_0 = 3 \times 10^{-1} M_p^4$ ,  $\beta = 1$ ,  $p = 3$ ,  $B_2 = M_p^4$ .

**For Case 2:**

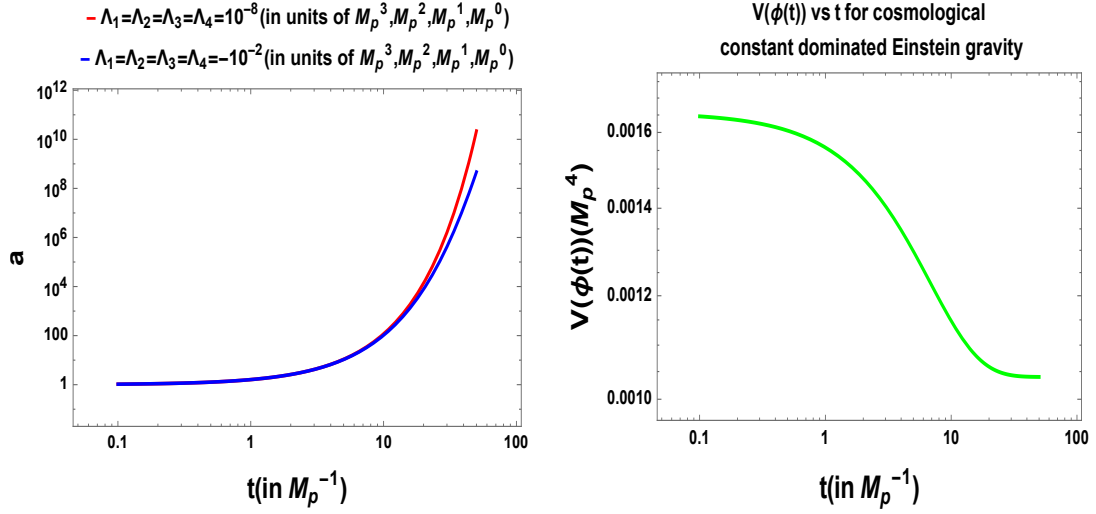
In Fig. 13, we have plotted the evolution of the scale factor and the potential during expansion for case 2. From the figures we can draw the following conclusions:

- Fig. 13(a) shows the variation of the scale factor with time for small field hilltop potential for two cases of parameter values for a scalar field dependent cosmological constant.
- Fig. 13(a) has been obtained from Eq. (5.84). Detail graphical analysis show that an expanding universe in the present scenario is possible only if the values of  $\Lambda_1$ ,  $\Lambda_2$ ,  $\Lambda_3$ ,  $\Lambda_4$  lies between  $-10^{-2}$  to  $10^{-2}$ . They can take any sign provided their magnitudes remain within the specified range. The expansion in this case is almost independent of the values of  $\beta$ ,  $p$  and  $V_0$ .
- In Fig. 13(a), we have shown two such cases which give rise to an expanding universe.
- Fig. 13(b) and Fig. 13(c) show the variation of the potential with time during expansion for case 2. Detail graphical analysis have shown that keeping the magnitude of the parameters within the above mentioned range, if we make  $\Lambda_1$  negative, then expansion is possible only if  $\Lambda_4$  is also negative or only slightly positive. This also requires a higher value of  $V_0$ . The other two parameters can be either positive or negative. Also, if the values of  $\Lambda_1$ ,  $\Lambda_3$  and  $\Lambda_4$  are very close to the upper bound, then we won't get the correct nature of the potential required for evolution.
- From Figs. 13(b) and 13(c), we can conclude that higher and positive parameter values increases the height of the potential. But smaller and negative values of the constants make the potential flatter. Also, from Fig. 13(c), only a negative value of  $\Lambda_4$  can produce the correct evolution of the potential if all the other constants are positive and small.

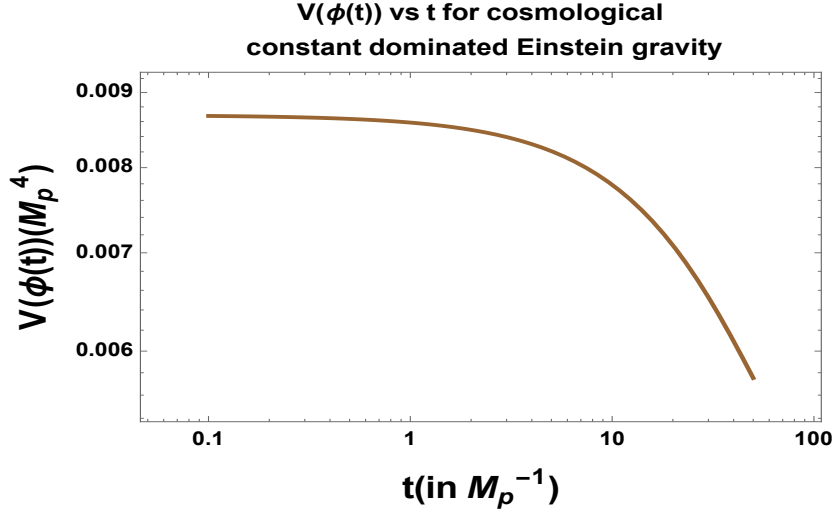
**For Case 3:**

In Fig. 14, we have plotted the evolution of the scale factor and the potential during expansion for case 3. From the figures we can draw the following conclusions:

- Fig. 14(a) shows the variation of the scale factor with time for small field hilltop potential for  $V_0 = 10^{-8} M_p^4$ ,  $B_{18} = M_p^{-2}$ ,  $\Lambda = 10^{-2} M_p^4$ ,  $B_{19} = 1$ .

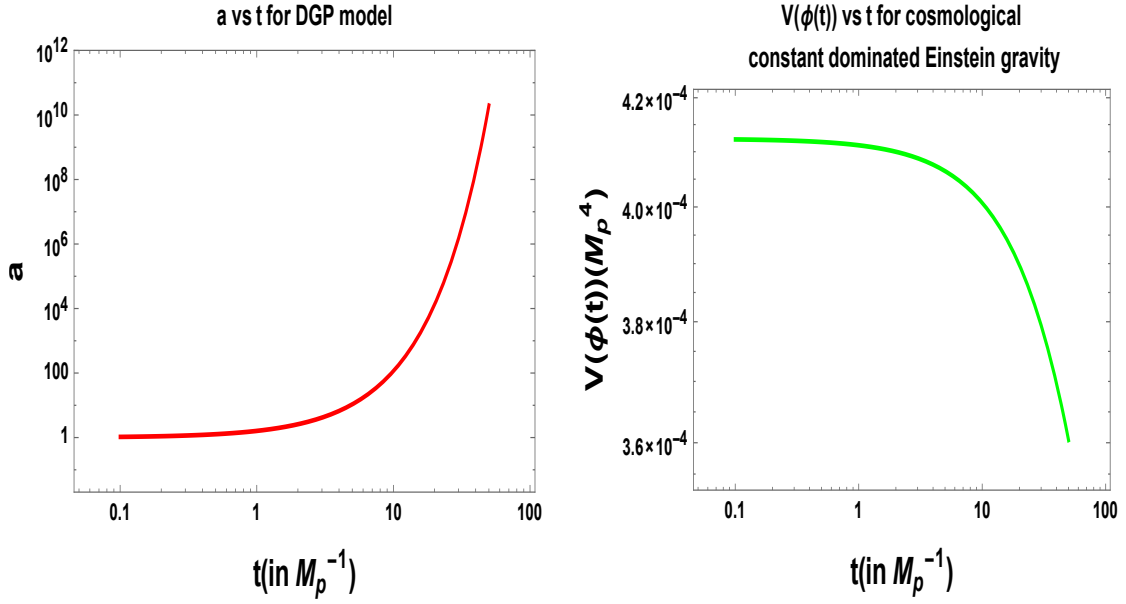


(a) An illustration of the behavior of the scale factor with time during expansion phase for  $\phi \ll M_p$  with  $V_0 = 10^{-8}M_p^4$ ,  $p = 2$ ,  $\beta = 1$ ,  $B_{14} = M_p^{-2}$ ,  $B_{15} = V_0 = 10^{-6}M_p^4$ ,  $p = 3$ ,  $\beta = 1$ ,  $B_{14} = M_p$ ,  $\Lambda_1 = 1$ ,  $\Lambda_1 = 10^{-8}M_p^3$ ,  $\Lambda_2 = 10^{-8}M_p^2$ ,  $\Lambda_3 = 10^{-8}M_p$ ,  $\Lambda_4 = -10^{-2}M_p^3$ ,  $\Lambda_2 = -10^{-2}M_p^2$ ,  $\Lambda_3 = -10^{-2}M_p$ ,  $\Lambda_4 = 10^{-8}$  for red curve and  $V_0 = 10^{-8}M_p^4$ ,  $p = 3$ ,  $\beta = -10^{-2}$ ,  $B_{14} = M_p^{-2}$ ,  $B_{15} = 1$ ,  $\Lambda_1 = -10^{-2}M_p^3$ ,  $\Lambda_2 = -10^{-2}M_p^2$ ,  $\Lambda_3 = -10^{-2}M_p$ ,  $\Lambda_4 = -10^{-2}$  for blue curve



(c) An illustration of the behavior of the potential with time during expansion phase for  $\phi \ll M_p$  with  $V_0 = 4 \times 10^{-6}M_p^4$ ,  $p = 3$ ,  $\beta = 1$ ,  $B_{14} = M_p$ ,  $\Lambda_1 = 10^{-4}M_p^3$ ,  $\Lambda_2 = 10^{-3}M_p^2$ ,  $\Lambda_3 = 4 \times 10^{-3}M_p$ ,  $\Lambda_4 = -3 \times 10^{-3}$ .

**Figure 13.** Graphical representation of the evolution of the scale factor and the potential during the expansion phase for the cosmological constant dominated Einstein gravity for case 2.



(a) An illustration of the behavior of the potential with time during expansion phase for  $\phi \ll M_p$  with  $V_0 = 10^{-8}M_p^4$ ,  $B_{18} = M_p^{-2}$ ,  $\Lambda = M_p$  with  $V_0 = 2 \times 10^{-4}M_p^4$ ,  $p = 3$ ,  $\beta = 1$ ,  $B_{18} = 10^{-2}M_p^4$ ,  $B_{19} = 1$ . (b) An illustration of the behavior of the potential with time during expansion phase for  $\phi \ll M_p$  with  $V_0 = 2 \times 10^{-4}M_p^4$ ,  $p = 3$ ,  $\beta = 1$ ,  $B_{18} = M_p^{-2}$ ,  $\Lambda = -10^{-3}M_p^4$ .

**Figure 14.** Graphical representation of the evolution of the scale factor and the potential during the expansion phase for the cosmological constant dominated Einstein gravity for case 3.

- Fig. 14(a) has been obtained from Eqn. (5.92). Detail graphical analysis show that an expanding universe in the present scenario is possible only if the value of  $\Lambda$  lies within the range  $-10^{-2}$  to  $10^{-2}$ . But as we go nearer to the upper bound, expansion occurs only for very small values (very close to unity) of  $B_{18}$ . The expansion in this case is independent of the values of  $\beta$ ,  $p$ . Higher values of  $V_0$  increases the amplitude of the expansion. But values of  $V_0$  greater than  $10^{-3}M_p^4$  do not give rise to an expanding universe.
- Fig. 14(b) shows the variation of the hilltop potential for an expanding universe for case 3 with  $\phi \ll M_p$  with  $V_0 = 2 \times 10^{-4}M_p^4$ ,  $p = 3$ ,  $\beta = 1$ ,  $B_{18} = M_p^{-2}$ ,  $\Lambda = -10^{-3}M_p^4$ . Graphical analysis show that within the allowed range of the parameter values, as discussed before, only a negative  $\Lambda$  can give the correct nature of the evolution of the potential when  $V_0$  is very small (around  $10^{-8}M_p^4$ ). For this case,  $\beta$  and  $p$  can take any values. But for larger values of  $V_0$ , we can increase the range of  $\Lambda$  and make it positive by making  $\beta$  positive. For example, if  $V_0 = 10^{-3}M_p^4$  and  $\Lambda = 8 \times 10^{-3}M_p^4$ , then the minimum value of  $\beta$  required to give the correct evolution of the potential is 5.

## 5.7.2 Case II: Natural potential

### For Case 1:

Fig. 15 show the evolution of the scale factor and the potential for the case of natural potential for case 1 during expansion. The following conclusions can be drawn from the graphs:

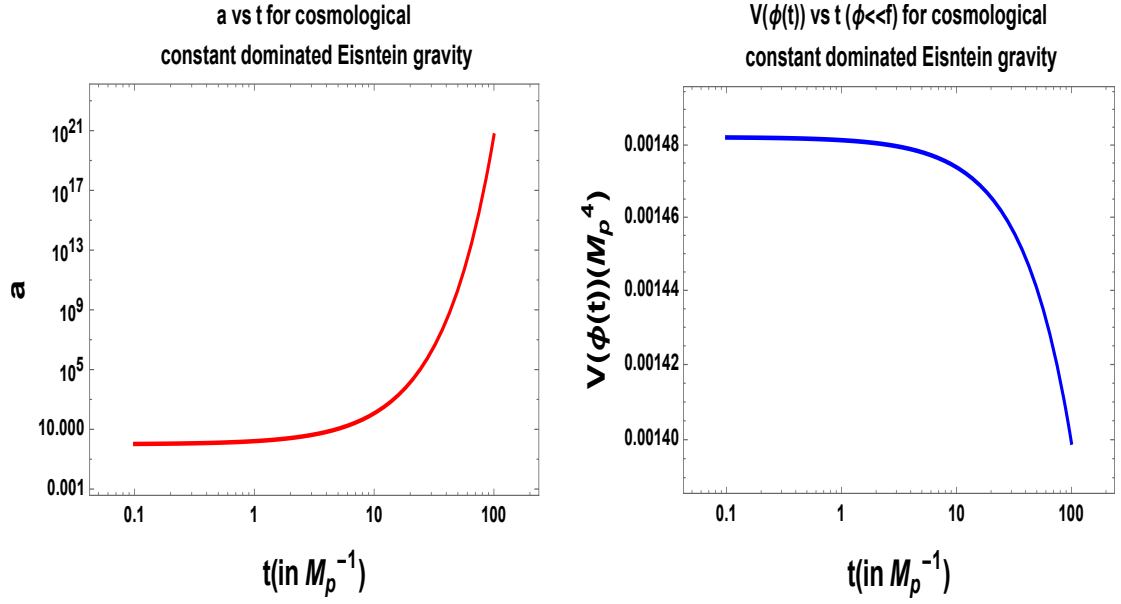
- Fig. 15(a), shows the plot of the scale factor in the small field limit for natural potential given by Eqn. (5.99).
- While obtaining the above plot, we kept the value of the integration constants  $B_6$  and  $B_7$  as 1. Higher values of the integration constants only results in an increase in the amplitude of the scale factor, not affecting the nature of the graph. Higher values of  $V_0$  also only results in an increase in amplitude of the scale factor.
- Fig. 15(b) shows the plot of the behavior of the potential with time for small field natural potential. This graph has been obtained with the help of Eqn. (5.97) with parameter values  $V_0 = 3.6 \times 10^{-3} M_p^4$ ,  $B_6 = 1$ ,  $f = 8M_p$ . Larger values of the parameters gives rise to larger amplitude of expansion, but the nature of the graph remains the same. If we compare Fig. 15(a) with Fig. 11(a), we find that there occurs a net increase in the amplitude of the scale factor after one expansion-contraction cycle.
- Fig. 15(c) shows the plot of the scale factor in the large field limit for natural potential given by Eqn. (5.104). This plot has been obtained for  $V_0 = 10^{-2} M_p^4$ ,  $B_8 = M_p$ ,  $B_9 = 1$ . Expansion is obtained only if the value of  $V_0$  is lesser than  $2M_p^4$ .
- Fig. 15(d) shows the plot of the behavior of the potential with time for large field natural potential. This graph has been obtained with the help of Eqn. (5.102) with parameter values  $V_0 = 10^{-2} M_p^4$ ,  $B_8 = M_p$ .

### For Case 2:

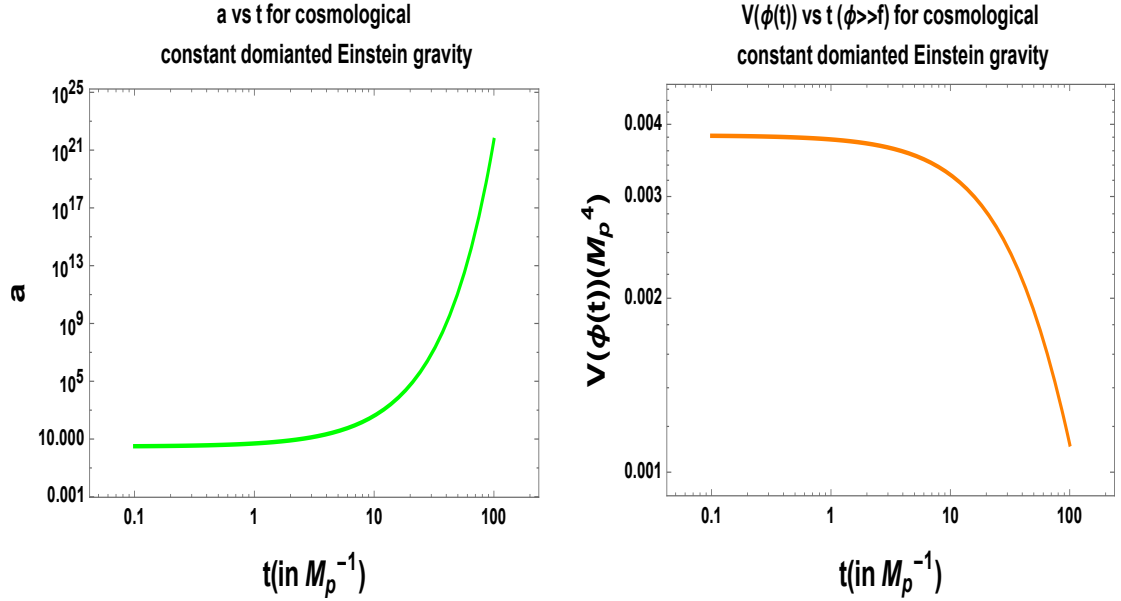
In Fig. 16, we have plotted the evolution of the scale factor and the potential during expansion for case 2. From the figures we can draw the following conclusions:

- Fig. 16(a) shows the variation of the scale factor with time for small field natural potential for two cases of parameter values for a scalar field dependent cosmological constant.



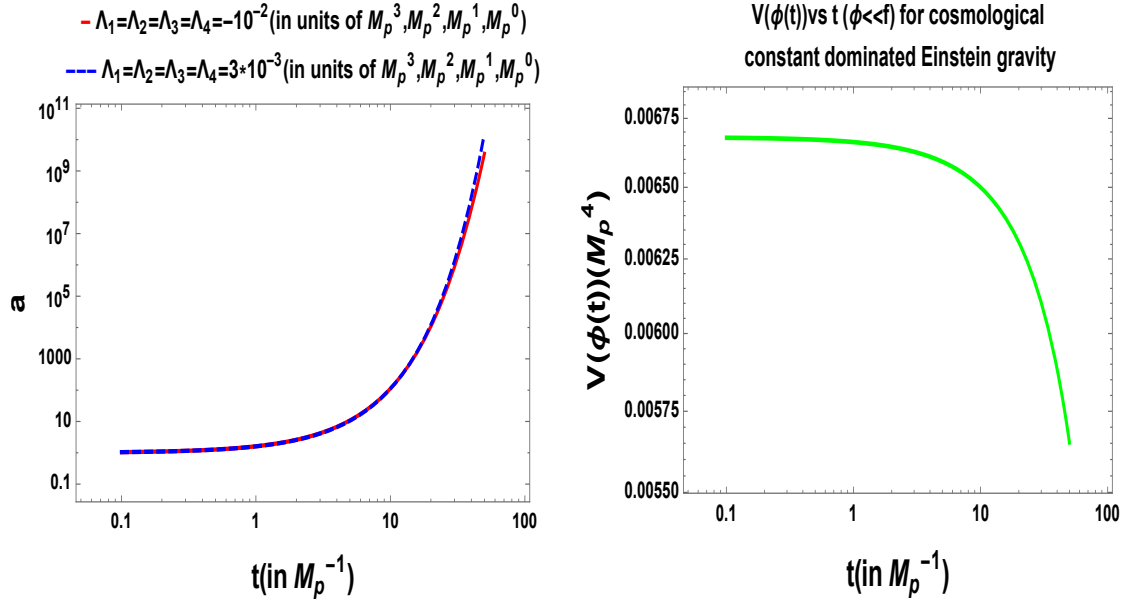


(a) An illustration of the behavior of the scale factor with time during expansion phase for  $\phi \ll f$  with  $V_0 = 10^{-8} M_p^4$ ,  $B_6 = 1$ ,  $B_7 = 1$ . (b) An illustration of the behavior of the potential during expansion phase for  $\phi \ll f$  with  $V_0 = 3.6 \times 10^{-3} M_p^4$ ,  $B_6 = 1$ ,  $f = 8 M_p$ .



(c) An illustration of the behavior of the scale factor with time during expansion phase for  $\phi \gg f$  with  $V_0 = 10^{-2} M_p^4$ ,  $B_8 = M_p$ ,  $B_9 = 1$ . (d) An illustration of the behavior of the potential with time during expansion phase for  $\phi \gg f$  with  $V_0 = 10^{-2} M_p^4$ ,  $B_8 = M_p$ .

**Figure 15.** Graphical representation of the evolution of the scale factor and the potential during the expansion and contraction phase for the cosmological constant dominated Einstein gravity for case 1.



(a) An illustration of the behavior of the scale factor with time during expansion phase for  $\phi \ll f$  with  $V_0 = 10^{-8}M_p^4$ ,  $f = 2M_p$ ,  $B_{16} = M_p^{-2}$ ,  $B_{17} = 1$ ,  $\Lambda_1 = V_0 = 4.4 \times 10^{-3}M_p^4$ ,  $f = 4M_p$ ,  $B_{16} = M_p^{-2}$ ,  $\Lambda_1 = -10^{-2}M_p^3$ ,  $\Lambda_2 = -10^{-2}M_p^2$ ,  $\Lambda_3 = -10^{-2}M_p$ ,  $\Lambda_4 = -10^{-2}M_p^3$ ,  $\Lambda_2 = 1.2 \times 10^{-3}M_p^2$ ,  $\Lambda_3 = 2.4 \times 10^{-3}M_p$ ,  $\Lambda_4 = -10^{-2}$  for red curve and  $V_0 = 10^{-8}M_p^4$ ,  $f = 6.5 \times 10^{-3}$ ,  $6M_p$ ,  $B_{16} = M_p^{-2}$ ,  $B_{17} = 1$ ,  $\Lambda_1 = 3 \times 10^{-3}M_p^3$ ,  $\Lambda_2 = 3 \times 10^{-3}M_p^2$ ,  $\Lambda_3 = 3 \times 10^{-3}M_p$ ,  $\Lambda_4 = 3 \times 10^{-3}$  for blue dashed curve .

**Figure 16.** Graphical representation of the evolution of the scale factor and the potential during the expansion phase for the cosmological constant dominated Einstein gravity for case 2.

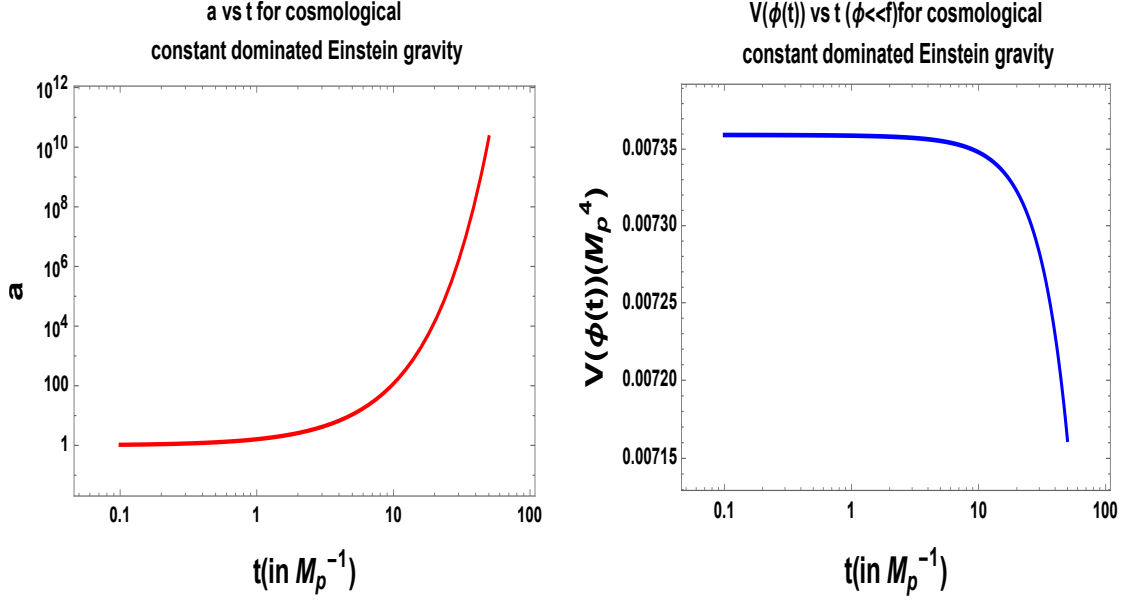
- Fig. 16(a) has been obtained from Eq. (5.118). Detail graphical analysis show that an expanding universe in the present scenario is possible only if the values of  $\Lambda_1$ ,  $\Lambda_2$ ,  $\Lambda_3$ ,  $\Lambda_4$  lies between  $-10^{-2}$  to  $10^{-2}$  similar to the case for hilltop potential. They can take any sign provided their magnitudes remain within the specified range. But expansion is possible only if  $f > 1M_p$  and value of  $B_{16}$  is very close to unity. If we make the value of  $B_{16}$  too large, then expansion is possible either if all the other constants are positive except  $\Lambda_2$  or if only  $\Lambda_2$  is positive and any two or all three other constants are negative. Increase in the value of  $V_0$  only increases the amplitude of scale factor.
- In Fig. 16(a), we have shown two such cases which give rise to an expanding universe.
- Fig. 16(b) shows the variation of the potential with time during expansion for case 2. Detail graphical analysis have shown that keeping the magnitude of

the parameters within the above mentioned range, expansion is possible only if  $\Lambda_3 > 3 \times 10^{-3} M_p$ ,  $\Lambda_4 > 5 \times 10^{-3}$  and  $V_0 > 10^{-6} M_p^4$ .

- Higher and positive parameter values increases the height of the potential.

**For Case 3:**

In Fig. 17, we have plotted the evolution of the scale factor and the potential



(a) An illustration of the behavior of the po- (b) An illustration of the behavior of the poten-  
 $\phi \ll f$  with  $V_0 = 10^{-8} M_p^4$ ,  $B_{20} = M_p^{-2}$ ,  $\Lambda =$  with  $V_0 = 4 \times 10^{-3} M_p^4$ ,  $f = 1$ ,  $B_{20} = M_p^{-2}$ ,  $\Lambda =$   
 $10^{-3} M_p^4$ ,  $B_{21} = 1.$   $-10^{-2} M_p^4.$

**Figure 17.** Graphical representation of the evolution of the scale factor and the potential during the expansion phase for the cosmological constant dominated Einstein gravity for case 3.

during expansion for case 3. From the figures we can draw the following conclusions:

- Fig. 17(a) shows the variation of the scale factor with time for small field natural potential for  $V_0 = 10^{-8} M_p^4$ ,  $B_{20} = M_p^{-2}$ ,  $\Lambda = 10^{-3} M_p^4$ ,  $B_{21} = 1$ .
- Fig. 17(a) has been obtained from Eq. (5.122). Detail graphical analysis show that an expanding universe in the present scenario is possible only if the value of  $\Lambda$  lies within the range  $-10^{-2}$  to  $10^{-2}$ . But if  $f < 1 M_p$ , expansion is possible only if  $B_{20}$  is very close to unity and  $\Lambda > -2.8 \times 10^{-2} M_p^4$ . For  $f > 1 M_p$ , expansion is possible if  $\Lambda$  lies within the range  $-10^{-2} M_p^4$  to  $10^{-2} M_p^4$

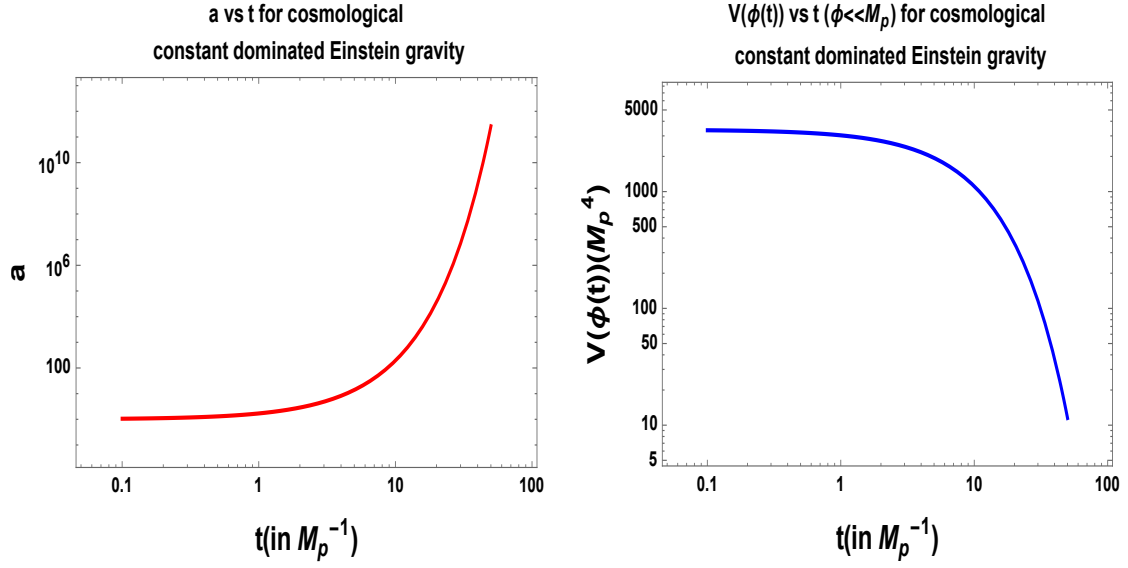
- Fig. 17(b) shows the variation of the natural potential for an expanding universe for case 3 with  $\phi \ll f$  with  $V_0 = 4 \times 10^{-3} M_p^4$ ,  $f = 1$ ,  $B_{20} = M_p^{-2}$ ,  $\Lambda = -10^{-2} M_p^4$ . Fig. 17(b) has been obtained with the help of Eqn. (5.120). Graphical analysis show that within the allowed range of the parameter values, as discussed before, larger values of  $V_0$  and  $\Lambda$  results in steeper fall of the potential and larger potential height.

### 5.7.3 Case III: Coleman-Weinberg potential

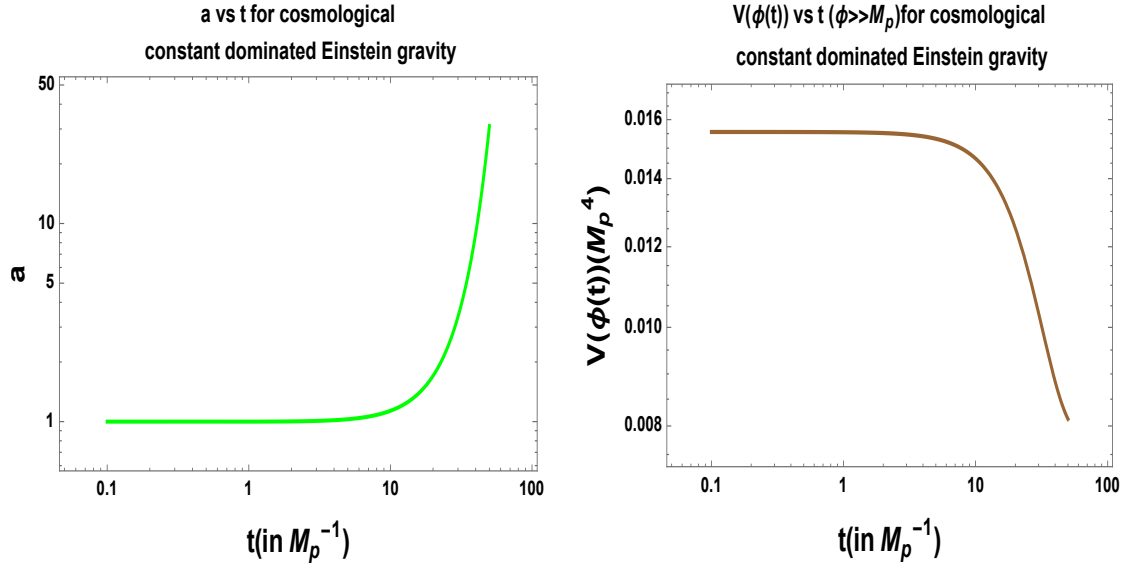
#### For Case 1:

Fig. 18 show the evolution of the scale factor and the potential for the case of supergravity potential for case 1 during expansion. The following conclusions can be drawn from the graphs:

- Fig. 18(a), shows the plot of the scale factor in the small field limit for supergravity potential given by Eqn. (5.131) with the parameter values  $V_0 = 2 \times 10^{-3} M_p^4$ ,  $B_{10} = M_p$ ,  $B_{11} = 1$ ,  $\alpha = 0.5$ ,  $\beta = 1$ .
- While obtaining the above plot, we kept the value of the integration constants  $B_{10}$  and  $B_{11}$  as 1. Higher values of the integration constants only results in an increase in the amplitude of the scale factor, not affecting the nature of the graph. Higher values of  $V_0$  also only results in an increase in amplitude of the scale factor. The evolution of the scale factor is almost independent of  $\alpha$ . Large increase in amplitude of the scale factor occurs for large value of  $\beta$  irrespective of its sign.
- Fig. 18(b) shows the plot of the behavior of the potential with time for small field supergravity potential. This graph has been obtained with the help of Eqn. (5.127) with parameter values  $V_0 = 4.6 \times 10^{-3} M_p^4$ ,  $B_{10} = 0.5$ ,  $\alpha = 0.18$ ,  $\beta = 2$ . Larger values of the parameters gives rise to larger amplitude of expansion, but the nature of the graph remains the same. If we compare Fig. 18(a) with Fig. 11(a), we find that there occurs a net increase in the amplitude of the scale factor after one expansion-contraction cycle.
- Fig. 18(c) shows the plot of the scale factor in the large field limit for supergravity potential given by Eqn. (5.139). This plot has been obtained for  $V_0 = 10^{-8} M_p^4$ ,  $B_{12} = 10^{-8} M_p$ ,  $B_{13} = 1$ ,  $\beta = 7$ . Proper expansion is obtained only if the value of  $B_{12}$  is  $\ll 1$  and the value of  $\beta$  is large. Larger value of  $V_0$  results in nearly constant expansion amplitude with a huge increase towards the later times. Expansion is possible for both negative and positive values of  $\beta$ .



(a) An illustration of the behavior of the scale factor with time during expansion phase for  $\phi \ll M_p$  with  $V_0 = 2 \times 10^{-3} M_p^4$ ,  $B_{10} = M_p$ ,  $B_{11} = V_0 = 4.6 \times 10^{-3} M_p^4$ ,  $B_{10} = 0.5$ ,  $\alpha = 0.18$ ,  $\beta = 2$ .  
 (b) An illustration of the behavior of the potential with time during expansion phase for  $\phi \ll M_p$  with  $V_0 = 2 \times 10^{-3} M_p^4$ ,  $B_{10} = M_p$ ,  $B_{11} = V_0 = 4.6 \times 10^{-3} M_p^4$ ,  $B_{10} = 0.5$ ,  $\alpha = 0.18$ ,  $\beta = 2$ .



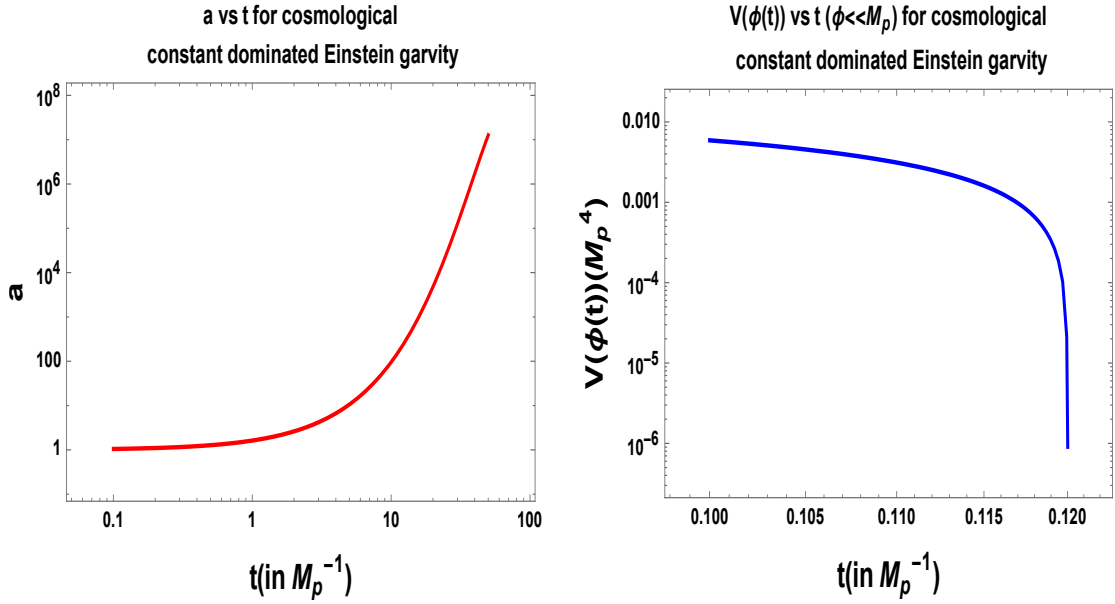
(c) An illustration of the behavior of the scale factor with time during expansion phase for  $\phi \gg M_p$  with  $V_0 = 10^{-8} M_p^4$ ,  $B_{12} = 10^{-8} M_p$ ,  $B_{13} = M_p$ .  
 (d) An illustration of the behavior of the potential with time during expansion phase for  $\phi \gg M_p$  with  $V_0 = 8 \times 10^{-3} M_p^4$ ,  $B_{12} = 10^{-8} M_p$ ,  $\alpha = 1$ ,  $\beta = -0.01$ .

**Figure 18.** Graphical representation of the evolution of the scale factor and the potential during the expansion and contraction phase for the cosmological constant dominated Einstein gravity for case 1.

- Fig. 18(d) shows the plot of the behavior of the potential with time for large field supergravity potential. This graph has been obtained with the help of Eqn. (5.137) with parameter values  $V_0 = 8 \times 10^{-3} M_p^4$ ,  $B_{12} = 10^{-8} M_p$ ,  $\alpha = 1$ ,  $\beta = -0.01$ . Proper evolution of the potential which will give rise to expanding universe is possible only if  $\beta < 0$  and  $B_{12}$  is  $\ll 1$ . Larger values of  $\alpha$  makes the potential fall more steeply. Larger values of  $V_0$  mildly increase the height of the potential.

**For Case 2:**

In Fig. 19, we have plotted the evolution of the scale factor and the potential



(a) An illustration of the behavior of the scale factor (b) An illustration of the behavior of the potential with time during expansion phase for  $\phi \ll M_p$  with time during expansion phase for  $\phi \ll M_p$  with  $V_0 = 1.3 \times 10^{-3} M_p^4$ ,  $B_{16} = M_p^{-2}$ ,  $B_{17} = 1$ ,  $\Lambda_1 = 2.1 \times 10^{-2} M_p^4$ ,  $\alpha = 10^{-4}$ ,  $B_{16} = 10^{-4} M_p^{-2}$ ,  $\Lambda_1 = 2.6 \times 10^{-2} M_p^3$ ,  $\Lambda_2 = -10^{-1} M_p^2$ ,  $\Lambda_3 = -10^{-1} M_p$ ,  $\Lambda_4 = -10^{-1} M_p^3$ ,  $\Lambda_2 = 7.9 \times 10^{-2} M_p^2$ ,  $\Lambda_3 = 7.9 \times 10^{-2} M_p$ ,  $\Lambda_4 = 8.8 \times 10^{-2}$ ,  $\alpha = 0.13$ ,  $\beta = -0.4$ .  $8.4 \times 10^{-1}$ ,  $\beta = -1.85$ .

**Figure 19.** Graphical representation of the evolution of the scale factor and the potential during the expansion phase for the cosmological constant dominated Einstein gravity for case 2.

during expansion for case 2. From the figures we can draw the following conclusions:

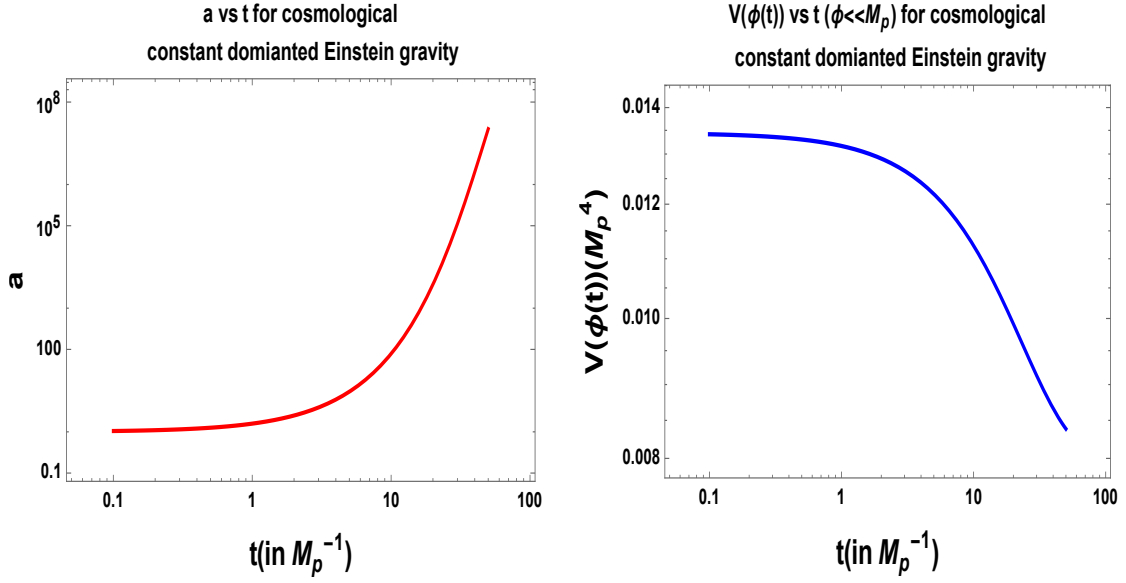
- Fig. 19(a) shows the variation of the scale factor with time for small field supergravity potential for case 2 with  $V_0 = 1.3 \times 10^{-3} M_p^4$ ,  $B_{16} = M_p^{-2}$ ,  $B_{17} = 1$ ,  $\Lambda_1 = 2.6 \times 10^{-2} M_p^3$ ,  $\Lambda_2 = -10^{-1} M_p^2$ ,  $\Lambda_3 = -10^{-1} M_p$ ,  $\Lambda_4 = 8.8 \times 10^{-2}$ ,  $\alpha = 0.13$ ,  $\beta = -0.4$

- Fig. 19(a) has been obtained from Eqn. (5.150). Detail graphical analysis show that an expanding universe in the present scenario is possible only if the values of  $\Lambda_1, \Lambda_2, \Lambda_3, \Lambda_4$  lies between  $-10^{-1}$  to  $10^{-1}$ . They can take any sign provided their magnitudes remain within the specified range. But expansion is possible for  $\beta > 0$  only if any two of the constants ( $\Lambda_1, \Lambda_2, \Lambda_3, \Lambda_4$ ) are positive and the other two take negative values. For  $\beta < 0$ , expansion is possible for any possible combination of signs of the constants. Large values of  $\alpha$  results in larger amplitude of expansion, but the nature remains the same.
- Fig. 19(b) shows the variation of the potential with time during expansion for case 2 obtained with the help of Eqn. (5.142) and with parameter values  $V_0 = 2.1 \times 10^{-2} M_p^4$ ,  $\alpha = 10^{-4}$ ,  $B_{16} = 10^{-4} M_p^{-2}$ ,  $\Lambda_1 = -10^{-1} M_p^3$ ,  $\Lambda_2 = 7.9 \times 10^{-2} M_p^2$ ,  $\Lambda_3 = 7.9 \times 10^{-2} M_p$ ,  $\Lambda_4 = 8.4 \times 10^{-1}$ ,  $\beta = -1.85$ . Detail graphical analysis have shown that keeping the magnitude of the parameters within the above mentioned range, potential evolves with the required nature to cause expansion only if  $\beta < 0$  and  $\alpha \leq 1$ .
- Higher and positive parameter values increases the height of the potential.

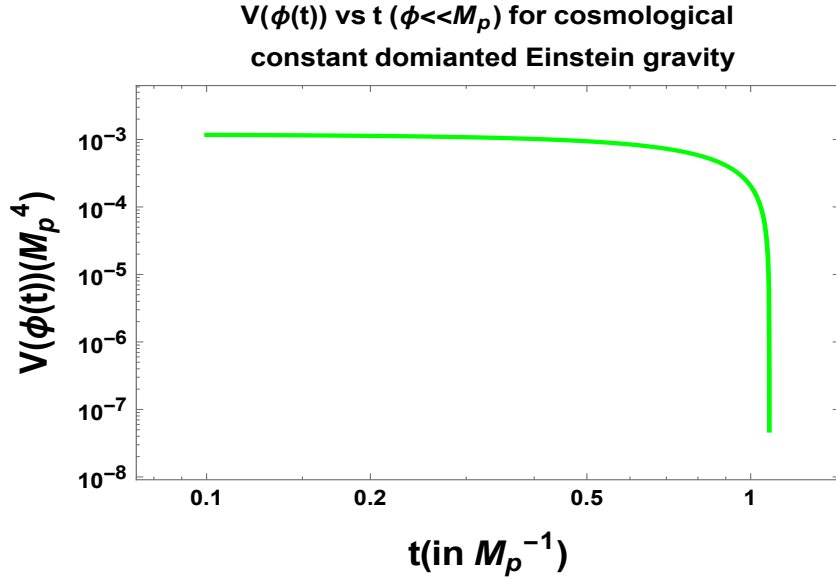
### For Case 3:

In Fig. 20, we have plotted the evolution of the scale factor and the potential during expansion for case 3. From the figures we can draw the following conclusions:

- Fig. 20(a) shows the variation of the scale factor with time for small field supergravity potential for  $V_0 = 1.5 \times 10^{-3} M_p^4$ ,  $B_{22} = M_p^{-2}$ ,  $\Lambda = 4 \times 10^{-3} M_p^4$ ,  $B_{23} = 1$ ,  $\alpha = 0.96$ ,  $\beta = 1$ .
- Fig. 20(a) has been obtained from Eqn. (5.161). Detail graphical analysis show that an expanding universe in the present scenario is possible only if the value of  $\Lambda$  lies within the range  $-10^{-1}$  to  $10^{-2}$ . If we decrease the value of  $V_0$  to  $10^{-7} M_p^4$  (say), then expansion is possible only for values of  $B_{22} \ll M_p^{-2}$ . Expansion is possible for both positive and negative values of  $\beta$ , however small positive values of  $\beta$  are more favourable for expansion.
- Figs. 20(b) and 20(c) show the variation of the supergravity potential for an expanding universe for case 3 with  $\phi \ll M_p$  for two sets of parameter values,  $V_0 = 8 \times 10^{-3} M_p^4$ ,  $\alpha = 0.8$ ,  $B_{22} = M_p^{-2}$ ,  $\beta = 0.15$ ,  $B_{23} = 1$ ,  $\Lambda = -3.6 \times 10^{-2} M_p^4$  and  $V_0 = 1.2 \times 10^{-3} M_p^4$ ,  $\alpha = 10^{-8}$ ,  $B_{22} = 10^{-8} M_p^{-2}$ ,  $\beta = -0.7$ ,  $B_{23} = 1$ ,  $\Lambda = 4.3 \times 10^{-3} M_p^4$  respectively. Figs. 20(b) and 20(c) have been obtained with the help of Eqn. (5.153). Graphical analysis show that within the allowed range of the parameter values, as discussed before, for values of  $\Lambda$  near the upper bound, expansion is possible only for negative values of  $\beta$  and values of other



(a) An illustration of the behavior of the potential with time during expansion phase for  $\phi \ll M_p$  with  $V_0 = 1.5 \times 10^{-3} M_p^4$ ,  $B_{22} = M_p^{-2}$ ,  $\Lambda = M_p$  with  $V_0 = 8 \times 10^{-3} M_p^4$ ,  $\alpha = 0.8$ ,  $B_{22} = 4 \times 10^{-3} M_p^4$ ,  $B_{23} = 1$ ,  $\alpha = 0.96$ ,  $\beta = 1$ . (b) An illustration of the behavior of the potential with time during expansion phase for  $\phi \ll M_p$  with  $V_0 = 1.5 \times 10^{-3} M_p^4$ ,  $B_{22} = M_p^{-2}$ ,  $\Lambda = M_p$  with  $V_0 = 8 \times 10^{-3} M_p^4$ ,  $\alpha = 0.8$ ,  $B_{22} = 4 \times 10^{-3} M_p^4$ ,  $B_{23} = 1$ ,  $\alpha = 0.96$ ,  $\beta = 1$ .



(c) An illustration of the behavior of the potential with time during expansion phase for  $\phi \ll M_p$  with  $V_0 = 1.2 \times 10^{-3} M_p^4$ ,  $\alpha = 10^{-8}$ ,  $B_{22} = 10^{-8} M_p^{-2}$ ,  $\beta = -0.7$ ,  $B_{23} = 1$ ,  $\Lambda = 4.3 \times 10^{-3} M_p^4$ .

**Figure 20.** Graphical representation of the evolution of the scale factor and the potential during the expansion phase for the cosmological constant dominated Einstein gravity for case 3.



parameters  $(\alpha, V_0, B_{22})$  much less than unity ( $\sim 10^{-8}$ ). For positive value of  $\beta$  expansion is possible if the value of  $V_0 > 10^{-4}M_p^4$  and that of  $\alpha$  is close to unity. In this case, in order to get an expanding universe,  $\Lambda$  must have small negative values. Larger the magnitude of  $\beta$ , steeper the fall of the potential.

## 6 Hysteresis from Loop Quantum gravity (LQG) model

Loop Quantum gravity (LQG) is one of the candidate theories of quantum gravity which successfully resolves the big bang singularity. It is primarily based on the quantum geometry effects of loop quantum gravity.

For the spatially flat case when the curvature parameter  $k = 0$ , the modified Friedmann equations in this model are given by:

$$H^2 = \left(\frac{\dot{a}}{a}\right)^2 = \frac{\rho}{3M^2} \left(1 - \frac{\rho}{\rho_c}\right), \quad (6.1)$$

$$\dot{H} + H^2 = \frac{\ddot{a}}{a} = -\frac{1}{6M^2} \left((\rho + 3p) - \frac{2\rho}{\rho_c}(2\rho + 3p)\right), \quad (6.2)$$

which is exactly same as that we get for RSII brane world cosmology (see Appendix). Since this analysis has already been done in detail by [11], we have not shown it here again. However the results of this analysis have been quoted in the Appendix for reference. Hence the rest of the conclusions remain same as that obtained for RSII brane world model.

Modified Friedmann equations for non flat case i.e. for  $k \neq 0$  in this model [76, 77] are given by:

$$H^2 = \left(\frac{\dot{a}}{a}\right)^2 = \frac{1}{3M^2} (\rho - \rho_1) \left(\frac{1}{\rho_c}(\rho_2 - \rho)\right), \quad (6.3)$$

$$\begin{aligned} \dot{H} + H^2 = \frac{\ddot{a}}{a} = & -\frac{1}{6M^2}(\rho + 3p) + \frac{2}{3M^2} \left(\frac{\rho}{\rho_c} + k\chi\right) \left(\rho + \frac{3}{2}p\right) \\ & + \frac{k\chi}{\gamma^2\Delta} \left(\frac{\rho}{\rho_c} + k\chi\right) - \frac{2\zeta k}{\gamma^2\Delta} \left(\frac{\rho}{\rho_c} + k\chi - \frac{1}{2}\right), \end{aligned} \quad (6.4)$$

where we introduce two new constants  $\rho_1$  and  $\rho_2$  are defined as:

$$\rho_1 := \frac{-3k\chi M^2}{\gamma^2\Delta} = -k\chi\rho_c, \quad (6.5)$$

$$\rho_2 := \rho_c(1 - k\chi). \quad (6.6)$$

Here the critical density  $\rho_c$ , the model parameters  $\Delta$ ,  $\chi$  and  $\zeta$  can be expressed within

LQG setup as [76, 77]:

$$\rho_c = \frac{3M_p^2}{\gamma^2 \Delta}, \quad (6.7)$$

$$\Delta = 4\sqrt{3}\pi\gamma l_p^2 = \bar{\mu}^2 p, \quad (6.8)$$

$$\chi = \begin{cases} \sin^2 \bar{\mu} - (1 + \gamma^2) \bar{\mu}^2, & \text{for } k = +1 \\ -\gamma^2 \bar{\mu}^2, & \text{for } k = -1. \end{cases} \quad (6.9)$$

$$\zeta = \sin^2 \bar{\mu} - \frac{\bar{\mu}}{2} \sin 2\bar{\mu}, \quad (6.10)$$

where  $p$  is the triad (which without any loss of generality will be chosen with positive orientation) and the Barbero-Immirzi parameter  $\gamma$  can be fixed by computing the black hole entropy in LQG. Now let us concentrate on the classical limit,  $\Delta \rightarrow 0$ , from LQG setup one can write:

$$\chi \rightarrow -\gamma^2 \bar{\mu}^2, \quad (6.11)$$

$$\rho_1 \rightarrow \frac{3kM_p^2}{p}, \quad (6.12)$$

$$\frac{(\rho_2 - \rho)}{\rho_c} \rightarrow 1. \quad (6.13)$$

Thus we recover the Friedmann equation in classical GR in the limit  $\Delta \rightarrow 0$ . In the next subsections we will discuss the detailed cosmological consequences as well the phenomena of cosmological hysteresis from this model.

### 6.1 Condition for bounce

Bounce occurs when the following condition holds good:

$$\rho = \rho_2, \quad (6.14)$$

where the universe reaches its minimum radius  $a_{min}$  and maximum density [77] is achieved:

$$\rho_{max} = \rho_2 |_{a_{min}} \approx \rho_c. \quad (6.15)$$

Therefore condition for bounce is given by:

$$\rho_b = \rho_c. \quad (6.16)$$

The mass at bounce (neglecting the constant factor) is given by:

$$M_b = \rho_b a_b^3 = \rho_c a_b^3. \quad (6.17)$$

Therefore an infinitesimal variation in mass at bounce can be expressed as:

$$\delta M = \rho_c \delta(a_b)^3. \quad (6.18)$$

By setting the following constraint condition:

$$\delta M = -\delta W = -\oint p dV, \quad (6.19)$$

we get the expression for change in amplitude of the scale factor at each successive cycle as:

$$\delta(a_{min})^3 = -\frac{1}{\rho_c} \oint p dV \quad (6.20)$$

Thus, the amplitude of the scale factor increases iff:

$$\oint p dV < 0 \quad (6.21)$$

as the critical density  $\rho_c > 0$  always. We also observe that now the increase in scale factor depends on the critical density  $\rho_c$  but is independent of the curvature parameter  $k$ . Hence the result holds good for  $k = \pm 1$  i.e. for both open and closed universe.

## 6.2 Condition for acceleration

From Eq. (6.4), at bounce the condition for acceleration is given by:

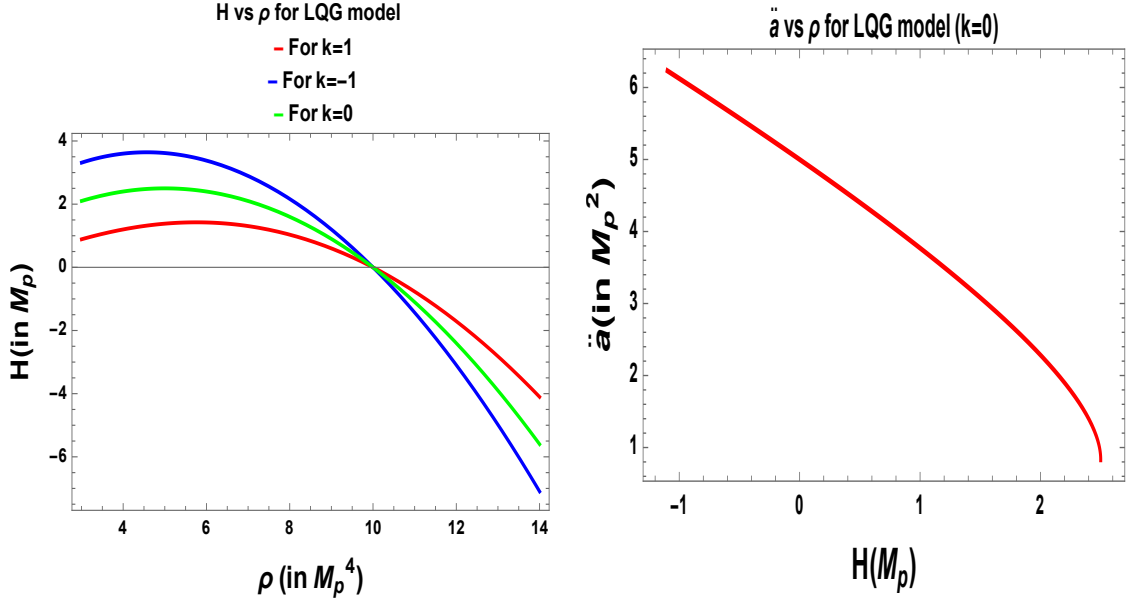
$$\begin{aligned} \frac{\ddot{a}}{a} = & -\frac{1}{6M^2}(\rho_c + 3p_b) + \frac{4}{6M^2}(1 + k\chi) \left( \rho_c + \frac{3}{2}p_b \right) \\ & + \frac{k\chi}{\gamma^2\Delta}(1 + k\chi) - \frac{2\zeta k}{\gamma^2\Delta} \left( k\chi + \frac{1}{2} \right) \end{aligned} \quad (6.22)$$

Thus it implies that whether the condition for acceleration violates the energy condition, now depends upon the values of different parameters of the LQG model present in the above expression.

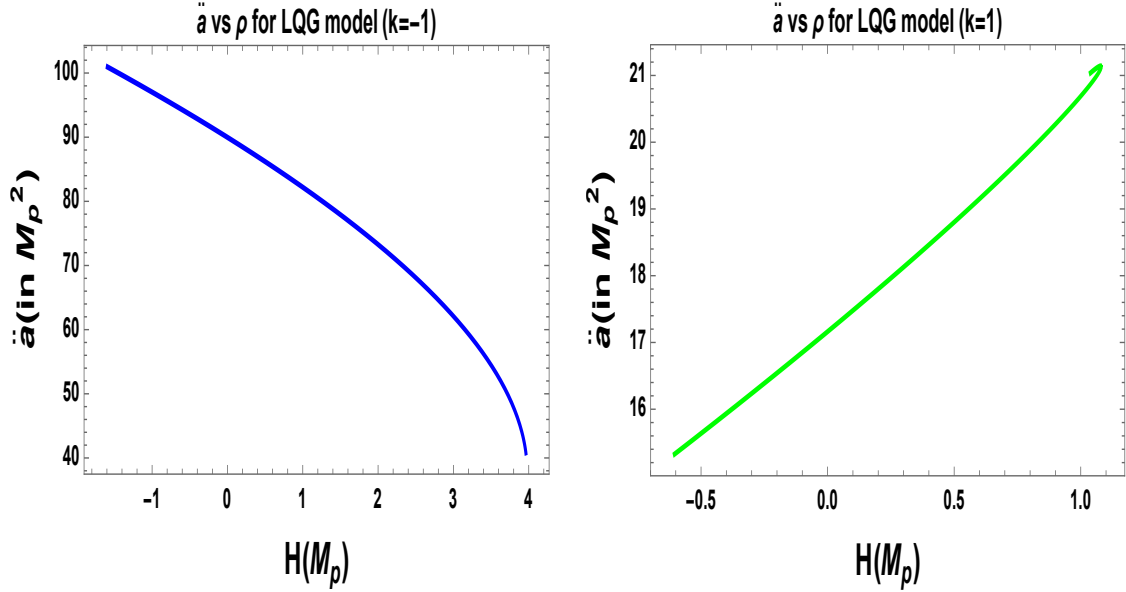
For different values of the curvature parameter  $k$  we get the following constraint conditions for acceleration at bounce as:

$$p_b > \begin{cases} -\frac{2\chi M^2(1+\chi)}{\gamma^2\Delta} + \frac{2\zeta M^2}{\gamma^2\Delta} - \frac{\rho_c(3+4\chi)}{3(1+2\chi)} & \text{for } k = +1 \\ \frac{2\chi M^2(1-\chi)}{\gamma^2\Delta} - \frac{2\zeta M^2}{\gamma^2\Delta} - \frac{\rho_c(3-4\chi)}{3(1-2\chi)} & \text{for } k = -1. \end{cases} \quad (6.23)$$

In Figs. 21, we have shown the phenomena of bounce and acceleration in the LQG model. We can draw the following conclusions from the above figures:



(a) An illustration of the bouncing condition for a universe with  $k = 1$ ,  $\rho_c = 10M^4$  for red curve and  $k = -1$ ,  $w = 1/3$ ,  $\rho_c = 10M^4$  for blue curve and  $k = -1$ ,  $w = 1/3$ ,  $\rho_c = 10M^4$  for green curve. (b) An illustration of the acceleration condition of state  $w = 0$ ,  $k = 0$ ,  $\rho_c = 10M^4$ .



(c) An illustration of the acceleration condition at the time of bounce for a universe with an equation of state  $w = 0$ ,  $k = -1$ ,  $\rho_c = 10M^4$ . (d) An illustration of the acceleration condition at the time of bounce for a universe with an equation of state  $w = 0$ ,  $k = 1$ ,  $\rho_c = 10M^4$ .

**Figure 21.** Graphical representation of the phenomena of bounce and acceleration for LQG model.

- In Fig. 21(a), we have plotted the r.h.s of Eq. (6.3) using the relation  $\rho = a^{-3(1+w)}$  with  $k = 1, \rho_c = 10M^4$  for red curve and  $k = 1, w = 1/3, \rho_c = 10M^4$  for blue curve and  $k = -1, w = 1/3, \rho_c = 10M^4$  for green curve.
- We have used  $w = 1/3$ , since we require a soft equation of state for causing the acceleration and expansion. The case  $w = 0$  causes bounce equally well. The value of  $\rho_c$  chosen is arbitrary.
- From Fig. 21(a), we can also say that the behavior of the Hubble parameter w.r.t. density is nearly same for any value of  $k$ .
- From Fig. 21(a), we get the bounce at  $\rho = \rho_b = 10M^4$  for all the three cases.
- Figs. 21(b) to 21(d), we have shown the necessary condition of acceleration ( $\ddot{a} > 0$ ) at the time of bounce for  $k = 0, -1, 1$ . Here we have plotted the r.h.s of Eqns. (6.4) and (6.3). These plots have also been obtained for  $w = 0, \rho_c = 10M^4$ .
- Thus from Fig. 21 we can conclude that for this model, bounce is possible for closed, open and flat universe.

### 6.3 Condition for turnaround

Turnaround or re-collapse occurs when the following criteria is achieved:

$$\rho = \rho_1, \quad (6.24)$$

when the universe reaches its maximum radius  $a_{max}$  and minimum density can be written as [77]:

$$\rho_1 = \rho_{min} \approx \frac{3kM^2}{a_{max}^2}. \quad (6.25)$$

Therefore, in place of Eq. (6.20), we get:

$$\delta a_{max} = -\frac{1}{3kM^2} \oint pdV \quad (6.26)$$

Unlike for the bounce case, the condition for an increase in expansion amplitude at turnaround now depends on the curvature parameter only (apart from the sign of the work done). Substituting the values of curvature parameter Eq. (6.26) can be recast in the following form:

$$\delta a_{max} = \begin{cases} -\frac{1}{3M^2} \oint pdV & \text{for } k = +1 \\ \frac{1}{3M^2} \oint pdV & \text{for } k = -1. \end{cases} \quad (6.27)$$

Let us explicitly mention the two possible physical outcomes from Eq. (6.29) appearing in the present context:

- For  $k = +1$ , in order to get an increase in the amplitude of the scale factor after each successive cycle, we need  $\oint pdV < 0$ .
- For  $k = -1$ , in order to get an increase in the amplitude of the scale factor after each successive cycle, we need  $\oint pdV > 0$ .

Rest of all the conclusions remain same as that we obtained for the case of bounce from LQG setup.

#### 6.4 Condition for deceleration

Using the definition of  $\rho_1 = -k\chi\rho_c$  from Eq. (6.4), at turnaround time scale the condition for acceleration is given by:

$$\rho_1 + 3p_t > \frac{6M^2\chi k}{\gamma^2\Delta}. \quad (6.28)$$

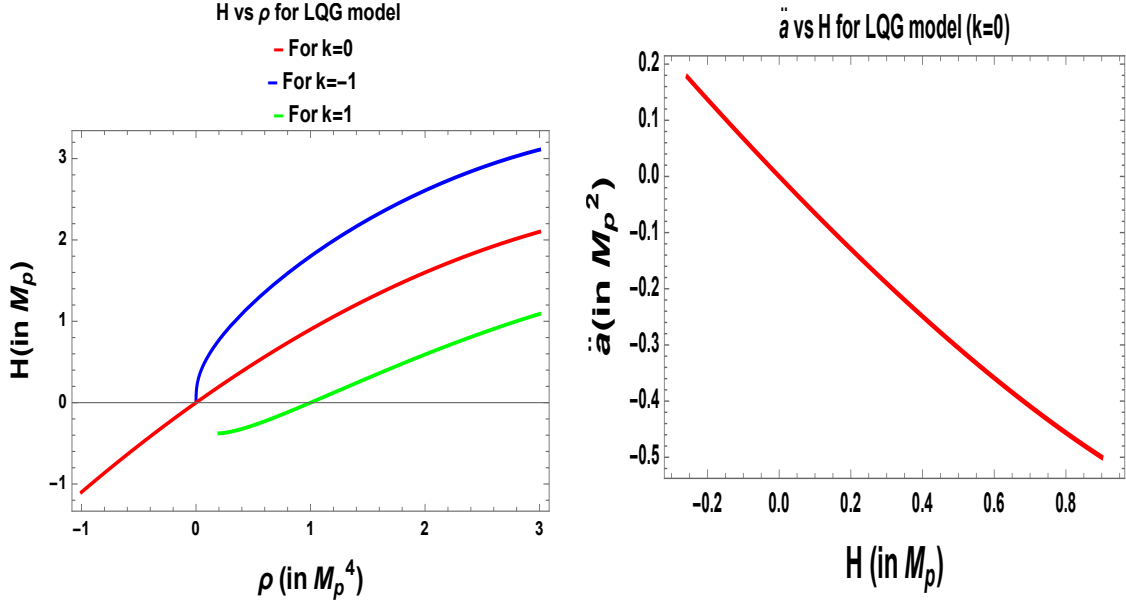
Further substituting the expression for  $\rho_1$  for different values of the curvature parameter  $k$  in non-flat case we get the following constraint conditions for acceleration at bounce as:

$$p_t = \begin{cases} M^2 \left( \frac{2\chi}{\gamma^2\Delta} - \frac{1}{a_t^2} \right) & \text{for } k = +1 \\ M^2 \left( \frac{2\chi}{\gamma^2\Delta} - \frac{1}{a_t^2} \right) & \text{for } k = -1. \end{cases} \quad (6.29)$$

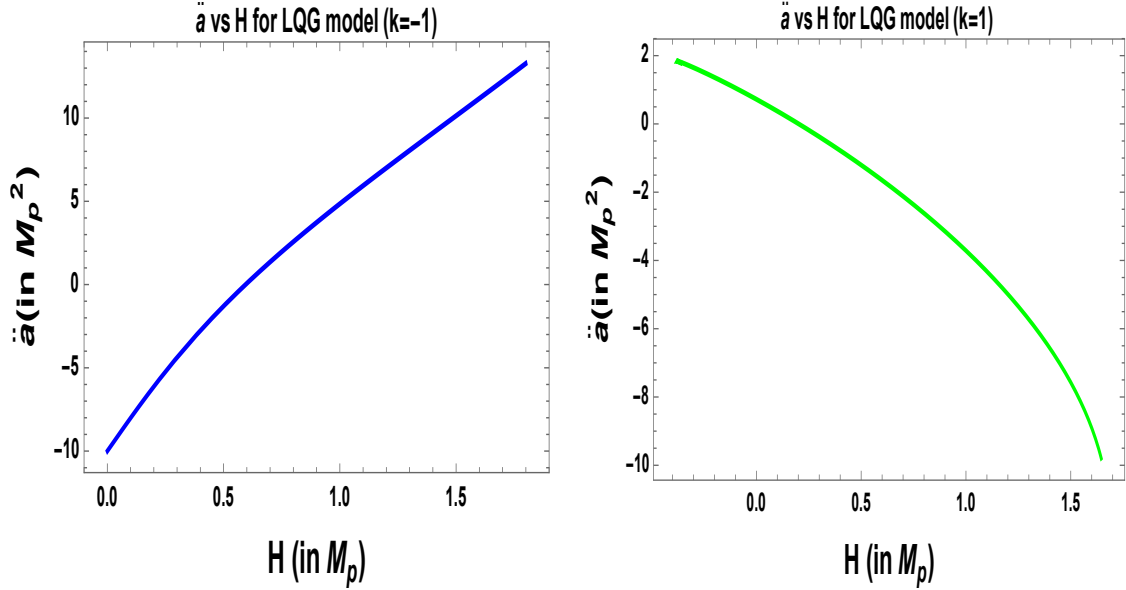
Just like the case of acceleration within LQG setup, the condition for deceleration at turnaround also depends on the LQG model parameters. Additionally it is important to note that whether this constraint violates the energy condition or not, solely governed by the numerical values of the constants.

In Fig. 22, we have shown the phenomena of turnaround and deceleration in LQG model. We can draw the following conclusions from the above figures:

- In Fig. 22(a), we have plotted the r.h.s of Eqns. (6.3), using the relation  $\rho = a^{-3(1+w)}$  with  $k = -1$ ,  $w = 1$ ,  $\rho_c = 10M^4$  for blue curve and  $k = 1$ ,  $w = 1$ ,  $\rho_c = 10M^4$  for green curve. For this case we have used  $w = 1$ , since we require a stiff equation of state for causing contraction and deceleration.
- From Fig. 22(a), we get the turnaround at  $\rho = \rho_t = 0$  for  $k = 0$ ,  $-1$  and at  $\rho = \rho_t = 1M^4$  respectively.



(a) An illustration of the turnaround condition for a universe with  $k = 0$ ,  $\rho_c = 10M^4$  for red at turnaround for a universe with  $k = 0$ ,  $\rho_c = 10M^4$  for blue curve,  $k = -1$ ,  $w = 1$ ,  $\rho_c = 10M^4$  for blue curve and  $k = 1$ ,  $w = 1$ ,  $\rho_c = 10M^4$  for green curve .



(c) An illustration of the deceleration condition at turnaround for a universe with an equation of state  $w = 1$ ,  $k = -1$ ,  $\rho_c = 10M^4$ . (d) An illustration of the deceleration condition at turnaround for a universe with an equation of state  $w = 1$ ,  $k = 1$ ,  $\rho_c = 10M^4$ .

**Figure 22.** Graphical representation of the phenomena of turnaround and deceleration for LQG model.

- Figs. 22(b), 22(c) and 22(d) show the necessary condition of deceleration ( $\ddot{a} < 0$ ) at the time of turnaround. Here we have plotted the r.h.s of Eqns. (6.4) and (6.3). This plot has also been obtained for the same parameter values as the earlier graph.
- Thus Fig. 22 shows graphically that the phenomenon of turnaround is possible for the DGP model having  $w = 1$ .

### 6.5 Evaluation of work done in one cycle

The expression for the total work done is same as that given by Eq. (4.52) in DGP model. But in order to get an expression similar to Eq. (4.63), we see that just like in DGP model, here also the Friedmann equations given by Eq. (6.3) and Eq. (6.4), which are highly complicated. Hence to get a analytical solution, just like in the case of DGP model, here also we can use the early and late time approximations to Eq. (6.3).

At early time,  $\rho \gg \rho_1$ , hence we can neglect  $\rho_1$  in Eq. (6.3). Then we get:

$$\left(\frac{\dot{a}}{a}\right)^2 = \frac{1}{3M^2} \rho \left(\frac{1}{\rho_c}(\rho_2 - \rho)\right) \quad (6.30)$$

Solving the above equation for  $\rho$  and using the following relation [76]:

$$\rho_1 + \rho_2 = \rho_c, \quad (6.31)$$

we get the following two-fold solution for the energy density:

$$\rho = \frac{\rho_c \pm \sqrt{\rho_c^2 - 4(3M^2\rho_c\left(\frac{\dot{a}}{a}\right)^2 + \rho_1\rho_2)}}{2}. \quad (6.32)$$

But we know that at the time of bounce ( $H = 0$ ), the solution of this equation is:

$$\rho = \rho_2 = \rho_c, \quad (6.33)$$

which we approximately get by setting  $H = 0$  in Eq. (6.32) and taking the positive signature in the solution. Therefore the physically acceptable solution for the density  $\rho$  is given by:

$$\rho_{phys} = \rho = \frac{\rho_c + \sqrt{\rho_c^2 - 4(3M^2\rho_c\left(\frac{\dot{a}}{a}\right)^2 + \rho_1\rho_2)}}{2}. \quad (6.34)$$

Using the energy conservation equation (continuity equation):

$$\dot{\rho} + 3H(\rho + p) = 0 \quad (6.35)$$

and Eq. (6.30), we get the following form of the second Friedmann equation written as:

$$\frac{\ddot{a}}{a} - \left(\frac{\dot{a}}{a}\right)^2 = \frac{1}{2M^2\rho_c}(2\rho - \rho_2)(\rho + p), \quad (6.36)$$



from which we get the following expression for the pressure  $p$  in early times as:

$$p = \frac{\dot{\phi}^2}{2} - V(\phi) = \frac{2M^2\rho_c}{(2\rho - \rho_2)} \left[ \left( \frac{\ddot{a}}{a} \right) - \left( \frac{\dot{a}}{a} \right)^2 \right] - \rho. \quad (6.37)$$

Further using Eq. (6.34) into Eq. (6.37), we get the following expression for the second and third integral of Eq. (4.53) as:

$$\begin{aligned} \int_{a^{i-1}}^{a_{min}^{i-1}} pdV &= \int_{a_{min}^{i-1}}^{a^{i-1}} pdV \\ &= \int 3 \left( \frac{2M^2\rho_c}{(2\rho - \rho_2)} \left[ \frac{\ddot{a}}{a} - \left( \frac{\dot{a}}{a} \right)^2 \right] - \frac{\rho_c}{2} \right) a^2 \dot{a} dt \\ &\quad + \int 3 \left( \frac{\sqrt{\rho_c^2 - 4 \left( 3M^2\rho_c \left( \frac{\dot{a}}{a} \right)^2 + \rho_1\rho_2 \right)}}{2} \right) a^2 \dot{a} dt. \end{aligned} \quad (6.38)$$

At late times,  $\rho \ll \rho_2$ , hence the following condition holds good:

$$\frac{(\rho_2 - \rho)}{\rho_c} \rightarrow 1. \quad (6.39)$$

Hence using  $\rho_1 = 3kM^2/a_{max}^2$ , Eq. (6.3) reduces to standard Friedmann equation given by:

$$\left( \frac{\dot{a}}{a} \right)^2 = \frac{(\rho - \rho_1)}{3M^2}. \quad (6.40)$$

Using the standard second Friedmann equation for acceleration and the above equation we get the following expression for pressure  $p$  as:

$$p = \frac{\dot{\phi}^2}{2} - V(\phi) = -M^2 \left[ \frac{2\ddot{a}}{a} + \left( \frac{\dot{a}}{a} \right)^2 + \frac{k}{a^2} \right]. \quad (6.41)$$

Therefore the expressions for the first and last integral in Eq. (4.53) are given by

$$\begin{aligned} \int_{a_{max}^{i-1}}^{a^{i-1}} pdV &= \int_{a^{i-1}}^{a_{max}^i} pdV \\ &= - \int 3M^2 (2\ddot{a}a + \dot{a}^3 + k\dot{a}) dt \end{aligned} \quad (6.42)$$

Therefore the complete expression of the work done in one single expansion-contraction

cycle is obtained by substituting Eq. (6.38) and Eq. (6.42) into Eq. (4.53) i.e.

$$\oint pdV = \int 3 \left( \frac{2M^2\rho_c}{(2\rho - \rho_2)} \left[ \frac{\ddot{a}}{a} - \left( \frac{\dot{a}}{a} \right)^2 \right] - \frac{\rho_c}{2} \right) a^2 \dot{a} dt$$

$$+ \int 3 \left( \frac{\sqrt{\rho_c^2 - 4 \left( 3M^2\rho_c \left( \frac{\dot{a}}{a} \right)^2 + \rho_1\rho_2 \right)}}{2} \right) a^2 \dot{a} dt$$

$$- \int 3M^2 (2\ddot{a}\dot{a}a + \dot{a}^3 + k\dot{a}) dt. \quad (6.43)$$

From the above expressions we can conclude that, at early times, work done depends on the LQG model parameters like the critical density  $\rho_c$ , but depends only on the curvature parameter  $k$  at late times.

## 6.6 Semi-analytical analysis for cosmological potentials

As we have done for the other models, here also we will consider the cases of three different potentials as mentioned earlier. In this subsection we will denote Planck mass by  $M_p$ .

### 6.6.1 Case I: Hilltop potential

Since we need to substitute the expression for the scale factor into Eq. (4.64), we need to find separate expressions for the scale factor for both early and late times during expansion and contraction phases of the Universe.

#### A. Expansion

##### i) Early time

At early time within the interval  $a_{min} < a < a'$  we will do the analysis for the case when the curvature parameter  $k \neq 0$ , because as we have already seen, that the curvature term is necessary for causing the turnaround at late times. To serve this purpose we can use the approximate Friedmann equation given by Eq. (6.30), where  $\rho$  is now given by the hilltop potential. Then substituting the resulting expression for the Hubble parameter  $H$  from LQG setup into Eq. (4.67), we get an integral equation of the following form:

$$\int d \left( \frac{\phi}{M_4} \right) \frac{\left( \frac{V_0}{3M_p^2} \right)^{1/2} \sqrt{\left( 1 + \beta \left( \frac{\phi}{M_p} \right)^p \right)} \sqrt{\left( 1 - \frac{V_0}{\rho_c} \left( 1 + \beta \left( \frac{\phi}{M_p} \right)^p \right) \right)}}{\beta p \left( \frac{\phi}{M_4} \right)^{p-1}} = - \frac{V_0}{3M_p^2} \int dt. \quad (6.44)$$

Now it is important to note that the exact analytical solution of the left hand side of the above integral equation is given in the Appendix for RSII model. But for LQG setup to get analytical result, we consider the following field redefinition:

$$\frac{\phi}{M_p} = e^\lambda, \quad (6.45)$$

where now we will solve for  $\lambda$  instead of  $\phi$ . Simplified analytical expression for  $\lambda$  was possible only if we consider the small field limiting case i.e.  $\phi/M_p \ll 1$ , which has been elaborately discussed below.

For this case we can expand the exponentials upto linear order and apply the following constraint conditions within LQG setup as:

$$\frac{p\beta\lambda}{(1+\beta)} \ll 1, \quad (6.46)$$

$$\frac{V_0(1+\beta(1+p\lambda))}{\rho_c} \ll 1. \quad (6.47)$$

Since we are in the small  $\lambda$  limit, these conditions are possible provided we choose the values of the parameters of the model accordingly. The solution for  $\lambda$  is now given by:

$$\lambda = \frac{\left(-\frac{V_0 t}{3M_p^2} + E_0\right)}{Q}, \quad (6.48)$$

where we introduce two constants  $Q$  and  $E_0$  given by:

$$Q = \left(\frac{V_0}{3M_p^2}\right)^{1/2} (1+\beta)^{1/2} \left(1 - \frac{V_0}{2\rho_c}(1+\beta)\right) \quad (6.49)$$

$$E_0 = Q\lambda_i + \frac{V_0 t_i}{3M_p^2} \quad (6.50)$$

Here  $\lambda_i$  is the value at bounce which corresponds to the time  $t = t_i$ .

Further substituting the expression for  $\lambda$  back into the approximated version of the Friedmann equation, we get the following expression for scale factor as:

$$a(t) = E_1 \exp \left[ \sqrt{\frac{V_0}{3M_p^2}} \left\{ \frac{\left( \left(1 - \frac{V_0}{2\rho_c}(1+\beta)\right) Q - \frac{E_0 p \beta V_0}{2\rho_c} + \frac{E_0 p \beta}{2(1+\beta)} \left(1 - \frac{V_0}{2\rho_c}(1+\beta)\right) \right) t}{Q} + \frac{\left( \frac{pV_0^2 \beta t^2}{12M_p^2 \rho_c} - \frac{V_0 p \beta t^2}{12M_p^2 (1+\beta)} \left(1 - \frac{V_0}{2\rho_c}(1+\beta)\right) \right)}{Q} \right\} \right], \quad (6.51)$$

where we introduce a new constant  $E_1$  given by:

$$E_1 = a_i \exp \left[ -\sqrt{\frac{V_0}{3M_p^2}} \left\{ \frac{\left( \left( 1 - \frac{V_0}{2\rho_c} (1 + \beta) \right) Q - \frac{E_0 p \beta V_0}{2\rho_c} + \frac{E_0 p \beta}{2(1+\beta)} \left( 1 - \frac{V_0}{2\rho_c} (1 + \beta) \right) \right) t_i}{Q} + \frac{\left( -\frac{p V_0^2 \beta t^2}{12 M_p^2 \rho_c} + \frac{V_0 p \beta t_i^2}{12 M_p^2 (1+\beta)} \left( 1 - \frac{V_0}{2\rho_c} (1 + \beta) \right) \right)}{Q} \right\} \right]. \quad (6.52)$$

ii) Late time:

At late times within the interval  $a' < a < a_{max}$ , the Friedmann equation is given by Eq. (6.40), which is the standard Friedmann equation appearing in the context of classical GR. Thus, in order to generate the condition for turnaround, we need to take the curvature parameter  $k \neq 0$  for this specific case. Thus, using the standard classical GR version of the Friedmann acceleration equation and considering that we have been solving for the cases when the contribution from the canonical kinetic term is smaller compared to the potential i.e.  $\rho \approx -p \approx V(\phi)$  for expansion and the contribution from the canonical kinetic term is larger compared to the potential i.e.  $\rho \approx p \approx \dot{\phi}^2/2$  for contraction, we get a differential equation for the scale factor of the form:

$$\frac{\ddot{a}}{a} - \left( \frac{\dot{a}}{a} \right)^2 - \frac{k}{a^2} = 0 \quad (6.53)$$

and solving this equation we get the two-fold expressions for the scale factor of the following form:

$$a(t) = \exp \left[ (\sqrt{E_2} t + E_2') \pm e^{2\sqrt{E_2} t + E_2'} - 2k \right] \quad (6.54)$$

and the form of  $E_2'$  and  $E_2$  can be evaluated from the appropriate boundary conditions.

Substituting the above expression back into the Friedmann equation, we get the expression for the potential as

$$V(\phi) = E_2 (1 + 2k e^{(E_2' + 2\sqrt{E_2} t)}) + e^{(-2E_2' - 2e^{(E_2' + 2\sqrt{E_2} t)} + 4k - 2\sqrt{E_2} t)}. \quad (6.55)$$

## B. Contraction

From Eq. (4.68), we see that for the contraction phase, under the approximation which we have assumed, the analysis becomes independent of the choice of the potential. Hence, the final results for the LQG model holds good for any form of the

potential.

i) Early time:

At early times within the interval  $a_{min} < a < a'$ , following the same analysis as we have already done for the case of expansion, with the new expression for density, the integral equation is now given by:

$$\int d\dot{\phi} \frac{1}{\frac{3\dot{\phi}^2}{\sqrt{6}M_p} \left(1 - \frac{\dot{\phi}^2}{2\rho_c}\right)^{1/2}} = - \int dt. \quad (6.56)$$

Solving the above integrals, we get the following expression for  $\dot{\phi}$  as:

$$\dot{\phi}^2 = \frac{2M_p^2}{3(t + E_3)^2 + \frac{M_p^2}{2\rho_c}} \quad (6.57)$$

where we introduce a new constant  $E_3$  defined as:

$$E_3 = -t_i \mp \frac{1}{\sqrt{3}} \left( \frac{2M_p^2}{\dot{\phi}_i} - \frac{M_p^2}{2\rho_c} \right)^{1/2}. \quad (6.58)$$

Here  $\dot{\phi}_i$  is the value of the derivative of the scalar field at bounce.

Integrating the above equation we get the solution for  $\phi$  as

$$\phi(t) = 2\sqrt{\frac{2}{3}} \frac{\sqrt{\rho_c}}{M_p} \tan^{-1}(\sqrt{6}(E_3 + t)\sqrt{\rho_c}/M_p) + E_3' \quad (6.59)$$

where

$$E_3' = \phi_i - 2\sqrt{\frac{2}{3}} \frac{\sqrt{\rho_c}}{M_p} \tan^{-1}(\sqrt{6}(E_3 + t_i)\sqrt{\rho_c}/M_p) \quad (6.60)$$

Further using the above expression in the Friedmann equation, we get the expression for scale factor as:

$$a(t) = E_4 \exp \left[ \frac{(-E_3 + t) \ln[M_p^2 + 3(E_3 - t)^2 \rho_c] \sqrt{\frac{M_p^2 \rho_c}{M_p^2 + 3(E_3 - t)^2 \rho_c}}}{6M_p \sqrt{\frac{(E_3 - t)^2 \rho_c}{M_p^2 + 3(E_3 - t)^2 \rho_c}}} \right] \quad (6.61)$$

where we introduce a new constant  $E_4$  defined as:

$$E_4 = a_i \exp \left[ - \frac{(-E_3 + t_i) \ln[M_p^2 + 3(E_3 - t_i)^2 \rho_c] \sqrt{\frac{M_p^2 \rho_c}{M_p^2 + 3(E_3 - t_i)^2 \rho_c}}}{6M_p \sqrt{\frac{(E_3 - t_i)^2 \rho_c}{M_p^2 + 3(E_3 - t_i)^2 \rho_c}}} \right], \quad (6.62)$$

where  $a_i$  is the value of the scale factor at the time of bounce  $t_i$ .

ii) Late time:

At late times within the interval  $a' < a < a_{max}$ , the Friedmann equation given by Eq. (6.40), which is the standard Friedmann equation as appearing in the context of classical GR. Thus, in order to generate the condition for turnaround, we need to take  $k \neq 0$  for this case. Thus, using the standard Friedmann acceleration equation and considering that we have been solving for the cases when the  $\rho \approx -p \approx V(\phi)$  for expansion and  $\rho \approx p \approx \dot{\phi}^2/2$  for contraction, we get a differential equation for the scale factor of the form:

$$\ddot{a} + \frac{2\dot{a}^2}{a} + \frac{2k}{a} = 0. \quad (6.63)$$

Now solving the above differential equation for  $a(t)$ , we get the following expression for the scale factor as:

$$a(t) = \text{InverseFunction} \left[ \frac{1}{-k \left( 1 + \text{ProductLog} \left[ \frac{e^{-1 - \frac{E_6}{k}} (K_1)^{2/k}}}{k} \right] \right)} \right] (t + E_7) \quad (6.64)$$

where  $E_6$ ,  $E_7$  and  $K_1$  are the arbitrary integration constants whose values are determined from the appropriate choice of boundary conditions <sup>3</sup>.

### C. Expression for work done

The expression for work done is given by the sum of Eq. (6.42) and Eq. (6.38). Evaluation of the integrals using the corresponding scale factor for small field limiting situation as have been calculated in this section gives

$$\oint pdV = W_1 + W_2, \quad (6.65)$$

---

<sup>3</sup> Here  $\text{InverseFunction}(f)(x)$  represents the inverse of the function  $f(x)$ .  $\text{ProductLog}$  or Lambert  $w$  function or omega function gives the principal solution for  $w$  in  $z = we^w$ , for any complex number  $z$ . By implicit differentiation, one can show that all branches of  $w$  satisfy the differential equation:  $\frac{dw}{dz} = \frac{w}{z(1+w)}$  for  $z \neq -\frac{1}{e}$ .

where  $W_1$  and  $W_2$  is defined as:

$$\begin{aligned}
W_1 = & k \operatorname{InverseFunction} \left[ \frac{1}{-k \left( 1 + \operatorname{ProductLog} \left[ \frac{-e^{-1 - \frac{E_6}{k}} (K_1)^{2/k}}{k} \right] \right)} \right] (t' - t_{max} + E_7) \\
& + 3 \operatorname{InverseFunction} \left[ \frac{1}{-k \left( 1 + \operatorname{ProductLog} \left[ \frac{-e^{-1 - \frac{E_6}{k}} (K_1)^{2/k}}{k} \right] \right)} \right] (t' - t_{max} + E_7)^3 \\
& - d_7 \left\{ \operatorname{Ei} \left[ \frac{d_6}{t_{min}} \right] - \operatorname{Ei} \left[ \frac{d_6}{t'} \right] \right\} \\
& + \frac{1}{9d_{18}} e^{-6d_{19}k} \left[ e^{3e^{d_{20}+d_{18}t_{max}}} (2 - 6e^{d_{20}+d_{18}t_{max}} + 9e^{2(d_{20}+d_{18}t_{max})}) \right. \\
& \left. + e^{3e^{d_{20}+d_{18}t'}} (-2 + 6e^{d_{20}+d_{18}t'} - 9e^{2(d_{20}+d_{18}t')}) + 9e^{4d_2k} (e^{d_{20}+d_{18}t_{max}} - e^{d_{20}+d_{18}t'}) k \right], \quad (6.66)
\end{aligned}$$

and

$$\begin{aligned}
W_2 = & -d_8 \left\{ \operatorname{Ei} \left[ \frac{3d_6}{t_{min}} \right] - \operatorname{Ei} \left[ \frac{3d_6}{t'} \right] \right\} - d_5 e^{d_6/t'} t' - d_5 e^{3d_6/t'} t' - e^{d_6/t_{min}} (d_9 + d_{10} e^{2d_6/t_{min}}) t_{min} \\
& + d_{11} \left\{ \operatorname{Ei} \left[ \frac{d_6}{t_{min}} \right] - \operatorname{Ei} \left[ \frac{d_6}{t'} \right] \right\} + d_{12} \left\{ \operatorname{Ei} \left[ \frac{3d_6}{t_{min}} \right] - \operatorname{Ei} \left[ \frac{3d_6}{t'} \right] \right\} \\
& + e^{d_6/t'} (d_9 + d_{10} e^{2d_6/t'}) t' + d_{13} e^{-d_{14}} \left\{ \operatorname{Erfi} \left[ \frac{d_{15} + 2d_{16}t_{min}}{2d_{13}} \right] - \operatorname{Erfi} \left[ \frac{d_{15} + 2d_{16}t'}{2d_{13}} \right] \right. \\
& \left. - \left( d_{17} \operatorname{Erfi} \left[ \frac{d_{15} + 2d_{16}t_{min}}{2d_{13}} \right] - d'_{17} \operatorname{Erfi} \left[ \frac{d_{15} + 2d_{16}t'}{2d_{13}} \right] \right) \right\} \\
& + \left( d_{17} \operatorname{Erfi} \left[ \frac{d_{15} + 2d_{16}t_{min}}{2d_{13}} \right] - d'_{17} \operatorname{Erfi} \left[ \frac{d_{15} + 2d_{16}t'}{2d_{13}} \right] \right) \\
& + d_5 e^{d_6/t_{min}} t_{min} + d_5 e^{3d_6/t_{min}} t_{min}, \quad (6.67)
\end{aligned}$$

where  $d_1 \dots d_{20}$  are constants that depends on the parameters of the model whose explicit forms have been given in the appendix. <sup>4</sup>.

## 6.6.2 Case II: Natural potential

### A. Expansion

#### i) Early time:

---

<sup>4</sup>Here  $\operatorname{Ei}(z)$  represents the exponential integral function, where  $\operatorname{Ei}(z) = \int \frac{e^{-z}}{z} dz$  and  $\operatorname{Erfi}$  represents the imaginary error function given by,  $\operatorname{Erfi}(z) = \frac{\operatorname{Erf}(iz)}{i}$ .

At early time, within the interval  $a_{min} < a < a'$ , we will do the analysis for the case when  $k \neq 0$ , because as we have seen, the curvature term is necessary for causing the turnaround at late times. We can use the approximate Friedmann equation given by Eq. (6.30), where  $\rho$  is now given by the natural potential. Then substituting the resulting expression of H into Eq. (4.67), we get an integral equation given by

$$\int \left( \frac{V_0}{3M_p^2} \right)^{1/2} \frac{\left( 1 + \cos \left( \frac{\phi}{f} \right) \right)^{1/2}}{\sin \left( \frac{\phi}{f} \right)} \left( 1 - \frac{V_0}{\rho_c} - \frac{V_0}{\rho_c} \cos \left( \frac{\phi}{f} \right) \right)^{1/2} = \frac{V_0}{3f^2} \int dt \quad (6.68)$$

The exact solutions of the above integrals are given in the Appendix. In order to simplify the expressions, we solve the above integrals for two limiting cases:

**a)  $\phi/f \ll 1$ :**

For this case we take small argument approximations of the trigonometric functions after which we get the solution for  $\phi$  as

$$\frac{\phi(t)}{f} = E_8 \exp \left[ \frac{V_0 t}{3\sqrt{2} f^2 \left( 1 - \frac{2V_0}{\rho_c} \right)^{1/2} \left( \frac{V_0}{3M_p^2} \right)^{1/2}} \right] \quad (6.69)$$

where

$$E_8 = \frac{\phi_i}{f} \exp \left[ - \frac{V_0 t_i}{3\sqrt{2} f^2 \left( 1 - \frac{2V_0}{\rho_c} \right)^{1/2} \left( \frac{V_0}{3M_p^2} \right)^{1/2}} \right] \quad (6.70)$$

Here  $\phi_i$  is the value of  $\phi$  at the initial time of bounce  $t_i$ .

Substituting the expression for  $\phi$  back into the Friedmann equation, we get the expression for scale factor as

$$a(t) = E_9 \exp \left[ \sqrt{2} \left( \frac{V_0}{3M_p^2} \left( 1 - \frac{2V_0}{\rho_c} \right)^{1/2} \right)^{1/2} t \right] \quad (6.71)$$

where

$$E_9 = a_i \exp \left[ - \sqrt{2} \left( \frac{V_0}{3M_p^2} \left( 1 - \frac{2V_0}{\rho_c} \right)^{1/2} \right)^{1/2} t_i \right] \quad (6.72)$$

Here  $a_i$  is the value of the scale factor at bounce.

**b)  $\phi/f \gg 1$ :**

For this case, considering the fact that for large argument the cosine function is



small and the sine function can be approximated to unity, the solution for  $\phi$  in this case simplifies to

$$\frac{\phi(t)}{f} = \frac{\left(\frac{V_0 t}{2f^2} + E_{10}\right)}{\left(1 - \frac{V_0}{2\rho_c}\right) \left(\frac{V_0}{3M_p^2}\right)^{1/2}} \quad (6.73)$$

where

$$E_{10} = \left(1 - \frac{V_0}{2\rho_c}\right) \left(\frac{V_0}{3M_p^2}\right)^{1/2} (\phi_i/f) - \frac{V_0 t_i}{3f^2} \quad (6.74)$$

Here  $\phi_i$  is the value of the scalar field at the time of bounce.

Substituting back the expression for  $\phi$  into the Friedmann equation and integrating, we get the expression for the scale factor as

$$a(t) = E_{11} \exp \left[ -\frac{\sqrt{\frac{V_0}{3M_p^2}}(V_0 - 2\rho_c)}{8V_0\rho_c^2} \left( -6\sqrt{\frac{V_0}{3M_p^2}} \sin\left(\frac{2(3E_{10}f^2 + tV_0)\rho_c}{3\sqrt{\frac{V_0}{3M_p^2}}f^2(V_0 - 2\rho_c)}\right)\rho_c \right) \right] \\ \exp \left[ -\frac{\sqrt{\frac{V_0}{3M_p^2}}(V_0 - 2\rho_c)}{8V_0\rho_c^2} \left( V_0(9\sqrt{\frac{V_0}{3M_p^2}}f^2 \sin\left(\frac{2(3E_{10}f^2 + tV_0)\rho_c}{3\sqrt{\frac{V_0}{3M_p^2}}f^2(V_0 - 2\rho_c)}\right) + 4t\rho_c) \right) \right] \quad (6.75)$$

where

$$E_{11} = a_i \exp \left[ \frac{\sqrt{\frac{V_0}{3M_p^2}}(V_0 - 2\rho_c)}{8V_0\rho_c^2} \left( -6\sqrt{\frac{V_0}{3M_p^2}} \sin\left(\frac{2(3E_{10}f^2 + t_i V_0)\rho_c}{3\sqrt{\frac{V_0}{3M_p^2}}f^2(V_0 - 2\rho_c)}\right)\rho_c \right) \right] \\ \exp \left[ \frac{\sqrt{\frac{V_0}{3M_p^2}}(V_0 - 2\rho_c)}{8V_0\rho_c^2} \left( V_0(9\sqrt{\frac{V_0}{3M_p^2}}f^2 \sin\left(\frac{2(3E_{10}f^2 + t_i V_0)\rho_c}{3\sqrt{\frac{V_0}{3M_p^2}}f^2(V_0 - 2\rho_c)}\right) + 4t_i\rho_c) \right) \right] \quad (6.76)$$

## ii) Late time:

At late times, within the interval  $a' < a < a_{max}$  the analysis is independent of the choice of the potential. Consequently the results shown in this subsection hold good for natural potential.

## **B. Contraction**

As has already been mentioned that while performing the analysis for expansion,

the conclusions for contraction phase is independent of any potential, hence remains same.

### C. Expression for work done

The expression for work done is given by the sum of Eq. (6.42) and Eq. (6.38). Evaluation of the integrals using the corresponding scale factor analytically has been possible for small field limiting situation, which as have been calculated in this section as shown below:

$$\oint pdV = D_1 + D_2, \quad (6.77)$$

where  $D_1$  and  $D_2$  is defined as:

$$\begin{aligned} D_1 = & k \operatorname{InverseFunction} \left[ \frac{1}{-k \left( 1 + \operatorname{ProductLog} \left[ \frac{-e^{-1 - \frac{E_6}{k}} (K_1)^{2/k}}{k} \right] \right)} \right] (t' - t_{max} + E_7) \\ & + 3 \operatorname{InverseFunction} \left[ \frac{1}{-k \left( 1 + \operatorname{ProductLog} \left[ \frac{-e^{-1 - \frac{E_6}{k}} (K_1)^{2/k}}{k} \right] \right)} \right] (t' - t_{max} + E_7)^3 \\ & + \frac{1}{9d_{18}} e^{-6d_{19}k} \left\{ e^{3e^{d_{20}+d_{18}t_{max}}} (2 - 6e^{d_{20}+d_{18}t_{max}} + 9e^{2(d_{20}+d_{18}t_{max})}) \right. \\ & \left. + e^{3e^{d_{20}+d_{18}t'}} (-2 + 6e^{d_{20}+d_{18}t'} - 9e^{2(d_{20}+d_{18}t')}) + 9e^{4d_2k} (e^{e^{d_{20}+d_{18}t_{max}}} - e^{e^{d_{20}+d_{18}t'}})k \right\}, \end{aligned} \quad (6.78)$$

and

$$\begin{aligned} D_2 = & d_5 e^{d_6/t_{min}} t_{min} + d_5 e^{3d_6/t_{min}} t_{min} \\ & - d_7 \left\{ \operatorname{Ei} \left[ \frac{d_6}{t_{min}} \right] - \operatorname{Ei} \left[ \frac{d_6}{t'} \right] \right\} - d_8 \left\{ \operatorname{Ei} \left[ \frac{3d_6}{t_{min}} \right] - \operatorname{Ei} \left[ \frac{3d_6}{t'} \right] \right\} \\ & - d_5 e^{d_6/t'} t' - d_5 e^{3d_6/t'} t' - e^{d_6/t_{min}} (d_9 + d_{10} e^{2d_6/t_{min}}) t_{min} \\ & + d_{11} \left\{ \operatorname{Ei} \left[ \frac{d_6}{t_{min}} \right] - \operatorname{Ei} \left[ \frac{d_6}{t'} \right] \right\} + d_{12} \left\{ \operatorname{Ei} \left[ \frac{3d_6}{t_{min}} \right] - \operatorname{Ei} \left[ \frac{3d_6}{t'} \right] \right\} \\ & + 3d_{21} (e^{d_{22}t_{min}} - e^{d_{22}t'}) - d_{23} (e^{3d_{22}t_{min}} - e^{3d_{22}t'}) \\ & + \frac{d_{24}}{3} (e^{3d_{22}t_{min}} - e^{3d_{22}t'}), \end{aligned} \quad (6.79)$$

where  $d_1 \dots d_{24}$  are constants that depends on the parameters of the model whose explicit forms have been given in the appendix. Hence from our analysis we can see that the phenomenon of hysteresis is achieved due to non-zero work done for natural

potential in LGG setup.

### 6.6.3 Case III: Coleman-Weinberg potential

#### A. Expansion

##### i) Early time:

At early time within the interval,  $a_{min} < a < a'$  to do the analysis we use non-vanishing curvature parameter  $k \neq 0$ , because as we have seen, the curvature term is necessary for causing the turnaround at late times. We can use the approximated version of the Friedmann equation as given by Eq. (6.30), where the energy density  $\rho$  is now characterized by the Coleman-Weinberg potential. Then substituting the resulting expression of H into Eq. (4.67), we get an integral equation given by

$$\int d\left(\frac{\phi}{M_p}\right) \frac{\sqrt{\left(\frac{V_0}{3M_p^2}\right) \left[1 + \left\{\alpha + \beta \ln\left(\frac{\phi}{M_p}\right)\right\} \left(\frac{\phi}{M_p}\right)^4\right] \left(1 - \frac{V_0}{3M_p^2 \rho_c} \left[1 + \left\{\alpha + \beta \ln\left(\frac{\phi}{M_p}\right)\right\} \left(\frac{\phi}{M_p}\right)^4\right]\right)}}{\left(\frac{\phi}{M_p}\right)^3 \left[4\alpha + \beta + 4\beta \ln\left(\frac{\phi}{M_p}\right)\right]} = -\frac{V_0}{3M_p^2} \int dt. \quad (6.80)$$

To compute the left hand side of the above integral equation, we consider the following field redefinition:

$$\frac{\phi}{M_p} = e^\lambda, \quad (6.81)$$

as we had done for the case of hilltop potential. Here now we will solve for the transformed or redefined field  $\lambda$  instead of  $\phi$ . Simplified analytical expressions for the above integral was possible only in the small field limiting case,  $\phi/M_p \ll 1$ , which has been elaborately discussed below.

For this case we can expand the exponentials upto linear order after which we get the following solution for  $\lambda$  as:

$$\lambda = \frac{\left(\frac{V_0}{3M_p^2}t - E_{12}\right) (4\alpha + \beta)}{(2 + \alpha) \left(\frac{V_0}{2\rho_c}\alpha + \frac{V_0}{2\rho_c} - 1\right) \left(\frac{V_0}{3M_p^2}\right)^{1/2}}, \quad (6.82)$$

where  $E_{12}$  is the arbitrary integration constant given in terms of the model parameters as:

$$E_{12} = \frac{V_0}{3M_p^2}t_i - \lambda_i(2 + \alpha) \left(\frac{V_0}{2\rho_c}\alpha + \frac{V_0}{2\rho_c} - 1\right) \left(\frac{V_0}{3M_p^2}\right)^{1/2}. \quad (6.83)$$

Here  $\lambda_i$  is the initial value at the time of bounce.

While obtaining the above expression we have assumed the following three constraint conditions:

$$\frac{V_0(1 + (\alpha + \beta\lambda)(1 + 4\lambda))}{\rho_c} \ll 1, \quad (6.84)$$

$$(\alpha + \beta\lambda)(1 + 4\lambda) \ll 1, \quad (6.85)$$

$$\frac{4\beta\lambda}{(4\alpha + \beta)} \ll 1. \quad (6.86)$$

Since we are in the small  $\lambda$  limit, these conditions are satisfied if we also choose the parameters of the model appropriately.

Further substituting the expression for  $\lambda$  back into the Friedmann equation, we get the following expression for scale factor as:

$$a(t) = E_{13} \exp \left[ \left( \frac{V_0}{3M_p^2} \right)^{1/2} \left( E't + t^2 \frac{\left( \frac{V_0}{3M_p^2} \right)}{2\left( \frac{V_0}{2\rho_c} + 4\alpha + \beta \right) \left( \frac{V_0}{3M_p^2} \right)^{1/2}} \right) \right],$$

where  $E_{13}$  is the arbitrary integration constant given in terms of the model parameters as:

$$E_{13} = a_i \exp \left[ - \left( \frac{V_0}{3M_p^2} \right)^{1/2} \left( E't_i - t_i^2 \frac{\left( \frac{V_0}{3M_p^2} \right)}{2\left( \frac{V_0}{2\rho_c} + 4\alpha + \beta \right) \left( \frac{V_0}{3M_p^2} \right)^{1/2}} \right) \right]$$

where we introduce two constants  $E'$  and  $E''$  defined as:

$$E' = \left( 1 + \frac{\alpha}{2} \right) \left( 1 - \frac{V_0}{2\rho_c} (1 + \alpha) \right) - E_{12} \frac{E''}{\frac{V_0}{2\rho_c} + 4\alpha + \beta}, \quad (6.87)$$

$$E'' = \left( 1 + \frac{\alpha}{2} \right) \left( 1 - \frac{V_0}{2\rho_c} (1 + \alpha) \right) + \left( \frac{V_0}{2\rho_c} + 4\alpha + \beta \right) \left( 1 + \frac{\alpha}{2} \right) - \left( 2\alpha + \frac{\alpha}{2} \right) \left( 1 - \frac{V_0}{2\rho_c} (1 + \alpha) \right). \quad (6.88)$$

Here  $a_i$  is the value of the scale factor at the time of bounce.

## ii) Late time:

At late time, within the interval  $a' < a < a_{max}$ , the result is independent of any specific choice of potential. We have already seen that for late times for the hilltop potential did not depend on the form of the potential, hence the results shown in that section holds good for Coleman-Weinberg potential.

## **B. Contraction**

As has already been mentioned that while performing the analysis for expansion, the conclusions for contraction phase is independent of any choice of potential, hence the conclusion remains the same as mentioned earlier for other potentials within LQG setup.

### C. Expression for work done

The expression for work done is given by the sum of Eq. (6.42) and Eq. (6.38). Since the evolution of the scale factor with time is same as that for the hilltop potential, the final expression for the work done also remains the same as that obtained for the hilltop potential. But now the constants depend on the parameters of this model under consideration. Hence we can see that the phenomenon of hysteresis is possible for Coleman-Weinberg potential in LQG setup.

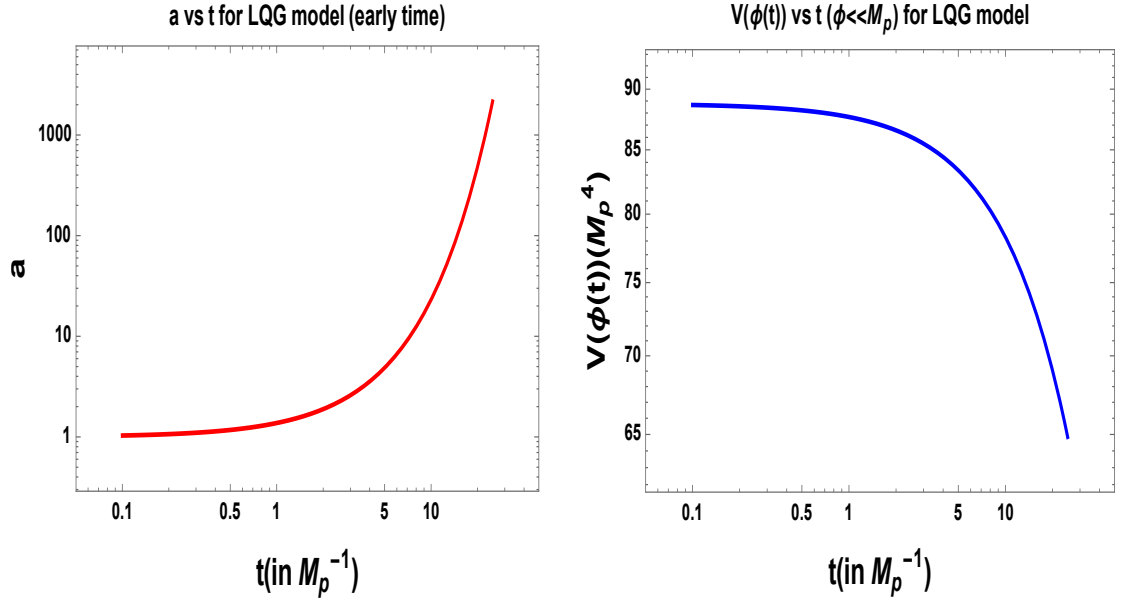
## 6.7 Graphical Analysis

### 6.7.1 Case I: Hilltop potential

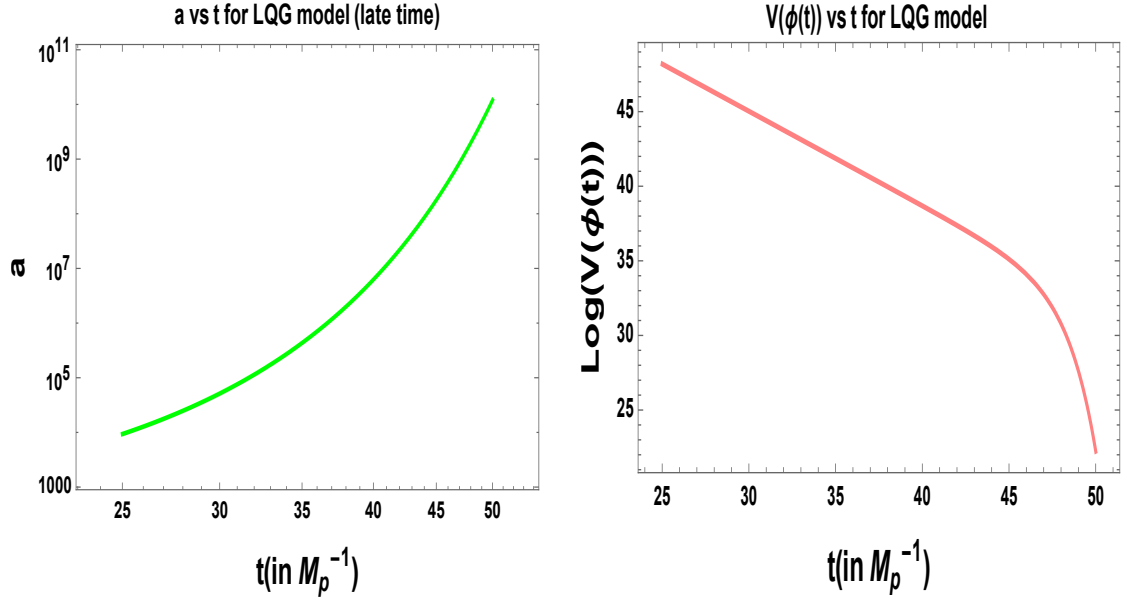
All the graphs in this section and in the following sections have been plotted in units of  $M_p = 1$ ,  $H_0 = 1$ ,  $c = 1$ , where  $M_p$  is the Planck mass,  $H_0$  is the present value of the Hubble parameter and  $c$  is the speed of light.

In Fig. 23 we have shown the evolution of the scale factor and the potential for early and late time expansion phase. From the above plots, we can draw the following conclusions:

- Fig. 23(a), shows the plot of the scale factor in the small field limit for hilltop potential given by Eq. (6.51) with the parameter values  $V_0 = 1.8 \times 10^{-3} M_p^4$ ,  $p = 3$ ,  $\beta = 1$ ,  $E_0 = 10 M_p$ ,  $\rho_c = 0.86 M_p^4$ ,  $E_1 = 1$ .
- Detail graphical analysis show that expansion is possible for both positive and negative values of  $\beta$ . However, for large positive values of  $\beta$  (such as  $> 2$ ) expansion is possible only if the values of  $V_0$  and  $E_0$  are large. For  $\beta < -1$ , expansion is not possible. And for  $\beta$  close to  $-1$ , expansion is obtained only if  $V_0$  and  $E_0$  is  $O(10^{-8})$ . Increase in  $p$  only results in an increase in the amplitude, keeping the pattern same. The plot is almost independent of the value of  $\rho_c$ .
- Fig. 23(b) shows the plot of the behavior of the potential with time for small field hilltop potential. This graph has been obtained with the help of Eqn. (6.48) with parameter values  $V_0 = 1.8 \times 10^{-3} M_p^4$ ,  $p = 3$ ,  $\beta = 1$ ,  $E_0 = 0.38 M_p$ ,  $\rho_c = 0.86 M_p^4$ . The evolution of the potential is not much affected



(a) An illustration of the behavior of the scale factor with time during the early expansion phase for  $\phi \ll M_p$  with  $V_0 = 1.8 \times 10^{-3} M_p^4$ ,  $p = 3$ ,  $\beta = 1$ ,  $E_0 = 10 M_p$ ,  $\rho_c = 0.86 M_p^4$ ,  $E_1 = 1$ .  
(b) An illustration of the behavior of the potential during early expansion phase for  $\phi \ll M_p$  with  $V_0 = 1.8 \times 10^{-3} M_p^4$ ,  $p = 3$ ,  $\beta = 1$ ,  $E_0 = 0.38 M_p$ ,  $\rho_c = 0.86 M_p^4$ .



(c) An illustration of the behavior of the scale factor with time during late time expansion phase with  $E_2 = M_p^2$ ,  $E'_2 = 0.6$ ,  $k = -1.0$ .  
(d) An illustration of the behavior of the potential during late time expansion phase with  $E_2 = 0.1 M_p^2$ ,  $E'_2 = -30$ ,  $k = 1.0$ .

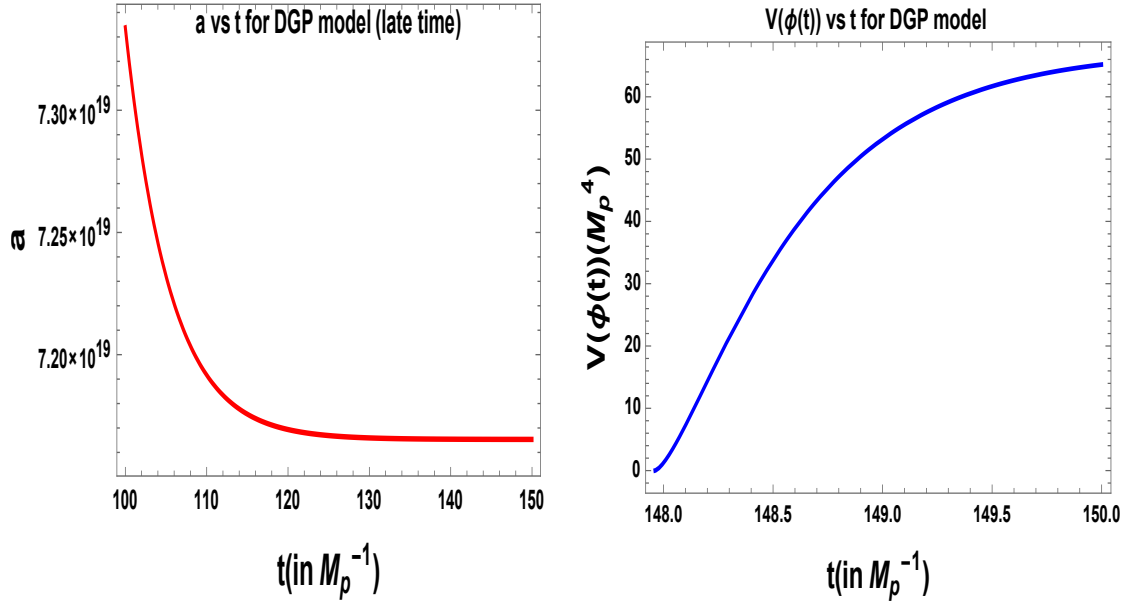
**Figure 23.** Graphical representation of the evolution of the scale factor and the potential during the expansion phase for LQG model.

by the value of  $p$  and  $\rho_c$  (only the amplitude changes).  $\beta < 0$  do not give the required evolution of the potential for causing expansion. Expansion is possible for larger positive values of  $\beta$  only if  $V_0$  is close to  $10^{-8}M_p^4$ . Larger the value of  $V_0$ , more linear the fall of the potential becomes. Expansion is possible only if the value of  $E_0 < 1M_p$ .

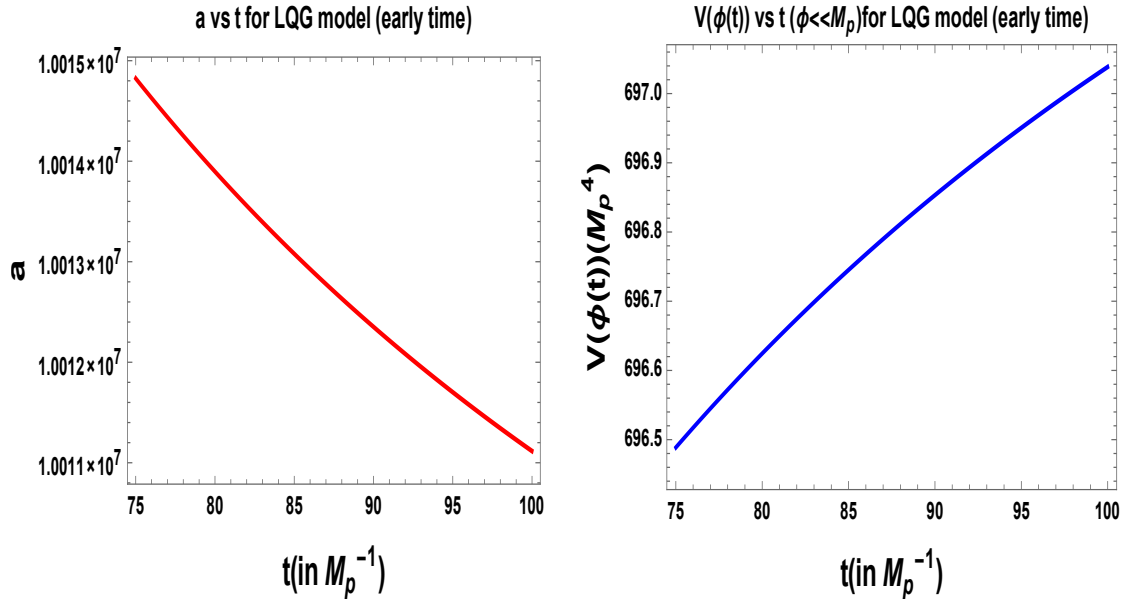
- Fig. 23(c) shows the plot of the scale factor in the late time expansion phase for hilltop potential given by Eqn. (6.54). This plot has been obtained for  $E_2 = M_p^2$ ,  $E'_2 = 0.6$ ,  $k = -1.0$ . Since the solution is true for any potential, Fig. 23(c) is also true for all the three potentials. Detail graphical analysis have shown that the pattern of the graph remains same for  $k = 1$ , only its amplitude decreases. Expansion is possible only for  $E'_2 < 1$ . Larger values of  $E_2$  increases the amplitude of expansion. Expansion is possible for both negative and positive values of the integration constants.
- Fig. 23(d) shows the evolution of the potential in the late time expansion phase for hilltop potential. Fig. 23(d) has been obtained by with the help of Eqn. (6.55) with the parameter values  $E_2 = 0.1M_p^2$ ,  $E'_2 = -30$ ,  $k = 1.0$ . Expansion is possible for negative values and slightly positive values of  $E'_2$  only and for getting the correct form of the potential with positive  $E'_2$ , we need to make  $E_2$  much less than unity. Very large values of  $E_2$  do not give the required nature of potential. Larger the magnitude of  $E'_2$ , larger is the height of the potential. In this case, we get a potential decreasing with time, which is required for expansion, only for  $k = 1$  and not for  $k = -1$ .

In Fig. 24 we have shown the evolution of the scale factor and the potential for early and late time contraction phase. From the above plots, we can draw the following conclusions:

- Fig. 24(c) shows the plot of the scale factor in the early time contraction phase for hilltop potential given by Eqn. (6.61). This plot has been obtained for  $E_3 = 10^{-8}M_p^{-1}$ ,  $E_4 = 10^7$ ,  $\rho_c = 0.86M_p^4$ . Detail graphical analysis have shown that as we increase the value of  $E_4$  and  $E_3$ , the amplitude of expansion increases but the nature of the graph remains the same. Both the amplitude and nature is almost independent of any change in the value of  $\rho_c$ .
- Fig. 24(d) shows the evolution of the potential in the early time contraction phase for hilltop potential. Fig. 24(d) has been obtained by with the help of Eqn. (6.59) with the parameter values  $V_0 = 6.3 \times 10^{-3}M_p^4$ ,  $p = 5$ ,  $\beta = 0.35$ ,  $E'_3 = 10.2M_p$ ,  $E_3 = 5M_p^{-1}$ ,  $\rho_c = 0.86M_p^4 = 1.4$ . Detail graphical analysis show that in order to get the correct nature of the potential which will result in contraction, we need  $\beta > 0$ . The other parameters do not affect the nature of the graph, but only increases its amplitude.



(a) An illustration of the behavior of the scale factor with time during the late contraction phase with  $A_4 = 100M_p^{-1}$ ,  $r = 6$ . (b) An illustration of the behavior of the potential during late contraction phase with  $V_0 = 6.1 \times 10^{-3} M_p^4$ ,  $A_3 = 152M_p^{-1}$ ,  $A_4 = 730M_p$ ,  $\beta = 0.52$ ,  $r = 1.62$ ,  $p = 1$ .



(c) An illustration of the behavior of the scale factor with time during early time contraction phase with  $E_3 = 10^{-8} M_p^{-1}$ ,  $E_4 = 10^7$ ,  $\rho_c = 0.86M_p^4$ . (d) An illustration of the behavior of the potential during early time contraction phase with  $V_0 = 6.3 \times 10^{-3} M_p^4$ ,  $p = 5$ ,  $\beta = 0.35$ ,  $E'_3 = 10.2M_p$ ,  $E_3 = 5M_p^{-1}$ ,  $\rho_c = 0.86M_p^4$ .

**Figure 24.** Graphical representation of the evolution of the scale factor and the potential during the contraction phase for LQG model.

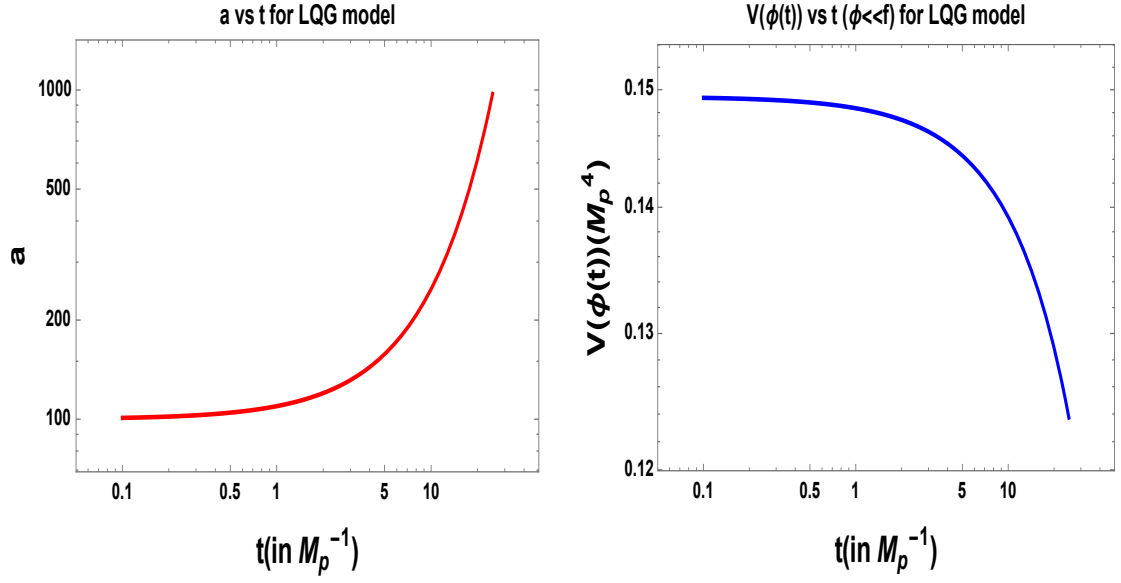


- The solution for the late time contraction phase given by Eqn. (6.64), contains inverse functions. Hence graphically solutions can be obtained only after solving the equation numerically.

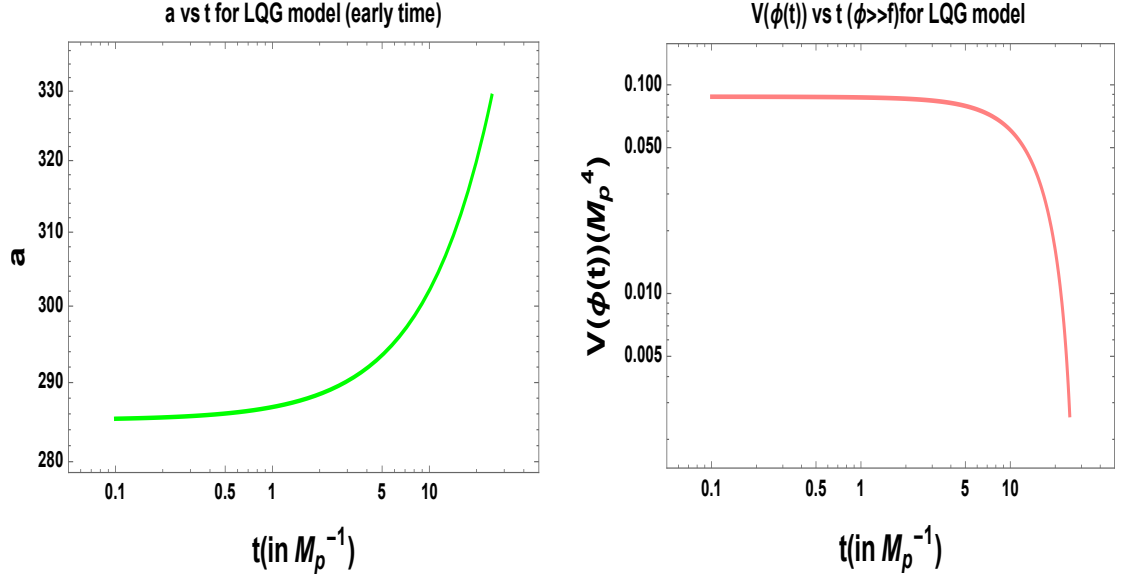
### 6.7.2 Case II: Natural potential

In Fig. 25 we have shown the evolution of the scale factor and the potential for early expansion phase. From the above plots, we can draw the following conclusions:

- Fig. 25(a), shows the plot of the scale factor in the small field limit for natural potential given by Eq. (6.71) with the parameter values  $V_0 = 4.1 \times 10^{-3} M_p^4$ ,  $E_9 = 10^2$  during the early phase of expansion.
- Higher values of  $V_0$  and  $E_9$  only increase the amplitude of expansion, keeping the nature of the plot unchanged. The change in the amplitude and nature of the plot is almost independent of the value of  $\rho_c$ .
- Fig. 25(b) shows the plot of the behavior of the potential with time for small field natural potential during the early phase of expansion. This graph has been obtained with the help of Eq. (6.69) with parameter values  $V_0 = 1.3 \times 10^{-1} M_p^4$ ,  $f = 20 M_p$ ,  $E_8 = 33$ ,  $\rho_c = 0.86 M_p^4$ . Large values of  $V_0$  and  $f$  increases the height of the potential. Only for certain range of values of  $E_8$ , we get the required evolution of the potential just like in case of the behavior of natural potential in DGP model. The evolution is almost independent of the value of  $\rho_c$ .
- The late time expansion plots remain same as given in Figs. 23(c) and 23(d). The amplitudes can be adjusted accordingly by changing the magnitudes of different parameters.
- Fig. 25(c), shows the plot of the scale factor in the large field limit for natural potential given by Eq. (6.75) with the parameter values  $V_0 = 1.5 \times 10^{-1} M_p^4$ ,  $f = 1 M_p$ ,  $E_{10} = 50 M_p$ ,  $E_{11} = 1$ ,  $\rho_c = 0.86 M_p^4$  during the early phase of expansion.
- Higher values of the  $\rho_c$ ,  $V_0$  and  $f$  only increase the amplitude of expansion, keeping the nature of the plot unchanged.
- Very large values of  $V_0$  (close to  $1 M_p^4$ ) makes the expansion uneven. Expansion is possible for both negative and positive values of  $E_{10}$ . Increasing the value of  $E_{10}$  can both increase and decrease the amplitude and makes the expansion more non linear and linear alternately.
- Fig. 25(d) shows the plot of the behavior of the potential with time for large field natural potential. This graph has been obtained with the help of Eqn. (6.73) with parameter values  $V_0 = 4.4 \times 10^{-2} M_p^4$ ,  $f = 1 M_p$ ,  $E_{10} = 6.4 M_p$ ,  $\rho_c =$



(a) An illustration of the behavior of the scale factor with time during the early expansion phase for  $\phi \ll f$  with  $V_0 = 4.1 \times 10^{-3} M_p^4$ ,  $E_9 = 10^2$ .  
 (b) An illustration of the behavior of the potential during early expansion phase for  $\phi \ll f$  with  $V_0 = 1.3 \times 10^{-1} M_p^4$ ,  $f = 20 M_p$ ,  $E_8 = 33$ ,  $\rho_c = 0.86 M_p^4$ .



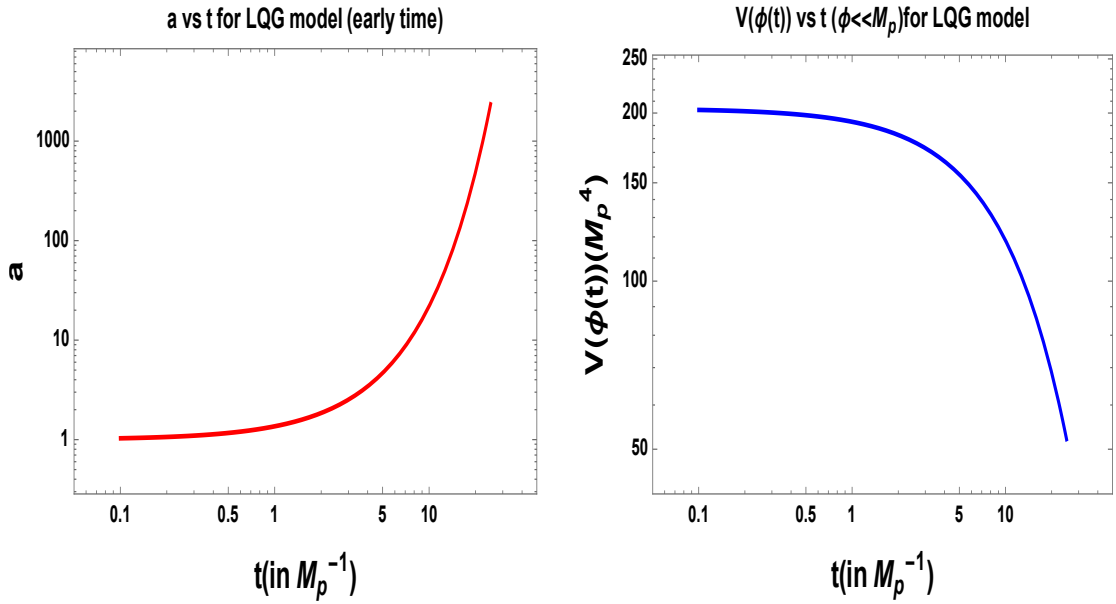
(c) An illustration of the behavior of the scale factor with time during early time expansion phase for  $\phi \gg f$  with  $V_0 = 1.5 \times 10^{-1} M_p^4$ ,  $f = 1 M_p$ ,  $E_{10} = 1 M_p$ ,  $E_{11} = 50 M_p$ ,  $E_{11} = 1$ ,  $\rho_c = 0.86 M_p^4$ .  
 (d) An illustration of the behavior of the potential during early time expansion phase for  $\phi \gg f$  with  $V_0 = 4.4 \times 10^{-2} M_p^4$ ,  $f = 1 M_p$ ,  $E_{10} = 6.4 M_p$ ,  $\rho_c = 0.86 M_p^4$ .

**Figure 25.** Graphical representation of the evolution of the scale factor and the potential during the early time expansion phase for the LQG model.

$0.86M_p^4$ . Detail analysis show that larger values of  $f$  gives smoother evolution of the potential. There are certain ranges of values for  $V_0$  and  $E_{10}$ , appearing after certain intervals, which gives rise to the correct nature of potential. Larger values of  $\rho_c$  may decrease or increase the height of the potential.

- If we compare the amplitudes of the scale factor in Fig. 24(c) with Fig. 25(a) or 25(c), we find that after one cycle of expansion and contraction, we can get a net increase in amplitude of the scale factor provided the parameters are chosen properly.

### 6.7.3 Case III: Coleman-Weinberg potential



(a) An illustration of the behavior of the scale factor with time during the early expansion phase for  $\phi \ll M_p$  with  $V_0 = 3 \times 10^{-4} M_p^4$ ,  $\alpha = M_p$ ,  $\beta = 0.4$ ,  $E_{12} = 0.08$ ,  $\beta = 0.7$ ,  $E' = 18.4$ ,  $\rho_c = 0.86$ ,  $E_{13} = 1$ . (b) An illustration of the behavior of the potential during early expansion phase for  $\phi \ll M_p$  with  $V_0 = 2.7 \times 10^{-3} M_p^4$ ,  $\beta = 0.4$ ,  $E_{12} = 0.08$ ,  $\beta = 0.7$ ,  $E' = 18.4$ ,  $\rho_c = 0.86$ ,  $E_{13} = 1$ ,  $\alpha = 0.02$ ,  $\rho_c = 0.86$ .

**Figure 26.** Graphical representation of the evolution of the scale factor and the potential during the early expansion phase for the LQG model.

In Fig. 26 we have shown the evolution of the scale factor and the potential for early small field expansion phase for supergravity potential. From the above plots, we can draw the following conclusions:

- Fig. 26(a), shows the plot of the scale factor in the small field limit for supergravity potential given by Eqn. (6.87) with the parameter values  $V_0 = 3 \times 10^{-4} M_p^4$ ,  $\alpha = 0.08$ ,  $\beta = 0.7$ ,  $E' = 18.4$ ,  $\rho_c = 0.86$ ,  $E_{13} = 1$  during the early phase of expansion.

- Expansion is possible for both negative and positive values of  $\beta$ . However, for negative values of  $\beta$ , expansion is possible only if  $\alpha > 0.5$  and  $E' > 1$ . Larger values of  $V_0$  and  $E'$  increases the amplitude of expansion. The expansion is almost independent of the value of  $\rho_c$ .
- Fig. 26(b) shows the plot of the behavior of the potential with time for small field supergravity potential during the early phase of expansion. This graph has been obtained with the help of Eqn. (6.82) with parameter values  $V_0 = 2.7 \times 10^{-3} M_p^4$ ,  $\beta = 0.4$ ,  $E_{12} = 0.61 M_p$ ,  $\alpha = 0.02$ ,  $\rho_c = 0.86$ . Correct form of the potential is obtained for both negative and positive values of  $\beta$ . However, for negative values of  $\beta$ ,  $E_{12}$  must be much less than unity. Larger the value of  $V_0$ , smaller the value of  $E_{12}$  allowed. For large positive  $\beta$ , proper evolution of the potential is possible only for very small value of  $V_0$ .  $\rho_c$  has very negligible effect on the evolution of the potential.
- If we compare the amplitudes of the scale factor in Fig. 26(a) with Fig. 24(c), we find that after one cycle of expansion and contraction, we can get a net increase in amplitude of the scale factor provided the parameters are chosen properly.

## 7 Hysteresis from Einstein-Gauss-Bonnet brane world gravity model

Einstein Gauss-Bonnet gravity is based on the theory of higher (five) dimensional brane world scenario where the simplest RS brane world action for single brane model (RSII) is modified by the addition of a Gauss Bonnet term ( $\mathcal{L}_{GB}$ ) which is a combination of the Ricci scalar  $\tilde{R}$ , the Ricci tensor  $\tilde{R}_{AB}$  and the Riemann tensor  $\tilde{R}_{ABCD}$  and is given by:

$$\mathcal{L}_{GB} = \tilde{R}^2 - 4\tilde{R}_{AB}\tilde{R}^{AB} + \tilde{R}_{ABCD}\tilde{R}^{ABCD}. \quad (7.1)$$

Consequently the action in five dimensional space-time takes the following form <sup>5</sup>:

$$S = \frac{1}{2\kappa_5^2} \int d^5 X \sqrt{-\tilde{g}} \left[ \tilde{R} - 2\Lambda + \alpha \left( \tilde{R}^2 - 4\tilde{R}_{AB}\tilde{R}^{AB} + \tilde{R}_{ABCD}\tilde{R}^{ABCD} \right) \right] + \int d^4 x \sqrt{-g} (\mathcal{L}_M^{\text{brane}} - \sigma), \quad (7.2)$$

where  $\tilde{g}_{AB}$  is the metric in the 5D bulk and

$$g_{\mu\nu} = \partial_\mu X^A \partial_\nu X^B \tilde{g}_{AB} \quad (7.3)$$

---

<sup>5</sup>One can generalize this action in arbitrary dimension  $D \geq 5$ . It is important to note that at  $D = 4$  the contribution from Gauss-Bonnet term is a topological invariant and does not contribute to the field equations. For rest of the analysis we fix the space-time dimension to be  $D = 5$  for the sake of simplicity.

is the induced metric on the brane with  $X^A(x^c)$  being the coordinates of an event on the brane labeled by  $x^c$ .

In the present context the modified Friedmann equation is given by [78]:

$$\frac{\kappa_5^4}{36}(\rho + \sigma)^2 = \left( \frac{h(a)}{a^2} + \varepsilon H^2 \right) \left[ 1 + \frac{4\alpha}{3} \left( \frac{3k - \varepsilon h(a)}{a^2} + 2H^2 \right) \right]^2, \quad (7.4)$$

where  $\sigma$  is the single brane tension,  $\alpha$  is the Gauss-Bonnet coupling,  $\Lambda$  is the 5-D cosmological constant,  $\varepsilon = +1, -1$  for space-like or time-like extra dimension respectively. Here the the function  $h(a)$  is given by the following expression:

$$h(a) = \varepsilon k + \frac{a^2}{4\alpha} \left( \varepsilon \mp \sqrt{1 + \frac{\alpha\mu}{a^4} + \frac{4}{3}\alpha\Lambda} \right), \quad (7.5)$$

where  $\mu$  is a constant.

Since the above equations are highly complicated, following the analysis of [78], we can write the above equation as:

$$C(\rho + \sigma)^2 = (A \pm H^2) (B + H^2)^2, \quad (7.6)$$

where  $\pm$  corresponds to  $\varepsilon = +1$  and  $\varepsilon = -1$  respectively. Here  $A, B$  and  $C$  are defined as:

$$A := \frac{k}{a^2} + \frac{h(a)}{a^2}, \quad (7.7)$$

$$B := \frac{3k}{2a^2} + \frac{3}{8\alpha} - \frac{\varepsilon h(a)}{2a^2} = \frac{3}{8\alpha} + \frac{3k}{2a^2} - \frac{\varepsilon A}{2}, \quad (7.8)$$

$$C := \frac{\kappa_5^4}{36} \left( \frac{3}{8\alpha} \right)^2 > 0. \quad (7.9)$$

## 7.1 Condition for bounce

### A. Space-like extra dimension with $\varepsilon = 1$

Let  $\rho = \rho_b$  is the corresponding energy density at which bounce occurs i.e. the Hubble parameter  $H = 0$  condition achieved. Hence substituting the Hubble parameter  $H = 0$  in Eq. (7.6), we get:

$$\rho_b = \frac{\sqrt{AB}}{C'} - \sigma \quad (7.10)$$

where  $C' = \sqrt{C}$  is also a constant,  $A, B$  are now fixed at the bounce.

Total mass at the bounce is given by

$$M_b = \rho_b a_b^3 = \left( \frac{\sqrt{AB}}{C'} - \sigma \right) a_b^3 \quad (7.11)$$

and infinitesimal change in mass at bounce can be expressed as:

$$\delta M_b = \frac{\sqrt{A}}{C'} \left( \frac{B\delta A a_b^3}{2A} + \delta B a_b^3 + 3B a_b^2 \delta a_b \right), \quad (7.12)$$

where infinitesimal change in  $A, B$  i.e.  $\delta A, \delta B$  can be expressed using Eq. (7.9) with  $\varepsilon = +1$  as:

$$\delta A = \frac{-2k}{a^3} \delta a + \frac{\mu a^{-5}}{\left(1 - \left(A - \frac{k}{a^2}\right) 4\alpha\right)} \delta a, \quad (7.13)$$

$$\delta B = -\frac{2k}{a^3} \delta a - \frac{\mu a^{-5}}{\left(1 - \left(A - \frac{k}{a^2}\right) 4\alpha\right)} \delta a. \quad (7.14)$$

Further substituting Eq.(7.13) and Eq. (7.14) into Eq. (7.12) and using the energy conservation equation (or continuity equation) we get the following expression for the change of the amplitude of the scale factor after one cycle as:

$$\delta a_{min} = \frac{\oint p dV}{(3\sigma a_{min}^2 - X')} \quad (7.15)$$

where we introduce a new model dependent parameter  $X'$  defined as:

$$X' = \frac{\sqrt{A}}{C'} \left[ \left( -2k + \frac{\mu a_{min}^{-2}}{\left(1 - \left(A - \frac{k}{a_{min}^2}\right) 4\alpha\right)} \right) \frac{B}{2A} - \left( 2k + \frac{\mu a_{min}^{-2}}{\left(1 - \left(A - \frac{k}{a_{min}^2}\right) 4\alpha\right)} \right) + 3B a_{min}^2 \right]. \quad (7.16)$$

Thus we see that the condition for an increase in the amplitude of the scale factor depends on  $A$  through  $X'$ , which in turn depends on the curvature parameter  $k$  and the model parameters like  $\mu, \alpha$  etc.

For  $k = +1, 0, -1$ , Eq. (7.15) can be rewritten as:

$$\delta a_{min} = \begin{cases} \frac{\oint p dV}{(3\sigma a_{min}^2 - Y')} & \text{for } k = +1 \\ \frac{\oint p dV}{(3\sigma a_{min}^2 - J')} & \text{for } k = 0 \\ \frac{\oint p dV}{(3\sigma a_{min}^2 - Z')} & \text{for } k = -1. \end{cases} \quad (7.17)$$

where  $Y'$ ,  $J'$  and  $Z'$  defined as:

$$X' = \begin{cases} Y' = \frac{\sqrt{A}}{C'} \left[ \left( -2 + \frac{\mu a_{min}^{-2}}{\left(1 - \left(A - \frac{1}{a_{min}^2}\right) 4\alpha\right)} \right) \frac{B}{2A} - \left( 2 + \frac{\mu a_{min}^{-2}}{\left(1 - \left(A - \frac{1}{a_{min}^2}\right) 4\alpha\right)} \right) + 3Ba_{min}^2 \right], & \text{for } k = +1 \\ J' = \frac{\sqrt{A}}{C'} \left[ \left( \frac{\mu a_{min}^{-2}}{(1-4A\alpha)} \right) \frac{B}{2A} - \left( \frac{\mu a_{min}^{-2}}{(1-4A\alpha)} \right) + 3Ba_{min}^2 \right], & \text{for } k = 0 \\ Z' = \frac{\sqrt{A}}{C'} \left[ \left( 2 + \frac{\mu a_{min}^{-2}}{\left(1 - \left(A + \frac{1}{a_{min}^2}\right) 4\alpha\right)} \right) \frac{B}{2A} - \left( -2 + \frac{\mu a_{min}^{-2}}{\left(1 - \left(A + \frac{1}{a_{min}^2}\right) 4\alpha\right)} \right) + 3Ba_{min}^2 \right], & \text{for } k = -1. \end{cases} \quad (7.18)$$

and now the expressions for  $A$  and  $B$  for different values of curvature parameter  $k = +1, 0, -1$  are given by:

$$A = \begin{cases} \frac{1}{a_{min}^2} + \frac{h(a_{min})}{a_{min}^2}, & \text{for } k = +1 \\ \frac{h(a_{min})}{a_{min}^2}, & \text{for } k = 0 \\ -\frac{1}{a_{min}^2} + \frac{h(a_{min})}{a_{min}^2}, & \text{for } k = -1. \end{cases} \quad (7.19)$$

and

$$B = \begin{cases} \frac{3}{2a_{min}^2} + \frac{3}{8\alpha} - \frac{h(a_{min})}{2a_{min}^2} = \frac{3}{8\alpha} + \frac{3}{2a_{min}^2} - \frac{A}{2}, & \text{for } k = +1 \\ \frac{3}{8\alpha} - \frac{h(a_{min})}{2a_{min}^2} = \frac{3}{8\alpha} - \frac{A}{2}, & \text{for } k = 0 \\ -\frac{3}{2a_{min}^2} + \frac{3}{8\alpha} - \frac{h(a_{min})}{2a_{min}^2} = \frac{3}{8\alpha} - \frac{3}{2a_{min}^2} - \frac{A}{2}, & \text{for } k = -1. \end{cases} \quad (7.20)$$

For the various values of the curvature parameter  $k = +1, 0, -1$  one can point out the following characteristics from our analysis:

- For  $k = +1$  case if we consider the situation where  $3\sigma a_{min}^2 > Y'$ , i.e. if the brane tension to be large, then an increase in the amplitude of the scale factor is possible for a positive sign of the work done i.e.  $\oint pdV > 0$ . And if the brane tension is small enough then a negative sign of the integral gives expansion with increasing amplitude.
- If we follow the analysis of [78], it shows pictorially that bounce does not occur when the extra dimension is space-like along with  $k = 0$ . We can also do similar pictorial study for the case when  $k \neq 0$  and see whether this statement remains true for  $k \neq 0$ .
- We also see that for  $k = -1$  case depending on the relative signs of  $A$ ,  $B$  and  $\sigma$ ,  $\delta a_{min}$  can be positive for both  $\oint pdV > or < 0$  cases. Thus just like for  $k = +1$ , if  $3\sigma a_{min}^2 > Z'$ , i.e. if we consider the brane tension to be large, then an increase in the amplitude of the scale factor is possible for a positive sign of the work done i.e.  $\oint pdV > 0$ . Additionally if the brane tension is small enough then a negative sign of the integral i.e.  $\oint pdV < 0$  gives expansion with increasing amplitude.

## B. Time-like extra dimension with $\varepsilon = -1$

In this context the condition for bounce is given by Eq. (7.10) with the expression of  $A$  and  $B$  now given by Eq. (7.9) with  $\varepsilon = -1$ . Hence the expression for infinitesimal change in mass at bounce  $\delta M_b$  is again given by Eq. (7.12), where the expressions for  $\delta A$  and  $\delta B$  are now given by:

$$\delta A = +\frac{2k}{a^3}\delta a - \frac{\mu a^{-5}}{(1 + (A + \frac{k}{a^2})4\alpha)}\delta a, \quad (7.21)$$

$$\delta B = -\frac{2k}{a^3}\delta a - \frac{\mu a^{-5}}{(1 + (A + \frac{k}{a^2})4\alpha)}\delta a. \quad (7.22)$$

Further substituting Eq. (7.21) and Eq. (7.22) into Eq. (7.12) and using the energy conservation equation (or continuity equation) we get the following expression for the change of the amplitude of the scale factor after one cycle as:

$$\delta a_{min} = \frac{\oint pdV}{(3\sigma a_{min}^2 - X')} \quad (7.23)$$



where the parameter  $X'$  is defined as:

$$X' = \frac{\sqrt{A}}{C'} \left[ \left( 2k + \frac{\mu a_{min}^{-2}}{\left(1 + \left(A + \frac{k}{a_{min}^2}\right) 4\alpha\right)} \right) \frac{B}{2A} - \left( 2k + \frac{\mu a_{min}^{-2}}{\left(1 + \left(A + \frac{k}{a_{min}^2}\right) 4\alpha\right)} \right) + 3Ba_{min}^2 \right]. \quad (7.24)$$

For  $k = +1, 0, -1$ , Eq. (7.23) can be rewritten as:

$$\delta a_{min} = \begin{cases} \frac{\oint pdV}{(3\sigma a_{min}^2 - Y')} & \text{for } k = +1 \\ \frac{\oint pdV}{(3\sigma a_{min}^2 - J')} & \text{for } k = 0 \\ \frac{\oint pdV}{(3\sigma a_{min}^2 - Z')} & \text{for } k = -1. \end{cases} \quad (7.25)$$

where  $Y'$ ,  $J'$  and  $Z'$  defined as:

$$X' = \begin{cases} Y' = \frac{\sqrt{A}}{C'} \left[ \left( 2 + \frac{\mu a_{min}^{-2}}{\left(1 + \left(A + \frac{1}{a_{min}^2}\right) 4\alpha\right)} \right) \frac{B}{2A} - \left( 2 + \frac{\mu a_{min}^{-2}}{\left(1 + \left(A + \frac{1}{a_{min}^2}\right) 4\alpha\right)} \right) + 3Ba_{min}^2 \right], & \text{for } k = +1 \\ J' = \frac{\sqrt{A}}{C'} \left[ \left( \frac{\mu a_{min}^{-2}}{(1+4A\alpha)} \right) \frac{B}{2A} - \left( \frac{\mu a_{min}^{-2}}{(1+4A\alpha)} \right) + 3Ba_{min}^2 \right], & \text{for } k = 0 \\ Z' = \frac{\sqrt{A}}{C'} \left[ \left( -2 + \frac{\mu a_{min}^{-2}}{\left(1 + \left(A - \frac{1}{a_{min}^2}\right) 4\alpha\right)} \right) \frac{B}{2A} - \left( -2 + \frac{\mu a_{min}^{-2}}{\left(1 + \left(A - \frac{1}{a_{min}^2}\right) 4\alpha\right)} \right) + 3Ba_{min}^2 \right], & \text{for } k = -1. \end{cases} \quad (7.26)$$

and now the expressions for  $A$  and  $B$  for different values of curvature parameter

$k = +1, 0, -1$  are given by:

$$A = \begin{cases} -\frac{1}{a_{min}^2} + \frac{1}{4\alpha} \left( \sqrt{-1 + \frac{\alpha\mu}{a_{min}^4} + \frac{4}{3}\alpha\Lambda - 1} \right), & \text{for } k = +1 \\ \frac{h(a)}{a_{min}^2}, & \text{for } k = 0 \\ \frac{1}{a_{min}^2} + \frac{1}{4\alpha} \left( \sqrt{-1 + \frac{\alpha\mu}{a_{min}^4} + \frac{4}{3}\alpha\Lambda - 1} \right), & \text{for } k = -1. \end{cases} \quad (7.27)$$

and

$$B = \begin{cases} \frac{3}{8\alpha} + \frac{3}{2a_{min}^2} + \frac{A}{2}, & \text{for } k = +1 \\ \frac{3}{8\alpha} + \frac{h(a_{min})}{2a_{min}^2} = \frac{3}{8\alpha} + \frac{A}{2}, & \text{for } k = 0 \\ \frac{3}{8\alpha} - \frac{3}{2a_{min}^2} + \frac{A}{2}, & \text{for } k = -1. \end{cases} \quad (7.28)$$

For the various values of the curvature parameter  $k = +1, 0, -1$  one can point out the following characteristics from our analysis:

- Here for  $k = +1$  case we see that depending on the relative signs of  $A$ ,  $B$  and  $\sigma$ ,  $\delta a_{min}$  can be positive for both  $\oint pdV > or < 0$ . Thus, if  $3\sigma a_{min}^2 > Y'$ , i.e. if we consider the brane tension to be large, then an increase in the amplitude of the scale factor is possible for a positive sign of the work done i.e.  $\oint pdV > 0$ . Additionally if the brane tension is small enough then a negative sign of the integral i.e.  $\oint pdV < 0$  gives expansion with increasing amplitude.
- In [78], the authors show pictorially that the bouncing condition is reached if either  $0 < B < 2A$  or  $B > 2A$  and  $\sigma < 0$  for  $k = 0$  case. We can also do similar pictorial study for the case when  $k \neq 0$  and see whether this statement remains true for  $k \neq 0$ .
- Also for  $k = -1$  case we see that depending on the relative signs of  $A$ ,  $B$  and  $\sigma$ ,  $\delta a_{min}$  can be positive for both  $\oint pdV > or < 0$ . Thus just like for  $k=+1$ , if  $3\sigma a_{min}^2 > Z'$ , i.e if we consider the brane tension to be large, then an increase

in the amplitude of the scale factor is possible for a positive sign of the work done i.e.  $\oint pdV > 0$ . And if the brane tension is small enough then a negative sign of the integral i.e.  $\oint pdV < 0$  gives expansion with increasing amplitude.

## 7.2 Condition for acceleration

### A. Space-like extra dimension with $\varepsilon = 1$

In order to get the condition for acceleration, we need to use the second Friedmann equation which we get after differentiating Eq. (7.6) w.r.t. time  $t$  for  $\varepsilon = +1$  and using the energy conservation equation to get rid of  $\dot{\rho}$ . The resulting equation is given by:

$$\dot{H} + H^2 = \frac{\ddot{a}}{a} = -\frac{3C'^2(\rho + p)(\rho + \sigma)}{Y} + \left(\frac{\dot{a}}{a}\right)^2 - \frac{Z}{Y} \quad (7.29)$$

where  $Z$  and  $Y$  are functions of  $A, B$  and their time derivatives, which are in turn functions of scale factor  $a(t)$  and its time derivative  $\dot{a}$  respectively. Their explicit expressions in terms of  $A, B$  and their derivatives are given by:

$$Y = 4AH^2 + 4AB + 2B^2 + 6H^4 + 8BH^2, \quad (7.30)$$

$$Z = \frac{\dot{A}B^2}{H} + 2\frac{AB\dot{B}}{H} + \dot{A}H^3 + 2H(\dot{A}B + A\dot{B} + B\dot{B} + \dot{B}H^2). \quad (7.31)$$

where  $H$  is the Hubble parameter.

The general condition for acceleration is given by the following expression:

$$(\rho + p)(\rho + \sigma) < \frac{1}{3C'^2}(H^2Y - Z) \quad (7.32)$$

Using Eq. (7.10) and setting  $H^2 = 0$  in the above equation, we get the following condition for acceleration at bounce as:

$$p_b < \frac{\sqrt{AB}}{C'} \left( -\frac{Z}{3AB^2} - 1 + \frac{\sigma C'}{\sqrt{AB}} \right) \quad (7.33)$$

where  $A, B, Z$  are fixed at bounce. Thus, whether this condition violates the energy condition or not, depends upon the values of the different parameters of the model.

Finally, in terms of the scalar field and its potential, the condition for acceleration can be written as:

$$\frac{\dot{\phi}^4}{2} < \frac{1}{3C'^2}(H^2Y - Z) - \frac{1}{2}\dot{\phi}^2(V(\phi) + \sigma) \quad (7.34)$$

Thus we see that the condition for acceleration in terms of the scalar field now not only depends on the kinetic term, but also on the fourth power of the time derivative of  $\phi$ .

## B. Time-like extra dimension with $\varepsilon = -1$

The second Friedmann equation is again given by Eq. (7.29) i.e.

$$\dot{H} + H^2 = \frac{\ddot{a}}{a} = -\frac{3C'^2(\rho + p)(\rho + \sigma)}{D} + \left(\frac{\dot{a}}{a}\right)^2 - \frac{E}{D}, \quad (7.35)$$

where now the expression for  $D$  and  $E$  are given by:

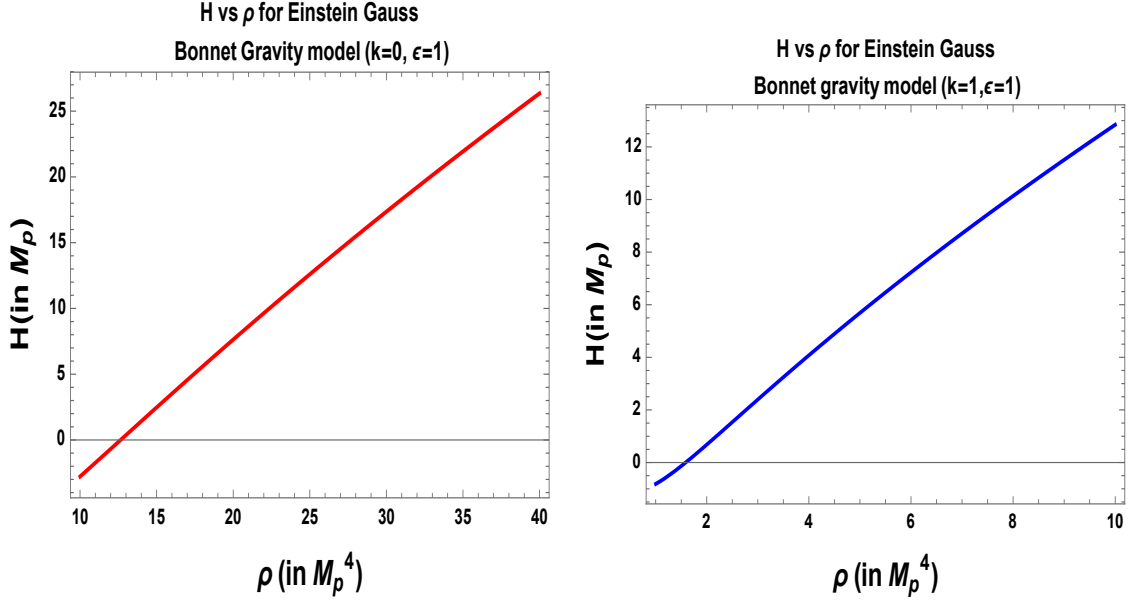
$$D = 4AH^2 + 4AB - 2B^2 - 6H^4 - 8BH^2, \quad (7.36)$$

$$E = \frac{\dot{A}B^2}{H} + 2\frac{AB\dot{B}}{H} + \dot{A}H^3 + 2H(\dot{A}B + A\dot{B} - B\dot{B} - \dot{B}H^2). \quad (7.37)$$

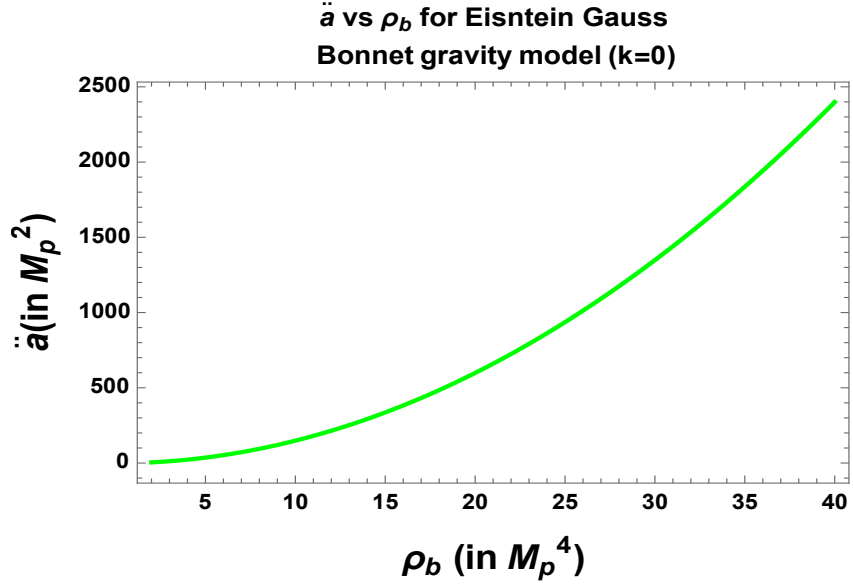
Rest all the conditions for acceleration in terms of the pressure and the scalar field remains the same with expressions for  $D$  and  $E$  now given by Eq. (7.36) and Eq. (7.37) respectively.

In Figs. 27, we have shown the phenomena of bounce and acceleration in the Einstein Gauss Bonnet gravity model. While performing this analysis, we have considered that  $\mu$  is very small and hence can be neglected. We can draw the following conclusions from the above figures:

- Figs. 27(a) and 27(b), have been plotted with the help of Eqns. (7.4), (7.5), (7.6) and (7.9) using the relation  $\rho = a^{-3(1+w)}$  with  $k = 0, A = 10M_p^2, B = 40M_p^2, \sigma = -10^{-9}M_4^4, C = 100$ . Bounce occurs for both negative and positive brane tension. Detail analysis of the scenarios under which bouncing is possible has been discussed extensively in [78].
- From Fig. 27(a), we get the bounce at  $\rho = \rho_b = 12.78M_p^4$ .
- In Fig. 27(b), we have shown the bouncing condition for  $k = 1, \varepsilon = 1, w = 1/3, C = 100, A = 10M_p^2, B = 40M_p^2, \sigma = -10^{-9}M_4^4, C = 100, \Lambda = 6 \times 10^{-3}M_p^2$ . The condition remains valid for the other combinations like ( $k = -1, \varepsilon = -1$ ), ( $k = 1, \varepsilon = -1$ ) and ( $k = -1, \varepsilon = 1$ ). But for the last case, bouncing occurs at a very small value of  $\rho$ , while for the other cases, it occurs at some larger value of  $\rho$ , which depends upon the choice of our parameters.
- For the cases ( $k = 1, \varepsilon = \pm 1$ ), bounce is possible only for negative brane tension. But for ( $k = -1, \varepsilon = \pm 1$ ), it is possible for both positive and negative brane tension. Bounce is also possible for  $w = 0$ . From Fig. 27(b), we get the bounce at  $\rho = \rho_b = 1.9M_p^4$ .



(a) An illustration of the bouncing condition for a universe with  $k = 0, A = 10M_p^2, B = 40M_p^2, \sigma = -10^{-9}M_4^4, C = 100$ .  
 (b) An illustration of the bouncing condition for a universe with  $k = 1, \epsilon = 1, w = 1/3, C = 100, A = 10M_p^2, B = 40M_p^2, \sigma = -10^{-9}M_4^4, C = 100, \Lambda = 6 \times 10^{-3}M_p^2$ .



(c) An illustration of the acceleration condition at the time of bounce for a universe with an equation of state  $w = 1/3, k = -0, A = -10M_p^2, B = 10M_p^2, C' = 10, \sigma = 1M_p^4$

**Figure 27.** Graphical representation of the phenomena of bounce and acceleration for Einstein Gauss Bonnet gravity model.

- Fig. 27(c), we have shown the necessary condition of acceleration ( $\ddot{a} > 0$ ) at the time of bounce for  $w = 1/3$ ,  $k = 0$ ,  $A = -10M_p^2$ ,  $B = 10M_p^2$ ,  $C' = 10$ ,  $\sigma = 1M_p^4$ . This plot has been obtained with the help of Eqn. (7.29). But since Eqn. (7.29) is highly complicated, in order to know the parameter space for which we get acceleration at bounce, we have instead set  $H^2 = 0$  and  $\rho = \rho_b$  in Eqn. (7.29) and analysed for what values of the parameters do we get acceleration at bounce. From detail graphical analysis, we have found that this possible if the condition  $4AB + 2B^2 < 0$  is satisfied for  $(\rho + \sigma) > 0$ , and vice versa. This is possible for both positive and negative values of  $A$ ,  $B$ ,  $\sigma$  provided the above conditions are satisfied. Similar analysis can be done for  $k = 1, -1$  also. The results remains nearly same.
- Thus from Fig. 27 we can conclude that for this model, bounce is possible for closed, open and flat universe.

### 7.3 Condition for turnaround

#### A. Space-like extra dimension with $\varepsilon = 1$

Following the same line of treatment as for bounce we get the condition for turnaround for  $\varepsilon = +1$  as:

$$\rho_t = \frac{\sqrt{AB}}{C'} - \sigma \quad (7.38)$$

where  $A$  and  $B$  are fixed at turnaround.

Following the same analysis as for bounce we get the following expression for change in the amplitude of the scale factor after each successive cycle is given by:

$$\delta a_{max} = \frac{\oint pdV}{(3\sigma a_{max}^2 - X)} = \begin{cases} \frac{\oint pdV}{(3\sigma a_{max}^2 - Y)} & \text{for } k = +1 \\ \frac{\oint pdV}{(3\sigma a_{max}^2 - J)} & \text{for } k = 0 \\ \frac{\oint pdV}{(3\sigma a_{max}^2 - Z)} & \text{for } k = -1. \end{cases} \quad (7.39)$$

where where the expressions for  $Y, J, Z$  remains same as in the bounce section

for  $Y', J', Z'$ , only with  $a_{min}$  replaced by  $a_{max}$  i.e.

$$X = \begin{cases} Y = \frac{\sqrt{A}}{C'} \left[ \left( -2 + \frac{\mu a_{max}^{-2}}{\left(1 - \left(A - \frac{1}{a_{max}^2}\right) 4\alpha\right)} \right) \frac{B}{2A} - \left( 2 + \frac{\mu a_{max}^{-2}}{\left(1 - \left(A - \frac{1}{a_{max}^2}\right) 4\alpha\right)} \right) + 3B a_{max}^2 \right], & \text{for } k = +1 \\ J = \frac{\sqrt{A}}{C'} \left[ \left( \frac{\mu a_{max}^{-2}}{(1-4A\alpha)} \right) \frac{B}{2A} - \left( \frac{\mu a_{max}^{-2}}{(1-4A\alpha)} \right) + 3B a_{max}^2 \right], & \text{for } k = 0 \\ Z = \frac{\sqrt{A}}{C'} \left[ \left( 2 + \frac{\mu a_{max}^{-2}}{\left(1 - \left(A + \frac{1}{a_{max}^2}\right) 4\alpha\right)} \right) \frac{B}{2A} - \left( -2 + \frac{\mu a_{max}^{-2}}{\left(1 - \left(A + \frac{1}{a_{max}^2}\right) 4\alpha\right)} \right) + 3B a_{max}^2 \right], & \text{for } k = -1. \end{cases} \quad (7.40)$$

and now the expressions for  $A$  and  $B$  for different values of curvature parameter  $k = +1, 0, -1$  are given by:

$$A = \begin{cases} \frac{1}{a_{max}^2} + \frac{h(a_{max})}{a_{max}^2}, & \text{for } k = +1 \\ \frac{h(a_{max})}{a_{max}^2}, & \text{for } k = 0 \\ -\frac{1}{a_{max}^2} + \frac{h(a_{max})}{a_{max}^2}, & \text{for } k = -1. \end{cases} \quad (7.41)$$

and

$$B = \begin{cases} \frac{3}{2a_{max}^2} + \frac{3}{8\alpha} - \frac{h(a_{max})}{2a_{max}^2} = \frac{3}{8\alpha} + \frac{3}{2a_{max}^2} - \frac{A}{2}, & \text{for } k = +1 \\ \frac{3}{8\alpha} - \frac{h(a_{max})}{2a_{max}^2} = \frac{3}{8\alpha} - \frac{A}{2}, & \text{for } k = 0 \\ -\frac{3}{2a_{max}^2} + \frac{3}{8\alpha} - \frac{h(a_{max})}{2a_{max}^2} = \frac{3}{8\alpha} - \frac{3}{2a_{max}^2} - \frac{A}{2}, & \text{for } k = -1. \end{cases} \quad (7.42)$$

Therefore the conclusions also remain same as for bounce case.

In [78], the authors show pictorially that for the case when  $k = 0$ , re-collapse occurs when  $A > 0, B > 0$  and  $\sigma < 0$  or is small but positive. We can also do similar pictorial study for the case when  $k \neq 0$  and find similar conditions on  $A, B$  and  $\sigma$  which gives re-collapse.

## B. Time-like extra dimension with $\varepsilon = -1$

The condition for turnaround remains same as Eq. (7.38).

Following the same analysis as for bounce we get the expression for change in the amplitude of the scale factor after each successive cycle as:

$$\delta a_{max} = \frac{\oint pdV}{(3\sigma a_{max}^2 - X)} = \begin{cases} \frac{\oint pdV}{(3\sigma a_{max}^2 - Y)} & \text{for } k = +1 \\ \frac{\oint pdV}{(3\sigma a_{max}^2 - J)} & \text{for } k = 0 \\ \frac{\oint pdV}{(3\sigma a_{max}^2 - Z)} & \text{for } k = -1. \end{cases} \quad (7.43)$$

where the expressions for  $Y, J, Z$  remains same as in the bounce section for  $Y', J', Z'$ , only with  $a_{min}$  replaced by  $a_{max}$  i.e.

$$X = \begin{cases} Y = \frac{\sqrt{A}}{C'} \left[ \left( 2 + \frac{\mu a_{max}^{-2}}{\left(1 + \left(A + \frac{1}{a_{max}^2}\right) 4\alpha\right)} \right) \frac{B}{2A} - \left( 2 + \frac{\mu a_{max}^{-2}}{\left(1 + \left(A + \frac{1}{a_{max}^2}\right) 4\alpha\right)} \right) + 3Ba_{max}^2 \right], & \text{for } k = +1 \\ J = \frac{\sqrt{A}}{C'} \left[ \left( \frac{\mu a_{max}^{-2}}{(1+4A\alpha)} \right) \frac{B}{2A} - \left( \frac{\mu a_{max}^{-2}}{(1+4A\alpha)} \right) + 3Ba_{max}^2 \right], & \text{for } k = 0 \\ Z = \frac{\sqrt{A}}{C'} \left[ \left( -2 + \frac{\mu a_{max}^{-2}}{\left(1 + \left(A - \frac{1}{a_{max}^2}\right) 4\alpha\right)} \right) \frac{B}{2A} - \left( -2 + \frac{\mu a_{max}^{-2}}{\left(1 + \left(A - \frac{1}{a_{max}^2}\right) 4\alpha\right)} \right) + 3Ba_{max}^2 \right], & \text{for } k = -1. \end{cases} \quad (7.44)$$

and now the expressions for  $A$  and  $B$  for different values of curvature parameter



$k = +1, 0, -1$  are given by:

$$A = \begin{cases} -\frac{1}{a_{max}^2} + \frac{1}{4\alpha} \left( \sqrt{-1 + \frac{\alpha\mu}{a_{max}^4} + \frac{4}{3}\alpha\Lambda - 1} \right), & \text{for } k = +1 \\ \frac{h(a)}{a_{max}^2}, & \text{for } k = 0 \\ \frac{1}{a_{max}^2} + \frac{1}{4\alpha} \left( \sqrt{-1 + \frac{\alpha\mu}{a_{max}^4} + \frac{4}{3}\alpha\Lambda - 1} \right), & \text{for } k = -1. \end{cases} \quad (7.45)$$

and

$$B = \begin{cases} \frac{3}{8\alpha} + \frac{3}{2a_{max}^2} + \frac{A}{2}, & \text{for } k = +1 \\ \frac{3}{8\alpha} + \frac{h(a_{max})}{2a_{max}^2} = \frac{3}{8\alpha} + \frac{A}{2}, & \text{for } k = 0 \\ \frac{3}{8\alpha} - \frac{3}{2a_{max}^2} + \frac{A}{2}, & \text{for } k = -1. \end{cases} \quad (7.46)$$

Therefore the conclusions also remain same as for bounce case.

In [78], the authors have shown pictorially that re-collapse occurs if  $0 < B < 2A$  for  $k = 0$ . We can also do similar pictorial study for the case when  $k \neq 0$  and find similar conditions on  $A, B$  and  $\sigma$  which gives re-collapse.

## 7.4 Condition for deceleration

### A. Space-like extra dimension with $\varepsilon = 1$

In this subsection the analysis again remains the same giving in place of Eq. (7.32), the governing constraint condition is given by:

$$(\rho + p)(\rho + \sigma) > \frac{1}{3C'^2}(H^2Y - Z), \quad (7.47)$$

and in place of Eq. (7.33) and Eq. (7.34), we get:

$$p_t > \frac{\sqrt{AB}}{C'} \left( -\frac{Z}{3AB^2} - 1 + \frac{\sigma C'}{\sqrt{AB}} \right), \quad (7.48)$$

$$\frac{\dot{\phi}^4}{2} > \frac{1}{3C'^2}(H^2Y - Z) - \frac{1}{2}\dot{\phi}^2(V(\phi) + \sigma). \quad (7.49)$$

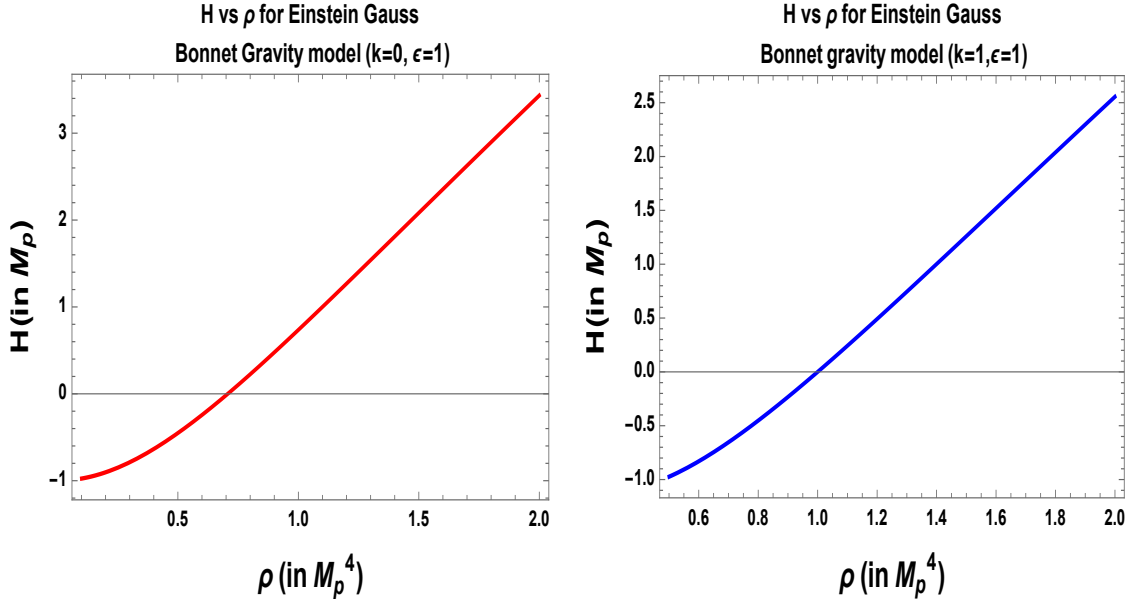
Thus we again see that this condition now depends on the fourth power of the time derivative of the scalar field as mentioned earlier.

## B. Time-like extra dimension with $\varepsilon = -1$

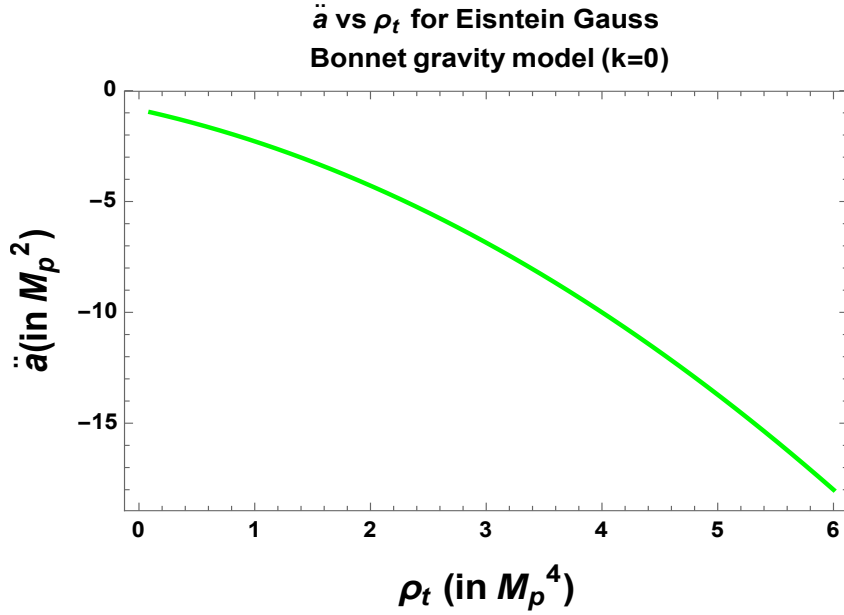
In the present context the analysis again remains the same as the final governing equations are exactly same as Eq. (7.47), Eq. (7.48) and Eq. (7.49) in which only the signatures of  $Y, Z, A, B$  changes accordingly due to  $\varepsilon = -1$ .

In Fig. 28, we have shown the phenomena of turnaround and deceleration in Einstein Gauss Bonnet gravity model. We can draw the following conclusions from the above figures:

- Fig. 28(a), has been plotted with the help of Eqns. (7.4), (7.5), (7.6) and (7.9) using the relation  $\rho = a^{-3(1+w)}$  with  $k = 0$ ,  $A = 1$ ,  $B = 10$ ,  $\sigma = -10^{-9}M_p^4$ ,  $C = 200$ . Detail graphical analysis show that the condition of turnaround is achieved only when  $A > 0$ ,  $B > 0$ ,  $\sigma < 0$  or is small positive. For further detail analysis of this case, one may refer to [78].
- From Fig. 28(a), we get the turnaround at  $\rho = \rho_t = 0.7M_p^4$ .
- Fig. 28(b) shows turnaround using Eqns. (Eqns. (7.4), (7.5), (7.6) and (7.9)) with  $w = 1$ ,  $k = 1$ ,  $\varepsilon = 1$ ,  $\sigma = -10^{-9}M_p^4$ ,  $C = 200$ . For this case we have used  $w = 1$ , since we require a stiff equation of state for causing contraction and deceleration. The parameter space causing turnaround remains same as that for bounce case. From Fig. 28(b), we get the turnaround at  $\rho = \rho_t = 1.0M_p^4$ .
- Fig. 28(c), we have shown the necessary condition of deceleration ( $\ddot{a} < 0$ ) at the time of turnaround for  $w = 1$ ,  $k = 0$ ,  $A = 10$ ,  $B = 15$ ,  $\sigma = 1M_p^4$ ,  $C' = 10$ . This plot has been obtained with the help of Eqn. (7.29). But since Eqn. (7.29) is highly complicated, in order to know the parameter space for which we get deceleration at turnaround, we have instead set  $H^2 = 0$  and  $\rho = \rho_b$  in Eqn. (7.29) and analysed for what values of the parameters do we get deceleration at turnaround (similar to the analysis done for bounce). From detail graphical analysis, we have found that this possible if the condition  $4AB + 2B^2 > 0$  is satisfied for  $(\rho + \sigma) > 0$ , and vice versa. This is possible for both positive and negative values of  $A$ ,  $B$ ,  $\sigma$  provided the above conditions are satisfied. Similar analysis can be done for  $k = 1, -1$  also. The results remains nearly same.
- Thus from Fig. 28 we can conclude that for this model, turnaround is possible for closed, open and flat universe.



(a) An illustration of the turnaround condition for a universe with  $k = 0$ ,  $A = 1M_p^2$ ,  $B = 10M_p^2$ ,  $\sigma = -10^{-9}M_p^4$ ,  $C = 200$ .  
 (b) An illustration of the turnaround condition for a universe with an equation of state  $w = 1$ ,  $k = 1$ ,  $\epsilon = 1$ ,  $\sigma = -10^{-9}M_p^4$ ,  $C = 200$ .



(c) An illustration of the deceleration condition at turnaround for a universe with an equation of state  $w = 1$ ,  $k = 0$ ,  $A = 10$ ,  $B = 15$ ,  $\sigma = 10^{-9}M_p^4$ ,  $C' = 10$ .

**Figure 28.** Graphical representation of the phenomena of turnaround and deceleration for Einstein Gauss Bonnet gravity model.

## 7.5 C. Evaluation of work done for one cycle

The expression for the total work done is same as that given by Eq. (4.52) in DGP model. But we can also express it in terms of the scale factor by using Eq. (7.29) and Eq. (7.6) in order to get an expression of the pressure in terms of the scale factor, which we can then substitute into the integral for the work done to get:

### A. Space-like extra dimension with $\varepsilon = 1$

$$\begin{aligned} \oint pdV &= \oint 3\dot{a} \frac{a^2}{C'} (A + H^2)^{1/2} (B + H^2) \left( \pm \frac{(H^2 Y - Z - \frac{\ddot{a}}{a} Y)}{3(A + H^2)(B + H^2)^2} \mp 1 \right) dt \\ &\quad + \oint 3\dot{a} \frac{a^2}{C'} (A + H^2)^{1/2} (B + H^2) \left( \frac{\sigma C'}{(A + H^2)^{1/2} (B + H^2)} \right) dt. \end{aligned} \quad (7.50)$$

### B. Time-like extra dimension with $\varepsilon = -1$

$$\begin{aligned} \oint pdV &= \oint 3\dot{a} \frac{a^2}{C'} (A - H^2)^{1/2} (B + H^2) \left( \pm \frac{(H^2 Y - Z - \frac{\ddot{a}}{a} Y)}{3(A - H^2)(B + H^2)^2} \mp 1 \right) dt \\ &\quad + \oint 3\dot{a} \frac{a^2}{C'} (A - H^2)^{1/2} (B + H^2) \left( \frac{\sigma C'}{(A - H^2)^{1/2} (B + H^2)} \right) dt. \end{aligned} \quad (7.51)$$

Thus the work done now depends not only on the scale factor, but also on the different parameters of the model like the coupling constant, brane tension etc within the present setup.

## 7.6 RSII limit

It has been shown in [79], that in the limit,  $\alpha \rightarrow 0$ , Eq. (7.4) reduces to RSII scenario. Then all the results shown in [11], for the case when all the other parameters are made zero and the extra dimension is time-like, will also hold true for the above model. These results have been shown once again in the appendix for the sake of clarity.

## 7.7 Semi-analytical analysis for cosmological potentials

In the analysis below, we will denote Planck mass by  $M_p$ . Here we will perform the analysis for  $k = 0$  case. One can repeat the analysis for  $k = \pm 1$  as well.

### 7.7.1 Case I: Hilltop potential

#### A. Expansion

##### A1. Space-like extradimension ( $\varepsilon = +1$ )

Using Eq. (4.67) and Eq. (7.6) for  $\varepsilon = +1$  and using the explicit form of  $\rho$ , which is specified by the hilltop potential as mentioned earlier, we get an integral equation of the following form:

$$\int d\left(\frac{\phi}{M_p}\right) \frac{\sqrt{\left[-\left(\sqrt{A} + \frac{1}{2}\frac{B}{\sqrt{A}}\right)2\sqrt{A} + \sqrt{A}\sqrt{\left\{R \pm 2\sqrt{\frac{C}{A}}V_0\left(1 + \beta\left(\frac{\phi}{M_p}\right)^p\right)\right\}}\right]}}{\sqrt{2}\beta p\left(\frac{\phi}{M_p}\right)^{p-1}} = -\frac{V_0}{3M_p^2} \int dt, \quad (7.52)$$

where

$$R = A + \frac{B^2}{4A} - 3B \pm 2\sqrt{\frac{C}{A}}\sigma \quad (7.53)$$

While arriving at the above integral, we have considered that  $\mu$  is small enough such that the term  $\alpha\mu/a^4$  can be neglected and  $\alpha$  should be small such that  $A$  is a large number hence the following constraint holds good:

$$\frac{H^2}{A} \ll 1. \quad (7.54)$$

By neglecting  $\mu$ , the quantities A and B becomes independent of scale factor, hence allowing us to attain some analytical approximate solutions. To compute the left hand side of the above integral equation, we will again use the following redefinition of the field:

$$\frac{\phi}{M_p} = e^\lambda. \quad (7.55)$$

Analytical solution was possible only for the case in the small field limiting case i.e. when  $\phi/M_p \ll 1$  which has been discussed below.

In this limit Expanding the exponentials upto linear order and applying two conditions:

$$\frac{\sqrt{C}\beta V_0\left(\frac{\phi}{M_p}\right)^p}{\left(A + \frac{B}{2A} - 3B \pm 4\sqrt{\frac{C}{A}}\sigma + 4\sqrt{\frac{C}{A}}V_0\right)} \ll 1, \quad (7.56)$$

$$\frac{\sqrt{C}\beta V_0}{\left(A + \frac{B}{2A} - 3B \pm 4\sqrt{\frac{C}{A}}\sigma + 4\sqrt{\frac{C}{A}}V_0 - \left(A + \frac{B}{2}\right)\right)} \ll 1, \quad (7.57)$$

we get the solution for  $\lambda$  as:

$$\lambda = \frac{-\frac{V_0 p \beta \sqrt{2}}{3M_p^2} t + F_0}{(\sqrt{R + 2\sqrt{C}V_0} - 2(A + \frac{B}{2}))^{1/2} S} \quad (7.58)$$

where we introduce a new constant  $F_0$ , which is defined in terms of the model parameters as:

$$F_0 = \lambda_i \left( \sqrt{R + 4\sqrt{\frac{C}{A}}V_0} - (A + \frac{B}{2}) \right)^{1/2} S + \frac{V_0 p}{3M_p^2} t_i, \quad (7.59)$$

where  $S$  is given by:

$$S = 1 \pm \frac{1}{2} \left( \frac{C}{(R + 2\sqrt{C}V_0) \left( \sqrt{R + 2\sqrt{C}V_0} - 2(A + \frac{B}{2}) \right)} \right)^{1/2} \beta. \quad (7.60)$$

Here  $\lambda_i$  is the value at bounce.

Substituting the above expression in the Friedmann equation, we get the expression for scale factor as

$$a(t) = F_1 \exp \left[ \left\{ \sqrt{R + 4\sqrt{\frac{C}{A}}V_0} - (A + \frac{B}{2}) \right\}^{1/2} \left( St + \frac{tp(S-1)F_0}{\sqrt{\left( \sqrt{R + 4\sqrt{\frac{C}{A}}V_0} - (A + \frac{B}{2}) \right) S}} \right) \mp \left\{ \sqrt{R + 4\sqrt{\frac{C}{A}}V_0} - (A + \frac{B}{2}) \right\}^{1/2} \frac{\frac{t^2}{2} p(S-1) \frac{V_0 p}{3M_p^2}}{\sqrt{\left( \sqrt{R + 4\sqrt{\frac{C}{A}}V_0} - (A + \frac{B}{2}) \right) S}} \right], \quad (7.61)$$

where the overall factor  $F_1$  can be expressed in terms of the model parameters as:

$$\begin{aligned}
F_1 = a_i \exp & \left[ \left\{ \sqrt{R + 2\sqrt{C}V_0} \right. \right. \\
& \left. \left. - 2\left(A + \frac{B}{2}\right) \right\}^{1/2} \left( S + \frac{p(S-1)F_0}{\sqrt{\left(\sqrt{R + 4\sqrt{\frac{C}{A}}V_0 - \left(A + \frac{B}{2}\right)\right)S}} \right) t_i \right. \\
& \left. \pm \left\{ \sqrt{R + 2\sqrt{C}V_0} \right. \right. \\
& \left. \left. - 2\left(A + \frac{B}{2}\right) \right\}^{1/2} \frac{\frac{t_i^2}{2}p(S-1)\frac{V_0p\beta\sqrt{2}}{3M_p^2}}{\sqrt{\left(\sqrt{R + 4\sqrt{\frac{C}{A}}V_0 - \left(A + \frac{B}{2}\right)\right)S}} \right]. \quad (7.62)
\end{aligned}$$

Here  $a_i$  is the value of the scale factor at the time of bounce. Thus we see that the scale factor varies exponentially with time in the small field limit during expansion.

## A2. Time-like extra dimension

The results remain same as for space-like extra dimension with the expression for  $R$  now given by:

$$R = A + \frac{B^2}{4A} + 3B \pm 2\sqrt{\frac{C}{A}}\sigma. \quad (7.63)$$

## B. Contraction

Following the same procedure as for the expansion phase, but with the expression for density is now given by  $\dot{\phi}^2/2$ , we get the following solutions:

$$\dot{\phi} = \frac{1 + \left[ 1 - \left\{ \left( -2\left(A + \frac{B}{2}\right) + \sqrt{AR} \right) (-t + F_2) + 1 \right\} \frac{1}{\sqrt{R(-2(A + \frac{B}{2}) + \sqrt{AR})}} \right]}{\frac{1}{\sqrt{R(-2(A + \frac{B}{2}) + \sqrt{AR})}}}, \quad (7.64)$$

$$\begin{aligned}
\phi(t) = 2t\sqrt{R} \left( -2\left(A + \frac{B}{2}\right) + \sqrt{AR} \right) - F_2 \left( -2\left(A + \frac{B}{2}\right) + \sqrt{AR} \right) t \\
+ \frac{\left( -2\left(A + \frac{B}{2}\right) + \sqrt{AR} \right) t^2}{2} + F_3, \quad (7.65)
\end{aligned}$$

where we introduce two arbitrary integration constants  $F_2$  and  $F_3$ , which is given in terms of model parameters as:

$$F_2 = \frac{\dot{\phi}_f - 2\sqrt{R} \left( -2 \left( A + \frac{B}{2} \right) + \sqrt{AR} \right)}{2A + B - \sqrt{AR}} - \frac{t_f(\sqrt{AR} - B - 2A)}{2A + B - \sqrt{AR}}, \quad (7.66)$$

$$F_3 = \phi_f - 2t_f\sqrt{R} \left( -2 \left( A + \frac{B}{2} \right) + \sqrt{AR} \right) + F_2 \left( -2 \left( A + \frac{B}{2} \right) + \sqrt{AR} \right) t_f + \frac{\left( -2 \left( A + \frac{B}{2} \right) + \sqrt{AR} \right) t_f^2}{2}. \quad (7.67)$$

Further substituting back into the Friedmann equation, we get the following solution for the scale factor as:

$$a(t) = F_4 \exp \left[ \sqrt{\frac{D''}{2}} \left( t - \frac{(-2 + D' + D'F_3D'' - D'D''t)^3}{3D'^2D''} \right) \right], \quad (7.68)$$

where we introduce a arbitrary integration constant  $F_4$ , which is given in terms of model parameters as:

$$F_4 = a_f \exp \left[ -\sqrt{\frac{D''}{2}} \left( t_f - \frac{(-2 + D' + D'F_3D'' - D'D''t_f)^3}{3D'^2D''} \right) \right]. \quad (7.69)$$

Here  $D'$  and  $D''$  is given by:

$$D' = \frac{1}{\sqrt{R} \left( -2 \left( A + \frac{B}{2} \right) + \sqrt{AR} \right)}, \quad (7.70)$$

$$D'' = -2 \left( A + \frac{B}{2} \right) + \sqrt{AR}, \quad (7.71)$$

and  $a_f$  is the value of the scale factor at turnaround. Here also the dependence is exponential but includes higher powers of time.

## C. Expression for work done

The expression for work done is obtained by substituting the expressions for scale factor into the Eq. (7.50), taking care of the assumptions that we have made earlier in the context of Einstein-Gauss-Bonnet brane world model.

### A1. Space-like extra dimension:



$$\begin{aligned}
\oint p dV = & f_8(-f_1 t_{max}^4 + f_2 t_{max}^5 - f_3 t_{max}^6 + f_4 t_{max}^7 - f_5 t_{max}^8 \\
& + f_6 t_{max}^9 - f_7 t_{max}^{10} + f_1 t_{min}^4 - f_2 t_{min}^5 + f_3 t_{min}^6 \\
& - f_4 t_{min}^7 + f_5 t_{min}^8 - f_6 t_{min}^9 + f_7 t_{min}^{10}) \\
& + f_9(Erf[(-f_{10} + f_{11} t_{max})] - Erf[(-f_{10} + f_{11} t_{min})])
\end{aligned} \tag{7.72}$$

where  $f_1 \dots f_{11}$  are the constants whose functional form depends on the parameters as appearing in the expression for the scale factor. Their explicit forms have been given in the appendix.

## B. Time like extra dimensions:

Since the solutions for the scale factor in the expansion and contraction phase remain same barring the constants, the final results for work done in this case also remain same.

Thus we see that since the work done after a complete cycle is non-zero, at least for the approximated expressions for the scale factor which we have evaluated in this paper. Thus hysteresis phenomenon can be explained for hilltop potential in the small field limit for Einstein Gauss Bonnet brane world gravity.

### 7.7.2 Case II: Natural potential

#### A. Expansion

Repeating the analysis as we have done for the hilltop potential, we get the expressions for the scalar field and scale factor for the two limiting cases-i) small field limit  $\phi/f \ll 1$  and ii) large field limit  $\phi/f \gg 1$ , which we discuss elaborately in the following subsections.

#### i) $\phi/f \ll 1$

##### A1. Space-like extra dimension ( $\varepsilon = +1$ )

Taking the small argument approximations of the trigonometric functions, we get

the solutions for the scale factor and scalar field as

$$a(t) = F_5 \exp \left[ \frac{1}{\sqrt{2}} \left( -2 \left( A + \frac{B}{2} \right) + \sqrt{U} \left( 1 \pm \frac{2\sqrt{C}V_0}{U} \right)^{1/2} \right)^{1/2} t \right], \quad (7.73)$$

$$\frac{\phi(t)}{f} = F_6 \exp \left[ \frac{V_0 t}{\left[ \frac{3f^2}{\sqrt{2}} \left( -2 \left( A + \frac{B}{2} \right) + \sqrt{U} \left( 1 \pm \frac{2\sqrt{C}V_0}{U} \right)^{1/2} \right)^{1/2} \right]} \right], \quad (7.74)$$

where we introduce three arbitrary integration constants  $F_5$ ,  $F_6$  and  $U$ , which are given in terms of model parameters as:

$$F_5 = a_i \exp \left[ -\frac{1}{\sqrt{2}} \left( -2 \left( A + \frac{B}{2} \right) + \sqrt{U} \left( 1 \pm \frac{2\sqrt{C}V_0}{U} \right)^{1/2} \right)^{1/2} t_i \right], \quad (7.75)$$

$$F_6 = \frac{\phi_i}{f} \exp \left[ -\frac{V_0 t_i}{\left[ \frac{3f^2}{\sqrt{2}} \left( -2 \left( A + \frac{B}{2} \right) + \sqrt{U} \left( 1 \pm \frac{2\sqrt{C}V_0}{U} \right)^{1/2} \right)^{1/2} \right]} \right], \quad (7.76)$$

$$U = \sqrt{A}R \pm 2\sqrt{C}V_0, \quad (7.77)$$

with the definition of  $R$  is same as appearing in the previous case i.e. for hilltop potential.

Thus the scale factor depends on time exponentially with only first power or linear power of time.

## A2. Time-like extra dimension ( $\varepsilon = -1$ ):

The conclusion remain same as was for the hilltop potential.

### ii) $\phi/f \gg 1$

## A1. Space-like extra dimension ( $\varepsilon = +1$ ):

Using the large argument approximations of the trigonometric functions and applying the conditions:

$$\frac{\sqrt{\frac{U}{W}}}{W} \ll 1, \quad (7.78)$$

$$W \gg \sqrt{\frac{C}{WU}}, \quad (7.79)$$

i.e.  $W$  is a large quantity where it is defined as:

$$W = \frac{1}{2} \left( \sqrt{U} - \left( \sqrt{A} + \frac{1}{2} \frac{B}{\sqrt{A}} \right) \right), \quad (7.80)$$

and  $U$  has already been defined before, we hence get the solution of the scalar field as:

$$\frac{\phi(t)}{f} = 2 \tan^{-1} \left[ \exp \left( \frac{V_0 t}{3f^2} + F_7 \right) \frac{f}{W} \right], \quad (7.81)$$

where we introduce three arbitrary integration constant  $F_7$ , which is given in terms of model parameters as:

$$F_7 = f \ln \left( \frac{W}{f} \tan \left( \frac{\phi_i}{2f} \right) \right) - \frac{V_0 t_i}{3f^2} \quad (7.82)$$

Substituting back into the approximate Friedmann equation we get the following expression for the scale factor as:

$$a(t) = F_8 \exp \left[ \sqrt{W} \left( \left( 1 - \frac{1}{W} \sqrt{\frac{C}{U}} \right) t - \frac{\frac{2}{W} \sqrt{\frac{C}{U}} \ln(1 + e^{\tilde{G}})}{\left( \frac{2V_0}{3f^2 W} \right)} + \frac{4}{W} \sqrt{\frac{C}{U}} t \right) \right] \quad (7.83)$$

where the functions  $G$  and  $F_8$  are given by:

$$\tilde{G} = \frac{2F_7}{W} + \frac{2V_0 t}{3f^2 W}, \quad (7.84)$$

$$F_8 = a_i \exp \left[ -\sqrt{W} \left( \left( 1 - \frac{1}{W} \sqrt{\frac{C}{U}} \right) t_i - \frac{\frac{2}{W} \sqrt{\frac{C}{U}} \ln(1 + e^G)}{\frac{2V_0}{3f^2 W}} + \frac{4}{W} \sqrt{\frac{C}{U}} t_i \right) \right]. \quad (7.85)$$

## A2. Time-like extra dimension ( $\varepsilon = -1$ ):

The conclusion remain same as was for the previous case.

## B. Contraction

### A1. Space-like extra dimension ( $\varepsilon = +1$ ):

Since the contraction phase is independent of any potential, the conclusions remain same as for hilltop potential

## A2. Time-like extra dimensions ( $\varepsilon = -1$ ):

In this case also the conclusions remain same as for hilltop potential

## C. Expression for work done

The expression for work done is obtained by substituting the expressions for scale factor into the Eq. (7.50), taking care of the assumptions that we have made earlier in the present context.

### A1. Space-like extra dimension ( $\varepsilon = +1$ ):

$$\begin{aligned} \oint p dV = & f_8(-f_1 t_{max}^4 + f_2 t_{max}^5 - f_3 t_{max}^6 + f_4 t_{max}^7 - f_5 t_{max}^8 \\ & + f_6 t_{max}^9 - f_7 t_{max}^{10} + f_1 t_{min}^4 - f_2 t_{min}^5 + f_3 t_{min}^6 \\ & - f_4 t_{min}^7 + f_5 t_{min}^8 - f_6 t_{min}^9 + f_7 t_{min}^{10}) \\ & + f_{12}(e^{f_{13} t_{min}} - e^{f_{13} t_{max}}), \end{aligned} \quad (7.86)$$

where  $f_1 \dots f_{13}$  are the constants whose form depends on the parameters in the expression for the scale factor. Explicit forms of the constants are given in the appendix.

### A2. Time-like extra dimensions ( $\varepsilon = -1$ ):

Since the solutions for the scale factor in the expansion and contraction phase remains same barring the constants, the results for work done also remains same.

Thus we see that since the work done after a complete cycle is non-zero, at least for the approximate expressions for the scale factor which we have evaluated in this subsection earlier. Thus hysteresis phenomenon is possible for the natural potential in the small field limit for Einstein Gauss Bonnet gravity.

## 7.7.3 Case III: Coleman-Weinberg potential

### A. Expansion

#### A1. Space-like extra dimension ( $\varepsilon = +1$ ):

The original integral equation being complicated, we follow the same procedure as has been done before i.e. use the field redefinition:

$$\phi/M_p = e^\lambda. \quad (7.87)$$

Analytical solutions were possible only for small field limit  $\phi/M_p \ll 1$  which we have discussed below.

In this limit expanding the exponentials upto linear order and applying the following constraint conditions:

$$\frac{2\sqrt{C}V_0(4\alpha + \beta)\lambda}{(\sqrt{U} + 2\sqrt{C}V_0\alpha)} \ll 1, \quad (7.88)$$

$$\frac{2\sqrt{C}V_0(4\alpha + \beta)}{\sqrt{H'} \left( \sqrt{AH'} - 2 \left( A + \frac{B}{2} \right) \right)} \ll 1, \quad (7.89)$$

$$\frac{4\beta\lambda}{(4\alpha + \beta)} \ll 1, \quad (7.90)$$

we get the solution for redefined or transformed field  $\lambda$  as:

$$\lambda = (4\alpha + \beta) \left( -\frac{V_0 t}{3M_p^2} + F_9 \right) \left( \frac{2}{\sqrt{AH'} - 2 \left( A + \frac{B}{2} \right)} \right)^{1/2}, \quad (7.91)$$

where we introduce two new constants  $H'$  and  $F_9$  defined in terms of the model parameters as:

$$H' = \sqrt{U} + 2\sqrt{C}V_0\alpha, \quad (7.92)$$

$$F_9 = \frac{\lambda_i}{(4\alpha + \beta) \left( \frac{2}{\sqrt{AH'} - 2 \left( A + \frac{B}{2} \right)} \right)^{1/2}} - \frac{V_0 t_i}{3M_p^2}. \quad (7.93)$$

Here  $\lambda_i$  is the value at bounce.

The solution for the scale factor turns out to be:

$$a(t) = F_{10} \exp \left[ \left\{ \left( \sqrt{AH'} - 2 \left( A + \frac{B}{2} \right) \right)^{1/2} + F_9 I (4\alpha + \beta) \right\} t - \frac{(4\alpha + \beta)t^2 \frac{V_0}{3M_p^2}}{2} \right] \quad (7.94)$$

where we introduce two new constants  $I$  and  $F_{10}$  defined in terms of the model parameters as:

$$I = \frac{\sqrt{2}V_0(4\alpha + \beta)}{\sqrt{H'} \left( \sqrt{AH'} - 2 \left( A + \frac{B}{2} \right) \right)}, \quad (7.95)$$

$$F_{10} = a_i \exp \left[ - \left\{ \left( \sqrt{AH'} - 2 \left( A + \frac{B}{2} \right) \right)^{1/2} + F_9 I (4\alpha + \beta) \right\} t_i + \frac{(4\alpha + \beta)t_i^2 \frac{V_0}{3M_p^2}}{2} \right]. \quad (7.96)$$

## A2. Time-like extra dimension ( $\varepsilon = -1$ ):

The conclusions remain same as for  $\varepsilon = 1$  case, only the expression for different parameters change with  $\varepsilon = 1$  replaced by  $\varepsilon = -1$ .

## B. Contraction

### A1. Space-like extra dimension ( $\varepsilon = +1$ ):

Conclusions for hilltop potential, holds true for this case also.

### A2. Time-like extra dimension ( $\varepsilon = -1$ ):

Conclusions remain same as for the case of hilltop potential.

## C. Expression for work done

### A1. Space-like extra dimension ( $\varepsilon = +1$ ):

The general expression for the scale factor i.e its time dependence is same for supergravity potential as for hilltop potential in the small field limit, hence the conclusions for work done remains valid for this case also, thus giving rise to the phenomenon of hysteresis.

### A2. Time-like extra dimension ( $\varepsilon = -1$ ):

The conclusion is same as above.

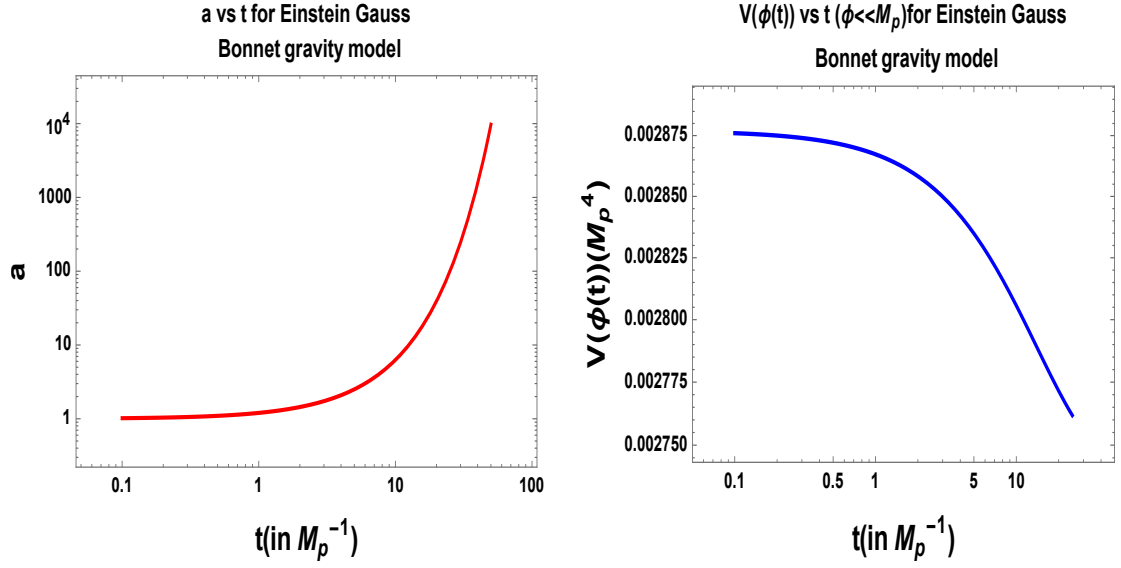
## 7.8 Graphical Analysis

### 7.8.1 Case I: Hilltop potential

All the graphs in this section and in the following sections have been plotted in units of  $M_p = 1$ ,  $H_0 = 1$ ,  $c = 1$ , where  $M_p$  is the Planck mass,  $H_0$  is the present value of the Hubble parameter and  $c$  is the speed of light.

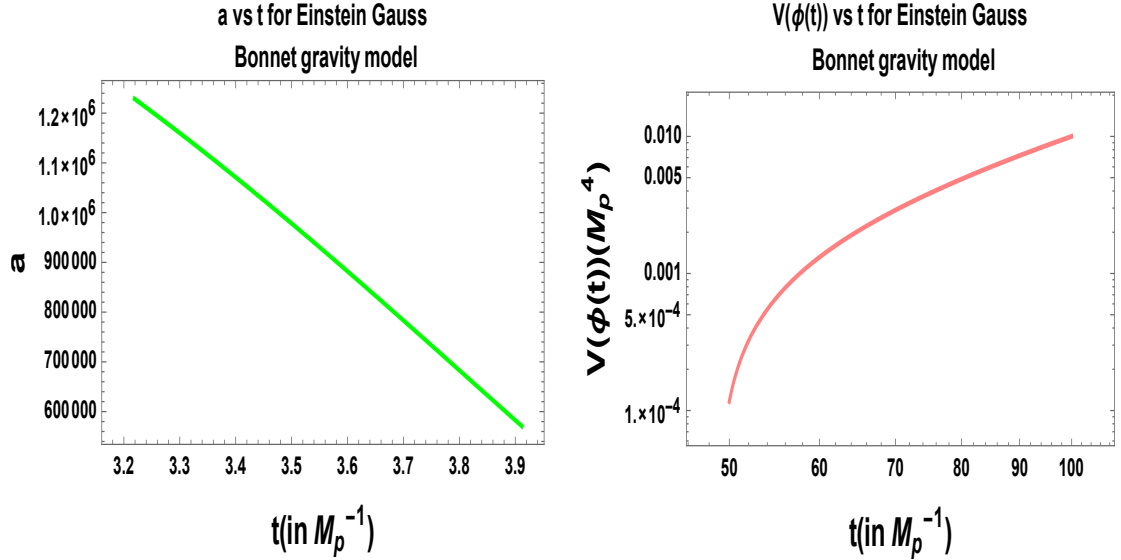
Fig. 29 shows the evolution of scale factor and potential during expansion and contraction phase for Einstein Gauss Bonnet gravity model. We can draw the following conclusions:

- Fig. 29(a), shows the plot of the scale factor in the small field limit for hilltop potential given by Eqn. (7.61) with  $V_0 = 10^{-8}M_p^4$ ,  $p = 3$ ,  $F_1 = 1$ ,  $F_0 =$



(a) An illustration of the behavior of the scale factor with time during expansion phase for  $\phi \ll M_p$  with  $M_p$  with  $V_0 = 10^{-8}M_p^4$ ,  $p = 3$ ,  $F_1 = 1$ ,  $F_0 = V_0 = 2.7 \times 10^{-3}M_p^4$ ,  $p = 4$ ,  $F_0 = 54M_p$ ,  $A = 0.1M_p$ ,  $A = 0.1M_p^2$ ,  $B = 0.1M_p^2$ ,  $C = 10$ ,  $S = 0.1M_p^2$ ,  $B = 0.1M_p^2$ ,  $C = 500$ ,  $R = 30M_p^2$ ,  $S = 0.1$ ,  $R = 0.1M_p^2$ .

(b) An illustration of the behavior of the potential with time during expansion phase for  $\phi \ll M_p$  with  $M_p$  with  $V_0 = 10^{-8}M_p^4$ ,  $p = 3$ ,  $F_1 = 1$ ,  $F_0 = V_0 = 2.7 \times 10^{-3}M_p^4$ ,  $p = 4$ ,  $F_0 = 54M_p$ ,  $A = 0.1M_p$ ,  $A = 0.1M_p^2$ ,  $B = 0.1M_p^2$ ,  $C = 10$ ,  $S = 0.1M_p^2$ ,  $B = 0.1M_p^2$ ,  $C = 500$ ,  $R = 30M_p^2$ ,  $S = 0.1$ ,  $R = 0.1M_p^2$ .



(c) An illustration of the behavior of the scale factor with time during contraction phase with  $V_0 = 10^{-6}M_p^4$ ,  $p = 1$ ,  $F_2 = 24M_p^{-1}$ ,  $F_3 = 1M_p$ ,  $A = 10M_p^2$ ,  $B = 20M_p^2$ ,  $F_3 = 150M_p$ ,  $F_4 = 1$ .

(d) An illustration of the behavior of the potential with time during contraction phase with  $V_0 = 10^{-6}M_p^4$ ,  $p = 1$ ,  $F_2 = 24M_p^{-1}$ ,  $F_3 = 1M_p$ ,  $A = 10M_p^2$ ,  $B = 20M_p^2$ ,  $F_3 = 150M_p$ ,  $F_4 = 1$ ,  $A = 2M_p^2$ ,  $B = -2M_p^2$ ,  $R = 10^{-3}M_p^2$ ,  $\beta = -0.9$ .

**Figure 29.** Graphical representation of the evolution of the scale factor and the potential during the expansion and contraction phase for Einstein Gauss Bonnet gravity model.

$0.1M_p$ ,  $A = 0.1M_p^2$ ,  $B = 0.1M_p^2$ ,  $C = 10$ ,  $S = 0.1$ ,  $R = 0.1M_p^2$ .

- Detail graphical analysis show that the amplitude of expansion increases with increase in the value of  $C$ , decrease in  $A$  and  $B$ . Expansion is not possible for  $A < 0$ . For  $R, S < 0$ , expansion is possible for large values of other parameters. For  $B < 0$ , expansion is possible if  $V_0$  and  $A$  are small,  $R$  and  $F$  are negative. In this case,  $S$  can be both negative and positive. Again for expansion to occur, the parameter space  $(R, F, S < 0)$ ,  $(A, B > 0)$  and  $(A, B, R > 0)$ ,  $(S, F < 0)$  not allowed. But if we look at the expression of  $F_0$ , then  $R, A$  cannot take negative values. This will make the expression imaginary, which is unphysical. For  $F < 0, S > 0$  but small, expansion is possible if  $p$  lies between 1 and 3.
- Fig. 29(b) shows the plot of the behavior of the potential with time for small field hilltop potential. This graph has been obtained with the help of Eqn. (7.58) with parameter values  $V_0 = 2.7 \times 10^{-3} M_p^4$ ,  $p = 4$ ,  $F_0 = 54 M_p$ ,  $A = 0.1 M_p^2$ ,  $B = 0.1 M_p^2$ ,  $C = 500$ ,  $R = 30 M_p^2$ ,  $S = 0.3$   $\beta = 0.05$ . Correct form of potential is possible for both negative and positive values of  $\beta$ . In this case, the condition

$$\sqrt{R + 2\sqrt{C}V_0} > 2(A + B/2) \quad (7.97)$$

should always be satisfied for getting real outputs which we can conclude from Eqn. (7.58). Larger values of  $S$  makes the potential flatter for longer time. Larger values of other parameters make the potential fall more linearly and decreases its slope. Both negative and positive values of  $B$  are allowed provided the above condition is satisfied.  $S < 0$  not allowed because we do not get the correct nature of the potential.

- In Fig. 29(c), we have plotted Eqn. (7.68), which results in the contraction phase of the universe provided we choose the value of the constants accordingly. This plot has been obtained for  $A = 10 M_p^2$ ,  $B = 20 M_p^2$ ,  $F_3 = 150 M_p$ ,  $F_4 = 1$ . Output is possible provided

$$\sqrt{AR}/2 > 2(A + B/2), \quad (7.98)$$

which we can also conclude from Eqn. (7.68). Contraction is possible provided

$$B, R > A \quad (7.99)$$

and

$$A, R, B > 0. \quad (7.100)$$

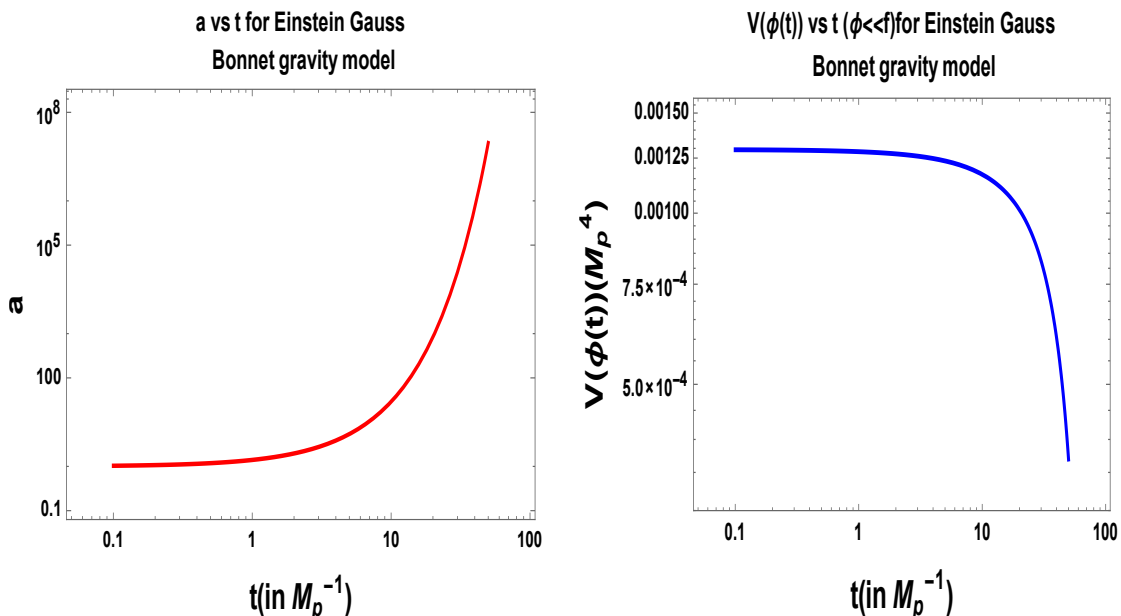
Higher values of the parameters increases the amplitude of expansion. If we compare Fig. 29(a) with Fig. 29(c), we find that there occurs a net increase in the amplitude of the scale factor after one expansion-contraction cycle.



- Fig. 29(d) shows the plot of the potential during the contraction phase given by Eqn. (7.65). This plot has been obtained for  $V_0 = 10^{-6}M_p^4$ ,  $p = 1$ ,  $F_2 = 24M_p^{-1}$ ,  $F_3 = 1M_p$ ,  $A = 2M_p^2$ ,  $B = -2M_p^2$ ,  $R = 10^{-3}M_p^2$ ,  $\beta = -0.9$ . Larger values of the integration constants  $F_2$  and  $F_3$  makes the rise more nonlinear. For  $\beta > 0$  rise of the potential is possible only for very large values of  $F_2$ . Larger values of other parameters increases the amplitude of the potential.

### 7.8.2 Case II: Natural potential

All the graphs in this section and in the following sections have been plotted in units of  $M_p = 1$ ,  $H_0 = 1$ ,  $c = 1$ , where  $M_p$  is the Planck mass,  $H_0$  is the present value of the Hubble parameter and  $c$  is the speed of light.



(a) An illustration of the behavior of the scale factor with time during expansion phase for  $\phi \ll f$  with  $V_0 = 8 \times 10^{-4}M_p^4$ ,  $F_5 = 1$ ,  $A = V_0 = 8 \times 10^{-4}M_p^4$ ,  $F_6 = 1$ ,  $A = 0.1M_p^2$ ,  $B = 0.8M_p^2$ ,  $B = 4.2M_p^2$ ,  $C = 1$ ,  $R = 40.6M_p^2$ . (b) An illustration of the behavior of the potential with time during expansion phase for  $\phi \ll f$  with  $V_0 = 8 \times 10^{-4}M_p^4$ ,  $F_5 = 1$ ,  $A = 0.1M_p^2$ ,  $C = 10$ ,  $R = 40.6M_p^2$ ,  $f = 0.1M_p$ .

**Figure 30.** Graphical representation of the evolution of the scale factor and the potential during the expansion for Einstein Gauss Bonnet gravity model.

Fig. 30 shows the evolution of scale factor and potential during expansion phase for Einstein Gauss Bonnet gravity model. We can draw the following conclusions:

- Fig. 30(a), shows the plot of the scale factor in the small field limit for natural potential given by Eqn. (7.74) with  $V_0 = 8 \times 10^{-4}M_p^4$ ,  $F_5 = 1$ ,  $A = 0.8M_p^2$ ,  $B = 4.2M_p^2$ ,  $C = 1$ ,  $R = 40.6M_p^2$ .

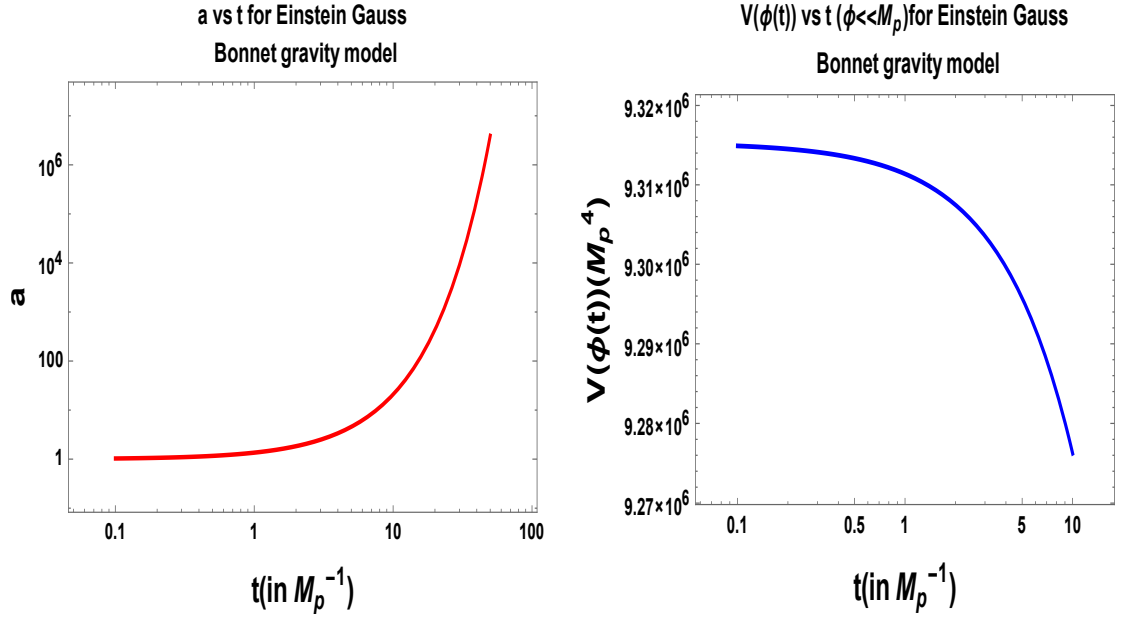
- Detail graphical analysis show that the amplitude of expansion increases with increase in the value of  $R$ . From Eqn. (7.74), we can conclude that  $R, A < 0$  not possible. Expansion is possible for  $B < 0$ . But large negative values of  $B$  expansion is not possible. The nature of the graph is almost independent of the value of  $C$  and  $V_0$ .
- Fig. 30(b) shows the plot of the behavior of the potential with time for small field natural potential. This graph has been obtained with the help of Eqn. (7.74) with parameter values  $V_0 = 8 \times 10^{-4} M_p^4$ ,  $F_6 = 1$ ,  $A = 0.1 M_p^2$ ,  $B = 0.1 M_p^2$ ,  $C = 10$ ,  $R = 40.6 M_p^2$ ,  $f = 0.1 M_p$ . The conclusions regarding the allowed parameter space for the expansion of the scale factor holds true for this case also. Very large values of  $V_0$  and  $A$  are not allowed since they cause uneven oscillations in the potential.
- For large field case given by Eqns. (7.83) and (7.81), the behavior is similar, hence have not been shown here explicitly.
- If we compare Fig. 30(a) with Fig. 29(c), we find that there occurs a net increase in the amplitude of the scale factor after one expansion-contraction cycle.

### 7.8.3 Case III: Coleman-Weinberg potential

All the graphs in this section and in the following sections have been plotted in units of  $M_p = 1$ ,  $H_0 = 1$ ,  $c = 1$ , where  $M_p$  is the Planck mass,  $H_0$  is the present value of the Hubble parameter and  $c$  is the speed of light.

Fig. 31 shows the evolution of scale factor and potential during expansion phase for Einstein Gauss Bonnet gravity model. We can draw the following conclusions:

- Fig. 31(a), shows the plot of the scale factor in the small field limit for supergravity potential given by Eqn. (7.94) with  $V_0 = 10^{-8} M_p^4$ ,  $F_9 = 1 M_p$ ,  $F_{10} = 1$ ,  $A = 0.1 M_p^2$ ,  $B = 0.1 M_p^2$ ,  $C = 1$ ,  $R = 4.4 M_p^2$ ,  $\beta = 1.5$ ,  $\alpha = 0.33$ .
- Detail graphical analysis show that the amplitude of expansion increases with increase in the value of  $R$ . But the expansion is almost independent of  $\alpha, \beta, F_9$ . Negative values of  $B$  gives large expansion. For larger values of  $R$ ,  $F_9$  cannot take large values. Expansion occurs for both negative and positive values of  $\beta$ . Larger values of  $V_0$  makes the graph more linear. For  $A < 0$ , expansion is not possible. However,  $B$  can take negative values, but both  $B$  and  $R$  taking negative values not allowed.
- Fig. 31(b) shows the plot of the behavior of the potential with time for small field supergravity potential. This graph has been obtained with the help of Eqn. (7.91) with parameter values  $V_0 = 1.2 \times 10^{-4} M_p^4$ ,  $F_9 = 6.6 M_p$ ,  $A =$



(a) An illustration of the behavior of the scale factor with time during expansion phase for  $\phi \ll M_p$  with  $V_0 = 10^{-8}M_p^4$ ,  $F_9 = 1M_p$ ,  $F_{10} = M_p$  with  $V_0 = 1.2 \times 10^{-4}M_p^4$ ,  $F_9 = 6.6M_p$ ,  $A = 1$ ,  $B = 0.1M_p^2$ ,  $C = 1$ ,  $R = 0.1M_p^2$ ,  $\alpha = 4.4M_p^2$ ,  $\beta = 1.5$ ,  $\alpha = 0.33$ .  
(b) An illustration of the behavior of the potential during expansion phase for  $\phi \ll M_p$  with  $V_0 = 1.2 \times 10^{-4}M_p^4$ ,  $F_9 = 6.6M_p$ ,  $A = 1$ ,  $B = 0.1M_p^2$ ,  $C = 10$ ,  $R = 20M_p^2$ ,  $\alpha = 0.38$ ,  $\beta = 0.85$ .

**Figure 31.** Graphical representation of the evolution of the scale factor and the potential during the expansion for Einstein Gauss Bonnet gravity model.

$0.1M_p^2$ ,  $B = 0.1M_p^2$ ,  $C = 10$ ,  $R = 20M_p^2$ ,  $\alpha = 0.38$ ,  $\beta = 0.85$ . The conclusions regarding the allowed parameter space for the expansion of the scale factor holds true for this case also. Very large negative values of  $\beta$  are not allowed. Expansion is possible only for small negative and positive values of  $\beta$ . Other parameter values only increases the amplitude, keeping the nature of the graph unchanged. The plot is almost independent of the value of  $C$  and  $R$ .

- If we compare Fig. 31(a) with Fig. 29(c), we find that there occurs a net increase in the amplitude of the scale factor after one expansion-contraction cycle.

## 8 Conclusion

In this paper, we have further explored the role of hysteresis in making cyclic models of universe as an alternative proposal to inflationary paradigm. The idea, originally proposed by the authors in refs. [10, 11], have been studied by us for a wide variety of cosmological models, especially, higher dimensional gravity setup. The basic analysis for getting the conditions which lead to an increase in expansion maximum, remains

the same as discussed in refs. [10, 11]. The most interesting outcome of this analysis is the dependence of the bouncing and turnaround conditions on the various model parameters. Through this analysis we find that the phenomenon of hysteresis is very robust and is eternal for all of these models. We study essentially those effective field theoretic models which can give rise to both the conditions for bounce and turnaround and at the same time also satisfies the observed features of the present universe. Like in the previous analysis as performed in the ref. [11], here also we find that inflationary conditions are not necessary for causing cosmological hysteresis. Hence the models analyzed in this paper can also be treated as an alternative prescription to inflation. Most of the results indicate that the value of the scale factor maximum and minimum after each cycle, depends not only on the signature of the hysteresis loop integral but also on the relative amplitudes of the model parameters, or in other words, we can fine tune the model parameters and get an amplitude increase after each cycle even if the signature of the hysteresis loop integral is positive. While doing the analysis we have not constrained the potential by any particular form. The potential can have any general form like a power series, oscillatory, etc, but with well defined minimum/minima which is essential for generating the required randomness or mixing of the field in the phase space  $(\dot{\phi}, \phi)$  so that its value during contraction and expansion are uncorrelated.

We have also tried to find the nature of dependence of the scale factor on time by directly solving the equation of motion for the scalar field under different scenarios and varying forms of the cosmological potential. Exact solutions of the equation of motion for the scalar field being highly complicated, we applied certain valid and possible approximations while doing the analysis by redefining the field in terms of other dynamical parameter, in order to get an approximate analytical expression for the dependence of the scale factor on time. This in turn helps us to directly guess the nature of the behavior of the scale factor as well as the scalar field during each cycle for different models. We have also derived an explicit expression for work done per cycle, hence have shown that its value comes out to be non zero for the cases which we have studied explicitly, provided we choose the parameters of the models accordingly. It shows that the phenomenon of hysteresis and a cyclic universe with an ever increasing scale factor, can be produced by a wide variety of models and potentials. This will also help us to constrain the parameters of the models and the potentials, such that we get the required results compatible with observations.

The future prospects of our work are mentioned below:

- Through this analysis we have seen the beautiful correlation between purely thermodynamical principle and relativistic models and how the former can be used for extracting interesting results from the later. But the models that we have considered are the variants of minimally coupled gravity frameworks. It

would therefore be interesting to investigate what new features arises once we relax this constraint. Also we can check whether modified gravity models like for variants of  $f(R)$  gravity, two brane-world model in presence of the Einstein-Hillbert term and the Einstein-Hillbert-Gauss-Bonnet gravity setup succeeds in generating a cyclic universe with increasing amplitude of expansion.

- One would also like to ask what other observational signatures we can get from such models which can be tested using CMB. We have also not yet verified whether these models produces a universe with the right amount of anisotropy and inhomogeneity present in the universe. In future we plan to connect these analyses with CMB observations, by rigorous study of the cosmological perturbation theory in various orders of metric fluctuations and computation of two point correlations to get the expressions for scalar and tensor power spectrum in this context. Hence we extend the study of this paper to compute the primordial non-Gaussianity in CMB from three and four point correlations. We also plan to derive the explicit expression for various modified consistency relations between the non-Gaussian as well as other cosmological parameters in the present context.
- Also, our present analysis have been performed for three different potentials. It would be interesting to check whether we can formulate any general form of a potential, which can be used to repeat the analysis of this paper for all the models.
- We also carry forward our analysis in the development of density inhomogeneities, which is the prime component to form large scale structures at late times. Also the specific role of cosmological hysteresis in the study of cosmological perturbations i.e. for interacting/decoupled dark matter and dark energy have not been explored at all earlier. We have some future plan to do some computations from this setup.
- Further using the reconstruction techniques we want to study the generic features of scalar field potentials in the framework of cosmological hysteresis.

## Acknowledgments

SC would like to thank Department of Theoretical Physics, Tata Institute of Fundamental Research, Mumbai for providing me Visiting (Post-Doctoral) Research Fellowship. SC take this opportunity to thank sincerely to Prof. Soumitra SenGupta, Prof. Sayan Kar, Prof. Sandip P. Trivedi, Prof. Shiraz Minwalla, Dr. Subhabrata Majumdar and Dr. Supratik Pal for their constant support and inspiration. SC take this opportunity to thank all the active members and the regular participants

of weekly student discussion meet ‘‘COSMOMEET’’ from Department of Theoretical Physics and Department of Astronomy and Astrophysics, Tata Institute of Fundamental Research for suggesting various crucial issues at the initial stage of the work, which finally helped us to improve the quality of the work. SC also thanks Indian Association for the Cultivation of Science (IACS), Kolkata and Physics and Applied Mathematics Unit (PAMU), Indian Statistical Institute (ISI), Kolkata for extending hospitality during the work. Additionally SC take this opportunity to thank the organizers of 28th IAGRG Meeting, 2015, Raman Research Institute (RRI) and Indian Institute of Science (IISC) for providing the local hospitality during the work. SB sincerely thanks Prof. T. P. Singh for constant support and inspiration. Last but not the least, we would all like to acknowledge our debt to the people of India for their generous and steady support for research in natural sciences, especially for theoretical physics.

## 9 Appendix

### 9.1 Hysteresis from RSII brane world model

Below we have quoted the results for RSII brane world cosmology with time like extra dimension necessary for causing the bounce, which was studied in detail by the authors of [11].

The Friedmann equations in this model are given by:

$$H^2 = \left(\frac{\dot{a}}{a}\right)^2 = \frac{8\pi G}{3}\rho \left\{1 - \frac{\rho}{\rho_c}\right\} - \frac{k}{a^2}, \quad (9.1)$$

$$\dot{H} + H^2 = \frac{\ddot{a}}{a} = -\frac{4\pi G}{3} \left\{(\rho + 3p) - \frac{2\rho}{\rho_c}(2\rho + 3p)\right\}. \quad (9.2)$$

#### 9.1.1 Condition for bounce

At bounce, by setting the Hubble parameter  $H = 0$ , we get:

$$\rho_b = \rho_c \quad (9.3)$$

The mass at bounce (neglecting the constant factor) is given by:

$$M_b = \rho_b a_b^3. \quad (9.4)$$

Therefore, the infinitesimal change in the mass content at bounce is given by:

$$\delta M = \delta(\rho_c a_b)^3. \quad (9.5)$$

From energy conservation, we get:

$$\delta M + \delta W = 0, \quad (9.6)$$

where  $\delta W$  is the work done during each expansion-contraction cycle which is given by  $\oint pdV$  which includes contribution from the area of the hysteresis loop.

Further setting

$$\delta M = -\delta W = -\oint pdV, \quad (9.7)$$

we get the expression for change in amplitude of the scale factor at each successive cycle as:

$$\delta(a_{\min})^3 \equiv \left\{ a_{\min}^{(i)} \right\}^3 - \left\{ a_{\min}^{(i-1)} \right\}^3 = -\frac{1}{\rho_c} \oint pdV, \quad (9.8)$$

Thus we see that the change in minimum of the expansion factor depends upon the work done and the density at bounce.

### 9.1.2 Condition for acceleration

From Eq. (9.2), condition for acceleration is given by:

$$4\pi G(\rho_c + p_c) > 0 \quad (9.9)$$

i.e. bounce can be obtained without violating the strong energy condition.

### 9.1.3 Condition for turnaround

Though the authors of [11] have suggested different ways of getting the condition for turnaround, but in there analysis they have used the presence of density which take negative values at late times to be the cause for turnaround. The authors of [11] have assumed that the late time behavior of the universe is governed by:

$$H^2 \simeq \kappa\rho - \frac{A}{a^n}, \quad (9.10)$$

where  $\kappa = \frac{8\pi G}{3}$ , and  $A > 0$ ,  $n \leq 2$ . Here  $A \equiv \Lambda < 0$ ,  $n = 0$  corresponds to a negative cosmological constant, whereas  $A = 1$ ,  $n = 2$  describes a universe which is spatially closed. Setting the Hubble parameter  $H = 0$ , we get the condition for turnaround as:

$$\kappa\rho_t = \frac{A}{a_t^n} \quad (9.11)$$

where  $\rho_t$  is the density and  $a_t$  the expansion factor at turnaround. They are connected via the following equation:

$$\rho_t = \frac{3M_4^2}{2} \left( \frac{k}{a_t^2} - \frac{1}{r_c^2} \right) \quad (9.12)$$

where  $\rho_t$  and  $a_t$  are the density and scale factor at turnaround respectively.

The change in amplitude of the scale factor after each successive cycle is given by:

$$\delta(a_{\max})^{3-n} \equiv \left\{ a_{\max}^{(i)} \right\}^{3-n} - \left\{ a_{\max}^{(i-1)} \right\}^{3-n} = -\frac{\kappa}{A} \oint pdV, \quad (9.13)$$

which is responsible for turnaround. Here two extreme physical situation correspond to:

- (i) the negative cosmological constant ( $n = 0$ ) for which

$$\delta a_{\max}^3 = -\frac{\kappa}{\Lambda} \oint pdV , \quad (9.14)$$

- (ii) the spatially closed universe ( $n = 2$ ) for which

$$\delta a_{\max} \equiv a_{\max}^{(i)} - a_{\max}^{(i-1)} = -\kappa \oint pdV . \quad (9.15)$$

#### 9.1.4 Condition for deceleration

Turnaround occurs only if:

$$\rho + 3p \geq 0 \quad (9.16)$$

Therefore, turnaround can be obtained without violating the energy condition in RSII setup.

## 9.2 Exact expressions for $\phi$ integrals

### DGP model-Hilltop potential

i) The exact solution to the left hand side of the integral in Eq. (4.70) for early times is given by

$$\begin{aligned} \mathcal{I}_1 = & \frac{(\phi/M_4)^{2-p} \left( -4\left(\frac{1}{2r_c} + \sqrt{\frac{V_0}{3M_4^2}(1 + (\phi/M_4)^p\beta)}\right) \right)}{4(-2+p)\beta p} \\ & + \frac{(\phi/M_4)^{2-p} \left( \sqrt{\frac{V_0}{3M_4^2}} p (\phi/M_4^2)^p \beta \operatorname{Hypergeometric2F1} \left[ \frac{1}{2}, \frac{2}{p}, \frac{2+p}{p}, -(\phi/M_4)^p\beta \right] \right)}{4(-2+p)\beta p} \end{aligned} \quad (9.17)$$

ii) The exact solution to the left hand side of Eq. (4.81) for late times is given by

$$\begin{aligned} \mathcal{I}_2 = & \frac{(\phi/M_4)^2 \left( -\frac{8V_0\beta}{3M_4^2} - 4D_G(\phi/M_4)^{-p} \right)}{4(-2+p) \left( D_G + \frac{2V_0\beta}{3M_4^2 t^p} \right)^{1/2}} \\ & + \frac{(\phi/M_4)^2 \left( \frac{2V_0\beta}{3M_4^2} p \sqrt{1 + \frac{2V_0\beta(\phi/M_4)^p}{3M_4^2 D_G}} \operatorname{Hypergeometric2F1} \left[ \frac{1}{2}, \frac{2}{p}, \frac{2+p}{p}, -\frac{2V_0\beta}{3M_4^2 D_G} (\phi/M_4)^p\beta \right] \right)}{4(-2+p) \left( D_G + \frac{2V_0\beta}{3M_4^2 t^p} \right)^{1/2}} \end{aligned} \quad (9.18)$$

where

$$D_G = \frac{2}{3} \frac{V_0}{M_4^2} + \frac{1}{r_c^2}. \quad (9.19)$$



### DGP model- Natural potential

i) Exact solution to the integral on left hand side of Eq. (4.110) for early times is given by

$$\mathcal{I}_3 = \left( \frac{V_0}{3M_4^2} \right)^{1/2} \left[ 1 + \cos \left( \frac{\phi}{f} \right) \right]^{1/2} \left[ -\ln \left( \cos \left( \frac{\phi}{4f} \right) \right) + \ln \left( \sin \left( \frac{\phi}{4f} \right) \right) \right] \sec \left( \frac{\phi}{2f} \right) \quad (9.20)$$

ii) Exact solution to the integral on left hand side of Eq. (4.115) for late times is given by

$$\mathcal{I}_4 = \sqrt{D_P - \frac{2V_0}{3M_4^2}} \tan^{-1} \left[ \frac{\sqrt{\frac{2V_0}{3M_4^2} + D_P \cos \left( \frac{\phi}{f} \right)}}{\sqrt{D_P - \frac{2V_0}{3M_4^2}}} \right] - \sqrt{D_P + \frac{2V_0}{3M_4^2}} \tan^{-1} \left[ \frac{\sqrt{\frac{2V_0}{3M_4^2} + D_P \cos \left( \frac{\phi}{f} \right)}}{\sqrt{D_P + \frac{2V_0}{3M_4^2}}} \right] \quad (9.21)$$

where

$$D_P = \frac{2V_0}{3M_4^2} + \frac{1}{r_c^2}. \quad (9.22)$$

### Cosmological constant model- Hilltop potential

Exact solution to the integral on left hand side of Eq. (4.110) for expansion is given by

$$\begin{aligned} \mathcal{I}_5 = & \frac{(\phi/M_4)^2 \left( -\frac{4V_0\beta}{3M_4^2} - 4D_\Lambda (\phi/M_4)^{-p} \right)}{4(-2+p) \left( D_\Lambda + \frac{V_0\beta}{3M_4^2 t^p} \right)^{1/2}} \\ & + \frac{(\phi/M_4)^2 \left( \frac{V_0\beta}{3M_4^2} p \sqrt{1 + \frac{V_0\beta (\phi/M_4)^p}{3M_4^2 D_\Lambda}} \text{Hypergeometric2F1} \left[ \frac{1}{2}, \frac{2}{p}, \frac{2+p}{p}, -\frac{V_0\beta}{D_\Lambda} (\phi/M_4)^p \beta \right] \right)}{4(-2+p) \left( D_\Lambda + \frac{V_0\beta}{3M_4^2 t^p} \right)^{1/2}} \end{aligned} \quad (9.23)$$

where

$$D_G = \frac{V_0}{3M_4^2} + \frac{\Lambda}{3}. \quad (9.24)$$

### Cosmological constant model- Natural potential

Exact solution to the integral on left hand side of Eq. (5.96) for expansion is given by

$$\mathcal{I}_6 = \sqrt{D_f - \frac{V_0}{3M_4^2}} \tan^{-1} \left[ \frac{\sqrt{\frac{V_0}{3M_4^2} + D_f \cos\left(\frac{\phi}{f}\right)}}{\sqrt{D_f - \frac{V_0}{3M_4^2}}} \right] - \sqrt{D_f + \frac{V_0}{3M_4^2}} \tan^{-1} \left[ \frac{\sqrt{\frac{V_0}{3M_4^2} + D_f \cos\left(\frac{\phi}{f}\right)}}{\sqrt{D_f + \frac{V_0}{3M_4^2}}} \right] \quad (9.25)$$

where

$$D_f = \frac{V_0}{3M_4^2} + \frac{\Lambda}{3}. \quad (9.26)$$

### LQG model- Hilltop potential

Exact solution to the integral on left hand side of Eq. (6.44) for early time expansion is given by:

$$\begin{aligned} \mathcal{I}_7 = & - \left( \frac{V_0}{3M_p^2} \right)^{1/2} \quad (9.27) \\ & \times \frac{(\phi/M_p)^{2-p} \sqrt{1 - \frac{V_0}{\rho_c} (1 + (\phi/M_p)^p \beta)} \text{AppellF1} \left[ -1 + \frac{2}{p}, -\frac{1}{2}, -\frac{1}{2}, \frac{2}{p}, -(\phi/M_p)^p \beta, \frac{V_0(\phi/M_p)^p \beta}{\rho_c(1 - (\frac{V_0}{\rho_c}))} \right]}{(-2 + p) \left( \frac{-1 + \frac{V_0}{\rho_c} + \frac{V_0(\phi/M_p)^p \beta}{\rho_c}}{-1 + (\frac{V_0}{\rho_c})} \right)^{1/2} \beta p} \end{aligned}$$

### LQC model- Natural potential

Exact solution to the integral on left hand side of Eq. (6.68) for early time expansion is given by

$$\begin{aligned} \mathcal{I}_8 = & \left( \frac{V_0}{3M_p^2} \right)^{1/2} \sec\left(\frac{\phi}{2f}\right) \sqrt{1 + \cos\left(\frac{\phi}{f}\right)} \left\{ -\sqrt{1 - 2\frac{V_0}{\rho_c}} \tanh^{-1} \left[ \frac{\sqrt{1 - 2\frac{V_0}{\rho_c} \cos(\phi/2f)}}{\sqrt{1 - \frac{V_0}{\rho_c} - \frac{V_0}{\rho_c} \cos(\phi/2f)}} \right] \right. \\ & \left. + \sqrt{-\frac{2V_0}{\rho_c}} \ln \left[ \sqrt{-\frac{2V_0}{\rho_c} \cos(\phi/2f)} + \sqrt{1 - \frac{V_0}{\rho_c} - \frac{V_0}{\rho_c} \cos\left(\frac{\phi}{f}\right)} \right] \right\} \quad (9.28) \end{aligned}$$

### 9.3 Expressions of the constants in work done analysis

#### 9.3.1 Dvali-Gabadadze-Porrati (DGP) brane world model

##### Hilltop potential

$$\begin{aligned}
a_6 &= \left( \left( \frac{V_0}{3M_4^2} \right)^{1/2} (1 + \beta)^{1/2} + \frac{1}{2r_c} + \beta p \frac{\left( \frac{V_0}{3M_4^2} \right)^{1/2}}{2(1 + \beta)^{1/2}} \left\{ \lambda_i + \frac{\frac{V_0}{3M_4^2}}{\left( \frac{V_0}{3M_4^2} \right)^{1/2} \frac{(1+\beta)^{1/2}}{\beta p} + \frac{1}{2r_c}} t_i \right\} \right) \\
a_7 &= \left( \beta p \frac{\left( \frac{V_0}{3M_4^2} \right)^{1/2}}{2(1 + \beta)^{1/2}} \right) \frac{\frac{V_0}{3M_4^2}}{2 \left( \frac{V_0}{3M_4^2} \right)^{1/2} \frac{(1+\beta)^{1/2}}{\beta p} + \frac{1}{2r_c}} \\
a_4 &= e^{\frac{3a_6^2}{4a_7}} a_i^3 \sqrt{\frac{\pi}{3}} \frac{(2 + (1 - \frac{1}{2r_c})^2)}{2\sqrt{a_7}} \\
a_5 &= \frac{1}{2} \sqrt{\frac{3}{a_7}} \\
a_1 &= e^{A_2/r_c} \\
a_2 &= a_1^{1/2} \\
a_3 &= a_1^{3/2}/r_c \\
a'_1 &= \frac{1}{2r_c} \\
a'_2 &= A_2'^3 \left( 2 + \left( 1 - \frac{1}{2r_c} \right)^2 \right) \frac{r_c}{3}
\end{aligned} \tag{9.29}$$

##### Natural potential

$$\begin{aligned}
b_2 &= \left( \sqrt{\frac{V_0}{3M_4^2}} \sqrt{2} + \frac{1}{2r_c} \right) \\
b_1 &= \frac{A_7^3}{3b_2} (2 + (1 - \frac{1}{2r_c})^2)
\end{aligned} \tag{9.30}$$

### 9.3.2 Cosmological constant dominated Einstein gravity model

#### Hilltop potential

$$\begin{aligned}
l_1 &= \sqrt{\left(\frac{V_0}{3M_p^2}(1+\beta) + \frac{\Lambda}{3}\right)} \\
l_2 &= \frac{\frac{V_0}{3M_p^2}\beta^2 p^2}{2\left(\frac{V_0}{3M_p^2}(1+\beta) + \frac{\Lambda}{3}\right)} B_0 \\
l_3 &= \frac{\left(\frac{V_0}{3M_p^2}\right)^2 \beta^2 p^2}{4\left(\frac{V_0}{3M_p^2}(1+\beta) + \frac{\Lambda}{3}\right)} \\
b_5 &= 2/p^2 \\
b_6 &= \frac{\beta^{1/2} p^2 B_2}{2\left(\frac{V_0}{3M_p^2}\right)^{1/2}} \\
b_7 &= \beta^{1/2} \frac{p^2}{2} \left(\frac{V_0}{3M_p^2}\right)^{1/2} \\
b_1 &= B_1 \frac{e^{3(l_1+l_2)^2/(2l_3)}}{\sqrt{l_3}} \\
b_2 &= l_1 \sqrt{3/(2l_3)} \\
b_3 &= \sqrt{3l_3/2}
\end{aligned} \tag{9.31}$$

#### Natural Potential

a)  $\phi \ll f$

$$\begin{aligned}
b_8 &= B_7^3 \\
b_9 &= \left(1 + \frac{\frac{V_0}{3M_p^2}}{\frac{V_0}{3M_p^2} + \frac{\Lambda}{3}}\right)^{1/2} \left(\frac{V_0}{3M_p^2} + \frac{\Lambda}{3}\right)^{1/2}
\end{aligned} \tag{9.32}$$

b)  $\phi \gg f$

$$\begin{aligned}
b_{10} &= \left( \frac{V_0}{3M_p^2} + \frac{\Lambda}{3} \right)^{1/2} \\
b_{13} &= \frac{\frac{V_0}{3M_p^2}}{2\left(\frac{V_0}{3M_p^2} + \frac{\Lambda}{3}\right)} \\
l_6 &= \frac{V_0}{3M_p^2} \\
l_7 &= \frac{\frac{V_0}{3M_p^2}}{\left(\frac{V_0}{3M_p^2} + \frac{\Lambda}{3}\right)^{1/2}} \\
b_{12} &= 1, \quad b_{11} = l_7/b_{10}, \quad b_{14} = B_8(-3 + \Lambda), \\
b_{15} &= \frac{l_6 l_7 - l_5 l_6 b_{10} + b_{10} l_6}{b_{10} l_6} - 1
\end{aligned} \tag{9.33}$$

### 9.3.3 Loop Quantum Gravity model

#### Hilltop potential

$$\begin{aligned}
q_1 &= \sqrt{\frac{V_0}{3M_p^2}} \left( \frac{\left( \left( 1 - \frac{V_0}{2\rho_c}(1+\beta) \right) Q - \frac{E_0 p \beta V_0}{2\rho_c} + \frac{E_0 p \beta}{2(1+\beta)} \left( 1 - \frac{V_0}{2\rho_c}(1+\beta) \right) \right)}{Q} \right) \\
q_2 &= \sqrt{\frac{V_0}{3M_p^2}} \left( \frac{\left( \frac{p V_0^2 \beta}{12 M_p^2 \rho_c} - \frac{V_0 p \beta}{12 M_p^2 (1+\beta)} \left( 1 - \frac{V_0}{2\rho_c}(1+\beta) \right) \right)}{Q} \right) \\
d_2 &= 1/M_p^2 \\
d_5 &= (1 + M_p^2)/\sqrt{6} \\
d_6 &= \sqrt{\frac{1 + M^2}{2}} \\
d_7 &= 1 \\
d_8 &= \frac{E_4^3 e^{3\rho_c/2}}{4\sqrt{1 + M_p^2}}.
\end{aligned} \tag{9.34}$$

$$\begin{aligned}
d_{11} &= 3E_4^2 e^{\rho_c} (1 + M_p^2) \sqrt{2\pi} (-12M_p^2 + \rho_c) \\
d_{12} &= 4k(1 + M_p^2) \sqrt{6\pi} \\
d_{19} &= 1 \\
d_{18} &= 2\sqrt{E_2} \\
d_{20} &= E_2' \\
d_{13} &= \sqrt{\frac{\pi}{q_2}} \frac{E_1^3 \rho_c}{4} \\
d_{14} &= \frac{3q_1^2}{4q_2} \\
d_{15} &= \frac{q_1}{2} \sqrt{\frac{3}{q_2}} \\
d_{16} &= \frac{\sqrt{3q_2}}{2} \\
d_{17} &= 12e^{q_1^2/(2q_2)} k \\
d_{17}' &= \sqrt{3} E_1^2 (12M_p^2 - \rho_c)
\end{aligned} \tag{9.35}$$

### Natural potential

$$\begin{aligned}
d_{22} &= \sqrt{2} \left( \frac{V_0}{3M_p^2} \left( 1 - \frac{2V_0}{\rho_c} \right)^{1/2} \right)^{1/2} \\
d_{21} &= \frac{6E_9 k}{d_{22}} \\
d_{23} &= \frac{E_9^3}{2d_{22}} \rho_c (12M_p^2 - \rho_c) \\
d_{24} &= \frac{E_9^3 \rho_c}{2d_{22}}
\end{aligned} \tag{9.36}$$

### 9.3.4 Einstein Gauss Bonnet Gravity brane world model

#### Hilltop potential

$$\begin{aligned}
g_1 &= \left( \sqrt{R + 4\sqrt{\frac{C}{A}} V_0} - (A + B/2)^{1/2} \right)^{1/2} S \\
g_2 &= \frac{p(S-1)F_0}{\sqrt{(\sqrt{R + 4\sqrt{\frac{C}{A}} V_0} - (A + B/2))S}} g_1 \\
g_3 &= \frac{p^2(S-1)\frac{V_0}{3M_p^2}}{\sqrt{(\sqrt{R + 4\sqrt{\frac{C}{A}} V_0} - (A + B/2))S}} g_1
\end{aligned} \tag{9.37}$$

$$\begin{aligned}
g_4 &= \sqrt{\frac{D''}{2}} \\
g_5 &= -2 + D' + D'F_3D'' \\
g_6 &= D'D'' \\
g_7 &= D^2D'' \\
f_1 &= 210g_1(28g_4^2g_5^6g_6^3 + 15g_4g_5^3(3g_4g_5 - 4g_6)g_6^2g_7 + 9g_6(3g_4^2g_5^2 - 6g_4g_5g_6 + g_6^2)g_7^2 + 9g_4^2g_7^3) \\
f_2 &= 504g_4^2g_6^2(14g_4g_5^5g_6^2 + 5g_4^2(4g_4g_5 - 3g_6)g_6g_7 + 3(3g_4g_5 - 2g_6)g_7^2) \\
f_3 &= 420g_4^2g_6^3(14g_4g_5^4g_6^2 + 3g_4(5g_4g_5 - 2g_6)g_6g_7 + 3g_4g_7^2) \\
f_4 &= -120g_4^2g_6^5(28g_4g_5^3g_6 + 18g_4g_5g_7 - 3g_4g_7) \\
f_5 &= 315g_4^3g_6^6(4g_4g_6 + g_7) \\
f_6 &= 280g_4^3g_5g_6^8 \\
f_7 &= 28g_4^3g_6^9 \\
f_8 &= \frac{1}{2520g_5g_7}\sqrt{1+A}(1+B)F_4^3\left(-1 + \frac{\sigma C'}{\sqrt{1+A}(1+B)}\right) \\
f_9 &= F_1^3 e^{\frac{3(g_1+g_2)^2/(2g_3)}{\sqrt{g_3}}} \\
f_{10} &= g_1\sqrt{3/(2g_3)} \\
f_{11} &= \sqrt{3g_3/2}
\end{aligned} \tag{9.38}$$

### Natural potential

$$\begin{aligned}
f_{13} &= \frac{1}{\sqrt{2}} \left( -2 \left( A + \frac{B}{2} \right) + \sqrt{U} \left( 1 \pm \frac{2\sqrt{C}V_0}{U} \right)^{1/2} \right)^{1/2} \\
f_{12} &= F_5^3 \frac{(\sqrt{1+A} + \sqrt{1+AB} - \sigma C')}{f_{13}C'}
\end{aligned} \tag{9.39}$$

### References

- [1] M. Eliade, *The Myth of the Eternal Return*, Pantheon, New York (1934).
- [2] S. L. Jaki, *Science and Creation: From eternal Cycles to an Oscillating Universe*, Science History Publ., New York (1974).
- [3] A. A. Starobinsky, *JETP Lett.* **30**, 719 (1979).
- [4] R. C. Tolman, *Relativity, Thermodynamics and Cosmology*, Clarendon Press, Oxford (1934).
- [5] P. J. Steinhardt and N. Turok, “Cosmic evolution in a cyclic universe,” *Phys. Rev. D* **65** (2002) 126003 [hep-th/0111098].
- [6] J. L. Lehners, “Ekpyrotic and Cyclic Cosmology,” *Phys. Rept.* **465** (2008) 223 [arXiv:0806.1245 [astro-ph]].

- [7] D. Baumann and L. McAllister, “*Inflation and String Theory*,” arXiv:1404.2601 [hep-th].
- [8] D. Baumann, “*TASI Lectures on Inflation*,” arXiv:0907.5424 [hep-th].
- [9] D. H. Lyth and A. Riotto, “*Particle physics models of inflation and the cosmological density perturbation*,” *Phys. Rept.* **314** (1999) 1 [hep-ph/9807278].
- [10] N. Kanekar, V. Sahni and Y. Shtanov, “*Recycling the universe using scalar fields*,” *Phys. Rev. D* **63** (2001) 083520 [astro-ph/0101448].
- [11] V. Sahni and A. Toporensky, “*Cosmological Hysteresis and the Cyclic Universe*,” *Phys. Rev. D* **85** (2012) 123542 [arXiv:1203.0395 [gr-qc]].
- [12] Y. F. Cai, E. McDonough, F. Duplessis and R. H. Brandenberger, “*Two Field Matter Bounce Cosmology*,” *JCAP* **1310** (2013) 024 [arXiv:1305.5259 [hep-th]].
- [13] Y. F. Cai, R. Brandenberger and P. Peter, “*Anisotropy in a Nonsingular Bounce*,” *Class. Quant. Grav.* **30** (2013) 075019 [arXiv:1301.4703 [gr-qc]].
- [14] Y. F. Cai, C. Gao and E. N. Saridakis, “*Bounce and cyclic cosmology in extended nonlinear massive gravity*,” *JCAP* **1210** (2012) 048 [arXiv:1207.3786 [astro-ph.CO]].
- [15] Y. F. Cai, D. A. Easson and R. Brandenberger, “*Towards a Nonsingular Bouncing Cosmology*,” *JCAP* **1208** (2012) 020 [arXiv:1206.2382 [hep-th]].
- [16] C. Li, R. H. Brandenberger and Y. K. E. Cheung, “*Big Bounce Genesis*,” *Phys. Rev. D* **90** (2014) 12, 123535 [arXiv:1403.5625 [gr-qc]].
- [17] R. H. Brandenberger, “*The Matter Bounce Alternative to Inflationary Cosmology*,” arXiv:1206.4196 [astro-ph.CO].
- [18] Y. F. Cai, R. Brandenberger and X. Zhang, “*The Matter Bounce Curvaton Scenario*,” *JCAP* **1103** (2011) 003 [arXiv:1101.0822 [hep-th]].
- [19] M. Lilley and P. Peter, “*Bouncing alternatives to inflation*,” arXiv:1503.06578 [astro-ph.CO].
- [20] F. T. Falciiano, M. Lilley and P. Peter, “*A Classical bounce: Constraints and consequences*,” *Phys. Rev. D* **77** (2008) 083513 [arXiv:0802.1196 [gr-qc]].
- [21] M. Lilley, F. Di Marco, J. Martin and P. Peter, “*Nonabelian Bosonic Currents in Cosmic Strings*,” *Phys. Rev. D* **82** (2010) 023510 [arXiv:1003.4601 [hep-th]].
- [22] M. Lilley, L. Lorenz and S. Clesse, “*Observational signatures of a non-singular bouncing cosmology*,” *JCAP* **1106** (2011) 004 [arXiv:1104.3494 [gr-qc]].
- [23] D. Battfeld and P. Peter, “*A Critical Review of Classical Bouncing Cosmologies*,” *Phys. Rept.* **571** (2015) 1 [arXiv:1406.2790 [astro-ph.CO]].
- [24] P. W. Graham, B. Horn, S. Kachru, S. Rajendran and G. Torroba, “*A Simple Harmonic Universe*,” *JHEP* **1402** (2014) 029 [arXiv:1109.0282 [hep-th]].
- [25] M. Koehn, J. L. Lehners and B. A. Ovrut, “*Cosmological super-bounce*,” *Phys. Rev. D* **90** (2014) 2, 025005 [arXiv:1310.7577 [hep-th]].



- [26] A. Vilenkin, “*Arrows of time and the beginning of the universe,*” *Phys. Rev. D* **88** (2013) 043516 [arXiv:1305.3836 [hep-th]].
- [27] S. Choudhury, B. K. Pal, B. Basu and P. Bandyopadhyay, “*Measuring CP violation within Effective Field Theory of inflation from CMB,*” arXiv:1409.6036 [hep-th].
- [28] S. Choudhury, A. Mazumdar and E. Pukartas, “*Constraining  $\mathcal{N} = 1$  supergravity inflationary framework with non-minimal Kahler operators,*” *JHEP* **1404** (2014) 077 [arXiv:1402.1227 [hep-th]].
- [29] S. Choudhury and A. Mazumdar, “*Primordial blackholes and gravitational waves for an inflection-point model of inflation,*” *Phys. Lett. B* **733** (2014) 270 [arXiv:1307.5119 [astro-ph.CO]].
- [30] S. Choudhury, T. Chakraborty and S. Pal, “*Higgs inflation from new Kahler potential,*” *Nucl. Phys. B* **880** (2014) 155 [arXiv:1305.0981 [hep-th]].
- [31] S. Choudhury and S. Pal, “*Fourth level MSSM inflation from new flat directions,*” *JCAP* **1204** (2012) 018 [arXiv:1111.3441 [hep-ph]].
- [32] T. Biswas, R. Mayes and C. Lattyak, “*Perturbations in Bouncing and Cyclic Models, a General Study,*” arXiv:1502.05875 [gr-qc].
- [33] T. Biswas, A. S. Koshelev, A. Mazumdar and S. Y. Vernov, “*Stable bounce and inflation in non-local higher derivative cosmology,*” *JCAP* **1208** (2012) 024 [arXiv:1206.6374 [astro-ph.CO]].
- [34] L. Battarra, M. Koehn, J. L. Lehners and B. A. Ovrut, “*Cosmological Perturbations Through a Non-Singular Ghost-Condensate/Galileon Bounce,*” *JCAP* **1407** (2014) 007 [arXiv:1404.5067 [hep-th]].
- [35] V. Sahni, Y. Shtanov and A. Toporensky, “*Arrow of time in dissipationless cosmology,*” arXiv:1506.01247 [gr-qc].
- [36] S. Choudhury and S. Pal, “*Primordial non-Gaussian features from DBI Galileon inflation,*” *Eur. Phys. J. C* **75** (2015) 6, 241 [arXiv:1210.4478 [hep-th]].
- [37] S. Choudhury, “*Constraining  $\mathcal{N} = 1$  supergravity inflation with non-minimal Kaehler operators using  $\delta N$  formalism,*” *JHEP* **1404** (2014) 105 [arXiv:1402.1251 [hep-th]].
- [38] X. Gao, M. Lilley and P. Peter, “*Production of non-gaussianities through a positive spatial curvature bouncing phase,*” *JCAP* **1407** (2014) 010 [arXiv:1403.7958 [gr-qc]].
- [39] X. Gao, M. Lilley and P. Peter, “*Non-Gaussianity excess problem in classical bouncing cosmologies,*” *Phys. Rev. D* **91** (2015) 2, 023516 [arXiv:1406.4119 [gr-qc]].
- [40] J. M. Maldacena, “*Non-Gaussian features of primordial fluctuations in single field inflationary models,*” *JHEP* **0305** (2003) 013 [astro-ph/0210603].
- [41] J. M. Maldacena and G. L. Pimentel, “*On graviton non-Gaussianities during inflation,*” *JHEP* **1109** (2011) 045 [arXiv:1104.2846 [hep-th]].
- [42] N. Arkani-Hamed and J. Maldacena, “*Cosmological Collider Physics,*” arXiv:1503.08043 [hep-th].

- [43] I. Mata, S. Raju and S. Trivedi, “*CMB from CFT*,” JHEP **1307** (2013) 015 [arXiv:1211.5482 [hep-th]].
- [44] A. Ghosh, N. Kundu, S. Raju and S. P. Trivedi, “*Conformal Invariance and the Four Point Scalar Correlator in Slow-Roll Inflation*,” JHEP **1407** (2014) 011 [arXiv:1401.1426 [hep-th]].
- [45] N. Kundu, A. Shukla and S. P. Trivedi, “*Constraints from Conformal Symmetry on the Three Point Scalar Correlator in Inflation*,” JHEP **1504** (2015) 061 [arXiv:1410.2606 [hep-th]].
- [46] S. Choudhury, “*Inflamagnetogenesis redux: Unzipping sub-Planckian inflation via various cosmoparticle probes*,” Phys. Lett. B **735** (2014) 138 [arXiv:1403.0676 [hep-th]].
- [47] S. Choudhury, “*Braneflamagnetogenesis from Cosmoparticle Physics after Planck*,” arXiv:1504.08206 [astro-ph.CO].
- [48] K. Subramanian, “*The origin, evolution and signatures of primordial magnetic fields*,” arXiv:1504.02311 [astro-ph.CO].
- [49] S. Choudhury and A. Mazumdar, “*Reconstructing inflationary potential from BICEP2 and running of tensor modes*,” arXiv:1403.5549 [hep-th].
- [50] S. Choudhury and A. Mazumdar, “*An accurate bound on tensor-to-scalar ratio and the scale of inflation*,” Nucl. Phys. B **882** (2014) 386 [arXiv:1306.4496 [hep-ph]].
- [51] S. Choudhury and A. Mazumdar, “*Sub-Planckian inflation & large tensor to scalar ratio with  $r \geq 0.1$* ,” arXiv:1404.3398 [hep-th].
- [52] S. Choudhury, “*Can Effective Field Theory of inflation generate large tensor-to-scalar ratio within Randall-Sundrum single braneworld?*,” Nucl. Phys. B **894** (2015) 29 [arXiv:1406.7618 [hep-th]].
- [53] J. E. Lidsey, A. R. Liddle, E. W. Kolb, E. J. Copeland, T. Barreiro and M. Abney, “*Reconstructing the inflation potential : An overview*,” Rev. Mod. Phys. **69** (1997) 373 [astro-ph/9508078].
- [54] T. P. Sotiriou and V. Faraoni, “ *$f(R)$  Theories Of Gravity*,” Rev. Mod. Phys. **82** (2010) 451 [arXiv:0805.1726 [gr-qc]].
- [55] A. De Felice and S. Tsujikawa, “ *$f(R)$  theories*,” Living Rev. Rel. **13** (2010) 3 [arXiv:1002.4928 [gr-qc]].
- [56] V. Faraoni, “ *$f(R)$  gravity: Successes and challenges*,” arXiv:0810.2602 [gr-qc].
- [57] S. Capozziello and M. De Laurentis, “*Extended Theories of Gravity*,” Phys. Rept. **509** (2011) 167 [arXiv:1108.6266 [gr-qc]].
- [58] S. Choudhury and S. Pal, “*DBI Galileon inflation in background SUGRA*,” Nucl. Phys. B **874** (2013) 85 [arXiv:1208.4433 [hep-th]].
- [59] S. Choudhury and S. Sengupta, “*Features of warped geometry in presence of Gauss-Bonnet coupling*,” JHEP **1302** (2013) 136 [arXiv:1301.0918 [hep-th]].

- [60] S. Choudhury, S. Sadhukhan and S. SenGupta, “*Collider constraints on Gauss-Bonnet coupling in warped geometry model,*” arXiv:1308.1477 [hep-ph].
- [61] S. Choudhury and A. Dasgupta, “*Galileogenesis: A new cosmophenomenological zip code for reheating through R-parity violating coupling,*” Nucl. Phys. B **882** (2014) 195 [arXiv:1309.1934 [hep-ph]].
- [62] S. Choudhury and S. SenGupta, “*A step toward exploring the features of Gravidilaton sector in Randall-ÅSundrum scenario via lightest Kaluza-ÅKlein graviton mass,*” Eur. Phys. J. C **74** (2014) 11, 3159 [arXiv:1311.0730 [hep-ph]].
- [63] S. Choudhury, J. Mitra and S. SenGupta, “*Modulus stabilization in higher curvature dilaton gravity,*” JHEP **1408** (2014) 004 [arXiv:1405.6826 [hep-th]].
- [64] S. Choudhury, J. Mitra and S. SenGupta, “*Fermion localization and flavour hierarchy in higher curvature spacetime,*” arXiv:1503.07287 [hep-th].
- [65] L. Randall and R. Sundrum, “*An Alternative to compactification,*” Phys. Rev. Lett. **83** (1999) 4690 [hep-th/9906064].
- [66] R. Maartens and K. Koyama, “*Brane-World Gravity,*” Living Rev. Rel. **13** (2010) 5 [arXiv:1004.3962 [hep-th]].
- [67] L. Randall and R. Sundrum, “*A Large mass hierarchy from a small extra dimension,*” Phys. Rev. Lett. **83** (1999) 3370 [hep-ph/9905221].
- [68] G. R. Dvali, G. Gabadadze and M. Porrati, “*4-D gravity on a brane in 5-D Minkowski space,*” Phys. Lett. B **485** (2000) 208 [hep-th/0005016].
- [69] E. J. Copeland, M. Sami and S. Tsujikawa, “*Dynamics of dark energy,*” Int. J. Mod. Phys. D **15** (2006) 1753 [hep-th/0603057].
- [70] K. Freese and W. H. Kinney, “*On: Natural inflation,*” Phys. Rev. D **70** (2004) 083512 [hep-ph/0404012].
- [71] S. Choudhury and S. Pal, “*Brane inflation in background supergravity,*” Phys. Rev. D **85** (2012) 043529 [arXiv:1102.4206 [hep-th]].
- [72] S. Choudhury and S. Pal, “*Reheating and leptogenesis in a SUGRA inspired brane inflation,*” Nucl. Phys. B **857** (2012) 85 [arXiv:1108.5676 [hep-ph]].
- [73] S. Choudhury and S. Pal, “*Brane inflation: A field theory approach in background supergravity,*” J. Phys. Conf. Ser. **405** (2012) 012009 [arXiv:1209.5883 [hep-th]].
- [74] B. Gumjudpai, “*Brane cosmology dynamics with induced gravity,*” Gen. Rel. Grav. **36** (2004) 747 [gr-qc/0308046].
- [75] P. A. R. Ade *et al.* [Planck Collaboration], “*Planck 2015 results. XIII. Cosmological parameters,*” arXiv:1502.01589 [astro-ph.CO].
- [76] P. Singh and F. Vidotto, “*Exotic singularities and spatially curved Loop Quantum Cosmology,*” Phys. Rev. D **83** (2011) 064027 [arXiv:1012.1307 [gr-qc]].
- [77] A. Ashtekar, T. Pawłowski, P. Singh and K. Vandersloot, “*Loop quantum cosmology of  $k = 1$  FRW models,*” Phys. Rev. D **75** (2007) 024035 [gr-qc/0612104].

- [78] H. Maeda, V. Sahni and Y. Shtanov, “*Braneworld dynamics in Einstein-Gauss-Bonnet gravity,*” *Phys. Rev. D* **76** (2007) 104028 [*Phys. Rev. D* **80** (2009) 089902] [[arXiv:0708.3237](#) [gr-qc]].
- [79] Y. Shtanov and V. Sahni, “*Bouncing brane worlds,*” *Phys. Lett. B* **557** (2003) 1 [[gr-qc/0208047](#)].